MARC A. MEYERS AND KRISHAN K. CHAWLA

# Mechanical Behavior of Materials

THIRD EDITION

# Mechanical Behavior of Materials

## Third Edition

Fully revised and updated, the new edition of this classic textbook provides a balanced mechanics-materials approach to understanding the mechanical behavior of materials.

It presents fundamental mechanisms operating at micro- and nanometer scales across a wide range of materials, in a way that is mathematically simple and requires no extensive knowledge of materials, and demonstrates how the microstructures and mesostructures of these materials determine their mechanical behavior.

Accompanied online by further resources for instructors, this is the ideal introduction for senior undergraduate and graduate students in materials science and engineering.

### New to this edition

New coverage of biomaterials, electronic materials, and cellular materials alongside established coverage of metals, polymers, ceramics, and composites.

New testing techniques such as micropillar compression and electron back-scattered diffraction.

Important new materials, such as high-entropy alloys, are introduced.

A stronger emphasis on real-world test data and tables, to train students in practical materials applications.

Over 40 new figures, over 100 worked examples, and over 740 exercises, including over 280 new exercises, to help cement student understanding.

**Marc A. Meyers** is a Distinguished Professor of Materials Science and Engineering at the University of California, San Diego, known for his expertise on the dynamic behavior of materials. He is a recipient of the TMS Educator Award (2013), the ASM International Albert Easton White Distinguished Teacher Award (2015), and the APS George Duvall Shock Compression Science Award (2017). He is a coauthor of *Biological Materials Science* (2014), and is a Fellow of TMS, ASM International, and the APS.

**Krishan K. Chawla** is an Emeritus Professor at the University of Alabama at Birmingham, and a former Program Director for Metals and Ceramics in the US NSF Division of Materials Research. He is the editor and chairman of the ASM Editorial Board for *International Materials Reviews*, the author of *Fibrous Materials*, 2nd edn. (2016), and a Fellow of ASM International.

# Mechanical Behavior of Materials

THIRD EDITION

**Marc A. Meyers**
University of California, San Diego

**Krishan K. Chawla**
University of Alabama at Birmingham

CAMBRIDGE
UNIVERSITY PRESS

CAMBRIDGE
UNIVERSITY PRESS

Shaftesbury Road, Cambridge CB2 8EA, United Kingdom

One Liberty Plaza, 20th Floor, New York, NY 10006, USA

477 Williamstown Road, Port Melbourne, VIC 3207, Australia

314–321, 3rd Floor, Plot 3, Splendor Forum, Jasola District Centre, New Delhi – 110025, India

103 Penang Road, #05–06/07, Visioncrest Commercial, Singapore 238467

Cambridge University Press is part of Cambridge University Press & Assessment,
a department of the University of Cambridge.

We share the University's mission to contribute to society through the pursuit of
education, learning and research at the highest international levels of excellence.

www.cambridge.org
Information on this title: www.cambridge.org/highereducation/isbn/9781108837903

DOI: 10.1017/9781108943383



First published in 1998 by Prentice-Hall
Second edition 2009 Cambridge University Press
6th printing 2013
Third edition 2025

*A catalogue record for this publication is available from the British Library.*

*Library of Congress Cataloging-in-Publication Data*
Names: Meyers, Marc A., author. | Chawla, Krishan Kumar, 1942– author.
Title: Mechanical behavior of materials / Marc A. Meyers, University of California, San Diego,
Krishan K. Chawla, University of Alabama, Birmingham.
Description: Third edition. | Cambridge ; New York, NY, USA : Cambridge University Press, [2025] |
Includes bibliographical references and index.
Identifiers: LCCN 2024014471 (print) | LCCN 2024014472 (ebook) | ISBN 9781108837903 (hardback) |
ISBN 9781108943383 (epub)
Subjects: LCSH: Strength of materials.
Classification: LCC TA403 .M554 2025 (print) | LCC TA403 (ebook) | DDC 620.1/12–dc23/eng/20240531
LC record available at https://lccn.loc.gov/2024014471
LC ebook record available at https://lccn.loc.gov/2024014472

ISBN 978-1-108-83790-3 Hardback

Additional resources for this publication at www.cambridge.org/mbm3

**Lovingly dedicated to the memory of my parents, Henri and Marie-Anne.**

**Marc André Meyers**

**Lovingly dedicated to the memory of my parents, Manohar L. and Sumitra Chawla.**

**Krishan Kumar Chawla**

# Contents

# Preface to the Third Edition

We are very pleased to offer this third edition of *Mechanical Behavior of Materials*. The first edition was published by Prentice-Hall in 1998. The second edition, a Cambridge University Press imprint, came out in 2009. The third edition is now seeing the light of the day in 2025. Needless to say, we have maintained the same fundamental theme of the book, viz., the fundamental mechanisms responsible for the mechanical properties of different materials under a variety of environmental conditions. The unique feature of the book is the presentation in a unified manner of important principles responsible for mechanical behavior of materials, metals, polymers, ceramics, composites, biological materials, electronic materials. The underlying theme is that structure (at the micro or nanometer level) of the material controls the properties of the material.

Although the basic theme of the book remains unchanged, the third edition has been updated with:

- State-of-the-art coverage of the major developments in materials, such as steels, ceramics, polymers, composites, biologic materials. Specifically, we discuss: unique characteristics of biological materials including the Arzt heptahedron and structural design elements which enable a quantitative engineering treatment in Chapter 1; the Euler equation, elasticity averaging methods of isostress and isostrain (Voigt and Reuss), and anisotropic effects to matrix formulation of stiffness in Chapter 2; High-Entropy Alloys in Chapter 10; Micropillar mechanical testing, EBSD (electron back-scattered diffraction), a powerful characterization method, and coincidence site lattice update in Chapter 5; fracture toughness of biological materials in Chapter 7.
- Many new figures to improve the presentation and to clarify the concepts presented.
- Fresh worked examples and exercises that help the students test their understanding.

The book is principally meant for use in the upper division and graduate level courses of mechanical engineering, and materials science and engineering departments. However, it will also be a great source of reference material to the practicing engineer, scientist, and researcher. We have kept the level of mathematics quite simple, and suggest the reader to refer back to Chapter 1 if needed, as it provides the basic materials-level information necessary to study this subject.

MAM would like to thank Sheron Tavares and Aomin Huang for their competent and dedicated work in the revision and permissions. This third edition would never have seen the day if it were not for them. He also thanks Boya Li for

contributing with exercises. He is grateful to his children Marc Meyers and Cristina Windsor, his granddaughters Claire, Isabelle, and Abigail, his brothers Pedro, Jacques, and Carlos for supporting him through this process. A special thanks is due to Linda Homayoun.

KKC is grateful to K. Carlisle, N. Chawla, A. Goel, M. Koopman, R. Kulkarni, A Mortensen, B. R. Patterson, P.D. Portella, and U. Vaidya, for their innumerable discussions and counsels. He is especially grateful to Kanika Chawla and M. Armstrong for their help with figures. As always, he is thankful to his family members, Anita, Kanika, Nikhil, Nimeesh, and Nivi for their forbearance.

# Preface to the Second Edition

The second edition of Mechanical Behavior of Materials has revised and updated material in every chapter to reflect the changes occurring in the field. In view of the increasing importance of bioengineering, a special emphasis is given to the mechanical behavior of biological materials and biomaterials throughout this second edition. A new chapter on environmental effects has been added. Professors Fine and Voorhees[1] make a cogent case for integrating biological materials into materials science and engineering curricula. This trend is already in progress at many US and European universities. Our second edition takes due recognition of this important trend. We have resisted the temptation to make a separate chapter on biological and biomaterials. Instead, we treat these materials together with traditional materials, viz., metals, ceramics, polymers, etc. In addition, taking due cognizance of the importance of electronic materials, we have emphasized the distinctive features of these materials from a mechanical behavior point of view.

The underlying theme in the second edition is the same as in the first edition. The text connects the fundamental mechanisms to the wide range of mechanical properties of different materials under a variety of environments. This book is unique in that it presents, in a unified manner, important principles involved in the mechanical behavior of different materials: metals, polymers, ceramics, composites, electronic materials, and biomaterials. The unifying thread running throughout is that the nano/microstructure of a material controls its mechanical behavior. A wealth of micrographs and line diagrams are provided to clarify the concepts. Solved examples and chapter-end exercise problems are provided throughout the text.

This text is designed for use in mechanical engineering and materials science and engineering courses by upper division and graduate students. It is also a useful reference tool for the practicing engineers involved with mechanical behavior of materials. The book does not presuppose any extensive knowledge of materials and is mathematically simple. Indeed, Chapter 1 provides the background necessary. We invite the reader to consult this chapter off and on because it contains very general material.

In addition to the major changes discussed above, the mechanical behavior of cellular and electronic materials was incorporated. Major reorganization of material has been made in the following parts: elasticity; Mohr circle treatment; elastic constants of fiber reinforced composites; elastic properties of biological and of biomaterials; failure criteria of composite materials; nanoindentation technique

[1] M. E. Fine and P. Voorhees, "On the evolving curriculum in materials science & engineering," *Daedalus*, Spring 2005, 134.

and its use in extracting material properties; etc. New solved and chapter-end exercises are added. New micrographs and line diagrams are provided to clarify the concepts.

We are grateful to many faculty members who adopted the first edition for classroom use and were kind enough to provide us with very useful feedback. We also appreciate the feedback we received from a number of students. MAM would like to thank Kanika Chawla and Jennifer Ko for help in the biomaterials area. The help provided by Marc H. Meyers and M. Cristina Meyers in teaching him the rudiments of biology has been invaluable. KKC would like thank K. B. Carlisle, N. Chawla, A. Goel, M. Koopman, R. Kulkarni, and B. R. Patterson for their help. KKC acknowledges the hospitality of Dr. P. D. Portella at Federal Institute for Materials Research and Testing (BAM), Berlin, Germany, where he spent a part of his sabbatical. As always, he is grateful to his family members, Anita, Kanika, Nikhil, and Nivi for their patience and understanding.

# A Note to the Reader

Our goal in writing *Mechanical Behavior of Materials* has been to produce a book that will be the pre-eminent source of fundamental knowledge about the subject. We expect this to be a guide to the student beyond his or her college years. There is, of course, a lot more material than can be covered in a normal semester-long course. We make no apologies for that in addition to being a classroom text, we want this volume to act as a useful reference work on the subject for the practicing scientist, researcher, and engineer.

Specifically, we have an introductory Chapter 1 (Materials: Structure, Properties, and Performance) dwelling on the themes of the book: structure, mechanical properties, and performance. This section introduces some key terms and concepts that are covered in detail in later chapters. We advise the reader to use this chapter as a handy reference tool, and consult it as and when required. We strongly suggest that the instructor use this first chapter as a self-study resource. Of course, individual sections, examples, and exercises can be added to the subsequent material as and when desired.

Enjoy!

# Chapter 1 Materials: Structure, Properties, and Performance

## 1.1 Introduction

Everything that surrounds us is matter. The origin of the word matter is *mater* (Latin) or *matri* (Sanskrit), for *mother*. In this sense, human beings anthropomorphized that which made them possible – that which gave them nourishment. Every scientific discipline concerns itself with matter. Of all matter surrounding us, a portion comprises materials. What are materials? They have been variously defined. One acceptable definition is "matter that human beings use and/or process." Another definition is "all matter used to produce manufactured or consumer goods." In this sense, a rock is not a material, intrinsically; however, if it is used in aggregate (concrete) by humans, it becomes a material. The same applies to all matter found on Earth: a tree becomes a material when it is processed and used by people, and a skin becomes a material once it is removed from its host and shaped into an artifact.

The successful utilization of materials requires that they satisfy a set of properties. These properties can be classified into thermal, optical, mechanical, physical, chemical, and nuclear, and they are intimately connected to the structure of materials. The structure, in its turn, is the result of synthesis and processing. A schematic framework that explains the complex relationships in the field of the mechanical behavior of materials, shown in Figure 1.1, is Thomas's iterative tetrahedron, which contains four principal elements: mechanical properties, characterization, theory, and processing. These elements are related, and changes in one are inseparably linked to changes in the others. For example, changes may be introduced by the synthesis and processing of, for instance, steel. The most common metal, steel has a wide range of strengths and ductilities (*mechanical properties*), which makes it the material of choice for numerous applications. While low-carbon steel is used as reinforcing bars in concrete and in the body of automobiles, quenched and tempered high-carbon steel is used in more critical applications such as axles and gears. Cast iron, much more brittle, is used in a variety of applications, including automobile engine blocks. These different applications require, obviously, different mechanical properties of the material. The different properties of the three materials, resulting in differences in performance, are attributed to differences in the internal structure of the materials.

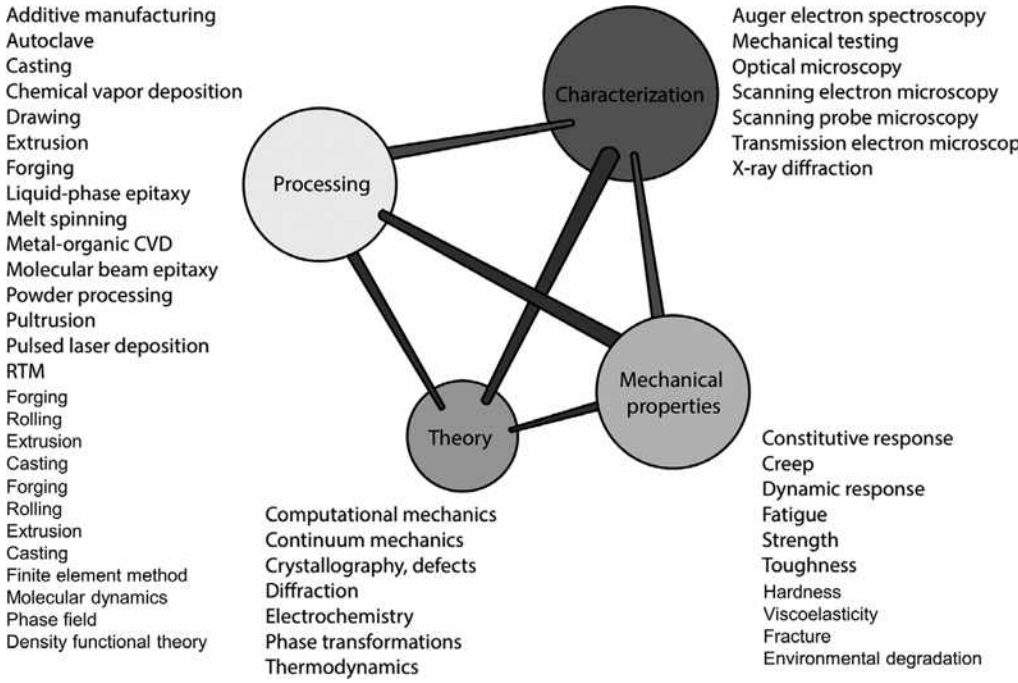


**Figure 1.1** Thomas's iterative materials tetrahedron applied to mechanical behavior of materials. (Figure courtesy of Annelies Zeeman.)

The understanding of the structure comes from *theory*. The determination of the many aspects of the micro-, meso-, and macrostructure of materials is obtained by *characterization*. Low-carbon steel has a primarily ferritic structure (body-centered cubic; see Section 1.3.1), with some interspersed pearlite (a ferrite–cementite mixture). The high hardness of the quenched and tempered high-carbon steel is due to its martensitic structure (body-centered tetragonal). The relatively brittle cast iron has a structure resulting directly from solidification, without subsequent mechanical working such as hot rolling. How does one obtain low-carbon steel, quenched and tempered high-carbon steel, and cast iron? By different *synthesis and processing* routes. The low carbon steel is processed from the melt by a sequence of mechanical working operations. The high-carbon steel is synthesized with a greater concentration of carbon (>0.5%) than the low-carbon steel (0.1%). Additionally, after mechanical processing, the high-carbon steel is rapidly cooled from a temperature of approximately 1,000 °C by throwing it into water or oil; it is then reheated to an intermediate temperature (tempering). The cast iron is synthesized with even higher carbon contents (~2%). It is poured directly into the molds and allowed to solidify in them. Thus, no mechanical working, except for some minor machining, is needed. These interrelationships among structure, properties, and performance, and their modification by synthesis and processing, constitute the central theme of materials science and engineering. The tetrahedron of

Figure 1.1 lists the principal processing methods, the most important theoretical approaches, and the most-used characterization techniques in materials science today.

The selection, processing, and utilization of materials have been part of human culture since its beginnings. Anthropologists refer to humans as "the toolmakers," and this is indeed a very realistic description of a key aspect of human beings responsible for their ascent and domination over other animals. It is the ability of humans to manufacture and use tools, and the ability to produce manufactured goods, that has allowed technological, cultural, and artistic progress and that has led to civilization and its development. Materials were as important to a Neolithic tribe in the year 10,000 BCE as they are to us today. The only difference is that today more complex synthetic materials are available in our society, while Neolithic tribes had only natural materials at their disposal: wood, minerals, bones, hides, and fibers from plants and animals. Although these naturally occurring materials are still used today, they are vastly inferior in properties to synthetic materials.

## 1.2 Monolithic, Composite, and Hierarchical Materials

The early materials used by humans were natural, and their structure varied widely. Rocks are crystalline, pottery is a mixture of glassy and crystalline components, wood is a fibrous organic material with a cellular structure, and leather is a complex organic material. Human beings started to synthesize their own materials in the Neolithic period: ceramics first, then metals, and later, polymers. In the twentieth century, simple monolithic structures were used first. The term *monolithic* comes from the Greek *mono* (one) and *lithos* (stone). It means that the material has essentially uniform properties throughout. Microstructurally, monolithic materials can have two or more phases. Nevertheless, they have properties (electrical, mechanical, optical, and chemical) that are constant throughout. Table 1.1 presents some of the important properties of metals, ceramics, and polymers. Their detailed structures will be described in Section 1.3. The differences in their structure are responsible for differences in properties. Metals have densities ranging from 2 to 19 g $cm^{-3}$; iron, nickel, chromium, and niobium have densities ranging from to 7 to 9 g $cm^{-3}$ aluminum has a density of 2.7 g $cm^{-3}$; and titanium has a density of 4.5 g $cm^{-3}$. Ceramics tend to have lower densities, ranging from 5 g $cm^{-3}$ (titanium carbide; TiC = 4.9) to 3 g $cm^{-3}$(alumina; $Al_2O_3$ = 3.95; silicon carbide; SiC = 3.2). Polymers have the lowest densities, fluctuating around 1 g $cm^{-3}$. Another marked difference among these three classes of materials is their ductility (ability to undergo plastic deformation). At room temperature, metals can undergo significant plastic deformation. Thus, metals tend to be ductile, although there are a number of exceptions. Ceramics, on the other hand, are very brittle, and the most ductile ceramics will be more brittle than most metals. Polymers have a behavior ranging from brittle (at temperatures below their glass transition temperature) to very deformable (in a nonlinear elastic material, such as rubber). The fracture toughness

**Table 1.1 Summary of Properties of Main Classes of Materials**

| Property | Metals | Ceramics | Polymers |
|---|---|---|---|
| Density (g $cm^{-3}$) | 2–20 | 1–14 | 1–2.5 |
| Electrical conductivity | high | low | low |
| Thermal conductivity | high | low | low |
| Ductility or strain-to-fracture (%) | 4–40 | <1 | 2–4 |
| Tensile strength (MPa) | 100–1,500 | 100–400 | – |
| Compressive strength (MPa) | 100–1,500 | 1,000–5,000 | – |
| Fracture toughness ($MNm^{-3/2}$) | 10–30 | 1–10 | 2–8 |
| Maximum service temperature (°C) | 1,000 | 1,800 | 250 |
| Corrosion resistance | low to medium | superior | medium |
| Bonding | metallic (free-electron cloud) | ionic or covalent | covalent |
| Structure | mostly crystalline (face-centered cubic, FCC; body-centered cubic, BCC; hexagonal close packed, HCP) | complex crystalline structure | amorphous or semicrystalline polymer |

is a good measure of the resistance of a material to failure and is generally quite high for metals and low for ceramics and polymers. Ceramics far outperform metals and polymers in high-temperature applications, since many ceramics do not oxidize even at very high temperatures (the oxide ceramics are already oxidized) and retain their strength to such temperatures. One can compare the mechanical, thermal, optical, electrical, and electronic properties of the different classes of materials and see that there is a very wide range of properties. Thus, monolithic structures built from primarily one class of material cannot provide all desired properties.

In the field of biomaterials (materials used in implants and life support systems), developments have also had far-reaching effects. The mechanical performance of implants is critical in many applications, including hipbone implants, which are subjected to high stresses, and endosseous implants in the jaw designed to serve as the base for teeth. Figure 1.2(a) shows the most successful design for endosseous implants in the jawbone. With this design, a titanium post is first screwed into the jawbone and allowed to heal. The tooth is fixed to the post and is effectively rooted into the jaw. The insertion of endosseous implants into the mandibles or maxillae, which was initiated in the 1980s, has been a revolution in dentistry. There is a little story associated with this discovery. Researchers were investigating the bone marrow of rabbits. They routinely used stainless steel hollow cylinders screwed into the bone. Through the hole, they could observe the bone marrow. It so happened that one of these cylinders was made of titanium. Since these cylinders were expensive, the researchers removed them periodically, in order to reuse them. When they tried to remove the titanium cylinder, it was tightly fused to the bone.

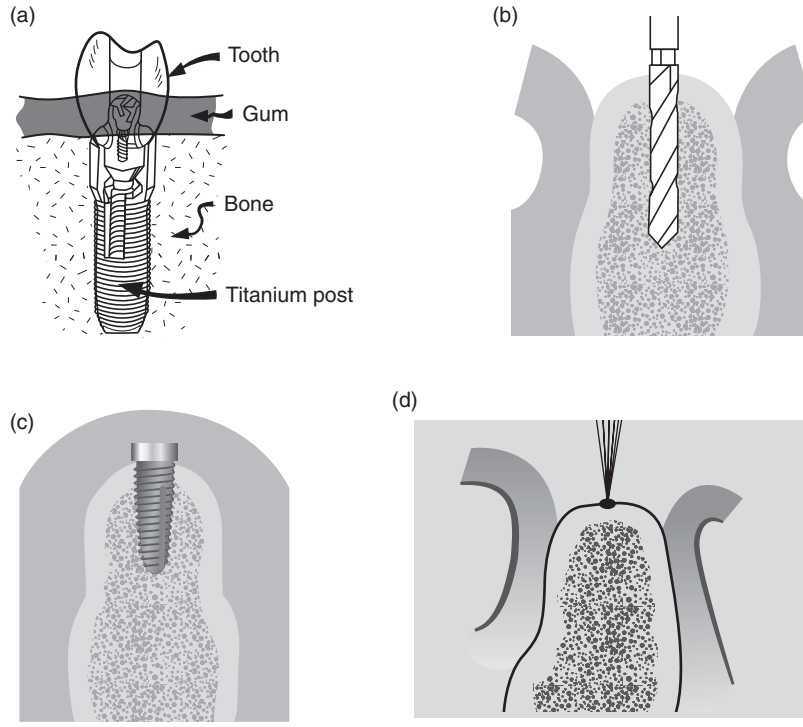


**Figure 1.2** (a) Complete endosseous implant, (b) a hole is drilled, and (c) a titanium post is screwed into jawbone. (d) Marking of site with small drill. (Figure courtesy of J. Mahooti.)

This triggered the creative intuition of one of the researchers, who said "What if. . .?".

Figure 1.2 shows the procedure used to insert the titanium implant. The site is first marked with a small drill that penetrates the cortical bone (Figure 1.2(d)). Then successive drills are used to create an orifice of the desired diameter (Figure 1.2(b)). The implant is screwed into the bone and the tissue is closed (Figure 1.2(c)). This implant is allowed to heal and fuse with the bone for approximately six months. Chances are that most readers will have these devices installed sometime in their lives.

Hip- and knee-replacement surgery is becoming commonplace. In the USA alone between 250,000 and 300,000 of each procedure are carried out annually. The materials of the prostheses have an important bearing on survival probability. Typical hip and knee prostheses are shown in Figure 1.3.

The hip prosthesis is made up of two parts: the acetabular component, or socket portion, which replaces the acetabulum, and the femoral component, or stem portion, which replaces the femoral head.

The femoral component is made of a metal stem with a metal ball on the extremity. In some prostheses a ceramic ball is attached to the metal stem. The acetabular component is a metal shell with a plastic inner socket liner made of

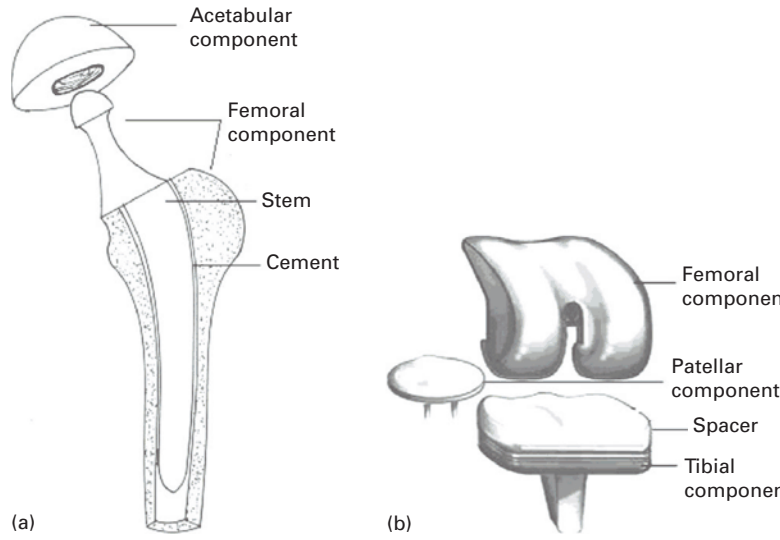


**Figure 1.3** (a) Total hip replacement prosthesis (b) total knee replacement prosthesis.

metal, ceramic, or a plastic called ultra-high-molecular-weight polyethylene (UHMWPE) that acts like a bearing. A *cemented* prosthesis is held in place by a type of epoxy cement that attaches the metal to the bone. An *uncemented* prosthesis has a fine mesh of holes on the surface area that touches the bone. The mesh allows the bone to grow into the mesh and become part of the bone. Biomaterial advances have allowed experimentation with new bearing surfaces, and there are now several different options when hip-replacement surgery is considered.

The metal has to be inert in the body environment. The preferred materials for the prostheses are Co–Cr alloys (Vitalium®) and titanium alloys. However, there are problems that have not yet been resolved: the metallic components have elastic moduli that far surpass those of bone. Therefore, they "carry" a disproportionate fraction of the load, and the bone is therefore unloaded. Since the health and growth of bone is closely connected to the loads applied to it, this unloading tends to lead to bone loss.

The most common cause of joint replacement failure is wear of the implant surfaces. This is especially critical for the polymeric components of the prosthesis. This wear produces debris which leads to tissue irritation. Another important cause of failure is loosening of the implant due to weakening of the surrounding bone. A third source of failure is fatigue.

*Biocompatibility* is a major concern for all implants, and ceramics are especially attractive because of their (relative) chemical inertness. Metallic alloys such as Vitalium® and titanium alloys have also proved to be successful, as have polymers such as polyethylene. A titanium alloy with a solid core surrounded by a porous periphery (produced by sintering of powders) has shown considerable potential. The porous periphery allows bone to grow and affords very effective fixation. Two new classes of materials that appear to present the best biocompatibility with bones are the Bioglass® and calcium phosphate ceramics. Bones contain calcium and

phosphorus, and Bioglass® is a glass in which the silicon has been replaced by those two elements. Thus, the bone "perceives" these materials as being another bone and actually bonds with it. Biomechanical properties are of great importance in bone implants, as are the elastic properties of materials. If the stiffness of a material is too high, then when implanted the material will carry more of the load placed on it than the adjacent bone. This could in turn lead to a weakening of the bone, since bone growth and strength depend on the stresses that the bone is subjected to. Thus, the elastic properties of bone and implant should be similar. Polymers reinforced with strong carbon fibers are also candidates for such applications. Metals, on the other hand, are stiffer than bones and tend to carry most of the load. With metals, the bones would be shielded from stress, which could lead to bone resorption and loosening of the implant.

Although new materials are being developed continuously, monolithic materials, with their uniform properties, cannot deliver the range of performance needed in any critical applications. *Composites* are a mixture of two classes of materials: metal–ceramic, metal–polymer, or polymer–ceramic. They have unique mechanical properties that are dependent on the amount and manner in which their constituents are arranged. Figure 1.4(a) shows schematically how different composites can be formed. Composites consist of a matrix and a reinforcing material. In making them, the modern materials engineer has at his or her disposal a very wide range of possibilities. However, the technological problems involved in producing some of them are immense, although there is a great deal of research addressing these problems. Figure 1.4(b) shows three principal kinds of reinforcement in composites: particles, continuous fibers, and discontinuous (short) fibers. The reinforcement usually has a higher strength than the matrix, which provides the ductility of the material. In ceramic-based composites, however, the matrix is brittle, and the fibers provide barriers to the propagating cracks, increasing the toughness of the material.

The alignment of the fibers is critical in determining the strength of a composite. The strength is highest along a direction parallel to the fibers and lowest along directions perpendicular to it. For the three kinds of composite shown in Figure 1.4(b), the polymer matrix plus (aramid, carbon, or glass) fiber is the most common combination if no high-temperature capability is needed.

Composites are becoming a major material in the aircraft industry. Carbon/epoxy and aramid/epoxy composites are being introduced in a large number of aircraft parts. These composite parts reduce the weight of the aircraft, increasing its economy and payload. The major mechanical property advantages of advanced composites over metals are better stiffness-to-density and strength-to-density ratios and greater resistance to fatigue. The values given in Table 1.2 apply to a unidirectional composite along the fiber reinforcement orientation. The values along other directions are much lower, and therefore the design of a composite has to incorporate the anisotropy of the materials. It is clear from the table that composites have advantages over monolithic materials. In most applications, the fibers are arranged along different orientations in different layers. For the central composite of Figure 1.4(b), these orientations are 0°, 45° 90°, and 135° to the tensile axis.

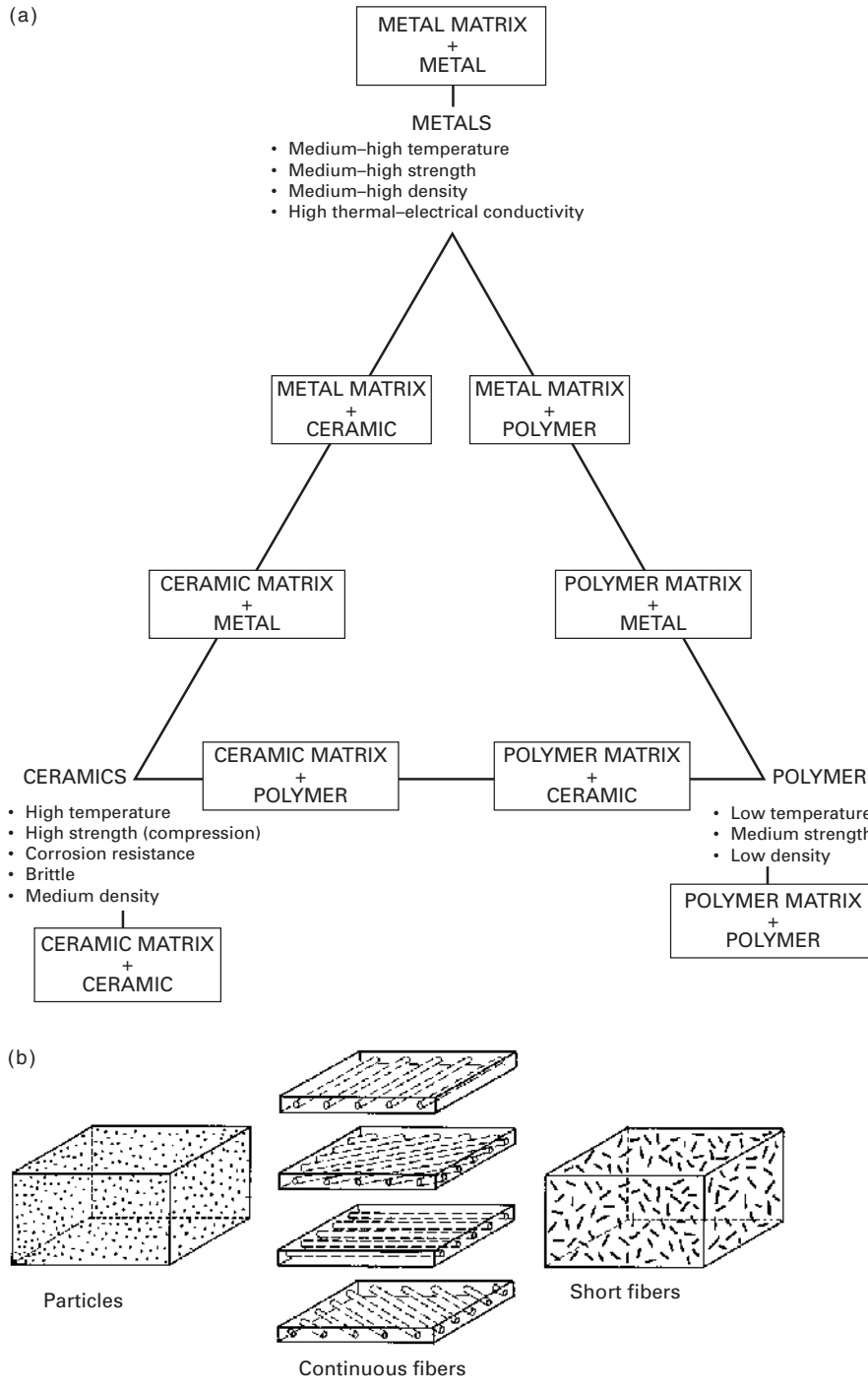


**Figure 1.4** (a) Schematic representations of different classes of composites. (b) Different kinds of reinforcement in composite materials. Composite with continuous fibers with four different orientations (shown separately for clarity).

**Table 1.2 Specific Modulus and Strength of Materials Used in Aircraft**

| Material | Elastic modulus/density (GPa/g $cm^{-3}$) | Tensile strength/density (MPa/g $cm^{-3}$) |
|---|---|---|
| Steel (AISI 4340) | 25 | 230 |
| Al (7075-T6) | 25 | 180 |
| Titanium (Ti-6Al-4V) | 25 | 250 |
| E glass/epoxy composite | 21 | 490 |
| S glass/epoxy composite | 47 | 790 |
| *Aramid/epoxy composite | 55 | 890 |
| HS (high tensile strength) carbon/epoxy composite | 92 | 780 |
| HM (high modulus) carbon/epoxy composite | 134 | 460 |

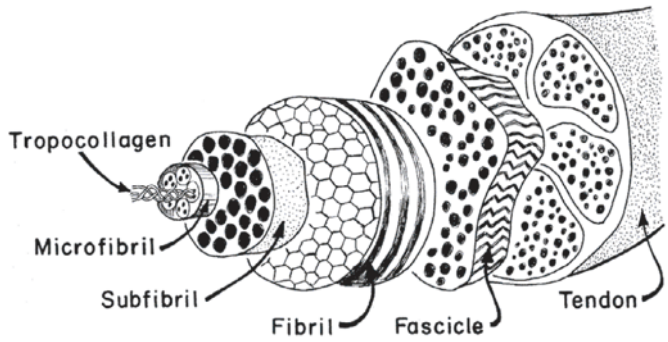


**Figure 1.5** A model of a hierarchical structure occurring in the human body. (Figure courtesy of E. Baer.)

Can we look beyond composites in order to obtain even higher mechanical performance? Indeed, we can: Nature is infinitely imaginative.

Our body is a complex arrangement of parts, designed, as a whole, to perform all the tasks needed to keep us alive. Scientists are looking into the make-up of soft tissue (skin, tendon, intestine, etc.), which is a very complex structure with different units active at different levels complementing each other. The structure of soft tissue has been called a *hierarchical* structure, because there seems to be a relationship between the ways in which it operates at different levels. Figure 1.5 shows the structure of a tendon. This structure begins with the tropocollagen molecule, a triple helix of polymeric protein chains. The tropocollagen molecule has a diameter of approximately 1.5 mm. The tropocollagen organizes itself into microfibrils, subfibrils, and fibrils. The fibrils, a critical component of the structure, are crimped when there is no stress on them. When stressed, they stretch out and then transfer their load to the fascicles, which compose the tendon. The fascicles have a diameter of approximately 150–300 μm and constitute the basic unit of the tendon. The hierarchical organization of the tendon is responsible for its toughness. Separate structural units can fail independently and thus absorb energy locally, without causing the failure of the entire tendon. Both experimental and analytical studies have been done, modeling the tendon as a composite of elastic, wavy fibers in a

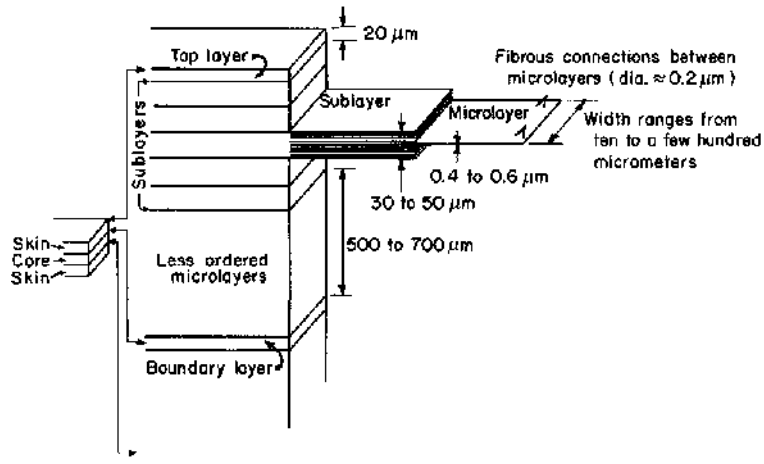


**Figure 1.6** Schematic illustration of a proposed hierarchical model for a composite (not drawn to scale).
(Figure courtesy of E. Baer.)

viscoelastic matrix. Local failures, absorbing energy, will prevent catastrophic failure of the entire tendon until enormous damage is produced.

Materials engineers are beginning to look beyond simple two component composites, imitating nature in organizing different levels of materials in a hierarchical manner. Baer[1] suggests that the study of biological materials could lead to new hierarchical designs for composites. One such example is shown in Figure 1.6, a layered structure of liquid-crystalline polymers consisting of alternating core and skin layers. Each layer is composed of sublayers which, in their turn, are composed of microlayers. The molecules are arranged in different arrays in different layers. The lesson that can be learned from this arrangement is that we appear to be moving toward composites of increasing complexity.

## 1.3 Structure of Materials

The *crystallinity*, or periodicity, of a structure, does not exist in gases or liquids. Among solids, the metals, ceramics, and polymers may or may not exhibit it, depending on a series of processing and composition parameters. Metals are normally crystalline. However, a metal cooled at a superfast rate from its liquid state called *splat cooling* can have an amorphous structure. (This subject is treated in greater detail in Section 1.3.4.) Silicon dioxide ($SiO_2$) can exist as amorphous (fused silica) or as crystalline (cristobalite or tridymite). Polymers consisting of molecular chains can exist in various degrees of crystallinity.

Readers not familiar with structures, lattices, crystal systems, and Miller indices should study these subjects before proceeding with the text. Most books on materials science, physical metallurgy, or X-rays treat the subjects completely. A brief introduction is presented next.

[1] E. Baer, *Sci. Am.* 254, No. 10 (1986) 179.

### 1.3.1 Crystal Structures

To date, seven crystal structures describe all the crystals that have been found. By translating the unit cell along the three crystallographic orientations, it is possible to construct a three-dimensional array. The translation of each unit cell along the three principal directions by distances that are multiples of the corresponding unit cell size produces the crystalline lattice.

Up to this point, we have not talked about atoms or molecules; we are just dealing with the mathematical operations of filling space with different shapes of blocks. We now introduce atoms and molecules, or "repeatable structural units." The unit cell is the smallest repetitive unit that will, by translation, produce the atomic or molecular arrangement. Bravais established that there are 14 space lattices. These lattices are based on the seven crystal structures. The points shown in Figure 1.7 correspond to atoms or groups of atoms. The 14 Bravais lattices can represent the

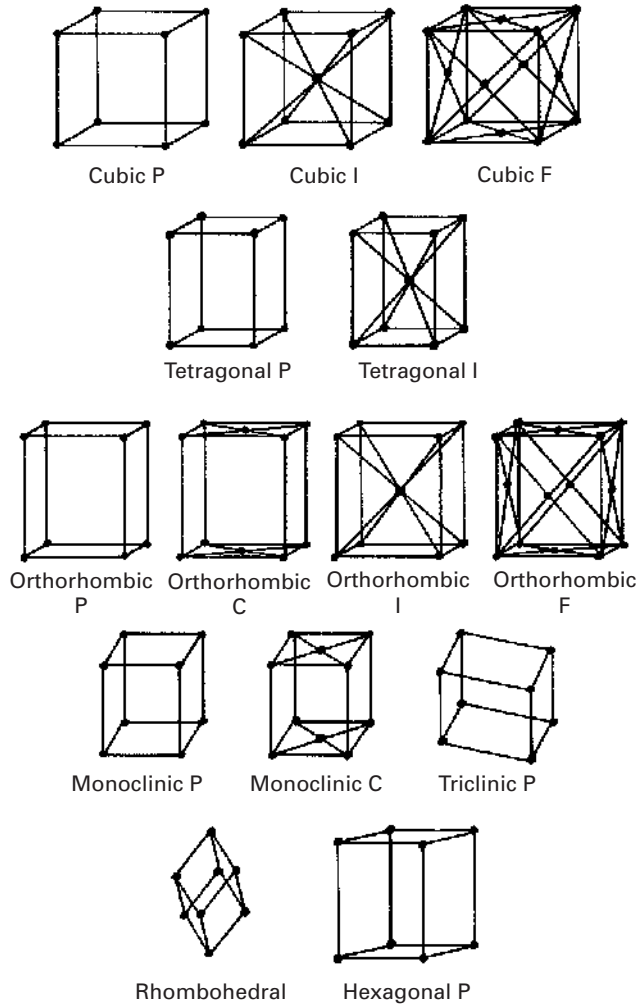


**Figure 1.7** The 14 Bravais space lattices ($P$ = primitive or simple; $I$ = body-centered cubic; $F$ = face-centered cubic; C = base-centered cubic).

**Table 1.3 Seven crystal systems and fourteen Bravais lattices**

| Name | Number of Bravais lattices | © Bart van Zeghbroeck 2007 Conditions | Primitive | Base-centered | Body-centered | Face-centered |
|---|---|---|---|---|---|---|
| Triclinic | 1 | $a_1 \neq a_2 \neq a_3, \alpha \neq \beta \neq \gamma$ | ✓ | | | |
| Monoclinic | 2 | $a_1 \neq a_2 \neq a_3, \alpha = \beta = 90^\circ \neq \gamma$ | ✓ | ✓ | | |
| Orthorhombic | 4 | $a_1 \neq a_2 \neq a_3, \alpha = \beta = \gamma = 90^\circ$ | ✓ | ✓ | ✓ | ✓ |
| Tetragonal | 2 | $a_1 = a_2 \neq a_3, \alpha = \beta = \gamma = 90^\circ$ | ✓ | | ✓ | |
| Cubic | 3 | $a_1 = a_2 = a_3, \alpha = \beta = \gamma = 90^\circ$ | ✓ | | ✓ | ✓ |
| Rhombohedral | 1 | $a_1 = a_2 = a_3, \alpha = \beta = \gamma < 120^\circ \neq 90^\circ$ | ✓ | | | |
| Hexagonal | 1 | $a_1 = a_2 \neq a_3, \alpha = \beta = 90^\circ, \gamma = 120^\circ$ | ✓ | | | |

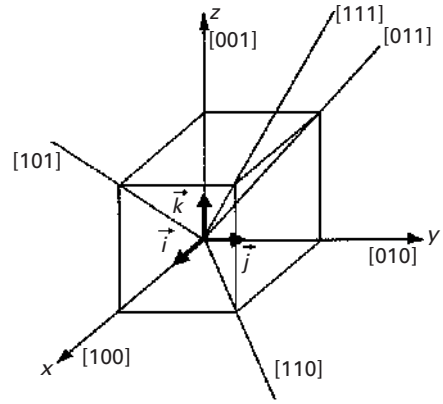


**Figure 1.8** Directions in a cubic unit cell.

unit cells for all crystals. Table 1.3 lists the 14 Bravais lattices as well as the respective lattice parameters. Figure 1.8 shows the indices used for directions in the cubic system. The same symbols are employed for different structures. We simply use the vector passing through the origin and a point ($m$, $n$, $o$):

$$\mathbf{V} = m\mathbf{i} + n\mathbf{j} + o\mathbf{k}.$$

If:

$$\mathbf{u} = u_1\mathbf{i} + u_2\mathbf{j} + u_3\mathbf{k}$$

and:

$$\mathbf{v} = v_1\mathbf{i} + v_2\mathbf{j} + v_3\mathbf{k}$$

we have:

$$\cos\ \alpha = \frac{u_1v_1 + u_2v_2 + u_3v_3}{\sqrt{u_1^2 + u_2^2 + u_3^2}\sqrt{v_1^2 + v_2^2 + v_3^2}}.$$

The angle between two directions **u** and **v** can be calculated through the cross product of the vectors:

$$\cos\alpha = \frac{\mathbf{u}\cdot\mathbf{v}}{|\mathbf{u}|\cdot|\mathbf{v}|}.$$

The notation used for a direction is

[m n o].

When we deal with a family of directions, we use the symbol $<mno>$.

The following family encompasses all equivalent directions:

$$< mno > \Rightarrow [mno], [mon], [omn], [onm], [nmo], [m\overline{n}o]$$
$$[mo\overline{n}], [om\overline{n}], [o\overline{n}m], [\overline{n}mo], \ldots$$

where an overbar indicates a negative sign in front of the variable. When the direction does not pass through the origin, and we have the head of the vector at $(m, n, o)$ and the tail at $(p, q, r)$, the vector **V** is given by

$$\mathbf{V} = (m-p)\mathbf{i} + (n-q)\mathbf{j} + (o-r)\mathbf{k}.$$

A direction not passing through the origin can be represented by

$$[(m-p)(n-q)(o-r)].$$

We can clear fractions, to reach smallest integer. Note that for the negative, we use a bar on top. For planes, we use the Miller indices, obtained from the intersection of a plane with the coordinate axes. Figure 1.9 shows a plane and its intercepts. We take

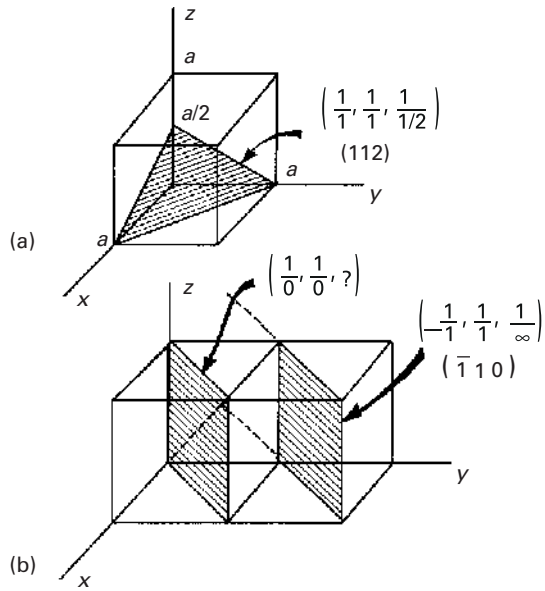


**Figure 1.9** Indexing of planes by Miller rules in the cubic unit cell; (a) (112); (b) $(\overline{1}10)$.

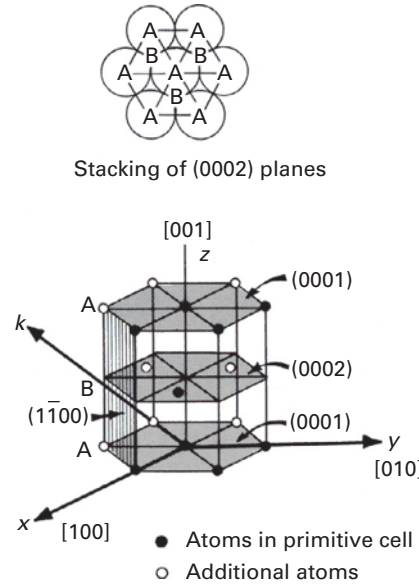


**Figure 1.10** Hexagonal structure consisting of a three-unit cell.

the inverse of the intercepts and multiply them by their common denominator so that we end up with integers. In Figure 1.9(a), we have

$$\frac{1}{1}, \frac{1}{1}, \frac{1}{1/2} \Rightarrow (112).$$

Figure 1.9 (b) shows an indeterminate situation. Thus, we have to translate the plane to the next cell, or else translate the origin. The indeterminate situation arises because the plane passes through the origin. After translation, we obtain intercepts (–1, 1, ∞). By inverting them, we get (110). The symbol for a family of planes is {m n o}. We do not reach to smallest integer. We use round parentheses ( ). For a family, we use { }. If the plane contains one of the axes, we move the origin to the next cell. If the plane is parallel to an axis, it intersects it at infinity. For instance, the spacing between (222) and (111) planes is different.

For hexagonal structures, we have a slightly more complicated situation. We represent the hexagonal structure by the arrangement shown in Figure 1.10. The atomic arrangement in the basal plane is shown in the top portion of the figure. Often, we use four axes ($x$, $y$, $k$, $z$) with unit vectors ($i$, $j$, $k$, $I$) to represent the structure. This is mathematically unnecessary, because three indices are sufficient to represent a direction in space from a known origin. Still, the redundancy is found by some people to have its advantages and is described here. We use the intercepts to designate the planes. The hatched plane (prism plane) has indices

$$\frac{1}{1}, \frac{1}{-1}, \frac{1}{\infty}, \frac{1}{\infty}.$$

After determining the indices of many planes, we learn that one always has

$$h + k = -i.$$

Thus, we do not have to determine the index for the third horizontal axis. If we use only three indices, we can use a dot to designate the fourth index, as follows:

$$(1\bar{1}\cdot 0).$$

For the directions, we can use either the three-index notation or a four-index notation. However, with four indices, the $h + k = -i$ rule will not apply in general, and one has to use special "tricks" to make the vector coordinates obey the rule.

If the indices in the three-index notation are $h'$, $k'$, and $\ell'$, the four index notation of directions can be obtained by the following simple equations:

$$h = \frac{1}{3}(2h' - k')$$
$$k = \frac{1}{3}(2k' - h')$$
$$i = -\frac{1}{3}(h' + k')$$
$$\ell = \ell'.$$

It can be easily verified that $h + k = -i$. Thus, the student is equipped to express the directions in the four-index notation.

### 1.3.2 Metals

The metallic bond can be visualized, in a very simplified way, as an array of positive ions held together by a "glue" consisting of electrons. These positive ions, which repel each other, are attracted to the "glue," which is known as an electron gas. Ionic and covalent bonding, on the other hand, can be visualized as direct attractions between atoms. Hence, these types of bonding, especially covalent bonding, are strongly directional and determine the number of neighbors that one atom will have, as well as their positions.

The bonding and the sizes of the atoms in turn determine the type of structure a material has. Often, the structure is very complicated for ionic and covalent bonding. On the other hand, the directionality of bonding is not very important for metals, and atoms pack into the simplest and most compact forms; indeed, they can be visualized as spheres. The structures favored by metals are the face-centered cubic (FCC), body-centered cubic (BCC), and hexagonal close packed (HCP) structures. In the periodic table, of the 81 elements to the left of the Zindl line, 53 have either the FCC or the HCP structure, and 21 have the BCC structure; the remaining 8 have other structures. The Zindl line defines the boundary of the elements with metallic character in the table. Some of them have several structures, depending on temperature. Perhaps the most complex of the metals is plutonium, which undergoes six polymorphic transformations.

Transmission electron microscopy can reveal the positions of the individual atoms of a metal, as shown in Figure 1.11 for molybdenum. The regular atomic array along a [001] plane can be seen. Molybdenum has a BCC structure.

## Example 1.1

Write the indices for the directions and planes marked in Figure E1.1.

**Figure E1.1**

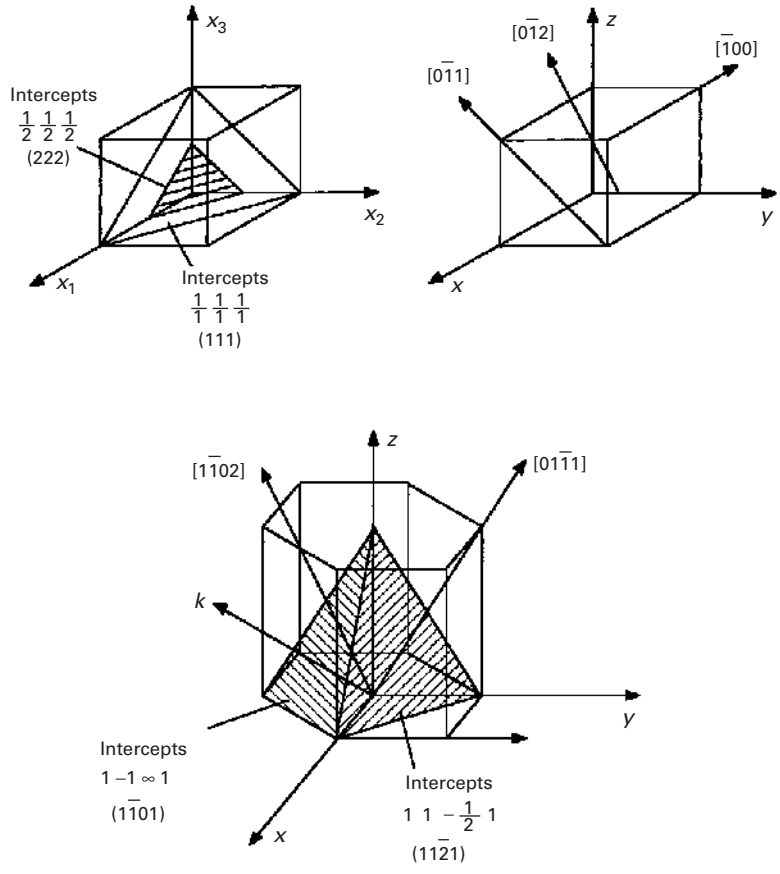


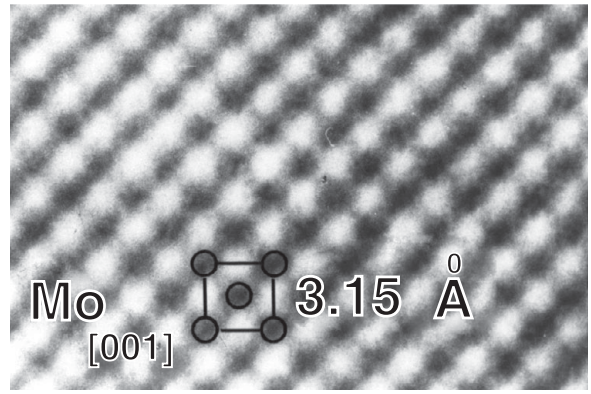


**Figure 1.11** Transmission electron micrograph at atomic resolution of (001) plane in molybdenum showing body-centered cubic arrangement of atoms.
(Figure courtesy of R. Gronsky.)

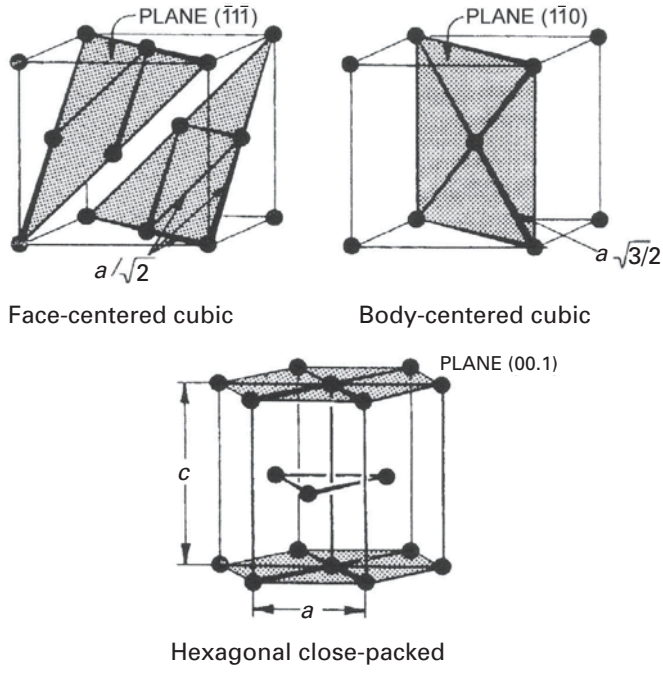


**Figure 1.12** Most closely packed planes in (a) FCC; (b) BCC; (c) HCP.

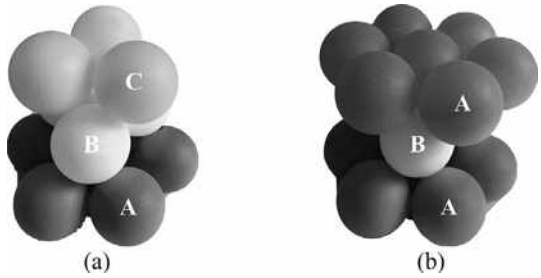


**Figure 1.13** Ball models showing stacking sequence in FCC and HCP structures. (© Sheron Tavares.)
(a) Layers of most closely packed atoms corresponding to (111) in FCC, forming ABC sequence.
(b) Corresponding layers for basal planes in HCP structure, forming ABAB sequence.

Figure 1.12 shows the three main metallic structures. The positions of the atoms are marked by small spheres and the atomic planes by dark sections. The small spheres do not correspond to the scaled-up size of the atoms, which would almost completely fill the available space, touching each other. For the FCC and HCP structures, the coordination number (the number of nearest neighbors of an atom) is 12; for the BCC structure, it is 8.

The ABC sequence of the FCC structure is also revealed in the three-layer model of Figure 1.13(a). The bottom layer (A) is formed of close-packed atoms. The middle layer (B) is also formed of close-packed atoms, whereas the top layer sits on top of three atoms of the B layer. The position of this atom does not correspond to a position in the A or B layers and therefore forms a separate layer C. This is the signature of the FCC structure. On the other hand, the HCP structure can be represented by the ABAB sequence. The third layer is in exact correspondence to the first layer (Figure 1.13(b)).

The planes with the densest packing are $(1\bar{1}1)$, $(1\bar{1}0)$, and (001) for the FCC, BCC, and HCP structures, respectively. These planes have an important effect on the directionality of deformation of the metal, as will be seen in Chapters 4 and 6. The distances between the nearest neighbors are also indicated in the figure. The reader should try to calculate them as an exercise. These distances are $a\sqrt{2}$, $(a\sqrt{3}/2)$, and $a$ for the FCC, BCC, and HCP structures, respectively.

The similarity between the FCC and HCP structures is much greater than might be expected from looking at the unit cells. Planes (111) for FCC and (001) for HCP have the same packing, as may be seen in Figure 1.13. The packing of a second plane similar to, and on top of, the first one (called *A*) can be made in two different ways; Figure 1.13 (a) indicates these two planes by the letters *B* and *C*. Hence, either alternative can be used. A third plane, when placed on top of plane *B*, would have two options: *A* or *C*. If the second plane is *C*, the third plane can be either *A* or *B*. If only the first and second layers are considered, the FCC and HCP structures are identical. If the position of the third layer coincides with that of the first (the *ABA* or *ACA* sequence), we have the HCP structure. Since this packing has to be systematically maintained in the lattice, one would have *ABABAB*... or *ACACAC*... If the third plane does not coincide with the first, we have one of two alternatives *ABC* or *ACB*. Since this sequence has to be systematically maintained, we have *ABCABCABC*... or *ACBACBACB*... This stacking sequence corresponds to the FCC structure. We thus conclude that the only difference between the FCC and HCP structures (the latter with a theoretical *c*/*a* ratio of 1.633) is the stacking sequence of the most densely packed planes. The difference resides in the next neighbors and in the greater symmetry of the FCC structure.

In addition to the metallic elements, intermediate phases and intermetallic compounds exist in great numbers, with a variety of structures. For instance, the beta phase in the copper-manganese-tin (Cu-Mn-Sn) system exhibits a special ordering for the composition $Cu_2MnSn$. The unit cell (BCC) is shown in Figure 1.14. However, the ordering of the Cu, Mn, and Sn atoms creates a super lattice composed of four BCC cells. This super lattice is FCC; hence, the unit cell for the ordered phase is FCC, whereas that for the disordered phase has a BCC unit cell. This ordering has important effects on the functional and structural (mechanical) properties and is discussed in Chapter 11. Although they are composed of three

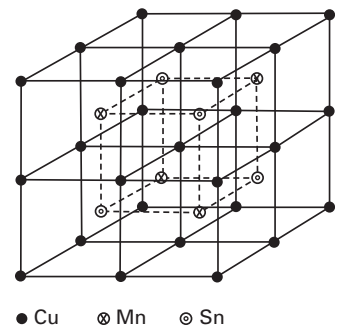


**Figure 1.14** $\beta$-ordered phase in Heusler alloys ($Cu_2MnSn$). (Reprinted from Observations on the ferromagnetic [beta] phase of the Cu-Mn-Sn system, *J. Appl. Cryst.* (1973). 6, 39–41, https://doi.org/10.1107/S0021889873008022, Copyright © International Union of Crystallography (1973).)

**Table 1.4 Some Important Intermetallic Compounds and Their Structures**

| Compound | Melting Point (°C) | Type of Structure |
|---|---|---|
| $Ni_3Al$ | 1,390 | $Ll_2$ (ordered FCC) |
| $Ti_3Al$ | 1,600 | $DO_{19}$ (ordered hexagonal) |
| TiAl | 1,460 | $Ll_0$ (ordered tetragonal) |
| Ni-Ti | 1,310 | CsCl |
| $Cu_3Au$ | 1,640 | $B_2$ (ordered BCC) |
| FeAl | 1,250–1,400 | $B_2$ (ordered BCC) |
| NiAl | 1,380–1,638 | $B_2$ (ordered BCC) |
| $MoSi_2$ | 2,025 | $C11_b$ (tetragonal) |
| $Al_3Ti$ | 1,300 | $DO_{22}$ (tetragonal) |
| $Nb_3Sn$ | 2,134 | $A1_5$ |
| $Nb_5Si_3$ | 2,500 | (tetragonal) |

nonferromagnetic elements, they are ferromagnetic. Heusler alloys were a scientific curiosity until 1984. It was discovered that they have spintronic properties and may lead the way to more efficient computers where information is stored by the spin of the electron. So, Moore's law, which states that the number of transistors in a certain size of computers doubles every two years, can continue for a few more years.

Table 1.4 lists some of the most important intermetallic compounds and their structures. Intermetallic compounds have a bonding that is somewhat intermediate between metallic and ionic/covalent bonding, and have properties that are most desirable for high-temperature applications. Nickel and titanium aluminides are candidates for high-temperature applications in jet turbines and aircraft applications.

## Example 1.2

Determine the ideal $c/a$ ratio for the hexagonal structure.

***Solution:*** The atoms in the basal $A$ plane form a closely packed array, as do the atoms in the $B$ plane going through the mid plane. If we take three atoms in the basal plane, with an atom in the $B$ plane resting among them, we have constructed a tetrahedron. The sides of the tetrahedron are $2r = a$, where $r$ is the atomic radius. The height of this tetrahedron is $c/2$, since the distance between planes is $c$. Hence, the problem is now reduced to finding the height, $c/2$, of a regular tetrahedron. In Figure E1.2, we have

$$DF = \frac{C}{2}$$

$$AB = AC = BC = AD = DB = DC = a.$$

## Example 1.2 (cont.)

**Figure E1.2**

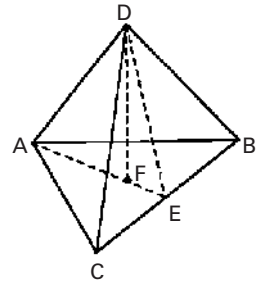


For triangle AEC,

$$AE^2 + EC^2 = AC^2$$

$$AE = \sqrt{a^2 - \frac{a^2}{4}} = \frac{a}{2}\sqrt{3.}$$

For triangle DFE,

$$EF^2 + DF^2 = DE^2.$$

But

$$EF = \frac{1}{3}AE = \frac{a}{6}\sqrt{3,}$$

$$DE = AE = \frac{a}{2}\sqrt{3,}$$

$$DF = \left(\frac{3a^2}{4} - \frac{3a^2}{36}\right)^{1/2},$$

$$\frac{c}{2} = a\left(\frac{2}{3}\right)^{1/2},$$

$$\frac{c}{a} = 2\left(\frac{2}{3}\right)^{1/2}.$$

Thus,

$$\frac{c}{a} = 1.633.$$

## Example 1.3

If the copper atoms have a radius of 0.128 nm, determine the density in FCC and BCC structures.

**(i)** In FCC structures, $4r = \sqrt{2}a_0$

$$a_0 = \frac{4}{\sqrt{2}}r = \frac{4}{\sqrt{2}} \times 0.128 \text{ nm}$$

$$a_0 = 0.362 \text{ nm}.$$

## Example 1.3 (cont.)

There are four atoms per unit cell in FCC. Atomic mass (or weight) of copper is 63.54 g $(g.mol)^{-1}$. So, the density of copper ($\rho$) in FCC structures is

$$\rho = \frac{63.54 \times 4}{\left(0.362 \times 10^{-7}\right)^3 \times \left(6.022 \times 10^{23}\right)} = 8.89 \text{ g cm}^{-3}.$$

↑
Avogadro's Number

**(ii)** In BCC structures, $4r = \sqrt{3}a_0$

$$a_0 = \frac{4}{\sqrt{3}}r = \frac{4}{\sqrt{3}} \times 0.128 \text{ nm}$$
$$a_0 = 0.296 \text{ nm}.$$

There are two atoms per unit cell in BCC structures.

$$\rho = \frac{63.54 \times 2}{\left(0.296 \times 10^{-7}\right)^3 \times \left(6.02 \times 10^{23}\right)} = 8.14 \text{ g cm}^{-3}.$$

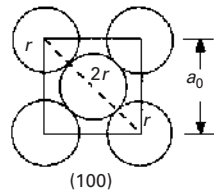


**Figure E1.3** The stable form of Cu is FCC. Only under unique conditions, such as Cu precipitates in iron, is the BCC form stable (because of the constraints of surrounding material).

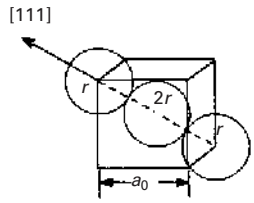


### 1.3.3 Ceramics

The name ceramic comes from the Greek *keramos* (pottery). The production of pottery made of clay dates from 6500 BCE. The production of silicate glass in Egypt dates from 1500 BCE The main ingredient of pottery is a hydrous aluminum silicate that becomes plastic when mixed, in fine powder form, with water. Thus, the early utilization of ceramics included both crystalline and glassy materials. Portland cement is also a silicate ceramic; by far the largest tonnage production of ceramics today – glasses, clay products (brick, etc.), cement – are silicate-based.

However, there have been dramatic changes since the 1970s and a wide range of new ceramics has been developed. These new ceramics are finding applications in

computer memories (due to their unique magnetic applications), in nuclear power stations ($UO_2$ fuel rods), in rocket nose cones and throats, in submarine sonar units (piezoelectric barium titanate), in jet engines (as coatings on metal turbine blades) as electronic packaging components ($Al_2O_3$, SiC substrates), as electrooptical devices (lithium niobate, capable of transforming optical into electrical information and vice versa), as optically transparent materials (ruby and yttrium garnet in lasers, optical fibers), as cutting tools (boron nitride, synthetic diamond, tungsten carbide), as refractories, as military armor ($Al_2O_3$, SiC, $B_4C$), and in a variety of structural applications.

The structure of ceramics is dependent on the character of the bond (ionic, covalent, or partly metallic), on the sizes of the atoms, and on the processing method. We will first discuss the crystalline ceramics.

## Example 1.4

Sketch the 12 members of the <110> family for a cubic crystal. Indicate the four {111} planes. You may use several sketches.

**Figure E1.4**

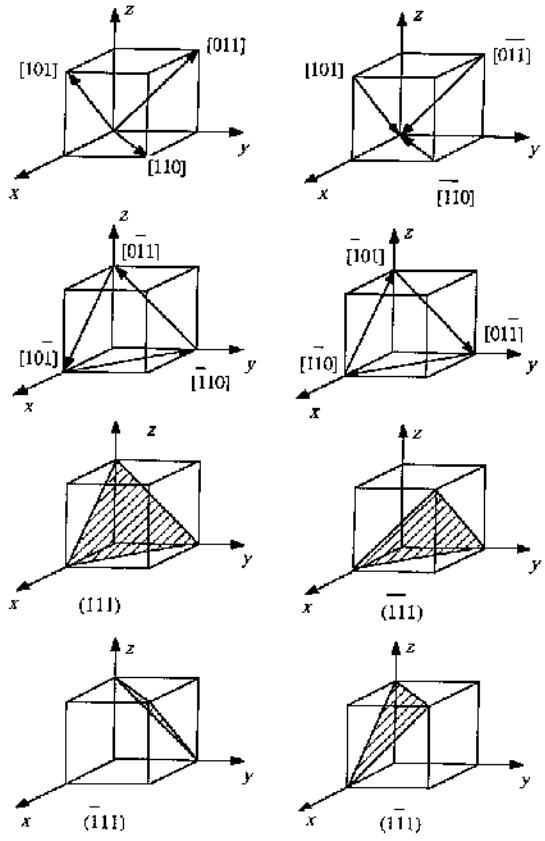

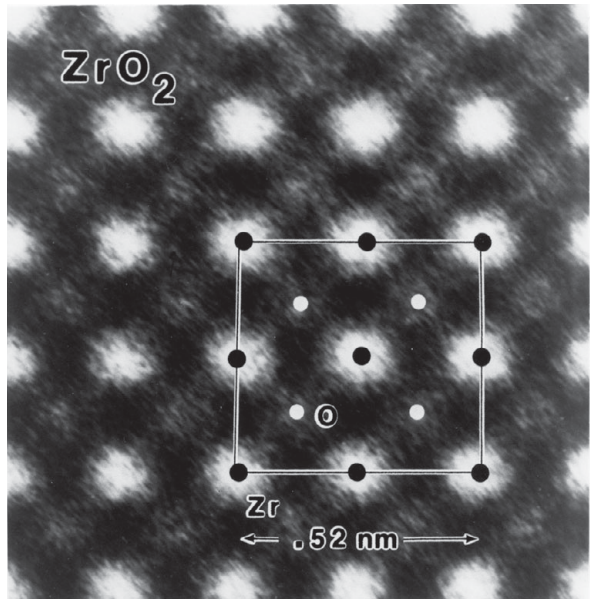


**Figure 1.15** Transmission electron micrograph of $ZrO_2$ at high resolution, showing individual Zr atoms and oxygen sites.
(Figure courtesy of R. Gronsky.)

Transmission electron microscopy has reached the point of development where we can actually image individual atoms, and Figure 1.15 shows a beautiful picture of the zirconium atoms in $ZrO_2$.The much lighter oxygen atoms cannot be seen but their positions are marked in the electron micrograph. By measuring the atomic distances along two orthogonal directions, one can see that the structure is not cubic, but tetragonal. The greater complexity of ceramics, in comparison to metallic structures, is evident from Figure 1.15. Atoms of different sizes have to be accommodated by a structure, and bonding (especially covalent) is highly directional. We will first establish the difference between ionic and covalent bonding.

The electronegativity value is a measure of an atom's ability to attract electrons. Compounds in which the atoms have a large difference in electronegativity are principally ionic, while compounds with the same electronegativity are covalent. In ionic bonding one atom loses electrons and is therefore positively charged (cation). The atom that receives the electrons becomes negatively charged (anion). The bonding is provided by the attraction between positive and negative charges, compensated by the repulsion between charges of equal signs. In covalent bonding the electrons are shared between the neighboring atoms. The quintessential example of covalent bonding is diamond. It has four electrons in the outer shell, which combine with four neighboring carbon atoms, forming a tridimensional regular diamond structure, which is a complex cubic structure. Figure 1.16 shows the diamond structure. The bond angles are fixed and equal to 70° 32'. The covalent bond is the strongest bond, and diamond has the highest hardness of all natural materials. There are synthetic materials that have an even higher hardness, such as graphene and some nanocrystalline structures. Another material that has covalent bonding is SiC.

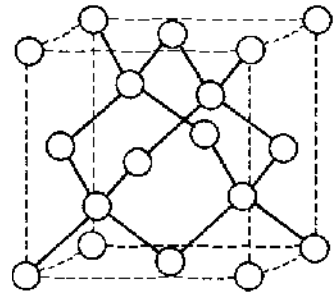

**Figure 1.16** Crystal structure of diamond.

## Example 1.5

(a) Calculate the packing factor of the diamond cubic structure. (b) Calculate the density of diamond. The atomic weight of carbon is 12 g $mol^{-3}$, and the lattice parameter of diamond is 0.357 nm at 300 K.

**Figure E1.5**

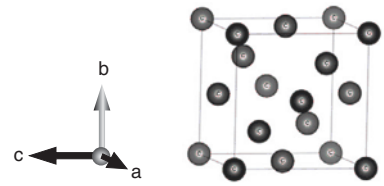


### *Solution:*

**(a)** 8 atoms/cell (4 from FCC + 4 at 1/4, 1/4, 1/4 from FCC atoms).
Nearest neighbor distance:

$$2r = \frac{a\sqrt{3}}{4}$$

$$r = \frac{a\sqrt{3}}{8}.$$

$$\text{Atomic packing factor (APF)} = \frac{\frac{4\pi}{3}\left(\frac{a\sqrt{3}}{8}\right)^{3*} 8}{a^3} = \frac{\pi\sqrt{3}}{16} = 0.34.$$

**(b)**

$$\rho\left(\text{g cm}^{-3}\right) = \frac{m}{V} = \frac{\sum_{i=1}^{N} N_i A_i\left(\text{g mol}^{-1}\right)}{(a\ \text{nm})^{3*}\left(\frac{1}{1*10^7\,\text{nm}}\right)^{3*}\left(6.022*10^{23}\text{g mol}^{-1}\right)}$$

$$\rho = \frac{(8\ \text{atoms})*\left(12\ \text{g mol}^{-1}\right)}{(0.357\ \text{nm})^{3*}\left(\frac{1\ \text{cm}}{1*10^7\,\text{nm}}\right)^{3*}\left(6.022*10^{23}\ \text{g mol}^{-1}\right)} = 3.503\ \text{g cm}^{-3}.$$

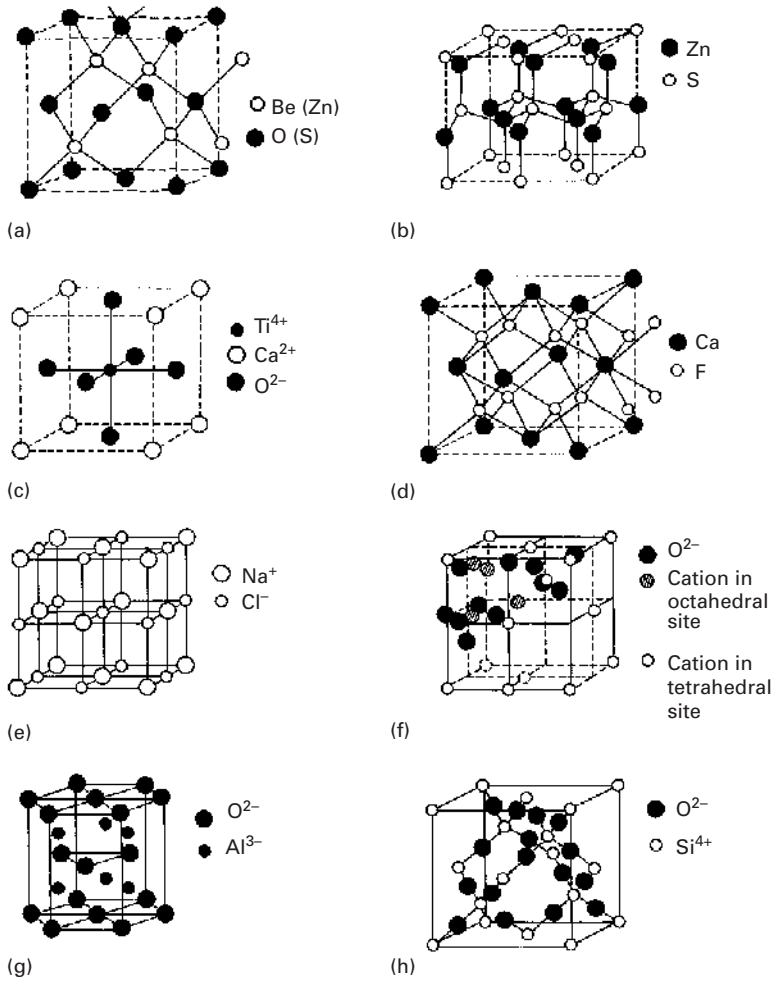


**Figure 1.17** Most common structures for ceramics. (a) Zinc blende (ZnS, BeO, SiC). (b) Wurtzite (ZnS, ZnO, SiC, BN). (c) Perovskite ($CoTiO_3$, $BaTiO_3$, $YCu_2Ba_3O_{7-x}$). (d) Fluorite ($ThO_2$, $UO_2$, $CeO_2$, $ZrO_2$, $PuO_2$). (e) NaCl (KCl, LiF, KBr, MgO, CaO, VO, MnO, NiO). (f) Spinel ($FeAl_2O_4$, $ZnAl_2O_4$, $MoAl_2O_4$). (g) Corundum ($Al_2O_3$, $Fe_2O_3$, $Cr_2O_3$, $Ti_2O_3$, $V_2O_3$). (h) Crystobalite ($SiO_2$-quartz). The CsCl stucture, which has one $Cs^+$ surrounded by four $Cl^-$ ions in cube edges, is not shown.

As the difference of electronegativity is increased, the bonding character changes from pure covalent to covalent-ionic, to purely ionic. Ionic crystals have a structure determined largely by opposite charge surrounding an ion. These structures are therefore established by the maximum packing density of ions. Compounds of metals with oxygen (MgO, $Al_2O_3$, $ZrO_2$, etc.) and with group VII elements (NaCl, LiF, etc.) are largely ionic. The most common structures of ionic crystals are presented in Figure 1.17. Evidently, there are more complex structures in ceramics than in metals because the combinations possible between the elements are so vast.

Ceramics also exist in the glassy state. Silica in this state has the unique optical property of being transparent to light, which is used technologically to great advantage. The building blocks of silica in crystalline and amorphous forms are the silica tetrahedra. Silicon bonds to four oxygen atoms, forming a tetrahedron. The oxygen atoms bond to just two silicon atoms. Numerous structures are possible, with different arrangements of the tetrahedra. Pure silica crystallizes into quartz, crystobalite, and tridymite. Because of these bonding requirements, the structure of silica is fairly open and, consequently, gives the mineral a low density. Quartz has a density of 2.65 g $cm^{-3}$,

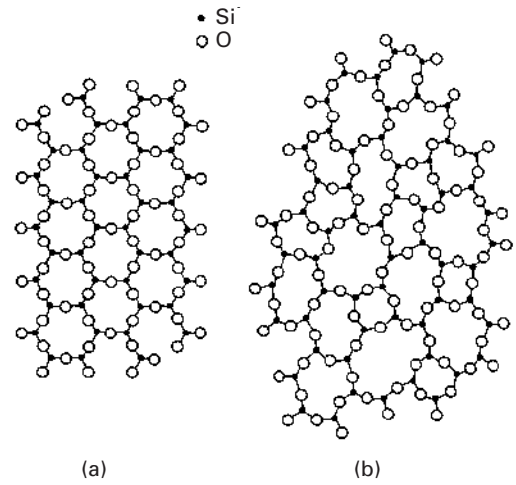


**Figure 1.18** Schematic two-dimensional representation of (a) ordered crystalline and (b) random-network glassy forms of silica.

compared with 3.59 g cm$^{-3}$ and 3.92 g cm$^{-3}$, for MgO and $A1_2O_3$, respectively. The structure of crystobalite (Figure 1.17(h)) shows clearly that each Si atom (open circle) is surrounded by four oxygen atoms (filled circles), while each oxygen atom binds two Si atoms. A complex cubic structure results. However, an amorphous structure in silica is more common when the mineral is cooled from the liquid state. Condensation of vapor on a cold substrate is another method by means of which thin, glassy films are made. One can also obtain glassy materials by electrodeposition, as well as by chemical reaction. Chapter 3 describes glassy metals in greater detail. Figure 1.18 provides a schematic representation of silica in its crystalline and glassy forms in an idealized two-dimensional pattern. The glassy state lacks long-range ordering; the three-dimensional silica tetrahedra arrays lack both symmetry and periodicity.

## Example 1.6

Determine the C–C–C–bonding angle in polyethylene.

***Solution:*** The easiest manner to visualize the bonding angle is to assume that one C atom is in the center of a cube and that it is connected to four other C atoms at the edges of the cube (see Figure E1.6 1) Suppose all angles are equal to $\alpha$.

**Figure E1.6**

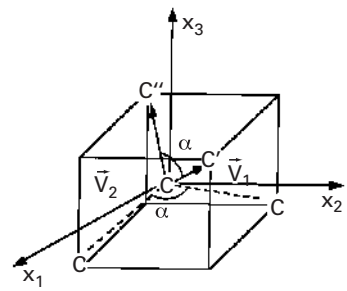

## Example 1.6 (cont.)

The problem is best solved vectorially. We set the origin of the axes at the center of the carbon atom and have two vectors connecting it to neighboring C atoms.

The angle between two vectors is (see Chapter 6 or any calculus text)

$$\cos\alpha = \frac{\frac{1}{2}\left(-\frac{1}{2}\right) + \frac{1}{2}\left(-\frac{1}{2}\right) + \frac{1}{2}\cdot\frac{1}{2}}{\sqrt{\frac{1}{4}+\frac{1}{4}+\frac{1}{4}}\cdot\sqrt{\frac{1}{4}+\frac{1}{4}+\frac{1}{4}}} = -\frac{1}{3}.$$

So

$$\alpha = 109.47^{\circ}.$$

(*Note*: When we have double bonds, the angle is changed.)

### 1.3.4 Glasses

As described earlier, glasses are characterized by a structure in which no long-range ordering exists. There can be short-range ordering, as indicated in the individual tetrahedral arrays of $SiO_4^{-4}$ in Figure 1.18, which shows both the crystalline and glassy forms of silica. Over distances of several atomic spacings, the ordering disappears, leading to the glassy state. It is possible to have glassy ceramics, glassy metals, and glassy polymers.

The structure of glass has been successfully described by the *Zachariasen* model. The *Bernal* model is also a successful one. It consists of drawing lines connecting the centers of adjacent atoms and forming polyhedra. These polyhedra represent the glassy structure of glass. Glassy structures represent a less efficient packing of atoms or molecules than the equivalent crystalline structures. This is very easily understood with the "suitcase" analog. We all know that by throwing clothes randomly into a suitcase, the end result is often a major job of sitting on the suitcase to close it. Neat packing of the same clothes occupies less volume. The same happens in glasses. If we plot the inverse of the density (called *specific volume*) versus temperature, we obtain the plot shown in Figure 1.19. Contraction occurs as the temperature is lowered. If the

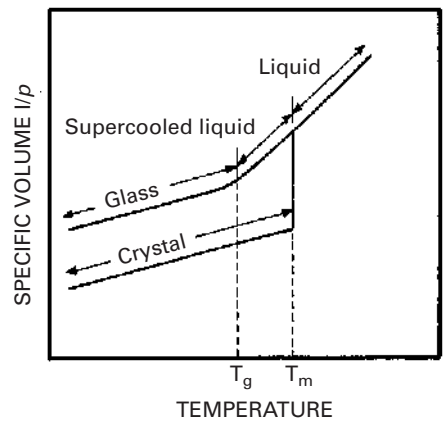


**Figure 1.19** Specific volume (inverse of density) as a function of temperature for glassy and crystalline forms of a material.

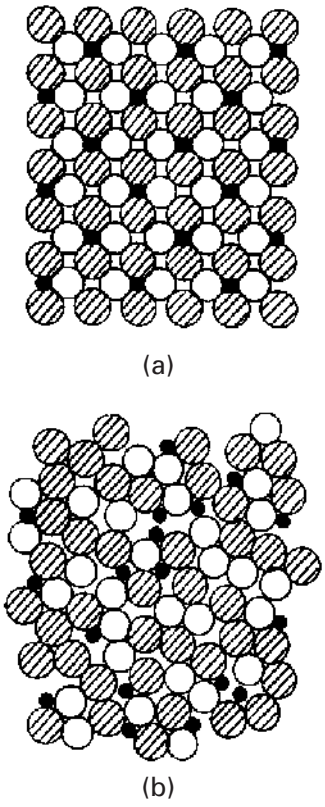


**Figure 1.20** Atomic arrangements in crystalline and glassy metals. (a) Crystalline metal section. (b) Glassy metal section. (Figure courtesy of L. E. Murr.)

material crystallizes, there is a discontinuity in the specific volume at the melting temperature $T_m$. If insufficient time is allowed for crystallization, the material becomes a super-cooled liquid, and contraction follows the liquid line. At a temperature $T_g$, called the *glass transition temperature*, the super-cooled liquid is essentially solid, with very high viscosity. It is then called a glass. This difference in specific volume between the two forms is often referred to as *excess volume*.

In ceramics, reasonably low cooling rates can produce glassy structures. The regular arrangement of the silica tetrahedra in Figure 1.18(a) requires a significant amount of time. The same is true for polymeric chains, which need to organize themselves into regular crystalline arrangements. For metals, this is more difficult. Only under extreme conditions it is possible to obtain solid metals in a noncrystalline structure. Figure 1.20 shows a crystalline and a glassy alloy with the same composition. The liquid state is frozen in, and the structure resembles that of glasses. It is possible to arrive at these special structures by cooling the alloy at such a rate that virtually no reorganization of the atoms into periodic arrays can take place. The required cooling rate is usually on the order of $10^6$ to $10^8$ K $s^{-1}$. It is also possible to arrive at the glassy state by means of solid-state processing (very heavy deformation and reaction) and from the vapor.

The original technique for obtaining metallic glasses was called splat cooling and was pioneered by Duwez and students.[2] An alloy in which the atomic sizes are quite dissimilar, such as Fe-B, is ideal for retaining the "glassy" state upon cooling. This technique consisted of propelling a drop of liquid metal with a high velocity against a heat-conducting surface such as copper. The interest in these alloys was mainly academic at the time. However, the unusual magnetic properties and high strength exhibited by the alloys triggered worldwide interest, and subsequent research has resulted in thousands of papers. The splat-cooling technique has been refined to the point where 0.07 to 0.12 mm-thick wires can be ejected from an orifice. Production rates as high as 1,800 m $min^{-1}$ can be obtained. Sheets and ribbons can be manufactured by the same technique. An alternative technique consists of vapor deposition on a substrate (sputtering). This seems a most promising approach, and samples with a thickness of several millimeters have been successfully produced.

The cooling rates required for the formation of the traditional amorphous metals are in the range of 100–1000 K $s^{-1}$. Thus, a splat-cooling technique must be used and only very thin layers can be produced. However, research at Tohoku University and the California Institute of Technology (Caltech) has yielded alloys based on La, Mg, Zr, Pd, Fe, Cu, and Ti, with critical cooling rates of 1–100 K $s^{-1}$, comparable to oxide glasses. Thus, thicker parts (several cm) can be fabricated. These alloys are known as Bulk Metallic Glasses (BMGs). The Caltech alloys are known as Vitreloy (41.2% Zr, 13.8% Ti, 12.5% Cu, 10% Ni, and 22.5% Be) and have strengths of 1700 MPa. Comparatively, $Ti_6Al_4V$ has a strength of 830 MPa. The bulk metallic glasses (BMGs) have been extensively studied due to their promising application and research value. Due to their glass transition temperature ($T_g$), they exhibit excellent properties such as high strength at low temperatures and appreciable ductility at high temperatures. Examples of applications are golf clubs, which have extraordinarily high coefficient of restitution.

## 1.3.5 Polymers

From a microstructural point of view, polymers are much more complex than metals and ceramics. On the other hand, they are cheap and easily processed. Polymers have lower strengths and moduli and lower temperature use limits than do metals or ceramics. Because of their predominantly covalent bonding, polymers are generally poor conductors of heat and electricity. Polymers are generally more resistant to chemicals than are metals, but prolonged exposure to ultraviolet light and some solvents can cause degradation of a polymer's properties.

### Chemical Structure

Polymers are giant chain-like molecules (hence, the name *macromolecules*), with covalently bonded atoms forming the backbone of the chain. Polymerization is the

[2] W. Klement, R. H. Willens, and P. Duwez, *Nature*, 187 (1960) 869.

process of joining together many monomers, the basic building blocks of polymers, to form the chains. For example, the ethyl alcohol monomer ($C_2H_3OH$) has the chemical structure:

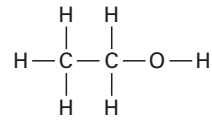

This yields the polymer polyethylene.

The monomer vinyl chloride has the chemical formula $C_2H_3Cl$, which, on polymerization, becomes polyvinyl chloride (PVC). The chemical structure of polyvinyl chloride is represented by:

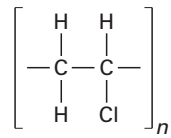

where $n$ is the degree of polymerization. There are numerous polymers with widely different properties: polyvinyl chloride (PVC), polystyrene (PS), poly(propylene) PP, polyether ether ketone (PEEK), etc.

## Types of Polymers

The difference in the behavior of polymers stems from their molecular structure and shape, molecular size and weight, and amount and type of bond (covalent or van der Waals). The different chain configurations are shown in Figure 1.21. A *linear polymer* consists of a long chain of atoms with attached side groups (Figure 1.21(a)). Examples include polyethylene, polyvinyl chloride, and polymethyl methacrylate. Note the coiling and bending of the chain. *Branched polymers* have branches attached to the main chain (Figure 1.21(b)). Branching can occur with linear, cross-linked, or any other types of polymers. A *crossed-linked* polymer has molecules of one chain bonded with those of another (Figure 1.21 (c)). Cross-linking of molecular chains results in a three-dimensional network. It is easy to see that cross-linking makes sliding of molecules past one another difficult, resulting in strong and rigid polymers. *Ladder polymers* have two linear polymers linked in a regular manner (Figure 1.21(d)). Not unexpectedly, ladder polymers are more rigid than linear polymers.

Yet another classification of polymers is based on the type of the repeating unit (see Figure 1.22). When we have one type of repeating unit, for example, *A*, forming the polymer chain, we call it a *homo polymer. Copolymers*, on the other hand, are polymer chains having two different monomers. If the two different monomers, *A* and *B*, are distributed randomly along the chain, then we have a *regular*, or *random, copolymer*. If, however, a long sequence of one monomer *A* is followed by a long sequence of another monomer *B*, we have a *block copolymer*. If we have a chain of one type of monomer *A* and branches of another type *B*, then we have a *graft copolymer*.

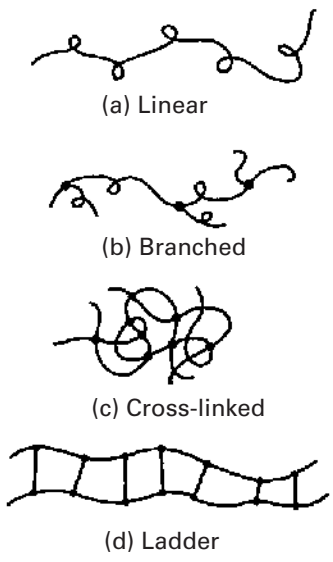


**Figure 1.21** Different types of molecular chain configurations.

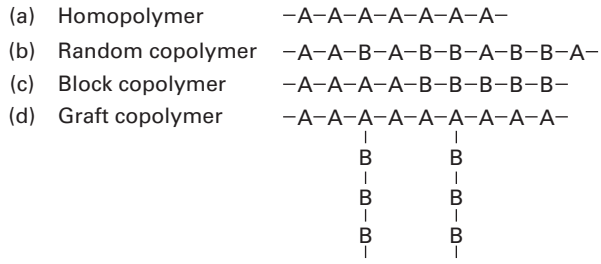


**Figure 1.22** (a) Homopolymer: one type of repeating unit. (b) Regular copolymer: two monomers, *A* and *B*, distributed randomly. (c) Block copolymer; a sequence of monomer B. (d) Graft copolymer; monomer *A* forms the main chain, while monomer *B* form the branched chain.

*Tacticity* has to do with the order of placement of side groups on a main chain. It can provide variety in polymers. Consider a polymeric backbone chain having side groups. For example, a methyl group ($CH_3$) can be attached to every second carbon atom in the polypropylene chain. By means of certain catalysts, it is possible to place the methyl groups all on one side of the chain or alternately on both sides, or to randomly distribute them in the chain. Figure 1.23 shows tacticity in polypropylene. When we have all the side groups on one side of the main chain, we have an *isotactic* polymer. If the side groups alternate from one side to another, we have a *syndiotactic* polymer. When the side groups are attached to the main chain in a random fashion, we get an *atactic* polymer.

## Thermosetting Polymers and Thermoplastics

Based on their behavior upon heating, polymers can be divided into two broad categories:

**(i)** thermosetting polymers,
**(ii)** thermoplastics.

**Figure 1.23** Tacticity, or the order of placement of side groups.

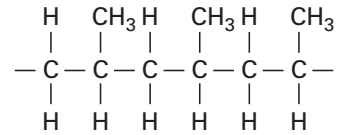

Isotactic polypropylene

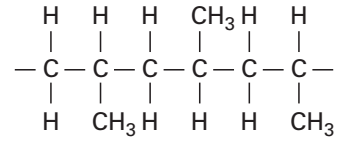

Syndiotactic polypropylene

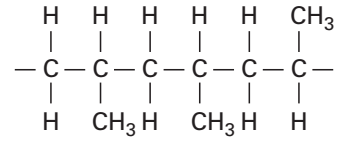

Atactic polypropylene

When the molecules in a polymer are cross-linked in the form of a network, they do not soften on heating. We call these cross-linked polymers *thermosetting* polymers. Thermosetting polymers decompose upon heating. As mentioned earlier, cross-linking makes sliding of molecules past one another difficult, which produces a strong and rigid polymer. A typical example is rubber cross-linked with sulfur, i.e., vulcanized rubber. Vulcanized rubber has 10 times the strength of natural rubber. Common examples of thermosetting polymers include phenolic, polyester, polyurethane, and silicone. Polymers that soften or melt upon heating are called *thermoplastics*. Suitable for liquid flow processing, they are mostly linear polymers, for example, low and high-density polyethylene and polymethyl methacrylate (PMMA).

Polymers can have an amorphous or partially crystalline structure. When the structure is amorphous, the molecular chains are arranged randomly, i.e., without any apparent order. Thermosetting polymers, such as epoxy, phenolic, and unsaturated polyester, have an amorphous structure. Semicrystalline polymers can be obtained by using special processing conditions. For example, by precipitating a polymer from an appropriate dilute solution, we can obtain small, plate-like crystalline lamellae, or crystallites. Such solution-grown polymer crystals are characteristically small. Figure 1.24 shows a transmission electron micrograph of a lamellar crystal of poly ($\varepsilon$-caprolactone). Note the formation of new layers of growth spirals around screw dislocations. The screw dislocations responsible for crystal growth are perpendicular to the plane of the micrograph. Polymeric crystals involve molecular chain packing, rather than the atomic packing characteristic of metals. Molecular

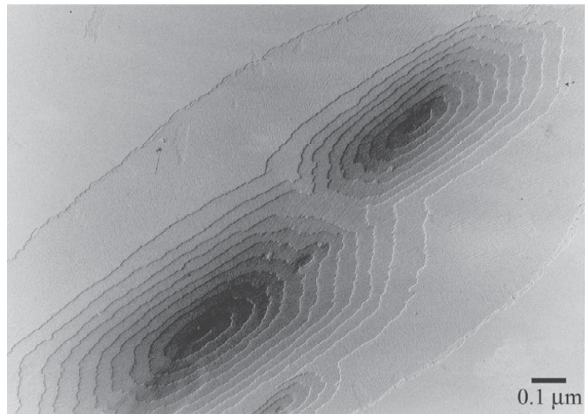


**Figure 1.24** Electron micrograph of a lamellar crystal showing growth spirals around screw dislocations.
(Figure courtesy of H. D. Keith.)

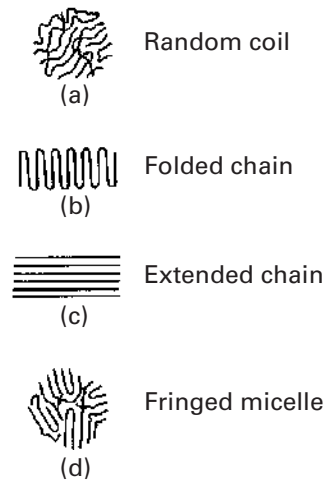


**Figure 1.25** Some important chain configurations.
(a) A flexible coiled chain structure. (b) A folding chain structure. (c) An extended and aligned chain structure.
(d) A fringed micelle chain structure.

chain packing requires a sufficiently stereographic regular chemical structure. Solution-grown polymeric crystals generally have a lamellar form, and the long molecular chains crystallize by folding back and forth in a regular manner. Lamellar polymeric crystals have straight segments of molecules oriented normal to the lamellar panes. Figure 1.25 depicts some important chain configurations in a schematic manner. The flexible, coiled structure is shown in Figure 1.25(a), while the chain-folding configuration that results in crystalline polymers is shown in Figure 1.25(b). Under certain circumstances, one can obtain an extended and aligned chain structure, shown in Figure 1.25(c). Such a structure, typically obtained in fibrous form, has very high strength and stiffness. A semi-crystalline configuration called a fringed micelle structure is shown in Figure 1.25(d). Almost all so-called semicrystalline polymers are, in reality, mixtures of crystalline and amorphous regions. Only by using very special techniques, such as solid-state polymerization, is it possible to prepare a 100% crystalline polymer. Polydiacetylene single crystals in the form of lozenges and fibers have been prepared by solid-state polymerization.

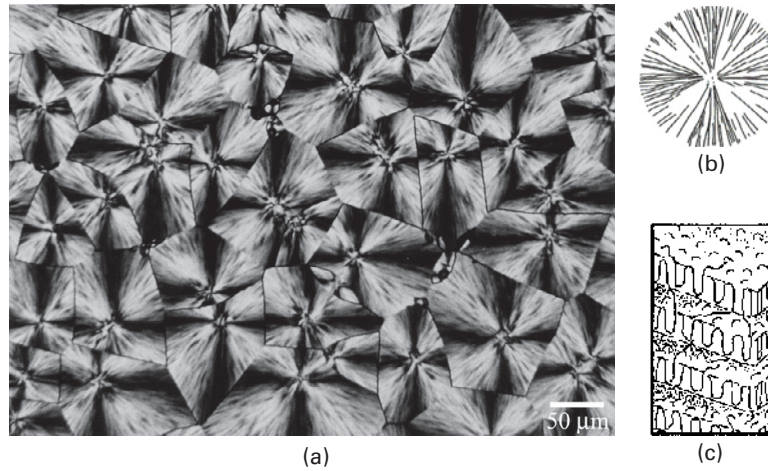


**Figure 1.26** Spherulitic structures.(a) A typical spherulitic structure in a melt-formed polymer film. (Figure courtesy of H. D. Keith.) (b) Schematic of a spherulite. Each spherulite consists of an assembly of radially arranged narrow crystalline lamellae. (c) Each lamella has tightly packed polymer chains folding back and forth. Amorphous regions fill the spaces between the crystalline lamellae.

Partially crystallized, or semicrystalline, polymers can also be obtained from melts. Generally, because of molecular chain entanglement, the melt-formed crystals are more irregular than those obtained from dilute solutions. A characteristic feature of melt-formed polymers is the formation of spherulites. When seen under cross-polarized light in an optical microscope, the classical spherulitic structure shows a Maltese cross pattern (see Figure 1.26(a). Figure 1.26(b) presents a schematic representation of a spherulite whose diameter can vary between a few tens to a few hundreds of micrometers. Spherulites can nucleate at a variety of points, as, for example, with dust or catalyst particles, in a quiescent melt and then grow as spheres. Their growth stops when the neighboring spherulites impinge upon each other. Superficially, the spherulites look like grains in a metal. There are, however, differences between the two. Each grain in a metal is a single crystal, whereas each spherulite in a polymer is an assembly of radially arranged, narrow crystalline lamellae. The fine-scale structure of these lamellae, consisting of tightly packed chains folding back and forth, is shown in Figure 1.26(c). Amorphous regions containing tangled masses of molecules fill the spaces between the crystalline lamellae.

## Degree of Crystallinity

The *degree of crystallinity* of a material can be defined as the fraction of the material that is fully crystalline. This is an important parameter for semicrystalline polymers. Depending on their degree of crystallinity, such polymers can show a range of densities, melting points, etc. It is worth repeating that a 100% crystalline polymer is very difficult to obtain in practice. The reason for the difficulty is the long chain

structure of polymers: some twisted and entangled segments of chains that get trapped between crystalline regions never undergo the conformational reorganization necessary to achieve a fully crystalline state. Molecular architecture also has an important bearing on a polymer's crystallization behavior. Linear molecules with small or no side groups crystallize easily. Branched chain molecules with bulky side groups do not crystallize as easily. For example, linear, high-density polyethylene can be crystallized to 90%, while branched polyethylene can be crystallized only to about 65%. Generally, the stiffness and strength of a polymer increase with the degree of crystallinity.

Like crystalline metals, crystalline polymers have imperfections. It is, however, not easy to analyze these defects, because the topological connectivity of polymer chains leads to large amounts and numerous types of disorder. Polymers are also very sensitive to damage by the electron beam in transmission electron microscopy (TEM), making it difficult to image them. Generally, polymer crystals are highly anisotropic. Because of covalent bonding along the backbone chain, polymeric crystals show low-symmetry structures, such as orthorhombic, monoclinic, or triclinic. Deformation processes such as slipping and twinning, as well as phase transformations that take place in monomeric crystalline solids, may also occur in polymeric crystals.

## Molecular Weight and Distribution

Molecular weight is a very important attribute of polymers, especially because it is not so important in the treatment of nonpolymeric materials. Many mechanical properties increase with molecular weight. In particular, resistance to deformation does so. Of course, concomitant with increasing molecular weight, the processing of polymers becomes more difficult.

The molecular weight of a polymer is given by the product of the molecular weight of the repeat unit (the ""mer") and the number of repeat units. The molecular weight of the ethylene repeat unit ($-CH_2-CH_2-$) is 28. We write the chemical formula: $H(-CH_2-CH_2-)_nH$. If $n$, the number of repeat units, is 10,000, the high-density polyethylene will have a molecular weight of 280,002. In almost all polymers, the chain lengths are not equal, but rather, there is a distribution of chain lengths. In addition, there may be more than one species of chain in the polymer. This makes for different parameters describing the molecular weight.

The number-averaged molecular weight ($M_n$) of a polymer is the total weight of all of the polymer's chains divided by the total number of chains:

$$M_n = \sum N_i, M_i / \sum N_i$$

where $N_i$ is the number of chains of molecular weight $M_i$.

The weight-averaged molecular weight ($M_w$) is the sum of the square of the total molecular weight divided by the total molecular weight. Thus,

$$M_w = \sum N_i M_i^2 / \sum M_i N_i.$$

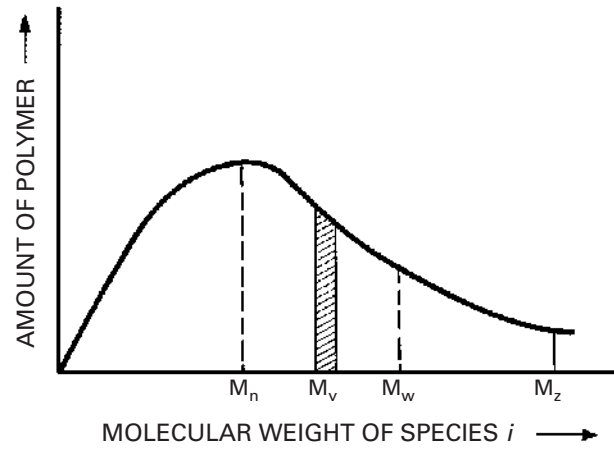


**Figure 1.27** A schematic molecular weight distribution curve. Various molecular weight parameters are indicated.

Two other molecular weight parameters are

$$M_z = \sum N_i M_i^3 / \sum N_i M_i^2$$

and

$$M_v = \left[ \sum N_i M_i^{(1+a)} / \sum N_i M_i \right]^{1/a},$$

where $a$ has a value between 0.5 and 0.8.

Typically, $M_n{:}M_w{:}M_z = 1{:}2{:}3$. Figure 1.27 shows a schematic molecular weight distribution curve with various molecular weight parameters indicated. Molecular weight distributions of the same polymer obtained from two different sources can be very different. Also, molecular weight distributions are not necessarily single peaked. For single-peaked distributions, $M_n$ is generally near the peak that is, the most probable molecular weight. The weight-averaged molecular weight, $M_w$, is always larger than $M_n$. The molecular weight characterization of a polymer is very important. The existence of a very high molecular-weight tail can make processing very difficult because of the enormous contribution of the tail to the melt viscosity of a polymer. The low end of the molecular-weight distribution, however, can be used as a plasticizer.

It is instructive to compare some monomers with low- and high-molecular-weight polymers. A very common monomer is a molecule of water, $H_2O$, with a molecular weight of 18. Benzene, on the other hand, is a low-molecular-weight organic solvent; its molecular weight is 78. By contrast, natural rubber has a molecular weight of about $10^4$, and polyethylene, a common synthetic polymer, can have a molecular weights greater than this. Polymers having such large molecular weights are sometimes called *high polymers*. Their molecular size is also very great.

It is interesting that the acetabular cup in total hip replacement, usually made of PE, has a performance that is highly dependent on its molecular weight. The life expectancy in high-molecular-weight polyethylene (HMWPE) is increased significantly for UHMWPE.

## Example 1.7

A polymer has three species of molecular weights: $3\times10^6$, $4\times10^6$, and $5\times10^6$. Compute its number-averaged molecular weight $M_n$ and weight-averaged molecular weight $M_w$.

***Solution:*** For the number-averaged molecular weight, we have

$$M_n = \frac{\sum N_i M_i}{\sum N_i} = \frac{3\times10^6 + 4\times10^6 + 5\times10^6}{3} = 4\times10^6.$$

The weight-averaged molecular weight is

$$M_w = \frac{\sum N_i M_i^2}{\sum N_i M_i} = \frac{\left(3\times10^6\right)^2 + \left(4\times10^6\right)^2 + \left(5\times10^6\right)^2}{3\times10^6 + 4\times10^6 + 5\times10^6} = \frac{50\times10^{12}}{12\times10^6} = 4.17\times10^6.$$

## Example 1.8

Estimate the molecular weight of polyvinyl chloride with degree of polymerization, $n$, equal to 800.

***Solution:*** The molecular weight of each "mer" of polyvinyl chloride ($C_2H_3Cl$) is

$$2(12) + 3(1) + 35.5 = 62.5.$$

For $n = 800$, the molecular weight is $800 \times 62.5 = 50{,}000$ g mol$^{-1}$.

## Example 1.9

Discuss how a polymer's density changes as crystallization proceeds from the melt.

***Answer:***

The density increases and the volume decreases as crystallization proceeds. This is because the molecular chains are more tightly packed in the crystal than in the molten or noncrystalline polymer. This phenomenon is, in fact, exploited in the so-called *density* method to determine the degree of crystallinity.

## Quasi Crystals

Quasi crystals represent a new state of solid matter. In a crystal, the unit cells are identical, and a single unit cell is repeated in a periodic manner to form the crystalline structure. Thus, the atomic arrangement in crystals has positional and orientational order. Orientational order is characterized by a rotational symmetry; that is, certain rotations leave the orientations of the unit cell unchanged. The theory of crystallography holds that crystals can have twofold, threefold, fourfold, or sixfold axes of rotational symmetry; a fivefold rotational symmetry is not allowed. A two-dimensional analogy of this is that one can tile a bathroom wall using a single shape of tile *if and only if* the tiles are rectangles (or squares), triangles, or hexagons, but not if the tiles are pentagons. One may obtain a glassy structure by rapidly cooling a vapor or liquid well below its melting point, until the disordered atomic arrangement characteristic of the vapor or liquid state gets frozen in. The atomic packing in the glassy state is dense but random. This can be likened to a mosaic formed by taking an infinite number of different shapes of tile and randomly joining them together. Clearly, the concept of a unit cell will not be valid in such a case. The atomic structure in the glassy state will have neither positional nor orientational order.

Quasi crystals are not perfectly periodic, but they do follow the rigorous theorems of crystallography. They can have any rotational symmetry axes which are prohibited in crystals. It is worth reminding the reader that a glassy structure shows an electron diffraction pattern consisting of diffuse rings for all orientations. A crystalline structure has an electron diffraction pattern that depends on the crystal symmetry.

Schectman et al. discovered that a rapidly solidified (melt-spun) aluminum-manganese alloy showed fivefold symmetry axis.[3] They observed a metastable phase that showed a sharp electron diffraction pattern with a perfect icosahedral symmetry. (Remember that sharp electron diffraction patterns are associated with the orderly atomic arrangement in crystals and icosahedral symmetry is forbidden in crystals.) At first, this was thought to be a paradox. However, some very careful and sophisticated electron microscopy work showed conclusively that it was indeed an icosahedral (20-fold) symmetry. Al-Mn alloys containing 18 to 25.3 wt% Mn examined by transmission electron microscopy showed the same anomalous diffraction. In particular, Al-25.3 wt% Mn alloy consisted almost entirely of one phase which has a composition close to $Al_6Mn$. The selected area diffraction pattern of $Al_6Mn$ showed a fivefold symmetry. This new kind of structure is neither amorphous nor crystalline; rather, the new phase in this alloy had a three-dimensional icosahedral symmetry.

Perhaps, it would be in order for us to digress a bit and explain this icosahedral symmetry. *Icosahedral* means 20 faces. An icosahedron has 20 triangular faces, 30 edges, and 12 vertices. Consider the two-dimensional case. As pointed out earlier,

[3] D. Schectman, I. A. Blech, D. Gratias, and J. W. Cahn, *Phys. Rev. Lett.*, 53 (1984) 1951.

one can tile a bathroom wall without leaving an open space (a *crack*) with hexagons. Three hexagons can be tightly packed without leaving a crack. Three pentagons, however, cannot be tightly packed. The reader may try this out. In three dimensions, four spheres pack tightly to form a tetrahedron; 20 tetrahedrons can, with small distortions, fit tightly into an icosahedron. Icosahedrons have fivefold symmetry (five triangular faces meet at each vertex) and they *cannot* fit together tightly, i.e., complete space filling is not possible with them. An icosahedron, therefore, cannot serve as a unit cell for a crystalline structure. Therefore, such structures are known as quasi crystals.

### 1.3.6 Liquid Crystals

A liquid crystal is a state of matter that shares some properties of liquids and crystals. Like all liquids, liquid crystals are fluids; however, unlike ordinary liquids, which are isotropic, liquid crystals can be anisotropic. Liquid crystals are also called *mesophases*. The liquid crystalline state exists in a specific temperature range, below which the solid crystalline state prevails and above which the isotropic liquid state prevails. That is, the liquid crystal has an order between that of a liquid and a crystalline solid. In a crystalline solid, the atoms, ions, or molecules are arranged in an orderly manner. This very regular three-dimensional order is best described in terms of a crystal lattice. Because of a different periodic arrangement in different directions, most crystals are anisotropic. Now consider a crystal lattice with rod-shaped molecules at the lattice points. In this case, we now have, in addition to a positional order, an orientational order. An analogy that is used to qualitatively describe the order in a liquid crystal is as follows. If a random pile of pencils is subjected to an external force, it will undergo an ordering process very much akin to that seen in liquid crystals. The pencils, long and rigid, tend to align themselves, with their long axes approximately parallel. By far the most important characteristic of liquid crystals is that their long molecules tend to organize according to certain patterns. The order of orientation is described by a directed line segment called the *director*. This order is the source of the rather large anisotropic effect in liquid crystals, a characteristic that is exploited in electrooptical displays or so-called liquid-crystal displays. Another important application of liquid crystals is the production of strong and stiff organic fibers such as aramid fiber, in which a rigid, rod-like molecular arrangement is provided by an appropriate polymer solution in the liquid crystalline state.[4] When a polymer manifests the liquid-crystalline order in a solution, we call it a *lyotropic* liquid crystal, and when the polymer shows the liquid crystalline state in the melt, it is called a *thermotropic* liquid crystal. The three types of order in the liquid crystalline state are nematic, smectic, and cholesteric, shown schematically in Figure 1.30. A nematic order is an approximately parallel array of polymer chains that remains disordered with regard to end groups or chain

[4] See K. K. Chawla, *Fibrous Materials* (Cambridge, U.K.: Cambridge University Press, 1998).

units; that is, there is no positional order along the molecular axis. Figure 1.30(a) shows this type of order, with the director vector *n* as indicated. In smectic order, we have one-dimensional, long-range positional order. Figure 1.30(b) shows smectic-A order, which has a layered structure with long-range order in the direction perpendicular to the layers. In this case, the director is perpendicular to the layer. Other more complex smectics are B, C, D, F, and G. The director in these may not be perpendicular to the layer, or there may exist some positional order as well. Cholesteric-type liquid crystals, shown in Figure 1.30(c), have nematic order with a superimposed spiral arrangement of nematic layers; that is, the director *n*, pointed along the molecular axis, has a helical twist.

## 1.3.7 Biological Materials and Biomaterials

### Biological Materials: Unique Characteristics

Seven unique aspects of biological materials distinguish them from their synthetic counterparts. It is through the understanding of each of them that we are advancing our knowledge with the goal of generating novel bioinspired materials and designs. These defining aspects comprise the Arzt heptahedron, presented in Figure 1.28. They are:

- *Evolution and environmental constraints*. Biological materials developed through a multimillion year process of evolution, driven by natural selection.

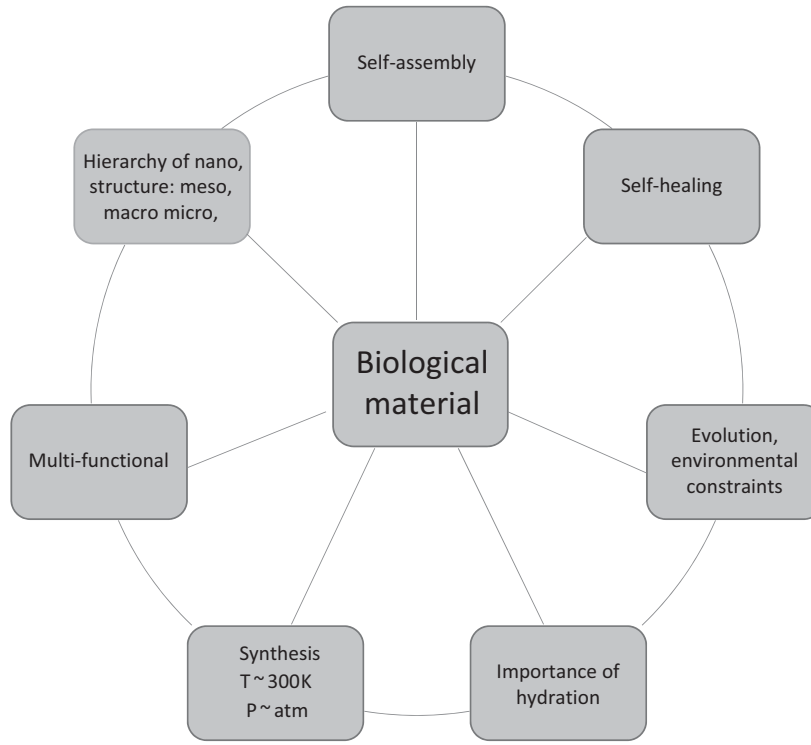


**Figure 1.28** Seven unique characteristics of biological materials: the Artz heptahedron.

- *Importance of hydration*. With notable exceptions, enamel and a few minerals, the level of hydration determines the mechanical properties.
- *Multifunctional.* Many tissues have more than one function, and this provides economy of space and mass.
- *Self-organization.* Nature uses a bottom-up approach to synthesize materials, whereas many of our processing methods are top-down. This bottom-up approach engenders self-organization and self-assembly.
- *Hierarchy of structure.* This is an aspect of utmost importance because it has direct relevance to mechanical properties. The structures at the nano, micro, meso, and ultra levels have different characteristics and work together synergistically.
- *Self-healing*. Many biological materials have a self-healing capability enabled by the cells and vascularity embedded in the extracellular matrix. Only a minute minority of synthetic materials have this capability.
- *Synthesis at ambient temperature and pressure.* Nature does not have at its disposal furnaces for high-temperature or autoclaves for high-pressure processing. Nor does she need them, since organisms exist mostly in a narrow range (–50 to +500 °C) of temperatures. There are isolated cases such as extremophiles and organisms living close to deep-sea vents, but they represent the exception. On the other hand, synthetic materials are designed to resist a variety of environments.

These unique characteristics render them intrinsically different from synthetic materials. Although there is a daunting variety of organisms (~8 million species), there are few recurring motifs in biological materials which have been identified.[5] This consists of seeking common structural designs in biological materials. Eight have been identified and are collectively named "structural design elements." They are amenable to analytical treatment and occur in different species through convergence and parallelism processes.

In spite of millions species of plants and animals on Earth, there is remarkable commonality in the structures observed among the diversity of biological materials. This is due to the fact that many different organisms have developed similar solutions to natural challenges. Our recent research has identified these common designs and named them *structural design elements*.

This new system new system of eight structural design elements enables a quantitative analytical treatment which can explain the mechanical properties, namely strength, stiffness, flexibility, fracture toughness, and energy absorption, of different biological materials for specific multifunctions (e.g. body support, joint movement, impact protection, mobility, flying). These structural design elements (visually displayed in Figure 1.29) are:

- *Fibrous* structures; offering high tensile strength when aligned in a single direction, with limited to nil compressive strength.

[5] M. A. Meyers, J. McKittrick, and P. Y. Chen, *Science*, 339 (2013) 773.

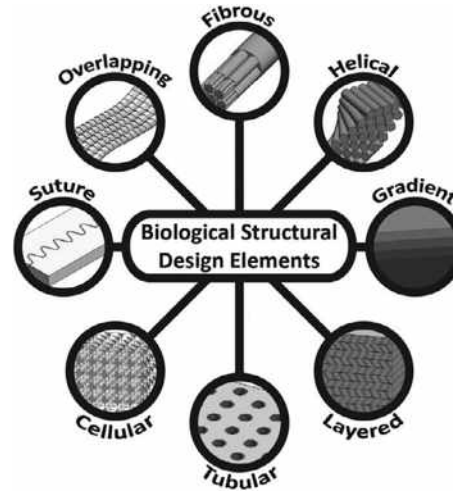


**Figure 1.29** The eight most common biological structural design elements.
(Reproduced from Marc A. Meyers, Joanna McKittrick, Michael M. Porter, et al, Structural Design Elements in Biological Materials: Application to Bioinspiration, *Advanced Materials*, Vol. 27, issue 37 (2015). With permission from John Wiley & Sons.)

- *Helical* structures; common to fibrous or composite materials, offering toughness in multiple directions and in-plane isotropy.
- *Gradient* structures; materials and interfaces that accommodate property mismatch (e.g. elastic modulus) through a gradual transition in order to avoid interfacial mismatch stress buildup, resulting in an increased toughness.
- *Layered* structures; complex composites that increase the toughness of (most commonly) brittle materials through the introduction of interfaces.
- *Tubular* structures; organized porosity that allows for energy absorption and crack deflection.
- *Cellular* structures; lightweight porous or foam architectures that provide directed stress distribution and energy absorption. These are often surrounded by dense layers to form sandwich structures.
- *Suture* structures; interfaces comprising wavy and interdigitating patterns that control the strength and flexibility.
- *Articulating* structures; featuring multiple plates or scutes that overlap to form flexible and often armored surfaces without interfaces.

As with all biological materials, these structural design elements are composed of biopolymers (e.g. collagen, chitin, keratin, cellulose) and biominerals (e.g. calcium carbonate, calcium phosphates, silica) that are hierarchically assembled from the nano to meso scales. However, the extraordinary mechanical properties observed in these natural materials are often a product of the intricate structural organization at higher spatial scales (micro, meso, and macro). As a result, in many cases organisms with different base materials will employ the same structure for the same purpose (e.g. tubules found in human dentin composed of hydroxyapatite/collagen and in a ram horns composed of keratin[6] can both absorb energy).

[6] S. E. Naleway, et al. *Adv Mat* 27.37 (2015) 5455–5476.

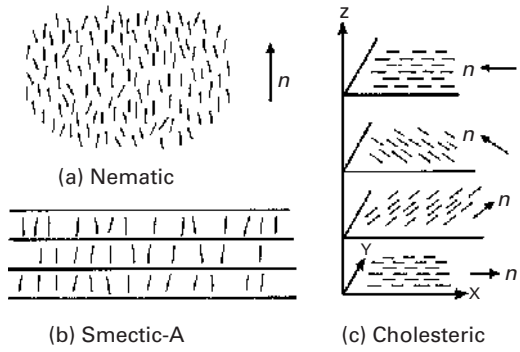


**Figure 1.30** Different types of order in the liquid crystalline state.

This is a new paradigm in the field of biological materials science: the structural design elements can serve as a toolbox for rationalizing the complex response of structural biological materials and for systematizing the development of bioinspired designs for structural applications. The ingenious manner by which these biocomposite structures are engineered is responsible for a mechanical response that is superior to that of synthetic materials

The mechanical properties of biological materials are, of course, of great importance, and the design of all living organisms is optimized for the use of these properties. Biological materials cover a very broad range of structures. The common feature is the hierarchical organization of the structure, so that failure at one level does not generate catastrophic fracture; the other levels in the hierarchy "take up" the load. Figure 1.31 demonstrates this fact. Figure 1.31(a) shows the response of the urether of three animals: guinea pig, dog, and rabbit. This muscle is a thick-walled cylindrical tube that has the ability to contract until the closure of the inner hole is complete. With a nonlinear elastic mechanical response, the urether is not unlike other soft tissues in that regard: its stiffness increases with loading, and the muscle becomes very stiff after a certain strain is reached. The unloading and loading responses are different, as shown in the figure, and this causes a hysteresis. Increases in length of 50% can be produced. Bone, on the other hand, is a material with drastically different properties: its strength and stiffness are much higher, and its maximum elongation is much lower. The structure of bones is quite complex, and they can be considered composite materials. Figure 1.31(b) illustrates the strength (in tension) of dry and wet bone. The maximum tensile strength is approximately 80 MPa, and Young's modulus is about 20 GPa.

The abalone shell and the shells of bivalve mollusks are often used as examples of a naturally occurring laminated composite material. These shells are composed of layers of calcium carbonate, glued together by a viscoplastic organic material. The calcium carbonate is hard and brittle. The effect of the viscoplastic glue is to provide a crack-deflection layer so that cracks have difficulty propagating through the composite. Figure 1.32 shows cracks that are deflected at each soft layer. The toughness of this laminated composite is vastly superior to that of a monolithic material, in which the crack would be able to propagate freely, without barriers.

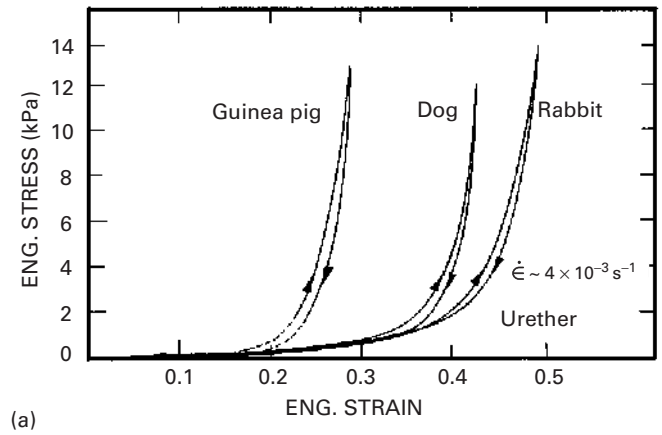


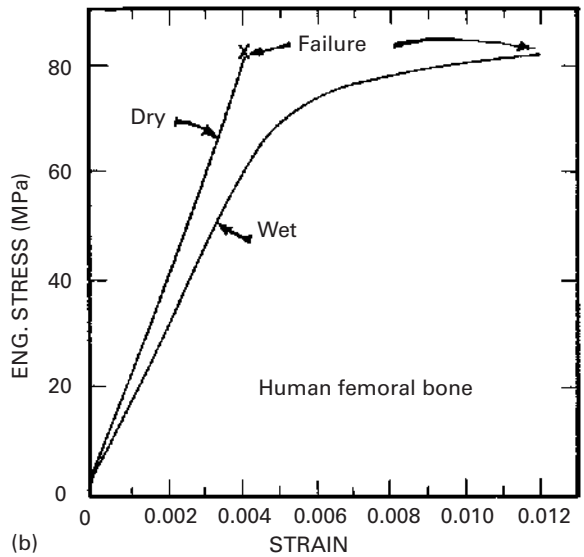


**Figure 1.31** Stress–strain curves for biological materials. (a) Urether. (Reproduced from the *American Journal of Physiology, Consolidated*, FC Yin, YC Fung, Vol. 221, 1971. © The American Physiological Society (APS).) (b) Human femur bone. (Reproduced from the *Journal of Applied Phisiology*, F. Gaynor Evans, Milton Lebow, Vol. 3, 1951, Pages 563–572. © The American Physiological Society (APS).)

The effect is shown at two scales: the mesoscale and the microscale. At the mesoscale, layers of calcium carbonate have a thickness of approximately 500 μm. At the microscale, each calcium carbonate layer is made up of small brick-shaped units (about $0.5 \times 7.5$ μm longitudinal section), glued together with the organic matter. The formation of this laminated composite results in a fracture toughness and strength (about 4 MPa $m^{-1/2}$ and approximately 150 MPa, respectively) that are much superior to those of the monolithic $CaCO_3$. The composite also exhibits a hierarchical structure; that is, the layers of $CaCO_3$ and organic glue exist at more

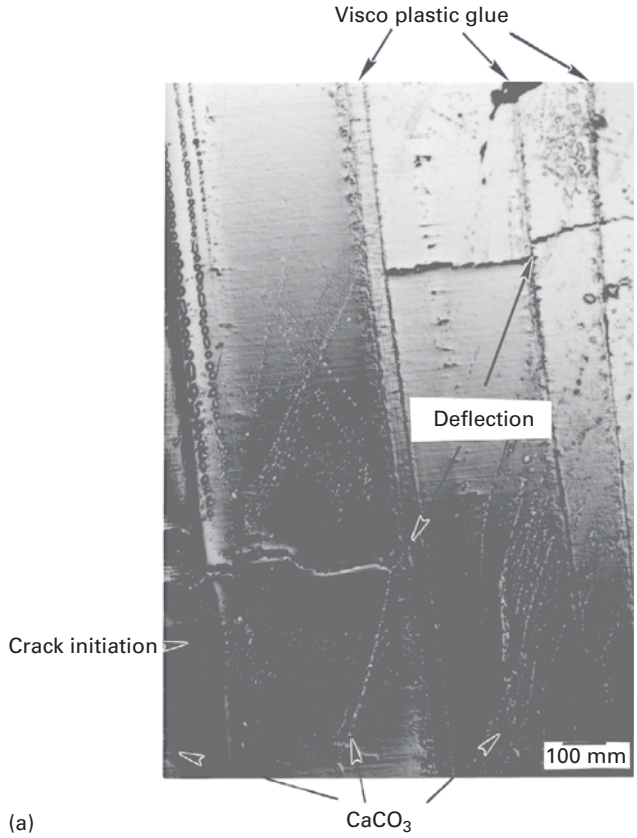


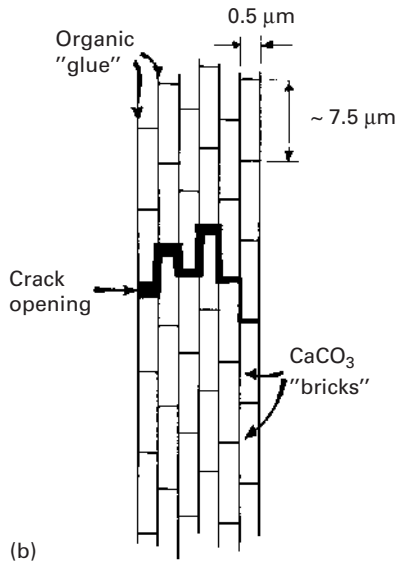


**Figure 1.32** (a) Cross-section of abalone shell showing how a crack, starting on the left, is deflected by a viscoplastic layer between calcium carbonate lamellae (mesoscale). (b) Schematic drawing showing the arrangement of calcium carbonate in nacre, forming a miniature "brick and mortar" structure (micro scale).

than one level (at the micro and meso levels). This naturally occurring composite has served as inspiration for the synthesis of $B_4C$-Al laminate composites, which exhibit superior fracture toughness.[7] In these synthetic composites, there is a 40% increase in both fracture toughness and strength over monolithic $B_4C$-Al cermets. (A cermet is a composite material consisting of ceramic (cer) and sintered metallic (met) materials.) *Biomimetics* is the field of materials science in which inspiration is sought from biological systems for the design of novel materials.

Another area of biomaterials in which mechanical properties have great importance is bioimplants. Complex interactions between the musculoskeletal system and these implants occur in applications where metals and ceramics are used as replacements for hips, knees, teeth, tendons, and ligaments. The matching of material and bone stiffness is important, as are the mechanisms of bonding tissue to these materials. The number of scientific and technological issues is immense, and the field of bioengineering focuses on these.

### 1.3.8 Porous and Cellular Materials

Wood, cancellous bone, Styrofoam, cork, and the insulating tiles of the Space Shuttle are examples of materials that are not compact; their structure has air as a major component. The great advantage of cellular structures is their low density. Techniques for making foam metals, ceramics, and polymers have been developed, and these cellular materials have found a wide range of applications, in insulation, in cushioning, as energy-absorbing elements, in sandwich panels for aircraft, as marine buoyancy components, in skis, and more.

The mechanical response of cellular materials is quite different from that of bulk materials. The elastic loading region is usually followed by a plateau that corresponds to the collapse of the pores, either by elastic, plastic buckling of the membranes or by their fracture. The third stage is an increase in the slope, corresponding to final densification. Figure 1.33(a) shows representative curves for polyethylene with different initial densities. The plateau occurs at different stress levels and extends to different strains for different initial densities. The bulk (fully dense) polyethylene is shown for comparison purposes. Cellular mullite, an alumina-silica solid solution, exhibits a plateau marked by numerous spikes, corresponding to the breakup of the individual cells (Figure 1.33(b)). Materials with initial densities as low as 5% of the bulk density are available as foams. Figure 1.33(c) shows a very important use of foams: sandwich structures, composed of end sheets of solid material in which a foam forms the core region, have numerous applications in the aerospace industry. The foam between the two panels makes them more rigid; this is accomplished without a significant increase in weight.

There are many biological examples of sandwich structures. The toucan beak (Figure 1.34(a)) is a structure with very low density (0.04 g $cm^{-3}$) that consists of an external layer of compact keratin. Figure 1.34(b) shows the keratin layer. It is

[7] M. Sarikaya, K. E. Gunnison, M. Yasrebi, and I. A. Aksay, *Mater. Soc. Symp. Proc.*, 174 (1990) 109.

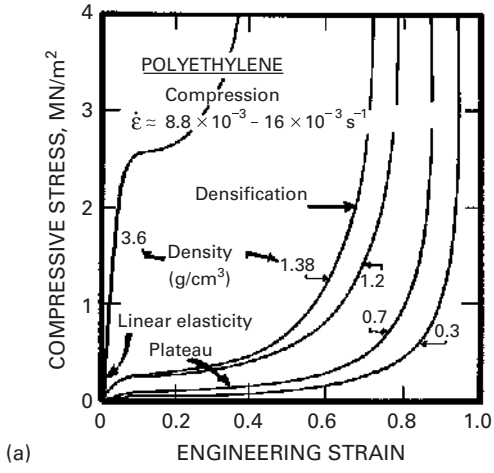


(a)

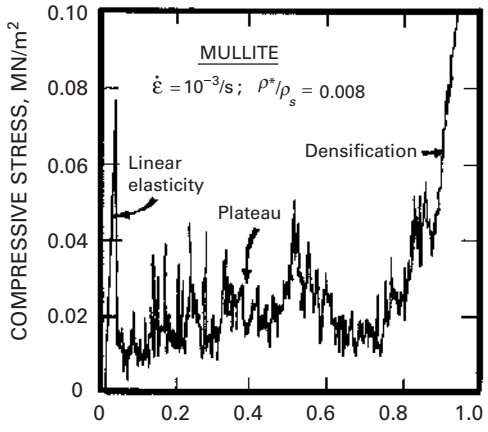


(b)

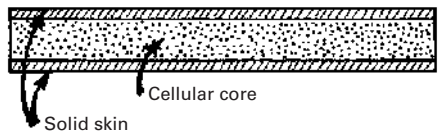


(c) Sandwich structure

**Figure 1.33** Compressive stress–strain curves for foams. (a) Polyethylene with different initial densities. (b) Mullite with relative density $\rho^*/\rho s = 0.08$. (Adapted from L. J. Gibson and M. F. Ashby, *Cellular Solids: Structure and Properties* (Oxford, U.K.: Pergamon Press, 1988), pp. 124, 125.) (c) Schematic of a sandwich structure. (Adapted from L.J. Gibson and M.F. Ashby, Cellular solids: Structure and properties. *Advances in Polymer Technology*, 9, issue 2 (1989). With permission from John Wiley & Sons.)

composed of superimposed scales. The extremely low density of the inside of the toucan beak is due to a foam-like (cellular) bone structure. The function of the cellular material is to provide structural rigidity to the system. In the absence of this foam, the external shell would buckle easily. Hence the toucan can fly without taking a nose dive.

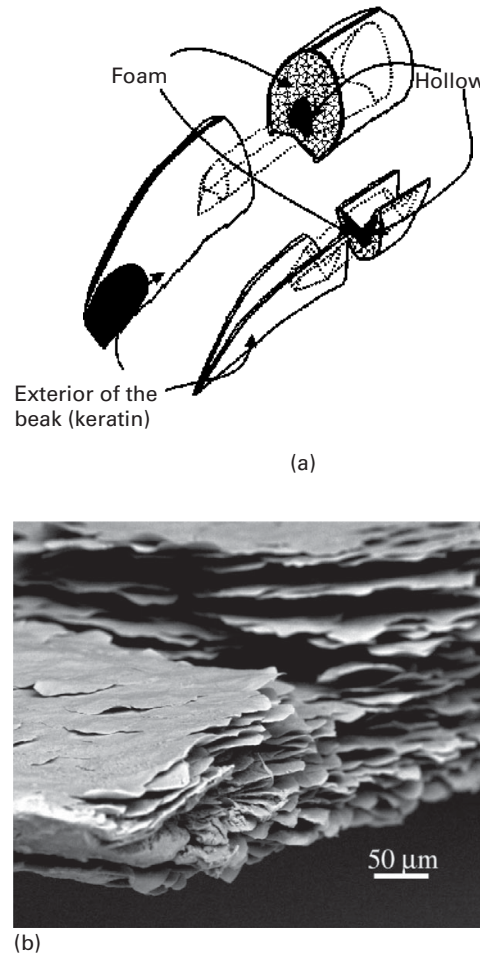


**Figure 1.34** (a) Toucan beak; (b) external shell made of keratin scales.
(Figure courtesy of Y. Seki.)

As examples of foams in synthetic and naturally occurring materials, we show in Figure 1.35 two structures. Figure 1.35(a) shows an open-celled aluminum foam. We sectioned the beak of the toucan and observed that the inside is composed of a foam with similar length scale Figure 1.34(b). Nature uses foams for the same purposes we do: to provide rigidity to structures with the addition of minimal weight. In Chapter 12 we give a detailed analysis of stresses involved in foams.

### 1.3.9 Nano- and Microstructures of Biological Materials

Biological materials are more complex than synthetic materials. They form complex arrays, hierarchical structures, and are often multifunctional, i.e., one material has more than one function. For example, bone has a structural function and serves as a producer of red blood cells (in marrow). We classify biological materials, from the mechanical property viewpoint, into soft and hard. Hard materials provide the skeleton, teeth, and nails in vertebrates and the exoskeleton in arthropods.

**Table 1.5 Occurrence of Different Biological Materials in the Body**

| Biological Material | Weight Percentage in Human Body |
|---|---|
| Proteins | 17 |
| Lipids | 15 |
| Carbohydrates | 1 |
| Minerals | 7 |
| DNA, RNA | 2 |
| Water | 58 |

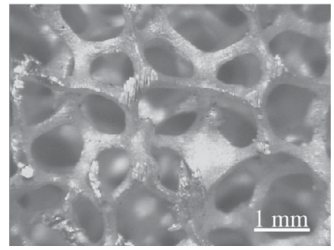


(a)

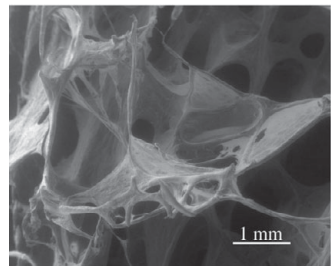


(b)

**Figure 1.35** Cellular materials: (a) synthetic aluminum foam. (Figure courtesy of K. S. Vecchio.) (b) Foam found in the inside of toucan beak. (Figure courtesy of M. S. Schneider.)

Soft biological materials build skin, muscle, internal organs, etc. Table 1.4 provides the distribution (on a weight percentage) of different constituents of the body.

Here are some examples of "hard" biological materials:

- Calcium phosphate (hydroxyapatite-$Ca_{10}(PO_4)_6(OH)_2$): teeth, bone.
- Chitin: nails.
- Keratin: bird beaks, horn, hair.
- Calcium carbonate (aragonite): mollusk shells, some reptile eggs (calcite): bird's eggs, crustaceans, mollusks.
- Amorphous silica ($SiO_2(H_2O)_n$): spicules in sponges.
- Iron oxide (magnetite – $Fe_3O_4$): teeth in chitons (a weird-looking marine worm), bacteria.

Of the above, iron oxide, calcium phosphate, silica, and iron oxide are minerals. Chitin is a polysaccharide and keratin is a protein.

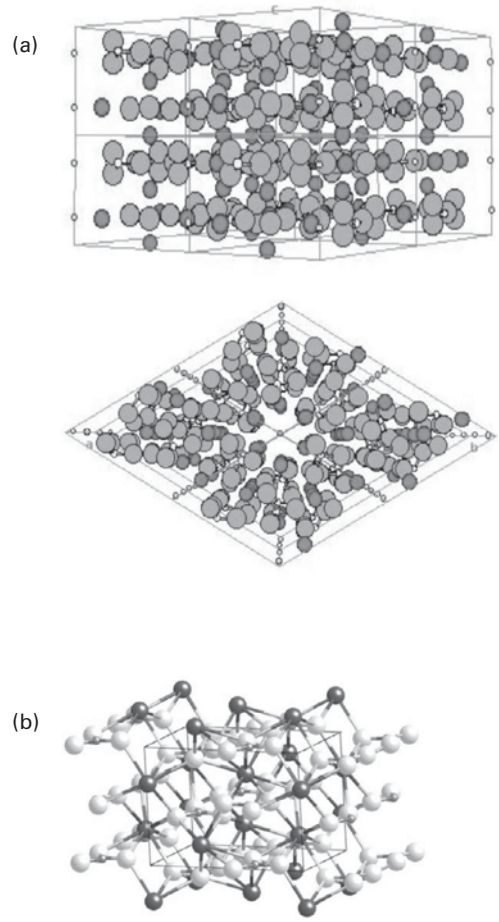


**Figure 1.36** Atomic structure of hydroxyapatite: (a) small white atoms (P), large gray atoms (O), black atoms (Ca). (b) Atomic structure of aragonite: large dark toms (Ca), small gray atoms (C), large white atoms (O).

Figure 1.36(a) shows the atomic arrangement of the calcium, phosphorus, and oxygen atoms in hydroxyapatite. The unit cell is quite complex and consists of four primitive hexagonal cells juxtaposed. We should remember that the hexagonal cell is composed of three primitive cells, brought together at their 120° angles ($3 \times 120 = 360$). In the case of the hydroxyapatite unit cell, there are four unit cells: two at the 60° angle and two at the 120° ($2 \times 60 + 2 \times 120 = 360$).

Figure 1.36(b) shows the aragonitic form of calcium carbonate. Aragonite has the orthorhombic structure. However, it is important to recognize that the minerals do not occur in isolation in living organisms. They are invariably intimately connected with organic materials, forming complex hierarchically structured composites. The resulting composite has mechanical properties that far surpass those of the monolithic minerals. Although we think of bone as a cellular mineral, it is actually composed of 60% collagen (on a volume percentage basis) and 30–40%

hydroxyapatite (on a weight basis). If the mineral is dissolved away, the entire collagen framework is retained.

The principal organic building blocks in living organisms are the proteins. The word comes from Greek (*Proteios*) which means "of first rank" and indeed proteins play a key role in most physiological processes. The soft tissues in the body are made of proteins. As seen above, they are also an important component of biominerals. In order to fully understand proteins, we have to start at the atomic/molecular level, as we did for polymers.

Actually, proteins can be conceived of as polymers with a greater level of complexity. We start with amino acids, which are compounds containing both an amine ($–NH_2$) and a carboxyl (–COOH) group. Most of them have the following structure, shown where R stands for a side chain (Table 1.6 shows some of them):

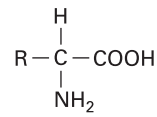

There are nine essential amino acids: histidine, isoleucine, leucine, lysine, methionine, phenylalanine, threonine, tryptophan, and valine. There are currently 20 amino acids found in proteins. In addition to these nine, we have the following: alanine, arginine, asparagine, aspartic acid, cysteine, glutamic acid, glutamine, glycine, proline, serine, and tyrosine.

In proteins, these amino acids combine themselves by forming links between the carboxyl group of one amino acid and the amino group of another. These linear chains, similar to polymer chains, are called polypeptide chains. The polypeptide chains acquire special configurations because of the formation of bonds (hydrogen, van der Waals, and covalent bonds) between amino acids on the same or different chains. The two most common configurations are the alpha helix and the beta sheet. Figure 1.37(a) shows how an alpha helix is formed. The NH and CO groups form hydrogen bonds between them in a regular pattern, and this creates the particular conformation of the chain that is of helical shape. One such bond is shown in Figure 1.37(a). In Figure 1.37(b) several hydrogen bonds are shown, causing the polypeptide chain to fold. The side chains stick out. The amino acid chain with the peptide group is shown in Figure 1.38(a). The amino acid chain with the peptide groups in a straight line is shown in Figure 1.38(b). Figure 1.38(c) shows the alpha helix conformation produced by the coiling of the amino acid chain. The peptide groups face each other and hydrogen bonds form. This keeps the helix stable.

Another common conformation of polypeptide chains is the beta sheet. In this conformation, separate chains are bonded. We can see that the radicals (large grey balls) of two adjacent chains stick out of the sheet plane on opposite sides. Successive chains can bond in such a fashion, creating pleated sheets.

We describe below the most important proteins: collagen, actin, myosin, elastin, resilin, abductin, keratin and silk, as well as cellulose and chitin, which are polysaccharides.

**Table 1.6 Eight amino acids found in proteins**

| Name | Chemical Structure |
|---|---|
| Alanine | 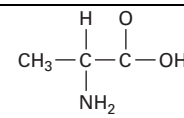 |
| Leucine | 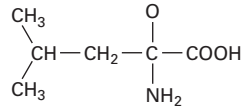 |
| Phenylalanine | 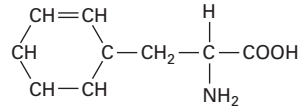 |
| Proline | 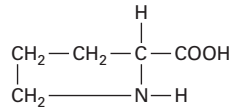 |
| Serine | 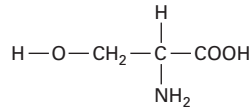 |
| Cysteine | 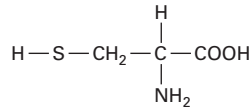 |
| Glutamate | 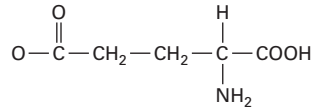 |
| Lysine | 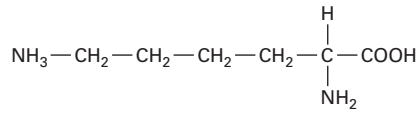 |

**Collagen** Collagen is a rather stiff and hard protein. It is a basic structural material for soft and hard bodies; it is present in different organs and tissues and provides structural integrity. Fung[8] compares it to steel, which is the principal load-carrying component in structures. In living organisms, collagen plays the same role: it is the main load-carrying component of blood vessels, tendons, bone, muscle, etc. In rats, 20% of the proteins are collagen. Humans are similar to rats in physiology and the same proportion should apply. Figure 1.39 shows the structure of collagen. It is a triple helix, each strand being made up of sequences of amino acids. Each strand is itself a left-handed helix with approximately 0.87 nm per turn. The triple helix has a right-handed twist with a period of 8.6 nm. The dots shown in a strand in

[8] Y. C. Fung, *Biomechanics: Mechanical Properties of Living Tissues* (Berlin: Springer, 1993).

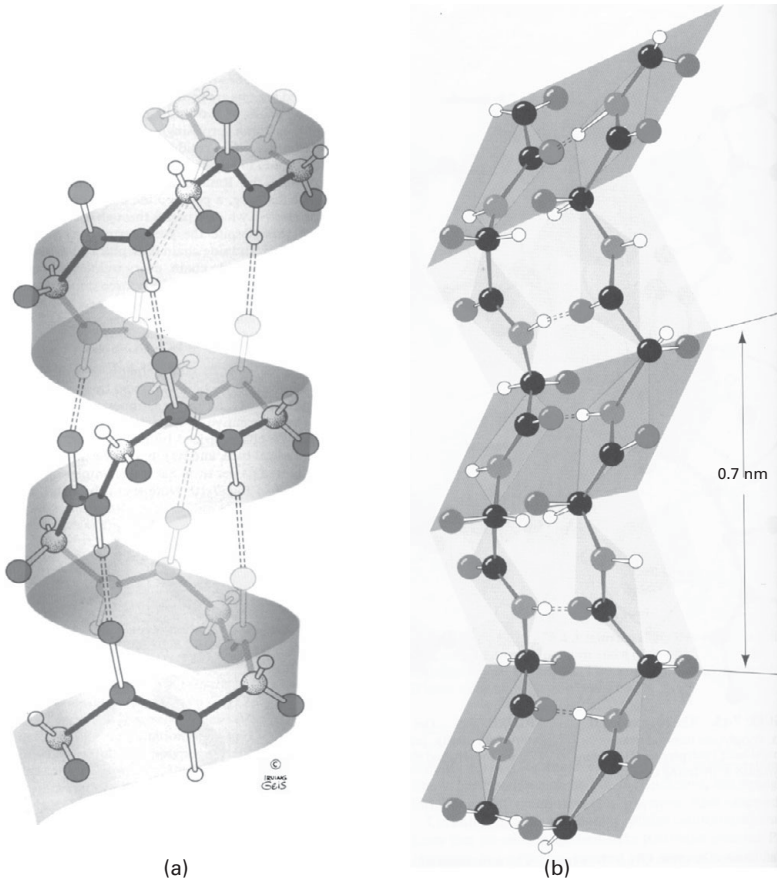


**Figure 1.37** (a) Structure of alpha helix; dotted double lines indicate hydrogen bonds. (b) Structure of beta sheet with two antiparallel polypeptide chains connected by hydrogen bonds (double-dotted lines).

Figure 1.39 represent glycine and different amino acids. There are over 10 types of collagen, called Type I, II, X, etc. Fiber-forming collagens organize themselves into fibrils.

Figure 1.40 shows the structural hierarchy of fibrillar collagen. In collagen formations, helical left-handed procollagen chains form a right-handed triple helix of roughly 300 nm in length. (b) Schematic representation of triple helix formed by three procollagen chains. Figure 1.40(c) shows the arrangement of triple helices into fibrils. Triple helices are arranged in a staggered manner, leading to a gap (0.54 d) and an overlap (0.46 d) region. The gap region has fewer triple helices across the section, and the overlap region has more. This gap and overlap has a periodicity, or d-period, of 67 nm, and is the cause of the visible banding in collagen fibrils. Figure 1.40 shows layers of collagen fibrils in a cross-section of skin. Figure 1.40(d) shows collagen fibrils of 100 nm diameter imaged by TEM. Fibrils clearly display the characteristic banding feature. Due to the viewing angle of the fibrils, d-period measurements decrease proportionally to the cosine of the viewing angle. A 90° viewing angle would lead to perfectly accurate measurements. (f) Atomic force microscopy (AFM) of hydrated collagen fibrils in an arapaima scale. 67nm d-period is measured.

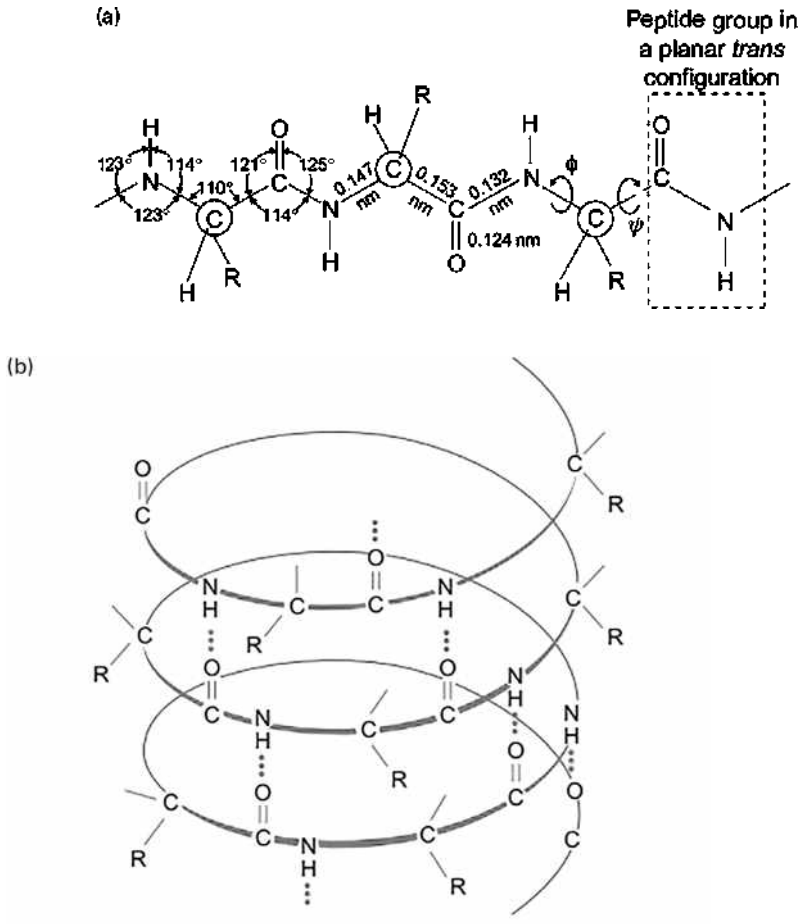


**Figure 1.38** (a) Geometry of a peptide (amide) linkage. (b) Hydrogen bonds in the alpha-helix. Coiling of an amino-acid chain brings peptide groups into juxtaposition so that the hydrogen bonds form and ensure the helical configuration. (Adapted from Journal of the Mechanical Behavior of Biomedical Materials, Vol 52, Vincent R. Sherman, Wen Yang, Marc A. Meyers, The materials science of collagen, 22–50, Copyright (2015), with permission from Elsevier.)

Fibrils, in turn, arrange themselves into fibers. Fibers are bundles of fibrils with diameters between 0.2 and 12 μm. In tendons, these fibers can be as long as the entire tendon. In tendons and ligaments, the collagen fibers form primarily one-dimensional networks. In skin, blood vessels, intestinal mucosa, and the female vaginal tract, the fibers organize themselves into more complex patterns leading to two- and three-dimensional networks.

The hierarchical organization of a tendon starts with tropocollagen (a form of collagen), and moves up, in length scale, to fascicles. There is a crimped, or wavy structure shown in the fascicles that has an important bearing on the mechanical properties. Figure 1.41 shows an idealized representation of a wavy fiber.

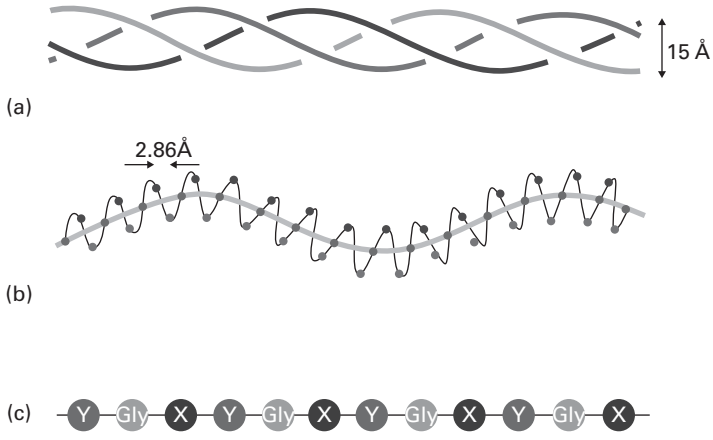


**Figure 1.39** Triple helix structure of collagen. (From Carlo Knupp, John M. Squire, Molecular Packing in Network-Forming Collagens, The Scientific World Journal, vol. 3, Article ID 157031, 20 pages, 2003. https://doi.org/10.1100/tsw.2003.40. Copyright © 2003 Carlo Knupp and John M. Squire.)

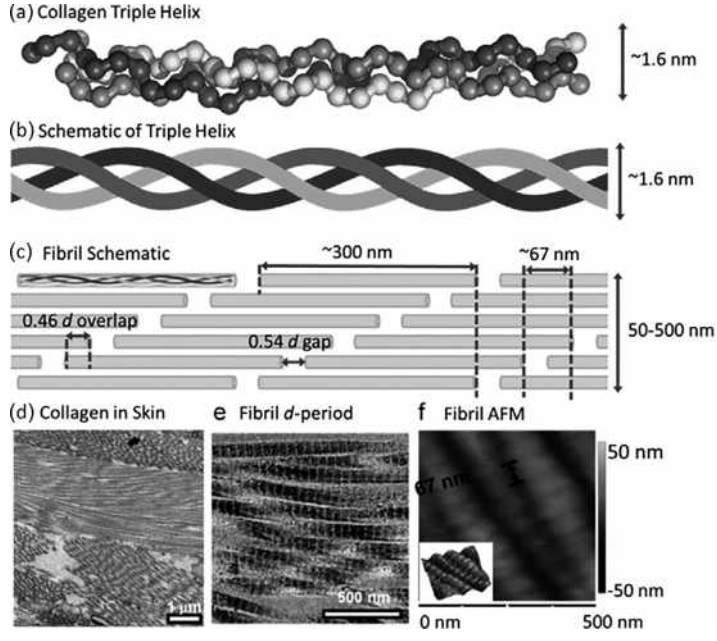


**Figure 1.40** Organization of collagen, starting with triple helix, and going to fibrils: (a) helical left-handed procollagen chains forming a right-handed triple helix of roughly 300 nm in length, (b) triple helix formed by three procollagen chains, (c) triple helices arranged in a staggered manner, leading to a gap (0.54 d) and an overlap (0.46 d) region; gap and overlap has a d-period, of 67 nm, (d) layers of collagen fibrils in a cross-section of skin; collagen fibrils of 100 nm diameter imaged by transmission electron microscopy, (f) atomic force microscopy of hydrated collagen fibrils in an arapaima scale. 67 nm d-period is measured.
(Reprinted from Journal of the Mechanical Behavior of Biomedical Materials, Vol 52, Vincent R. Sherman, Wen Yang, Marc A. Meyers, The materials science of collagen, 22–50, Copyright (2015), with permission from Elsevier.)

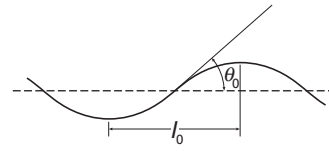


**Figure 1.41** Idealized configuration of a wavy collagen fiber.

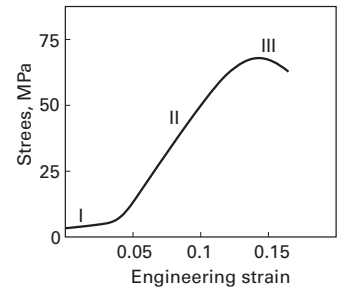


**Figure 1.42** Stress–strain curve of collagen with three characteristic stages.

Two parameters define it: the wavelength $2l_0$ and the angle $\theta_0$. Typical values for the Achilles tendon of a mature human are $l_0 = 20$–$50$ μm and $\theta_0 = 6$–$8°$. These bent collagen fibers stretch out in tension. When the load is removed, the waviness returns. When the tendon is stretched beyond the straightening of the waviness, damage starts to occur. Figure 1.42 shows a schematic stress–strain curve for tendons. The tendon was stretched until rupture. There are essentially three stages:

- Region I: toe part, in which the slope rises rapidly. This is the physiological range in which the tendon operates under normal conditions.
- Region II: linear part, with a constant slope.
- Region III: slope decreases with strain and leads to failure.

The elastic modulus of collagen is approximately 1 GPa and the maximum strain is in the 10–20% range. Cross-linking increases with age, and collagen becomes less flexible.

**Actin and Myosin** These are the principal proteins of muscles, leukocytes (white blood cells), and endothelial cells. Muscles contract and stretch through the controlled gliding/grabbing of the myosin with respect to the actin fibers. Figure 1.43(a) shows an actin fiber. It is composed of two polypeptides in a helical arrangement. Figure 1.43(b) shows the myosin protein. It has little heart-shaped "grapplers" called cross-bridges. The tips of the cross-bridges bind and unbind to the actin filaments. Figure 1.43(c) shows the myosin and actin filaments, and the cross-bridges at different positions. The cross-bridges are hinged to the myosin and can attach themselves to different positions along the actin filaments as the actin is displaced to the left. Thus, the muscles operate by a micro-telescoping action of these two proteins.

Figure 1.44 shows how the filaments organize themselves into myofibrils. Bundles of myofibrils form a muscle fiber. The $Z$ line represents the periodicity

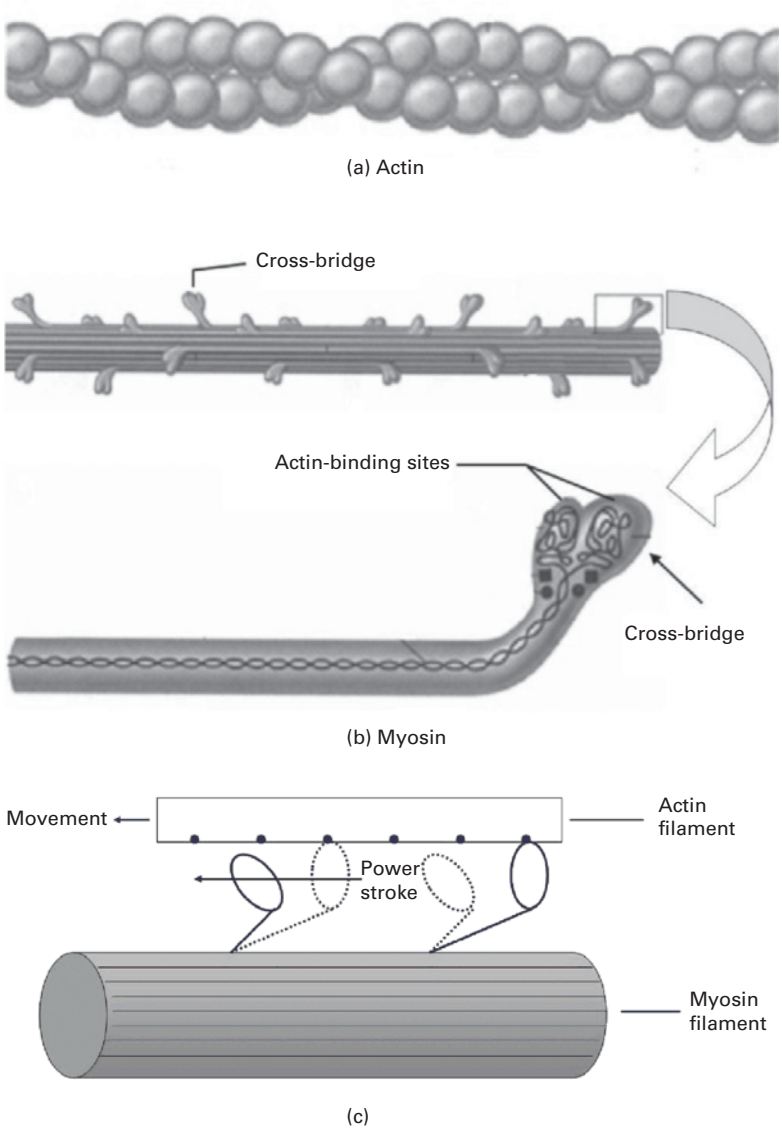


**Figure 1.43** Molecular structure of (a) actin and (b) myosin; (c) action of cross-bridges when actin filament is moved to the left with respect to the myosin filament; notice how cross-bridges detach themselves, then reattach themselves to the actin.

in the myosin-actin units (called sarcomeres) and is approximately equal to 3 μm in the stretched configuration. It shortens when the muscle is contracted. This gives the muscle a striated pattern when observed at high magnification. They resemble a coral snake in the microscope. Myofibrils have a diameter of approximately 1–2 μm.

**Elastin** Elastin is found in skin, walls of arteries and veins, and lung tissue. A prominent place is in the "*ligamentum nuchae*, a long ligament that runs along the top of the neck in horses and is constantly under tension. Other vertebrates have it too, but it is less pronounced. In this manner, the horse can keep its head up

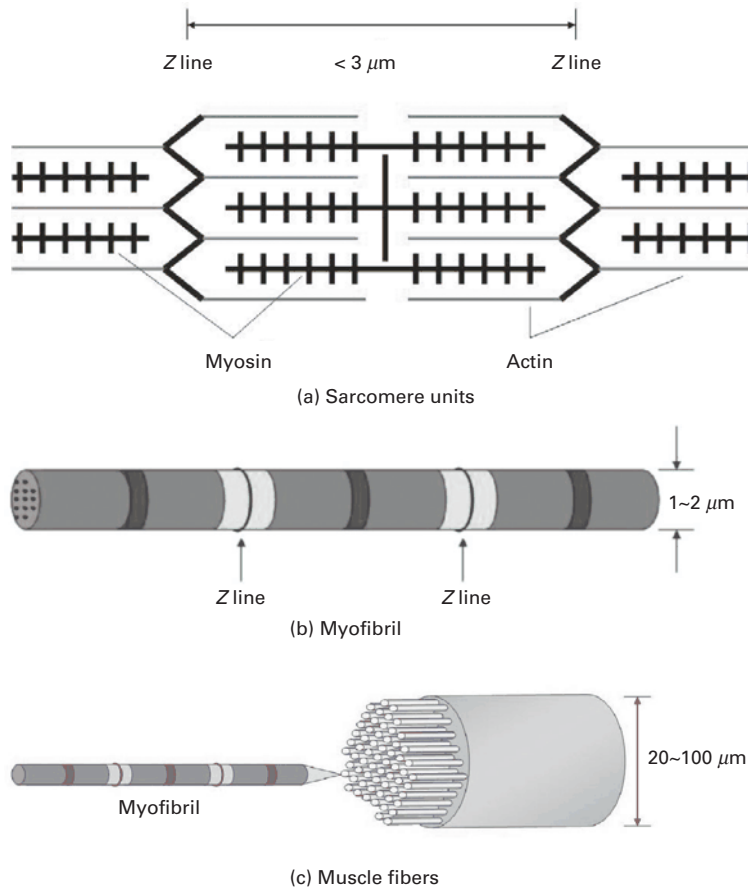


**Figure 1.44** Structure of muscle from (a) the sarcomere units, to (b) myofibril, and finally to (c) muscle fibers.

without using muscles. The "ligamentum nuchae plays a role similar to the cables in a suspension bridge. It is a rather robust cylinder.

**Resilin and Abductin** These are found in arthropods. They have properties similar to those of elastin, but occur in totally different animals and have a different structure.

**Keratin** Keratin is found in hair, horn, bird beaks and feathers, and whale baleen. The toucan beak presented in Section 1.3.8 is made of keratin. It has a structure similar to collagen (three interwoven helices). These helices combine themselves to form micro fibrils with a diameter of 8 nm. Interestingly, it undergoes a phase transformation under tensile load, which increases its elongation.

**Cellulose** Cellulose is the most abundant biological structural material, and is present in wood (which is a composite of cellulose and lignin) and cotton (almost pure cellulose). Cellulose is a cross-linked crystalline polymer. Its basic building block is a fibril with 3.5 nm diameter and 4 nm periodicity.

**Chitin** Chitin is a polysaccharide found in many invertebrates. The exoskeleton of insects is made of chitin.

**Silk** Silk is composed of two proteins: fibroin (tough strands) and sericin, a gummy glue. The mechanical properties (strength and maximum elongation) can vary widely, depending on the application intended by the animal. For instance, among the silks produced by spiders are dragline and spiral. Dragline, used in the radial components of the web, is the structural component, and has high tensile strength (600 mPa) and a strain at failure of about 6%. The spiral tangential components are intended to capture prey, and are "soft" and "sticky." The strain at failure in this case can exceed 16, i.e. 1,600%.

## Example 1.10

Determine the maximum strain that the collagen fibers can experience without damage if their shape is as given in Figure 1.41 with a ratio between amplitude and wavelength of 0.2.

We can assume a sine function of the form:

$$y = k \sin 2\pi x/\lambda.$$

The maximum of $y$ is reached when $x = \pi/4$.

Hence:

$$y_{\max} = k = \lambda/5.$$

We can integrate over the length of the sine wave from 0 to $2\pi$ . However, this will lead to an elliptical integral of difficult solution. A simple approximation is to consider the shape of the wavy protein as an ellipse with major axis $2a$ and minor axis $2b$. The circumference is given by the approximate expression (students should consult a mathematics text to obtain this expression)

$$L \approx \pi\left[\frac{3}{2}(a+b) - (ab)^{1/2}\right].$$

In the sine function, we have two arms, one positive and one negative. Their sum corresponds, in an approximate manner, to the circumference of the ellipse. The strain is equal to

$$\varepsilon = \frac{L - 4a}{4a} = \frac{\pi\left[\frac{3}{2}(a+b) - (ab)^{1/2}\right] - 4a}{4a}.$$

Thus:

$$\varepsilon = \frac{\pi}{4}\left[\frac{3}{2}\left(1 + \frac{b}{a}\right) - \left(\frac{b}{a}\right)^{1/2}\right] - 1.$$

## Example 1.10 (cont.)

The following ratio is given:

$$\frac{b}{2a} = 0.2 \quad \text{and} \quad \frac{b}{a} = 0.4.$$

The corresponding strain is:

$$\varepsilon = 0.53.$$

Beyond this strain, the collagen will break.

### 1.3.10 The Sponge Spicule: An Example of a Biological Material

Marine sponges have long tentacles that are called spicules. These spicules act as antennas, which are subjected to marine currents and other stresses. These long silica rods have properties that dramatically exceed the strength of synthetic silica. Figure 1.43 shows the flexure strength of both spicule and synthetic silica. The difference in flexure strength between sponge spicule and synthetic silica is remarkable. The synthetic silica fractures at a relatively low stress of 200 mPa compared to the yield stress of the spicule at 870 mPa. The area under the stress–strain curve gives a reasonable idea of the toughness. Clearly the toughness of the spicule is many times higher than that of synthetic silica. As evidenced by Figure 1.45, failure

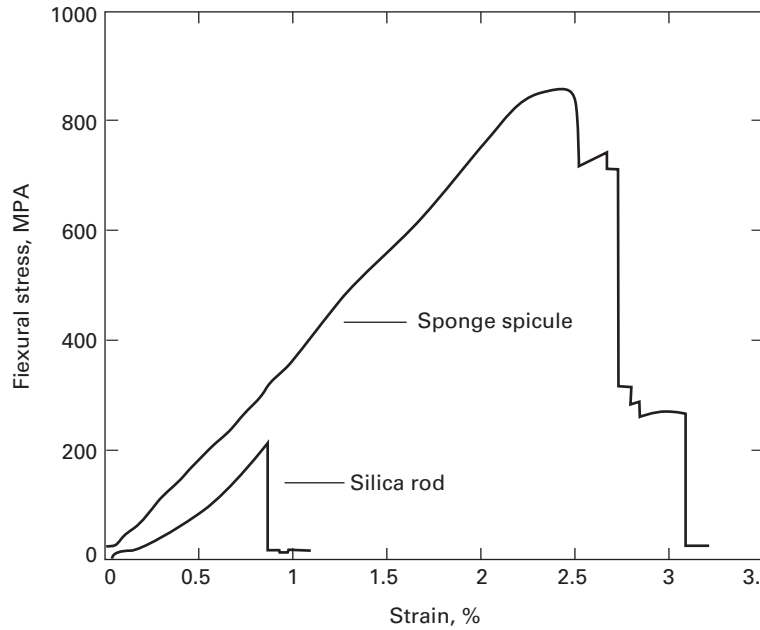


**Figure 1.45** stress deflection responses of synthetic silica rod and sponge spicule in flexure testing. (Figure courtesy of George Mayer.)

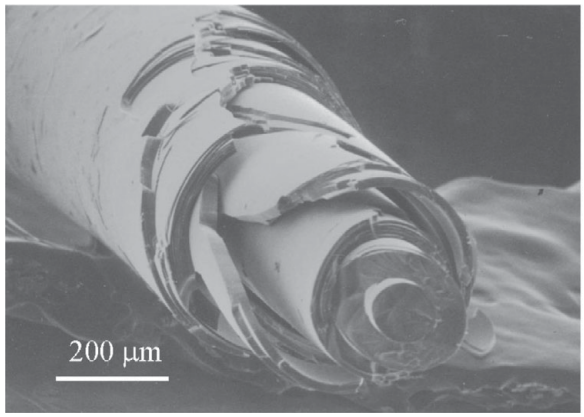


**Figure 1.46** SEM of fractured sponge spicule showing two-dimensional onion-skin structure of concentric layers.
(Figure courtesy of George Mayer.)

does not occur catastrophically in the spicule. Instead, the spicule fails "gracefully," which is a considerable advantage.

Figure 1.46 shows the microstructure of a fracture surface. The spicule consists of many concentric layers. This onion-like structure is responsible for the strengthening effect observed. When stress is applied to a silica rod, a crack will initiate at the weakest point in the material and propagate through the silica rod in a catastrophic manner. In contrast, crack propagation in the spicule will be arrested at each interface. This type of "graceful" failure is extremely useful. We can truly learn and apply this lesson from nature to modern material applications.

### 1.3.11 Active (or Smart) Materials

Technology puts greater and greater demand on materials and there is a constant push to develop materials with enhanced capabilities. The term *multifunctional materials* has been coined to describe materials with more than one capability. This is inspired by nature, where materials often have more than one function. For example, the trunk of a tree is at the same time a structural component and a carrier for the sap. Bones have a structural as well as a blood-cell-producing function.

Another category of advanced materials are *active materials*. They are also called "smart" materials. Active materials have responses that can be used in all kinds of devices. Given below are the main classes of active materials.

- Shape memory alloys: The most common is a NiTi alloy known as Nitinol. It can undergo strains of 1–5% through a martensitic transformation that is reversible. There are numerous applications through two effects: the shape memory effect and the super elastic (or pseudoelastic) effect: dental braces, stents, etc. A detailed description of these alloys is given in Chapter 11.
- Magnetorheological materials: These materials exhibit a viscosity that depends on an externally applied magnetic field. The suspension system of a US-made luxury

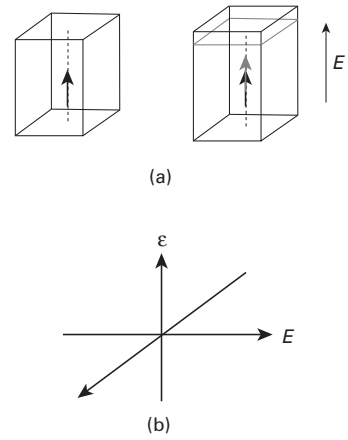


**Figure 1.47** (a) Effect of applied field $E$ on dimension of ferroelectric material. (b) Linear relationship between strain and electric field.
(Figure courtesy of G. Ravichandran.)

automobile uses this material. The stiffness can be adjusted by varying the magnetic field.

- Piezoelectric ceramics and ferroelectricity[9]: These materials generate an electric field when strained. Conversely, if an electric current is passed through them, they change their dimensions. Barium titanate and lead zirconate titanate (Pb(Zr, Ti)$O_3$) are examples. They have the perovskite structure with composition $ABO_3$, where A and B are metals. They are characterized by a linear strain–electric-field response. The maximum strain is on the order of 0.2%. Applications include vibration control, micropositioning devices, ultrasonics, and nondestructive evaluation.

It is a property of ferroelectrics to exhibit polarization in the absence of an electric field. Polarization is defined as dipole moment per unit volume or charge per unit area on the surface. The material is divided into domains, which are regions with uniformly oriented polarization. Ferroelectrics are characterized by a linear relationship between stress $\sigma$ and polarization $P$:

$$P = d\sigma.$$

There is a converse relationship between strain $\varepsilon$ and electric field, $E$:

$$\varepsilon = dE,$$

where $d$ is called the polarizability tensor. Figure 1.47(a) shows how the application of an externally applied electric field $E$ results in a change in length of the specimen. Figure 1.47(b) shows the linear relationship between the strain and the field. This is a property of ferroelectric crystals, certain noncentrosymmetric crystals (e.g. quartz, ZnO), textured polycrystals, and polycrystals with a net spontaneous polarization. Applications include adaptive optics, active rotors and control surfaces, robotics,

[9] K. Bhattacharya and G. Ravichandran, *Acta Mater.*, 51 (2003) 5941.

and MEMS/NEMS (microelectromechanical system/nanoelectromechanical system) actuators.

### 1.3.12 Electronic Materials

Electronic materials are composed, for the most part, of thin films arranged in several layers and deposited on a substrate. The most common substrate is monocrystalline silicon (the silicon wafer). Integrated circuits form the heart of modern computers and the silicon chip is a primary example. Figure 1.48 shows a schematic of the materials and structure used in a CMOS (complementary metal oxide semiconductor) transistor device. The *pn* junctions form transistors. The substrate is silicon, which in this case is *n* doped. The thin film layers are vapor-deposited and there are a number of mechanical aspects that are of considerable importance. In Figure 1.48 we have monocrystalline and polycrystalline silicon, oxide, glass, metal, and a dielectric passivation layer.

The thin films deposited on the substrate have dimensions of a few nanometers to a few micrometers. These films may be under residual stresses as high as 500 MPa. These stresses are due to:

- Thermal expansion coefficient effects: When the film cools it contracts. The thermal expansion coefficients of the different layer scan be different, creating internal stresses.
- Phase transformations: The phases in thin films are often nonequilibrium phases.

There are a number of mechanical problems associated with these stresses. Dislocations at the interface between substrate and thin film, cracking of the

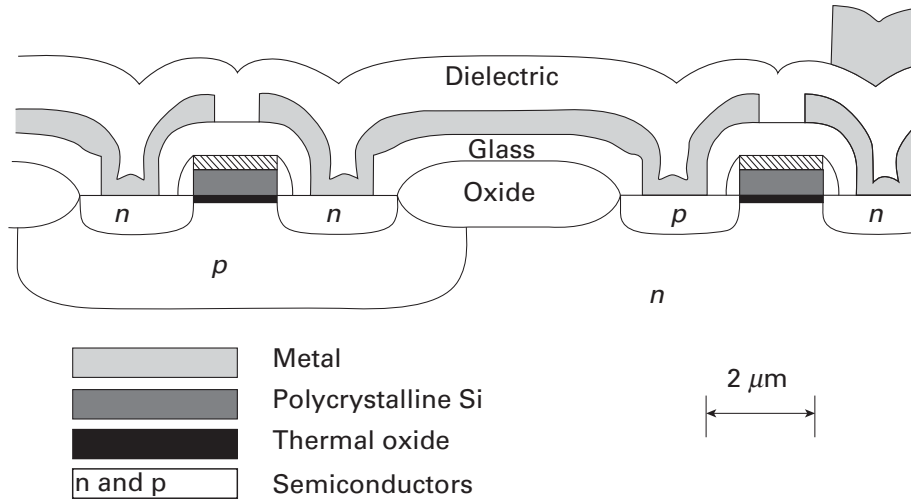


**Figure 1.48** Cross-section of a complementary metal-oxide semiconductor (CMOS). (Adapted by permission of Springer Nature: *Metallurgical Transactions, A, Physical Metallurgy and Materials Science*, Mechanical properties of thin films, William D. Nix, Copyright (1989).)

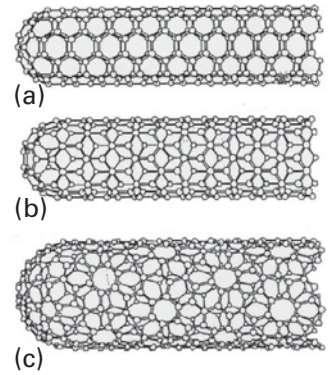


**Figure 1.49** Three configurations for single-wall carbon nanotubes: (a) armchair, (b) "zig-zag", (c) chiral.
(Adapted from *Carbon*, Vol. 33, M.S. Dresselhaus, G. Dresselhaus, R. Saito, Physics of carbon nanotubes, Pages 883–891. Copyright 1995, with permission from Elsevier.)

passivation layer, and bending of the substrate/thin-film system are a few examples. We will briefly describe these effects in Chapters 2, 6, 9, and 13.

Magnetic hard disks are also made of thin films. The aluminum disk, upon which a thin layer of magnetic material is deposited, rotates at surface velocities approaching 80 km $h^{-1}$, while the "head" flies aerodynamically over it. The distance between head and disk is as low as 0.3 μm. Some of the mechanical problems are friction, wear, and the unavoidable collisions between disk and head.

### 1.3.13 Nanotechnology

Nanotechnology[10, 11] refers to the structure and properties of materials and devices at the nanometer level. Developments in synthesis and characterization methods have resulted in materials that are designed from the "bottom up," rather than from the "top down." These terms were first used by the famous physicist Richard Feynman. The traditional method used in the design of new materials is to develop synthesis and processing techniques at the macro scale, and then to carry out detailed characterization at the micrometer and nanometer scale. The new approach is to start with atoms, then assemble them into small arrays and characterize their structure and properties at that level. This approach was led by the semiconductor revolution. As the sizes of devices become smaller, we approach atomic dimensions. At that level, it is being found that many materials possess unique properties. Many biological processes also use the bottom-up approach. Atoms aggregate themselves into molecules and complex arrays through genetic messages. The atoms come together and self-organize themselves into complex arrays of amino acids, which in their turn form proteins. It is hoped that we will be able to fully harness this approach in the future. There are already applications of nanotechnology in the marketplace.

A material that is showing great potential because of unique characteristics is the carbon nanotube. The first nanotube was produced in Japan by S. Iijima. One can

[10] C. P. Poole and F. J. Owens, *Introduction to Nanotechnology* (Hoboken, NJ: Wiley-Interscience, 2003).
[11] M. Ratner and D. Ratner, *Nanotechnology* (Englewood Cliffs, NJ: Prentice Hall, 2003).

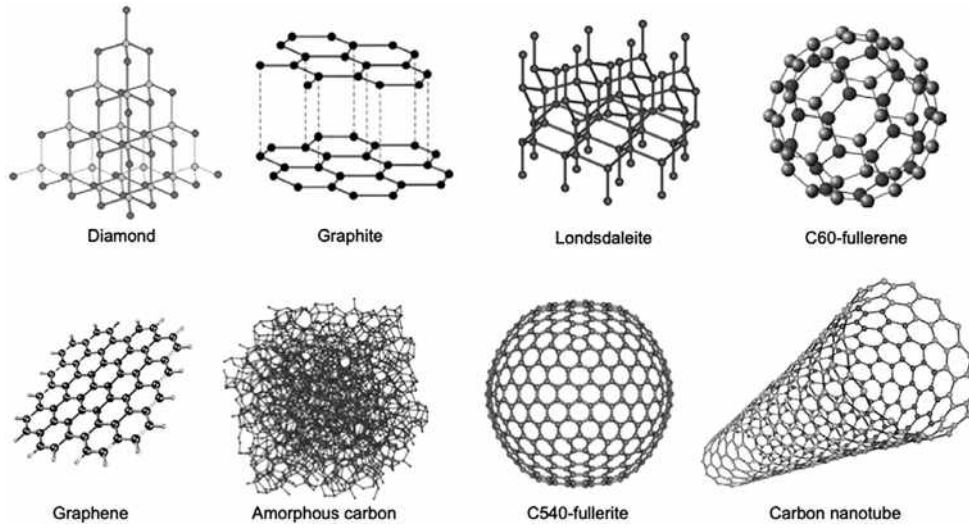


**Figure 1.50** Different arrangements of carbon atoms.
(Reprinted by permission from Springer Nature: Topics in Current Chemistry, Carbon nanotubes in biomedicine, Viviana Negri et al, Copyright (2020).)

envisage a carbon nanotube by rolling a single layer of carbon atoms into a hollow cylinder. The ends can be semispherical caps (one half of a "Bucky ball"). There are three morphologies for carbon nanotubes, shown in Figure 1.47: armchair, zig-zag, and chiral. They differ in the following:

- Armchair: the hexagons have the "pointy" side perpendicular to cylinder axis.
- Zig-zag: the hexagons have the pointy side aligned with the cylinder axis.
- Chiral: The hexagons are inclined with respect to the cylinder axis, and the carbon sheet wraps itself helically around the cylinder.

These carbon nanotubes have typically a diameter between 5 and 20 nm and length between 1 and 100 μm. They have outstanding mechanical properties, since they are based on the C–C bond, the strongest in nature. There are varying estimates of their strength, and values between 45 and 200 GPa are quoted. This would make them the strongest material known, ranking with diamond. Although the nanotubes are very short, one can envisage a day where continuous nanotubes are manufactured. Their incorporation as reinforcements in composites presents a bright prospect.

Figure 1.50 shows several carbon allotropes: diamond, graphite, lonsdaleite, C60-fullerene, graphene, amorphous carbon, C540-fullerite, and single-walled carbon nanotube. Outstanding properties can be achieved by the different configurations of the carbon atoms. This topic, nanostructured materials, is treated in Chapter 5.

Two-dimensional structures, especially graphene and $MoSi_2$, are becoming increasingly important.

## 1.4 Strength of Real Materials

Materials deform and fail through defects. These defects (cracks, point defects, dislocations, twins, martensitic phase transformations, etc.) are discussed in Chapters 4 through 8. The two principal mechanisms are crack growth, and dislocations and plastic flow:

- Crack growth: Real materials can have small internal cracks, at whose extremities high-stress concentrations are set up. Hence, the theoretical cleavage strength can be achieved at the tip of the crack at applied loads that are only a fraction of that stress. Griffith's theory (see Chapter 7) explains this situation very clearly. These stress concentrations are much lower in ductile materials, since plastic flow can take place at the tip of a crack, blunting the crack's tendency to grow.
- Dislocations and plastic flow: Before the theoretical shear stress is reached, dislocations are generated and move in the material; if they are already present, they start moving and multiply. These dislocations are elementary carriers of plastic deformation and can move at stresses that are a small fraction of the theoretical shear stress. They will be discussed in detail in Chapter 4.

In sum, cracks prevent brittle materials from obtaining their theoretical cleavage stress, while dislocations prevent ductile materials from obtaining their theoretical shear stress.

To achieve the theoretical strength of a crystalline lattice, there are two possible methods: (1) eliminating all defects and (2) creating so many defects, that their interactions render them inoperative. The first approach has yielded some materials with extremely high strength. Unfortunately, this has been possible only in special configurations called "whiskers." The second approach is the one more commonly pursued, because of the obvious dimensional limitations of the first; the strength levels achieved in bulk metals have steadily increased by an ingenious combination of strengthening mechanisms, but are still much lower than the theoretical strength. Maraging steels with useful strengths up to 2 GPa have been produced, as have patented steel wires with strengths of up to 4.2 GPa; the latter are the highest strength steels.

Figure 1.51 compares the ambient-temperature strength of tridimensional, filamentary, and whisker materials. The whiskers have a cross-sectional diameter of only a few micrometers and are usually monocrystalline (although polycrystalline whiskers have also been developed). Whiskers are one of the strongest materials developed by human beings. The dramatic effect of the elimination of two dimensions is shown clearly in Figure 1.51 and in Table 1.7. The strongest whiskers are ceramics. Figure 1.51 provides some illustrative examples. Iron whiskers with a strength of 12.6 GPa have been produced, compared with 2 GPa for the strongest bulk steels. The value of 12.6 GPa is essentially identical to the theoretical shear stress, because the normal stress is twice the shear stress. In general, FCC whiskers tend to be much weaker than BCC whiskers and ceramics. For instance, Cu whiskers have a strength of about 2 GPa. This is consistent with the much lower

**Table 1.7 Room Temperature Strength of Some Whiskers**

| Material | Diameter | Maximum tensile strength (GPa) | Source |
|---|---|---|---|
| Cu | 1.2 to 15 μm | 2–6 | [a] |
| Ag | 1.2 to 15 μm | 1.5–4 | [a] |
| Fe | 1.2 to 15 μm | 3–9 | [a] |
| SiC | 4–6 μm | 8.4 | [b] |
| $Al_2O_3$ | 82–320 nm | 49 | [c] |
| $Si_3N_4$ | 40–800 nm | 17–59 | [d] |
| Graphite | 1–5 μm | 20 | [e] |

[a] S. Brenner, *J. Appl. Phys.*, 27(1956)1484–1497.
[b] J. J. Petrovic, J. V. Milewski, D. L. Rohr, F. D. Gac, *J. Matls. Sci.*, 20(1985) 1167–1177.
[c] S. Wang, Y. He, H. Huang, J. Zhou, G. J. Auchterlonie, B. Huang, *Nanotechnology*, 24(2013) 285703.
[d] H. Iwanaga, C, Kawai, *JACS*, 81(1998) 773–776.
[e] R. Bacon, *J. Appl. Phys.*, 31(1960) 283–290.
Adapted with permission from A. Kelly, *Strong Solids* (Oxford, U.K.: Clarendon Press, 1973), p. 263s.

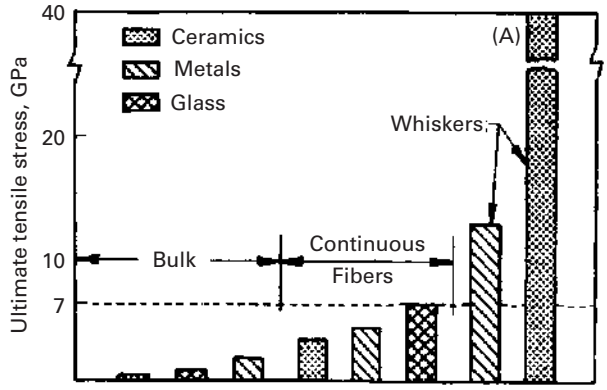


**Figure 1.51** Theoretical strength of continuous fibers and whiskers. The strength of the SiC whisker produced by the Philips Eindhoven Laboratory is indicated by (A).

theoretical shear strength exhibited by copper whiskers. It turns out that silver, gold, and copper have $\tau_{max}/G$ ratios of 0.039 (see Chapter 4). Hence, they are not good whisker materials. Figure 1.52 shows a stress–strain curve for a tin whisker. The stress drops vertically after the yield point. In contrast, the stress–strain curve for the polycrystal is barely different from the abscissa axis. This demonstrates, for a real material, the dramatic effect that a small lateral dimension can have on the strength and ductility.

In the elastic range, the curve deviates slightly from Hooke's law and exhibits some temporary inflections and drops (not shown in the figure). In many cases, for both metals and nonmetals, failure occurs at the elastic line, without appreciable plastic strain. When plastic deformation occurs, as, for example, in copper and zinc, a very large yield drop is observed. Although the strength of whiskers is not completely understood, it is connected to the absence of dislocations. This is also exemplified in Figure 1.52, which compares the strength of single crystalline tin in the form of whiskers with the bulk polycrystalline form. The whiskers have a strength around

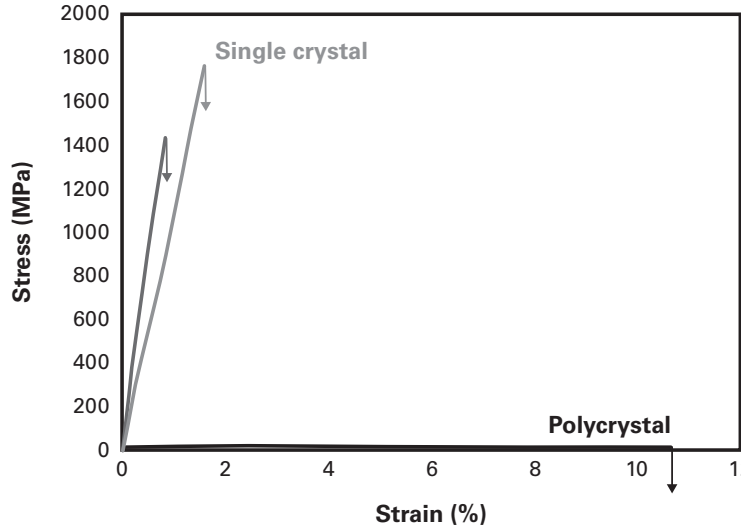


**Figure 1.52** Stress–strain curve of tin whisker and comparison with strength of polycrystal. (Reprinted by permission from Springer Nature: Journal of Electronic Materials, Tensile Behavior of Single-Crystal Tin Whiskers, S.S. Singh et al., Copyright (2014).)

1.6 GPa, whereas the polycrystal strength is in the low MPa range. It is impossible to produce a material virtually free of dislocations, in other words, perfect. However, for whiskers, dislocations can easily escape out of the material during elastic loading. Their density and mean free path are such that they will not interact and produce other sources of dislocation. Hence, the yield point is the stress required to generate dislocations from surface sources. The irregularities often observed in the elastic range indicate that existing dislocations move and escape out of the whisker. At a certain stress, the whisker becomes essentially free of dislocations. When the stress required to activate surface sources is reached, the material yields plastically, or fails.

## Example 1.11

Calculate the stresses generated in a turbine blade if its cross-sectional area is 10 $cm^2$ and the mass of each blade is 0.2 kg.

***Solution:*** This is an example of a rather severe environment where the material properties must be predicted with considerable detail. For example the blade may be in a jet engine. Figure E 1.11 shows a section of the compressor stage of a jet. The individual blades are fixed by a dovetail arrangement to the turbine vanes. Assume a rotational velocity $\omega$ =10,000 rpm and a mean radius $R$ = 0.5 m. The centripetal acceleration in the bottom of each turbine blade is

$$a_c = \omega^2 R = \left[10,000 \times \frac{1}{60} \times 2\pi\right]^2 \times 0.5 = 5.4 \times 10^5 \text{m s}^{-2}.$$

## Example 1.11 (cont.)

The stress that is generated is

$$\sigma = \frac{F}{A} = \frac{ma_c}{A} = \frac{0.2 \times 5.4 \times 10^5}{10 \times 10^{-4}} = 100 \text{ MPa},$$

where $F$ is the centripetal force and $A$ is the cross-sectional area. This stress of 100 MPa is significantly below the flow stress of nickel-based superalloys at room temperature, but can be quite significant at higher temperatures.

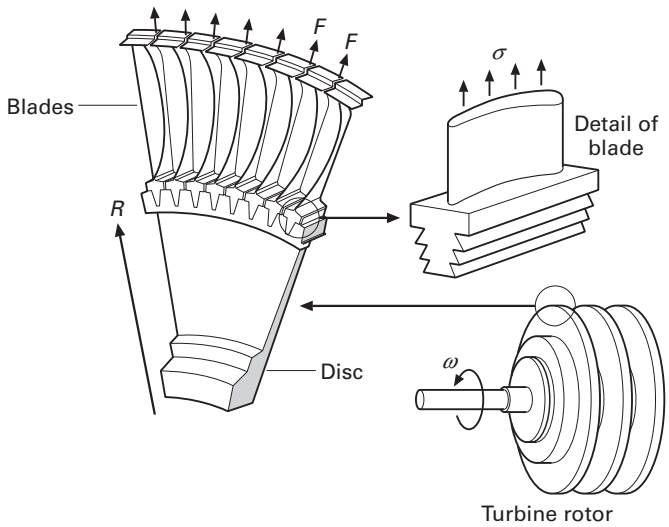


**Figure E1.11** Turbine blade subjected to centripetal force during operation.

## SUGGESTED READING

### Materials in General

J. F. Shackelford. *Introduction to Materials Science for Engineers*, 4th edn. Upper Saddle River, NJ: Prentice Hall, 1996.

W. F. Smith. *Principles of Materials Science and Engineering*, 3rd edn. New York, NY: McGraw Hill, 1996.

D. R. Askeland and P. Phule. *The Science and Engineering of Materials*, 4th edn. Pacific Grove, CA: Thomson, 2003.

W. D. Callister. Jr. *Materials Science and Engineering*, 4th edn. New York, NY: Wiley, 2003.

### Metals

C. S. Barrett and T. B. Massalski. *Structure of Metals*, 3rd rev. edn. Oxford, U.K: Pergamon, 1980.

M. A. Meyers and K. K. Chawla. *Mechanical Metallurgy*. Englewood Cliffs, NJ: Prentice-Hall, 1984.

## Ceramics

W. D. Kingery, H. K. Bowen, and D. R. Uhlmann. *Introduction to Ceramics*, 2nd edn. New York, NY, Wiley, 1976.
Y.-M. Chiang, D. Birnie III, and W. D. Kingery, *Physical Ceramics*, New York, NY: Wiley, 1997.

## Polymers

D. C. Bassett. *Principles of Polymer Morphology*. Cambridge, U.K.: Cambridge University Press, 1981.
Hiltner (ed.) *Structure-Property Relationships of Polymeric Solids*. New York, NY: Plenum Press, 1983.
R. J. Young. *Introduction to Polymers*. London: Chapman & Hall, 1986.
B. Wunderlich. *Macromolecular Physics, Vol. 1: Crystal Structure*. New York, NY: Academic Press, 1973.
B. Wunderlich. *Macromolecular Physics, Vol. 2: Crystal Nucleation*. New York, NY: Academic Press, 1976.

## Composite Materials

K. Chawla. *Composite Materials: Science & Engineering*. 2nd edn. New York, NY: Springer, 1998.
K. Chawla. *Ceramic Matrix Composites*, 2nd edn. Boston, MA: Kluwer, 2003.
N. Chawla and K. K. Chawla. *Metal Matrix Composites*, New York, NY: Springer, 2006.

## Liquid Crystals

A Ciferri, W. R. Krigbaum, and R. B. Meyer (eds.). *Polymer Liquid Crystals*. New York, NY: Academic Press, 1982.

## Biomaterials

M. Elices (ed.). *Structural Biological Materials*, Amsterdam, the Netherlands: Pergamon, 2000.
J. F. V. Vincent. *Structural Biomaterials*. Princeton, NJ: Princeton University Press, 1991.
Y.C. Fung. *Biomechanics: Mechanical Properties of Living Tissues*. New York, NY: Springer, 1981.

## Cellular Materials

J. Gibson and M. F. Ashby. *Cellular Solids: Structure and Properties*. Oxford, U.K.: Pergamon Press, 1988.

## Electronic Materials

W. D. Nix. Mechanical Properties of Thin Films, *Met. Trans.*, 20A (1989) 2217.
L.B. Freund and S. Suresh. *Thin Film Materials: Stress, Defect Formation and Surface Evolution*. Cambridge, U.K.: Cambridge University Press, 2003.

## EXERCISES

**1.1** A jet turbine rotates at a velocity of 7,500 rpm. Calculate the stress acting on the turbine blades if the turbine disc radius is 70 cm and the cross-sectional area is 15 $cm^2$. Take the length to be 10 cm and the alloy density to be 8.5 g $cm^{-3}$.

**1.2** The material of the jet turbine blade in Problem 1.1, Super alloy IN 718, has a room-temperature yield strength equal to 1.2 G Pa; it decreases with temperature as

$$\sigma = \sigma_0 \left(1 - \frac{T - T_0}{T_m - T_0}\right)$$

where $T_0$ is the room temperature and $T_m$ is the melting temperature in K ($T_m = 1{,}700$ K). At what temperature will the turbine flow plastically under the influence of centripetal forces?

**1.3** **(a)** Describe the mechanical properties that are desired in a tennis racket, and recommend different materials for the different parts of the racket.

**(b)** Describe the mechanical properties that are desired in a golf club, and recommend different materials for the different parts of the club.

**1.4** On eight cubes that have one common vertex, corresponding to the origin of axes, draw the family of {111} planes. Show that they form an octahedron and indicate all <110> directions.

**1.5** The frequency of loading is an important parameter in fatigue. Estimate the frequency of loading (in cycles per second, or Hz) of an automobile tire in the radial direction when the car speed is 100 km $h^{-1}$ and the wheel diameter is 0.5 m.

**1.6** Indicate, by their indices and in a drawing, six directions of the <112> family.

**1.7** The density of Cu is 8.9 g $cm^{-3}$ and its atomic weight (or mass) is 63.546. It has the FCC structure. Determine the lattice parameter and the radius of atoms.

**1.8** The lattice parameter for W(BCC) is $a = 0.32$ nm. Calculate the density, knowing that the atomic weight (or mass) of W is 183.85.

**1.9** Consider the unit cell of CsCl which has NaCl structure. The radius of $Cs^+$ is 0.169 nm and that of $Cl^-$ is 0.181 nm. (a) Determine the packing factor of the structure, assuming that $Cs^+$ and $Cl^-$ ions touch each other along the diagonals of the cube. (b) Determine the density of CsCl if the atomic weight of Cs is 132.905 and that of Cl is 35.453.

**1.10** MgO has the same structure as NaCl (simple cubic). If the radii of $O^{2-}$ and $Mg^{2+}$ ions are 0.14 nm and 0.070 nm, respectively, determine (a) the packing factor and (b) the density of the material. The atomic weight of $O_2$ is 16 and that of Mg is 24.3.

**1.11** Germanium has the diamond cubic structure with interatomic spacing of 0.245 nm. Calculate the packing factor and density. (The atomic weight of germanium is 72.6.)

**1.12** The basic unit (or mer) of polytetrafluoroethylene (PTFE) or Teflon is $C_2F_4$. If the mass of the PTFE molecule is 45,000 amu, what is the degree of polymerization?

**1.13** Using the representation of the orthorhombic unit cell of polyethylene (see Figure E1.13), calculate the theoretical density. How does this value compare with the density values of polyethylene obtained in practice?

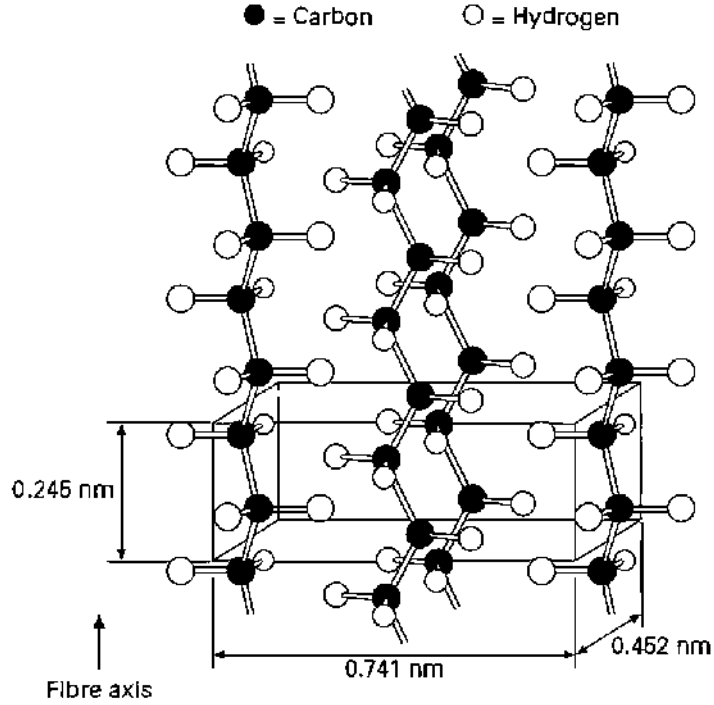


**Figure E1.13** Crystalline form of polyethylene with orthorhombic unit cell.

**1.14** A pitch blend sample has five different molecular species with molecular masses of $0.5 \times 10^6$, $0.5 \times 10^7$, $1 \times 10^7$, $4 \times 10^7$, and $6 \times 10^7$. Compute the number-averaged molecular weight and weight-averaged molecular weight of the sample.

**1.15** Different polymorphs of a material can have different mechanical properties. Give some examples.

**1.16** What are smart materials? Give some examples.

**1.17** What are glass-ceramics? Explain their structure and properties. (Hint: think of Corning ware.)

**1.18** Explain how the scale of microstructure can affect the properties of a material. Use steel, an alloy of iron and carbon, as an example.

**1.19** For a cubic system, calculate the angle between (a) [100] and [111], (b) [111] and [112], (c) [112] and [221].

**1.20** Recalculate the bicycle stiffness ratio for a titanium frame. (See Examples 1.1 and 1.2.) Find the stiffness and weight of the bicycle if the radius of the tube is 25 mm. Use the following information:

$$\begin{aligned} \text{Alloy} &: \text{Ti} - 6\%\text{Al} - 4\%\text{V}, \\ \sigma_y &= 1,150 \text{ MPa}, \\ \text{Density} &= 4.5 \text{ g cm}^{-3}, \\ E &= 106\text{GPa}, \\ G &= 40\text{GPa}. \end{aligned}$$

**1.21** Calculate the packing factor for NaCl, given that $r_{\text{Na}} = 0.186$ nm and $R_{\text{Cl}} = 0.107$ nm.

**1.22** Determine the density of BCC iron structure if the iron atom has a radius of 0.124 nm.

**1.23** Draw the following direction vectors in a cubic unit cell:

(a) [100] and [110], (b) [112], (c) $[\bar{1}10]$, (d) $[\bar{3}2\bar{1}]$.

**1.24** Calculate the stress generated in a turbine blade if its cross-sectional area is 0.002 $m^2$ and the mass of each blade is 0.5 kg. Assume that the rotational velocity $\omega = 15{,}000$ rpm and the turbine disk radius is 1 m.

**1.25** Suppose that the turbine blade from the last problem is part of a jet turbine. The material of the jet turbine is a nickel-based superalloy with yield strength, $\sigma_y = 1.5$ G Pa; it decreases with temperature as:

$$\sigma_y = \sigma_0[(1 - (T - T_0)/(T_m - T_0)],$$

where $T_0 = 293$ K is room temperature and $T_m = 1{,}550$ K is the melting temperature. Find the temperature at which the turbine will flow plastically under the influence of centripetal forces.

**1.26** Calculate the lattice parameter of Ni (FCC) knowing that the atomic diameter of nickel is 0.249 nm.

**1.27** A jet turbine blade, made of MARM 200 (a nickel-based superalloy) rotates at 10,000 rpm. The radius of the disk is 50 mm. The cross-sectional area is 20 $cm^2$ and the length of the blade is equal to 12 cm. The density of MARM 200 is 8.5 g $cm^{-3}$.

**(a)** What is the stress acting on the turbine blade in MPa?

**(b)** If the room temperature strength of MARM 200 is equal to 800 MPa, what is the maximum operational temperature in kelvin?

The yield stress varies with temperature as:

$$\sigma = \sigma_0 \left[ 1 - \left( \frac{(T - T_0)}{(T_m - T_0)} \right)^m \right],$$

where $T_m$ is the melting temperature ($T_m = 1{,}700$ K) and $T_0$ is the room temperature; $m = 0.5$.

**1.28** Generate a three-dimensional unit cell for the intermetallic compound $AuCu_3$ that has a cubic structure. The Au atoms are at the cube corners and the Cu atoms at the center of the faces. Given:

**Figure Ex 1.28**

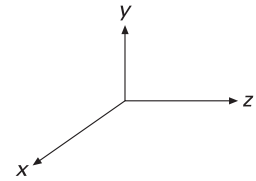


$r_{Cu} = 0.128$ nm $AN_{Cu}$ (atomic number) $= 63.55$ amu
$r_{Au} = 0.144$ nm $AN_{Au} = 196.97$ amu.
(a) Find the lattice parameter in nanometers.
(b) What is the atomic mass of the unit cell in grams?
(c) What is the density of the compound in g $cm^{-3}$?

**1.29** Draw the following unit cells with the planes (one plane per cube with the coordinate axes): (a) $(\bar{1}01)$, (b) $(1\bar{1}1)$, (c) $(0\bar{1}2)$, (d) (301).

**1.30** Show how the atoms pack in the following planes by drawing circles (atoms) in the appropriate spots: (a) (111) in FCC, (b) (110) in FCC, (c) (111) in BCC, (d) (110) in BCC.

**1.31** BET is a technique for measuring the surface area of particles, which is of obvious importance in nanomaterials. Describe this technique. Don't forget to mention what the acronym BET stands for.

**1.32** "Tin plate" is one of the largest tonnage steel products. It is commonly used for making containers. If it is a steel product why is it called tin plate?

**1.33** Using Figure 1.7, list the important symmetry operations in the following crystal systems: (a) triclinic, (b) monoclinic, (c) orthorhombic.

**1.34** The only possible rotation operations that can be used to define crystal systems are rotations of the type $n = 1$, 2, 3, 4, and 6. Using other values of $n$ will result in unit cells which, when joined together, will not fill all space. Demonstrate this by giving a simple mathematical proof. (*Hint*: consider two lattice points separated by a unit translation vector.)

**1.35** Calculate the APF (atomic packing factor) for BCC and FCC unit cells, assuming the atoms are represented as hard spheres. Do the same for the diamond cubic structure.

**1.36** Draw the following crystallographic planes in BCC and FCC unit cells along with their atoms that intersect the planes: (a) (101), (b) (110), (c) (441), (d) (111), (e) (312).

**1.37** A block copolymer has macromolecules of each polymer attached to the other as can be seen in Figure 1.22(c). The total molecular weight is 100,000 g $mol^{-1}$. If 140 g of A and 60 g of B were added, determine the degree of polymerization for each polymer. A: 56 g $mol^{-1}$; B: 70 g $mol^{-1}$.

**1.38** Sketch the following planes within the unit cell. Draw one cell for each solution. Show new origin and ALL necessary calculations.
(a) $(0\bar{1}\bar{1})$, (b) (102), (c) (002), (d) $(1\bar{3}0)$, (e) $(\bar{2}12)$, (f) $(3\bar{1}\bar{2})$.

**1.39** Sketch the following directions within the unit cell. Draw one cell for each solution. Show new origin and ALL necessary calculations.
(a) [101], (b) $[0\bar{1}0]$, (c) $[12\bar{2}]$, (d) [301], (e) $[\bar{2}01]$, (f) $[2\bar{1}3]$.

**1.40** Suppose we introduce one carbon atom for every 100 iron atoms in an interstitial position in BCC iron, giving a lattice parameter of 0.2867 nm. For the Fe-C alloy, find the density and the packing factor.
Given:
Atomic mass of C = 12,
Atomic mass of Fe = 55.89,
$a_{Fe} = 0.2867$ nm,
Avogadro's number, $N = 6.02 \times 10^{23}$.

**1.41** Determine the maximum length of a polymer chain made with 1,500 molecules of ethylene, knowing that the carbon bond length is 0.13 nm.

**1.42** Calculate the atomic packing factor (APF) of diamond cubic.

**1.43** SiC has the diamond cubic structure. Calculate the APF of SiC ($r_{Si} = 0.11$ nm and $r_C = 0.07$ nm).

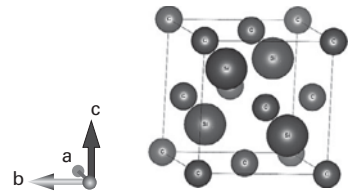


**Figure Ex 1.43**

**1.44** **(a)** How can the development of composites influence future aircraft?
**(b)** What are the principal features of composites?

**1.45** If steel is as strong as aluminum alloys in terms of strength, why are planes built with aluminum alloys?

**1.46** What composite materials are used in the Boeing 787?

**1.47** Draw the direction vectors in a cubic unit cell: [111], [201] and $[\bar{2}31]$.

**1.48** (a) Determine the interplanar spacing of (110) planes in a tetragonal unit cell ($a = b \neq c$, $\alpha = \beta = \gamma = 90^\circ$ ) with lattice parameters of $a = 0.3963$ nm and $c = 0.3671$ nm. (b) Determine the areas of the following planes $(\bar{1}10)$, $(1\bar{2}0)$ and $(00\bar{1})$.

**1.49** There are face-centered and body-centered structures in cubic systems, but no base-centered cubic. Show that the base-centered cubic structure is equivalent to another structure of the Bravais lattices.

**1.50** Explain the concept of free volume in glass transition in condensed matter. Why we can easily make a polymer which is composed of small molecules like metals in a glassy state but not in a crystalline state (though certain metallic glasses can be made easily).

**1.51** Stress–strain diagrams for three different polymers can be found in the following plot. It is known that one of the polymers is in a rubbery state, one is in a glassy state and the third is in a semicrystalline state. Please indicate the corresponding curves for the rubber, glassy, and semicrystalline polymers.

**1.52** Why is the percentage of composite materials increasing as time goes by? What are the advantages of using composite materials over traditional metallic materials?

**1.53** If gold atoms have a radius of 0.144 nm, determine the density and APF (atomic packing factor) in FCC and BCC structures. (Atoms are in contact along the face diagonal and body diagonal directions; $a = 0.407$ nm.)

**1.54** Find the indices of planes and directions in the HCP crystal structure.

**Figure Ex 1.54**

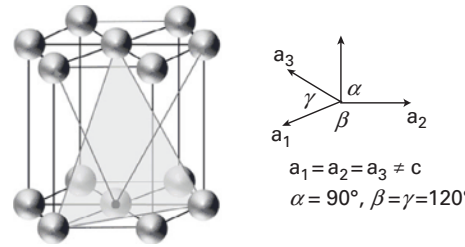


**1.55** How many major types of composite materials are there? What is the main component of composite materials?

**1.56** Draw three types of composite material.

**1.57** It is known that FCC and HCP possess relatively high APFs (atomic packing factors). Determine (a) the stacking pattern of FCC, HCP and BCC, (b) the closest packing plane of the FCC and BCC structures.

**1.58** Explain the difference between homopolymer, copolymer and block polymer by drawing them.

**1.59** Dental implant surgery is a procedure to replace the tooth roots with man-made materials. After the surgery, the artificial teeth will function as real ones. Stainless steel used to be the primary choice for implants. However, titanium is chosen over stainless steel nowadays. What is the advantage of titanium over stainless steel in this case?

**1.60** A continuous and aligned glass-fiber-reinforced composite consists of 25 vol% glass fibers with an elastic modulus of 80 GPa and 75 vol% of a polymer with an elastic modulus of 4.2 GPa.

**(a)** Compute the elastic modulus of this material in the longitudinal direction.

**(b)** If the cross-sectional area is 300 $mm^2$ and a stress of 40 MPa is applied along longitudinal direction, determine the load on the reinforcement and matrix phases respectively.

**(c)** What is the displacement and strain of the matrix and reinforcement phases under these conditions?

**1.61** Given that the lattice parameter of Ti is $a = 0.2950$nm and $c/a = 1.588$, determine the atomic packing factor and density of Ti. (The atomic weight of Ti is 48 g $mol^{-1}$ and the radius of a Ti atom is 147 pm.)

# Chapter 2 Elasticity and Viscoelasticity

## 2.1 Introduction

Elasticity deals with elastic stresses and strains, their relationship, and the external forces that cause them. An *elastic strain* is defined as a strain that disappears instantaneously once the forces that cause it are removed. The theory of elasticity for Hookean solids in which stress is proportional to strain is rather complex in its more rigorous treatment. However, it is essential to the understanding of micro- and macromechanical problems. Examples of the former are stress fields around dislocations, incompatibilities of stresses at the interface between grains, and dislocation interactions in work hardening; examples of the latter are the stresses developed in drawing and rolling wire, and the analysis of specimen machine interactions interesting for tensile strength. This chapter is structured in such a way as to satisfy the needs of both the undergraduate and the graduate student. A simplified treatment of elasticity is presented, in a manner so as to treat problems in an undergraduate course. Stresses and strains are calculated for a few simplified cases; the tridimensional treatment is kept at a minimum. A graphical method for the solution of two-dimensional stress problems (the Mohr circle) is described. On the other hand, the graduate student needs more powerful tools to handle problems that are somewhat more involved. In most cases, the stress and strain systems in tridimensional bodies can be better treated as tensors, with the indicial notation. Once this tensor approach is understood, the student will have acquired a very helpful visualization of stresses and strains as tridimensional entities. Important problems whose solutions require this kind of treatment involve stresses around dislocations, interactions between dislocations and solute atoms, fracture mechanics, plastic waves in solids, stress concentrations caused by precipitates, the anisotropy of individual grains and the stress state in a composite material.

## 2.2 Longitudinal Stress and Strain

Figure 2.1 shows a cylindrical specimen being stressed in a machine that tests materials for tensile strength. The upper part of the specimen is screwed to the crosshead of the machine. The coupled rotation of the two lateral screws causes the crosshead to move.

MARC A. MEYERS AND KRISHAN K. CHAWLA

# Mechanical Behavior of Materials

THIRD EDITION

# Mechanical Behavior of Materials

## Third Edition

Fully revised and updated, the new edition of this classic textbook provides a balanced mechanics-materials approach to understanding the mechanical behavior of materials.

It presents fundamental mechanisms operating at micro- and nanometer scales across a wide range of materials, in a way that is mathematically simple and requires no extensive knowledge of materials, and demonstrates how the microstructures and mesostructures of these materials determine their mechanical behavior.

Accompanied online by further resources for instructors, this is the ideal introduction for senior undergraduate and graduate students in materials science and engineering.

### New to this edition

New coverage of biomaterials, electronic materials, and cellular materials alongside established coverage of metals, polymers, ceramics, and composites.

New testing techniques such as micropillar compression and electron back-scattered diffraction.

Important new materials, such as high-entropy alloys, are introduced.

A stronger emphasis on real-world test data and tables, to train students in practical materials applications.

Over 40 new figures, over 100 worked examples, and over 740 exercises, including over 280 new exercises, to help cement student understanding.

**Marc A. Meyers** is a Distinguished Professor of Materials Science and Engineering at the University of California, San Diego, known for his expertise on the dynamic behavior of materials. He is a recipient of the TMS Educator Award (2013), the ASM International Albert Easton White Distinguished Teacher Award (2015), and the APS George Duvall Shock Compression Science Award (2017). He is a coauthor of *Biological Materials Science* (2014), and is a Fellow of TMS, ASM International, and the APS.

**Krishan K. Chawla** is an Emeritus Professor at the University of Alabama at Birmingham, and a former Program Director for Metals and Ceramics in the US NSF Division of Materials Research. He is the editor and chairman of the ASM Editorial Board for *International Materials Reviews*, the author of *Fibrous Materials*, 2nd edn. (2016), and a Fellow of ASM International.

# Mechanical Behavior of Materials

THIRD EDITION

**Marc A. Meyers**
University of California, San Diego

**Krishan K. Chawla**
University of Alabama at Birmingham

CAMBRIDGE
UNIVERSITY PRESS

CAMBRIDGE
UNIVERSITY PRESS

Shaftesbury Road, Cambridge CB2 8EA, United Kingdom

One Liberty Plaza, 20th Floor, New York, NY 10006, USA

477 Williamstown Road, Port Melbourne, VIC 3207, Australia

314–321, 3rd Floor, Plot 3, Splendor Forum, Jasola District Centre, New Delhi – 110025, India

103 Penang Road, #05–06/07, Visioncrest Commercial, Singapore 238467

Cambridge University Press is part of Cambridge University Press & Assessment,
a department of the University of Cambridge.

We share the University's mission to contribute to society through the pursuit of
education, learning and research at the highest international levels of excellence.

www.cambridge.org
Information on this title: www.cambridge.org/highereducation/isbn/9781108837903

DOI: 10.1017/9781108943383



First published in 1998 by Prentice-Hall
Second edition 2009 Cambridge University Press
6th printing 2013
Third edition 2025

*A catalogue record for this publication is available from the British Library.*

*Library of Congress Cataloging-in-Publication Data*
Names: Meyers, Marc A., author. | Chawla, Krishan Kumar, 1942– author.
Title: Mechanical behavior of materials / Marc A. Meyers, University of California, San Diego,
Krishan K. Chawla, University of Alabama, Birmingham.
Description: Third edition. | Cambridge ; New York, NY, USA : Cambridge University Press, [2025] |
Includes bibliographical references and index.
Identifiers: LCCN 2024014471 (print) | LCCN 2024014472 (ebook) | ISBN 9781108837903 (hardback) |
ISBN 9781108943383 (epub)
Subjects: LCSH: Strength of materials.
Classification: LCC TA403 .M554 2025 (print) | LCC TA403 (ebook) | DDC 620.1/12–dc23/eng/20240531
LC record available at https://lccn.loc.gov/2024014471
LC ebook record available at https://lccn.loc.gov/2024014472

ISBN 978-1-108-83790-3 Hardback

Additional resources for this publication at www.cambridge.org/mbm3

**Lovingly dedicated to the memory of my parents, Henri and Marie-Anne.**

**Marc André Meyers**

**Lovingly dedicated to the memory of my parents, Manohar L. and Sumitra Chawla.**

**Krishan Kumar Chawla**

# Contents

# Preface to the Third Edition

We are very pleased to offer this third edition of *Mechanical Behavior of Materials*. The first edition was published by Prentice-Hall in 1998. The second edition, a Cambridge University Press imprint, came out in 2009. The third edition is now seeing the light of the day in 2025. Needless to say, we have maintained the same fundamental theme of the book, viz., the fundamental mechanisms responsible for the mechanical properties of different materials under a variety of environmental conditions. The unique feature of the book is the presentation in a unified manner of important principles responsible for mechanical behavior of materials, metals, polymers, ceramics, composites, biological materials, electronic materials. The underlying theme is that structure (at the micro or nanometer level) of the material controls the properties of the material.

Although the basic theme of the book remains unchanged, the third edition has been updated with:

- State-of-the-art coverage of the major developments in materials, such as steels, ceramics, polymers, composites, biologic materials. Specifically, we discuss: unique characteristics of biological materials including the Arzt heptahedron and structural design elements which enable a quantitative engineering treatment in Chapter 1; the Euler equation, elasticity averaging methods of isostress and isostrain (Voigt and Reuss), and anisotropic effects to matrix formulation of stiffness in Chapter 2; High-Entropy Alloys in Chapter 10; Micropillar mechanical testing, EBSD (electron back-scattered diffraction), a powerful characterization method, and coincidence site lattice update in Chapter 5; fracture toughness of biological materials in Chapter 7.
- Many new figures to improve the presentation and to clarify the concepts presented.
- Fresh worked examples and exercises that help the students test their understanding.

The book is principally meant for use in the upper division and graduate level courses of mechanical engineering, and materials science and engineering departments. However, it will also be a great source of reference material to the practicing engineer, scientist, and researcher. We have kept the level of mathematics quite simple, and suggest the reader to refer back to Chapter 1 if needed, as it provides the basic materials-level information necessary to study this subject.

MAM would like to thank Sheron Tavares and Aomin Huang for their competent and dedicated work in the revision and permissions. This third edition would never have seen the day if it were not for them. He also thanks Boya Li for

contributing with exercises. He is grateful to his children Marc Meyers and Cristina Windsor, his granddaughters Claire, Isabelle, and Abigail, his brothers Pedro, Jacques, and Carlos for supporting him through this process. A special thanks is due to Linda Homayoun.

KKC is grateful to K. Carlisle, N. Chawla, A. Goel, M. Koopman, R. Kulkarni, A Mortensen, B. R. Patterson, P.D. Portella, and U. Vaidya, for their innumerable discussions and counsels. He is especially grateful to Kanika Chawla and M. Armstrong for their help with figures. As always, he is thankful to his family members, Anita, Kanika, Nikhil, Nimeesh, and Nivi for their forbearance.

# Preface to the Second Edition

The second edition of Mechanical Behavior of Materials has revised and updated material in every chapter to reflect the changes occurring in the field. In view of the increasing importance of bioengineering, a special emphasis is given to the mechanical behavior of biological materials and biomaterials throughout this second edition. A new chapter on environmental effects has been added. Professors Fine and Voorhees[1] make a cogent case for integrating biological materials into materials science and engineering curricula. This trend is already in progress at many US and European universities. Our second edition takes due recognition of this important trend. We have resisted the temptation to make a separate chapter on biological and biomaterials. Instead, we treat these materials together with traditional materials, viz., metals, ceramics, polymers, etc. In addition, taking due cognizance of the importance of electronic materials, we have emphasized the distinctive features of these materials from a mechanical behavior point of view.

The underlying theme in the second edition is the same as in the first edition. The text connects the fundamental mechanisms to the wide range of mechanical properties of different materials under a variety of environments. This book is unique in that it presents, in a unified manner, important principles involved in the mechanical behavior of different materials: metals, polymers, ceramics, composites, electronic materials, and biomaterials. The unifying thread running throughout is that the nano/microstructure of a material controls its mechanical behavior. A wealth of micrographs and line diagrams are provided to clarify the concepts. Solved examples and chapter-end exercise problems are provided throughout the text.

This text is designed for use in mechanical engineering and materials science and engineering courses by upper division and graduate students. It is also a useful reference tool for the practicing engineers involved with mechanical behavior of materials. The book does not presuppose any extensive knowledge of materials and is mathematically simple. Indeed, Chapter 1 provides the background necessary. We invite the reader to consult this chapter off and on because it contains very general material.

In addition to the major changes discussed above, the mechanical behavior of cellular and electronic materials was incorporated. Major reorganization of material has been made in the following parts: elasticity; Mohr circle treatment; elastic constants of fiber reinforced composites; elastic properties of biological and of biomaterials; failure criteria of composite materials; nanoindentation technique

[1] M. E. Fine and P. Voorhees, "On the evolving curriculum in materials science & engineering," *Daedalus*, Spring 2005, 134.

and its use in extracting material properties; etc. New solved and chapter-end exercises are added. New micrographs and line diagrams are provided to clarify the concepts.

We are grateful to many faculty members who adopted the first edition for classroom use and were kind enough to provide us with very useful feedback. We also appreciate the feedback we received from a number of students. MAM would like to thank Kanika Chawla and Jennifer Ko for help in the biomaterials area. The help provided by Marc H. Meyers and M. Cristina Meyers in teaching him the rudiments of biology has been invaluable. KKC would like thank K. B. Carlisle, N. Chawla, A. Goel, M. Koopman, R. Kulkarni, and B. R. Patterson for their help. KKC acknowledges the hospitality of Dr. P. D. Portella at Federal Institute for Materials Research and Testing (BAM), Berlin, Germany, where he spent a part of his sabbatical. As always, he is grateful to his family members, Anita, Kanika, Nikhil, and Nivi for their patience and understanding.

# A Note to the Reader

Our goal in writing *Mechanical Behavior of Materials* has been to produce a book that will be the pre-eminent source of fundamental knowledge about the subject. We expect this to be a guide to the student beyond his or her college years. There is, of course, a lot more material than can be covered in a normal semester-long course. We make no apologies for that in addition to being a classroom text, we want this volume to act as a useful reference work on the subject for the practicing scientist, researcher, and engineer.

Specifically, we have an introductory Chapter 1 (Materials: Structure, Properties, and Performance) dwelling on the themes of the book: structure, mechanical properties, and performance. This section introduces some key terms and concepts that are covered in detail in later chapters. We advise the reader to use this chapter as a handy reference tool, and consult it as and when required. We strongly suggest that the instructor use this first chapter as a self-study resource. Of course, individual sections, examples, and exercises can be added to the subsequent material as and when desired.

Enjoy!

# Chapter 1 Materials: Structure, Properties, and Performance

## 1.1 Introduction

Everything that surrounds us is matter. The origin of the word matter is *mater* (Latin) or *matri* (Sanskrit), for *mother*. In this sense, human beings anthropomorphized that which made them possible – that which gave them nourishment. Every scientific discipline concerns itself with matter. Of all matter surrounding us, a portion comprises materials. What are materials? They have been variously defined. One acceptable definition is "matter that human beings use and/or process." Another definition is "all matter used to produce manufactured or consumer goods." In this sense, a rock is not a material, intrinsically; however, if it is used in aggregate (concrete) by humans, it becomes a material. The same applies to all matter found on Earth: a tree becomes a material when it is processed and used by people, and a skin becomes a material once it is removed from its host and shaped into an artifact.

The successful utilization of materials requires that they satisfy a set of properties. These properties can be classified into thermal, optical, mechanical, physical, chemical, and nuclear, and they are intimately connected to the structure of materials. The structure, in its turn, is the result of synthesis and processing. A schematic framework that explains the complex relationships in the field of the mechanical behavior of materials, shown in Figure 1.1, is Thomas's iterative tetrahedron, which contains four principal elements: mechanical properties, characterization, theory, and processing. These elements are related, and changes in one are inseparably linked to changes in the others. For example, changes may be introduced by the synthesis and processing of, for instance, steel. The most common metal, steel has a wide range of strengths and ductilities (*mechanical properties*), which makes it the material of choice for numerous applications. While low-carbon steel is used as reinforcing bars in concrete and in the body of automobiles, quenched and tempered high-carbon steel is used in more critical applications such as axles and gears. Cast iron, much more brittle, is used in a variety of applications, including automobile engine blocks. These different applications require, obviously, different mechanical properties of the material. The different properties of the three materials, resulting in differences in performance, are attributed to differences in the internal structure of the materials.

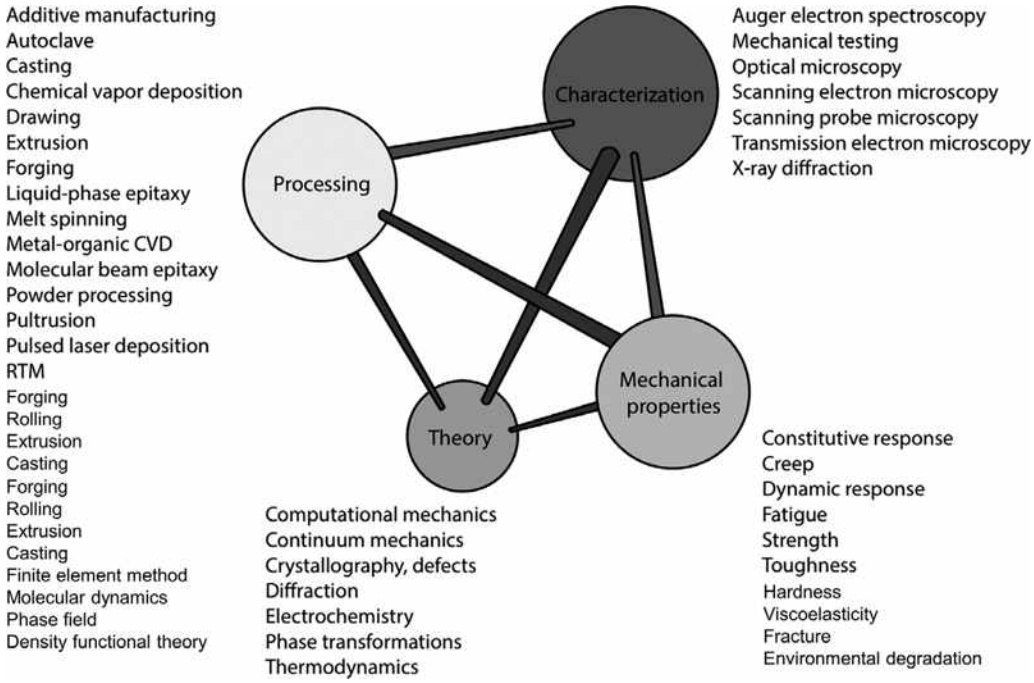


**Figure 1.1** Thomas's iterative materials tetrahedron applied to mechanical behavior of materials. (Figure courtesy of Annelies Zeeman.)

The understanding of the structure comes from *theory*. The determination of the many aspects of the micro-, meso-, and macrostructure of materials is obtained by *characterization*. Low-carbon steel has a primarily ferritic structure (body-centered cubic; see Section 1.3.1), with some interspersed pearlite (a ferrite–cementite mixture). The high hardness of the quenched and tempered high-carbon steel is due to its martensitic structure (body-centered tetragonal). The relatively brittle cast iron has a structure resulting directly from solidification, without subsequent mechanical working such as hot rolling. How does one obtain low-carbon steel, quenched and tempered high-carbon steel, and cast iron? By different *synthesis and processing* routes. The low carbon steel is processed from the melt by a sequence of mechanical working operations. The high-carbon steel is synthesized with a greater concentration of carbon (>0.5%) than the low-carbon steel (0.1%). Additionally, after mechanical processing, the high-carbon steel is rapidly cooled from a temperature of approximately 1,000 °C by throwing it into water or oil; it is then reheated to an intermediate temperature (tempering). The cast iron is synthesized with even higher carbon contents (~2%). It is poured directly into the molds and allowed to solidify in them. Thus, no mechanical working, except for some minor machining, is needed. These interrelationships among structure, properties, and performance, and their modification by synthesis and processing, constitute the central theme of materials science and engineering. The tetrahedron of

Figure 1.1 lists the principal processing methods, the most important theoretical approaches, and the most-used characterization techniques in materials science today.

The selection, processing, and utilization of materials have been part of human culture since its beginnings. Anthropologists refer to humans as "the toolmakers," and this is indeed a very realistic description of a key aspect of human beings responsible for their ascent and domination over other animals. It is the ability of humans to manufacture and use tools, and the ability to produce manufactured goods, that has allowed technological, cultural, and artistic progress and that has led to civilization and its development. Materials were as important to a Neolithic tribe in the year 10,000 BCE as they are to us today. The only difference is that today more complex synthetic materials are available in our society, while Neolithic tribes had only natural materials at their disposal: wood, minerals, bones, hides, and fibers from plants and animals. Although these naturally occurring materials are still used today, they are vastly inferior in properties to synthetic materials.

## 1.2 Monolithic, Composite, and Hierarchical Materials

The early materials used by humans were natural, and their structure varied widely. Rocks are crystalline, pottery is a mixture of glassy and crystalline components, wood is a fibrous organic material with a cellular structure, and leather is a complex organic material. Human beings started to synthesize their own materials in the Neolithic period: ceramics first, then metals, and later, polymers. In the twentieth century, simple monolithic structures were used first. The term *monolithic* comes from the Greek *mono* (one) and *lithos* (stone). It means that the material has essentially uniform properties throughout. Microstructurally, monolithic materials can have two or more phases. Nevertheless, they have properties (electrical, mechanical, optical, and chemical) that are constant throughout. Table 1.1 presents some of the important properties of metals, ceramics, and polymers. Their detailed structures will be described in Section 1.3. The differences in their structure are responsible for differences in properties. Metals have densities ranging from 2 to 19 g $cm^{-3}$; iron, nickel, chromium, and niobium have densities ranging from to 7 to 9 g $cm^{-3}$ aluminum has a density of 2.7 g $cm^{-3}$; and titanium has a density of 4.5 g $cm^{-3}$. Ceramics tend to have lower densities, ranging from 5 g $cm^{-3}$ (titanium carbide; TiC = 4.9) to 3 g $cm^{-3}$(alumina; $Al_2O_3$ = 3.95; silicon carbide; SiC = 3.2). Polymers have the lowest densities, fluctuating around 1 g $cm^{-3}$. Another marked difference among these three classes of materials is their ductility (ability to undergo plastic deformation). At room temperature, metals can undergo significant plastic deformation. Thus, metals tend to be ductile, although there are a number of exceptions. Ceramics, on the other hand, are very brittle, and the most ductile ceramics will be more brittle than most metals. Polymers have a behavior ranging from brittle (at temperatures below their glass transition temperature) to very deformable (in a nonlinear elastic material, such as rubber). The fracture toughness

**Table 1.1 Summary of Properties of Main Classes of Materials**

| Property | Metals | Ceramics | Polymers |
|---|---|---|---|
| Density (g $cm^{-3}$) | 2–20 | 1–14 | 1–2.5 |
| Electrical conductivity | high | low | low |
| Thermal conductivity | high | low | low |
| Ductility or strain-to-fracture (%) | 4–40 | <1 | 2–4 |
| Tensile strength (MPa) | 100–1,500 | 100–400 | – |
| Compressive strength (MPa) | 100–1,500 | 1,000–5,000 | – |
| Fracture toughness ($MNm^{-3/2}$) | 10–30 | 1–10 | 2–8 |
| Maximum service temperature (°C) | 1,000 | 1,800 | 250 |
| Corrosion resistance | low to medium | superior | medium |
| Bonding | metallic (free-electron cloud) | ionic or covalent | covalent |
| Structure | mostly crystalline (face-centered cubic, FCC; body-centered cubic, BCC; hexagonal close packed, HCP) | complex crystalline structure | amorphous or semicrystalline polymer |

is a good measure of the resistance of a material to failure and is generally quite high for metals and low for ceramics and polymers. Ceramics far outperform metals and polymers in high-temperature applications, since many ceramics do not oxidize even at very high temperatures (the oxide ceramics are already oxidized) and retain their strength to such temperatures. One can compare the mechanical, thermal, optical, electrical, and electronic properties of the different classes of materials and see that there is a very wide range of properties. Thus, monolithic structures built from primarily one class of material cannot provide all desired properties.

In the field of biomaterials (materials used in implants and life support systems), developments have also had far-reaching effects. The mechanical performance of implants is critical in many applications, including hipbone implants, which are subjected to high stresses, and endosseous implants in the jaw designed to serve as the base for teeth. Figure 1.2(a) shows the most successful design for endosseous implants in the jawbone. With this design, a titanium post is first screwed into the jawbone and allowed to heal. The tooth is fixed to the post and is effectively rooted into the jaw. The insertion of endosseous implants into the mandibles or maxillae, which was initiated in the 1980s, has been a revolution in dentistry. There is a little story associated with this discovery. Researchers were investigating the bone marrow of rabbits. They routinely used stainless steel hollow cylinders screwed into the bone. Through the hole, they could observe the bone marrow. It so happened that one of these cylinders was made of titanium. Since these cylinders were expensive, the researchers removed them periodically, in order to reuse them. When they tried to remove the titanium cylinder, it was tightly fused to the bone.

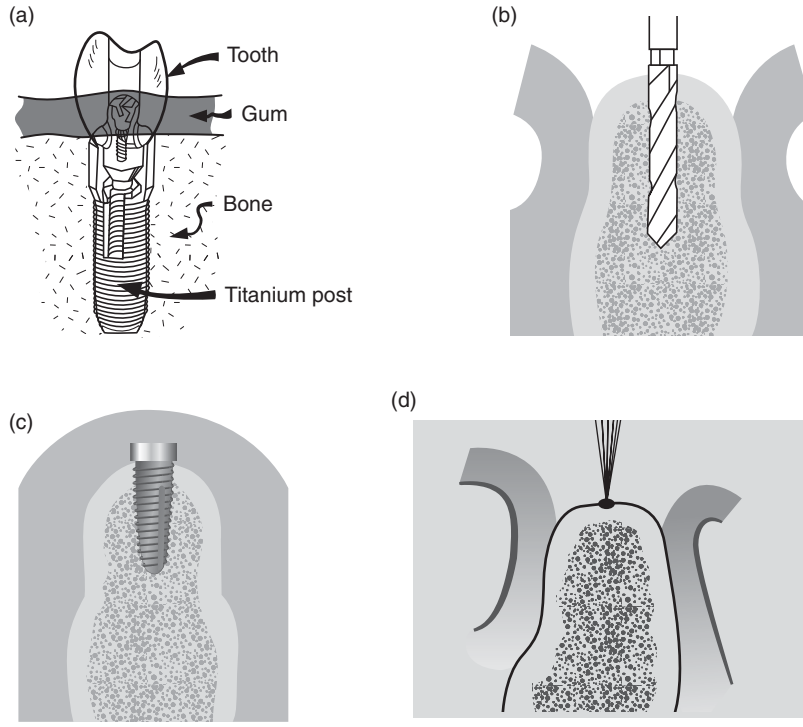


**Figure 1.2** (a) Complete endosseous implant, (b) a hole is drilled, and (c) a titanium post is screwed into jawbone. (d) Marking of site with small drill. (Figure courtesy of J. Mahooti.)

This triggered the creative intuition of one of the researchers, who said "What if. . .?".

Figure 1.2 shows the procedure used to insert the titanium implant. The site is first marked with a small drill that penetrates the cortical bone (Figure 1.2(d)). Then successive drills are used to create an orifice of the desired diameter (Figure 1.2(b)). The implant is screwed into the bone and the tissue is closed (Figure 1.2(c)). This implant is allowed to heal and fuse with the bone for approximately six months. Chances are that most readers will have these devices installed sometime in their lives.

Hip- and knee-replacement surgery is becoming commonplace. In the USA alone between 250,000 and 300,000 of each procedure are carried out annually. The materials of the prostheses have an important bearing on survival probability. Typical hip and knee prostheses are shown in Figure 1.3.

The hip prosthesis is made up of two parts: the acetabular component, or socket portion, which replaces the acetabulum, and the femoral component, or stem portion, which replaces the femoral head.

The femoral component is made of a metal stem with a metal ball on the extremity. In some prostheses a ceramic ball is attached to the metal stem. The acetabular component is a metal shell with a plastic inner socket liner made of

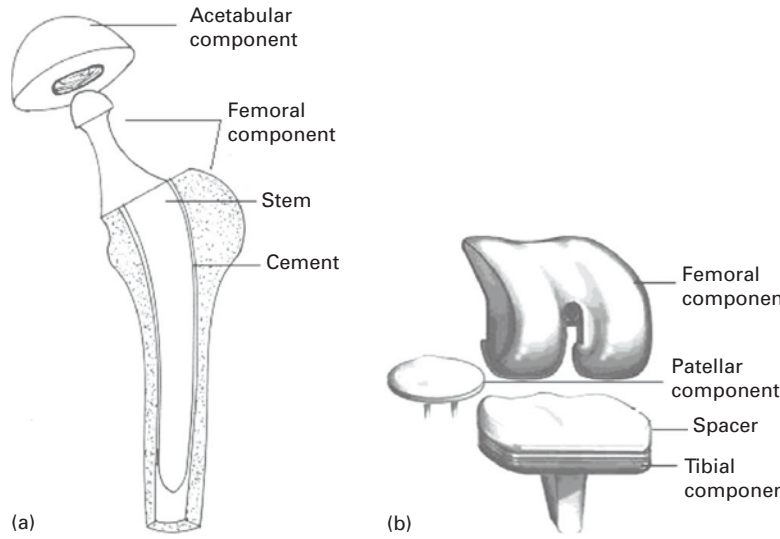


**Figure 1.3** (a) Total hip replacement prosthesis (b) total knee replacement prosthesis.

metal, ceramic, or a plastic called ultra-high-molecular-weight polyethylene (UHMWPE) that acts like a bearing. A *cemented* prosthesis is held in place by a type of epoxy cement that attaches the metal to the bone. An *uncemented* prosthesis has a fine mesh of holes on the surface area that touches the bone. The mesh allows the bone to grow into the mesh and become part of the bone. Biomaterial advances have allowed experimentation with new bearing surfaces, and there are now several different options when hip-replacement surgery is considered.

The metal has to be inert in the body environment. The preferred materials for the prostheses are Co–Cr alloys (Vitalium®) and titanium alloys. However, there are problems that have not yet been resolved: the metallic components have elastic moduli that far surpass those of bone. Therefore, they "carry" a disproportionate fraction of the load, and the bone is therefore unloaded. Since the health and growth of bone is closely connected to the loads applied to it, this unloading tends to lead to bone loss.

The most common cause of joint replacement failure is wear of the implant surfaces. This is especially critical for the polymeric components of the prosthesis. This wear produces debris which leads to tissue irritation. Another important cause of failure is loosening of the implant due to weakening of the surrounding bone. A third source of failure is fatigue.

*Biocompatibility* is a major concern for all implants, and ceramics are especially attractive because of their (relative) chemical inertness. Metallic alloys such as Vitalium® and titanium alloys have also proved to be successful, as have polymers such as polyethylene. A titanium alloy with a solid core surrounded by a porous periphery (produced by sintering of powders) has shown considerable potential. The porous periphery allows bone to grow and affords very effective fixation. Two new classes of materials that appear to present the best biocompatibility with bones are the Bioglass® and calcium phosphate ceramics. Bones contain calcium and

phosphorus, and Bioglass® is a glass in which the silicon has been replaced by those two elements. Thus, the bone "perceives" these materials as being another bone and actually bonds with it. Biomechanical properties are of great importance in bone implants, as are the elastic properties of materials. If the stiffness of a material is too high, then when implanted the material will carry more of the load placed on it than the adjacent bone. This could in turn lead to a weakening of the bone, since bone growth and strength depend on the stresses that the bone is subjected to. Thus, the elastic properties of bone and implant should be similar. Polymers reinforced with strong carbon fibers are also candidates for such applications. Metals, on the other hand, are stiffer than bones and tend to carry most of the load. With metals, the bones would be shielded from stress, which could lead to bone resorption and loosening of the implant.

Although new materials are being developed continuously, monolithic materials, with their uniform properties, cannot deliver the range of performance needed in any critical applications. *Composites* are a mixture of two classes of materials: metal–ceramic, metal–polymer, or polymer–ceramic. They have unique mechanical properties that are dependent on the amount and manner in which their constituents are arranged. Figure 1.4(a) shows schematically how different composites can be formed. Composites consist of a matrix and a reinforcing material. In making them, the modern materials engineer has at his or her disposal a very wide range of possibilities. However, the technological problems involved in producing some of them are immense, although there is a great deal of research addressing these problems. Figure 1.4(b) shows three principal kinds of reinforcement in composites: particles, continuous fibers, and discontinuous (short) fibers. The reinforcement usually has a higher strength than the matrix, which provides the ductility of the material. In ceramic-based composites, however, the matrix is brittle, and the fibers provide barriers to the propagating cracks, increasing the toughness of the material.

The alignment of the fibers is critical in determining the strength of a composite. The strength is highest along a direction parallel to the fibers and lowest along directions perpendicular to it. For the three kinds of composite shown in Figure 1.4(b), the polymer matrix plus (aramid, carbon, or glass) fiber is the most common combination if no high-temperature capability is needed.

Composites are becoming a major material in the aircraft industry. Carbon/epoxy and aramid/epoxy composites are being introduced in a large number of aircraft parts. These composite parts reduce the weight of the aircraft, increasing its economy and payload. The major mechanical property advantages of advanced composites over metals are better stiffness-to-density and strength-to-density ratios and greater resistance to fatigue. The values given in Table 1.2 apply to a unidirectional composite along the fiber reinforcement orientation. The values along other directions are much lower, and therefore the design of a composite has to incorporate the anisotropy of the materials. It is clear from the table that composites have advantages over monolithic materials. In most applications, the fibers are arranged along different orientations in different layers. For the central composite of Figure 1.4(b), these orientations are 0°, 45° 90°, and 135° to the tensile axis.

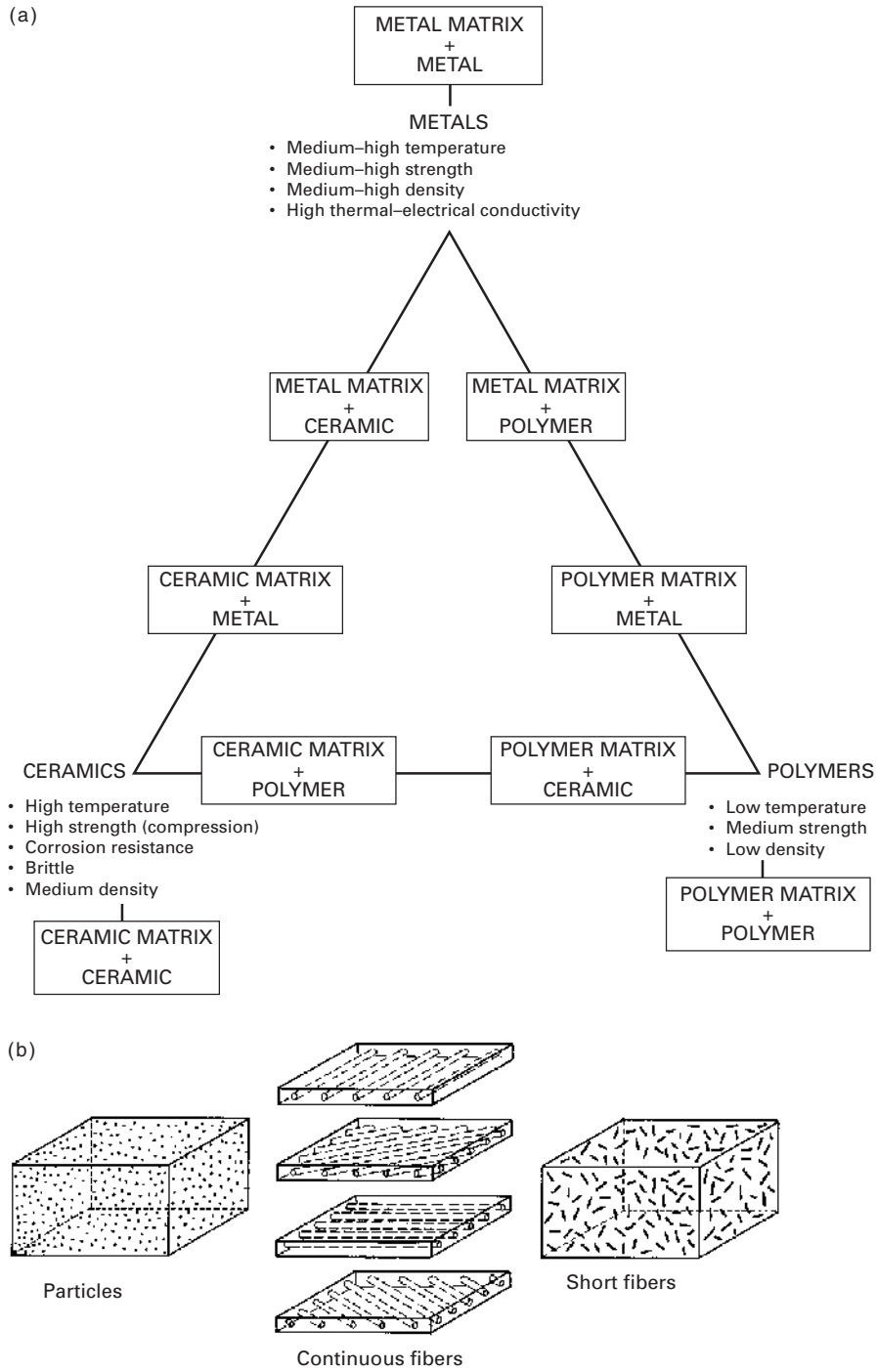


**Figure 1.4** (a) Schematic representations of different classes of composites. (b) Different kinds of reinforcement in composite materials. Composite with continuous fibers with four different orientations (shown separately for clarity).

**Table 1.2 Specific Modulus and Strength of Materials Used in Aircraft**

| Material | Elastic modulus/density (GPa/g cm$^{-3}$) | Tensile strength/density (MPa/g cm$^{-3}$) |
|---|---|---|
| Steel (AISI 4340) | 25 | 230 |
| Al (7075-T6) | 25 | 180 |
| Titanium (Ti-6Al-4V) | 25 | 250 |
| E glass/epoxy composite | 21 | 490 |
| S glass/epoxy composite | 47 | 790 |
| *Aramid/epoxy composite | 55 | 890 |
| HS (high tensile strength) carbon/epoxy composite | 92 | 780 |
| HM (high modulus) carbon/epoxy composite | 134 | 460 |

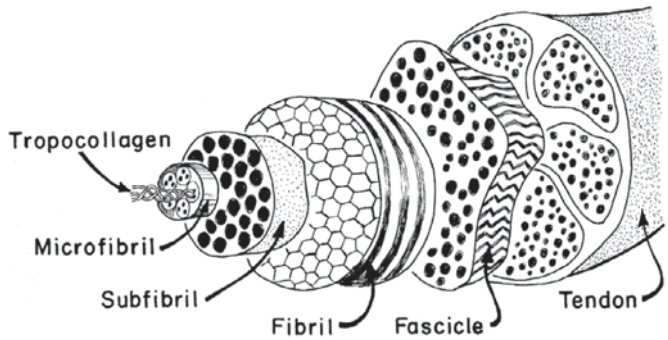


**Figure 1.5** A model of a hierarchical structure occurring in the human body. (Figure courtesy of E. Baer.)

Can we look beyond composites in order to obtain even higher mechanical performance? Indeed, we can: Nature is infinitely imaginative.

Our body is a complex arrangement of parts, designed, as a whole, to perform all the tasks needed to keep us alive. Scientists are looking into the make-up of soft tissue (skin, tendon, intestine, etc.), which is a very complex structure with different units active at different levels complementing each other. The structure of soft tissue has been called a *hierarchical* structure, because there seems to be a relationship between the ways in which it operates at different levels. Figure 1.5 shows the structure of a tendon. This structure begins with the tropocollagen molecule, a triple helix of polymeric protein chains. The tropocollagen molecule has a diameter of approximately 1.5 mm. The tropocollagen organizes itself into microfibrils, subfibrils, and fibrils. The fibrils, a critical component of the structure, are crimped when there is no stress on them. When stressed, they stretch out and then transfer their load to the fascicles, which compose the tendon. The fascicles have a diameter of approximately 150–300 μm and constitute the basic unit of the tendon. The hierarchical organization of the tendon is responsible for its toughness. Separate structural units can fail independently and thus absorb energy locally, without causing the failure of the entire tendon. Both experimental and analytical studies have been done, modeling the tendon as a composite of elastic, wavy fibers in a

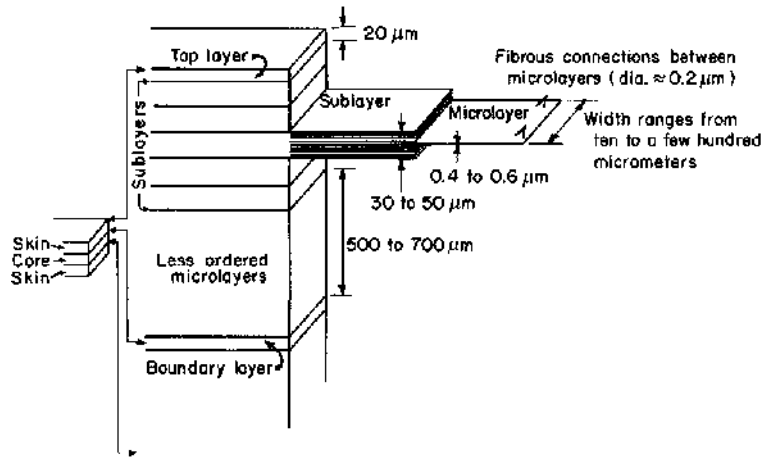


**Figure 1.6** Schematic illustration of a proposed hierarchical model for a composite (not drawn to scale).
(Figure courtesy of E. Baer.)

viscoelastic matrix. Local failures, absorbing energy, will prevent catastrophic failure of the entire tendon until enormous damage is produced.

Materials engineers are beginning to look beyond simple two component composites, imitating nature in organizing different levels of materials in a hierarchical manner. Baer[1] suggests that the study of biological materials could lead to new hierarchical designs for composites. One such example is shown in Figure 1.6, a layered structure of liquid-crystalline polymers consisting of alternating core and skin layers. Each layer is composed of sublayers which, in their turn, are composed of microlayers. The molecules are arranged in different arrays in different layers. The lesson that can be learned from this arrangement is that we appear to be moving toward composites of increasing complexity.

## 1.3 Structure of Materials

The *crystallinity*, or periodicity, of a structure, does not exist in gases or liquids. Among solids, the metals, ceramics, and polymers may or may not exhibit it, depending on a series of processing and composition parameters. Metals are normally crystalline. However, a metal cooled at a superfast rate from its liquid state called *splat cooling* can have an amorphous structure. (This subject is treated in greater detail in Section 1.3.4.) Silicon dioxide ($SiO_2$) can exist as amorphous (fused silica) or as crystalline (cristobalite or tridymite). Polymers consisting of molecular chains can exist in various degrees of crystallinity.

Readers not familiar with structures, lattices, crystal systems, and Miller indices should study these subjects before proceeding with the text. Most books on materials science, physical metallurgy, or X-rays treat the subjects completely. A brief introduction is presented next.

[1] E. Baer, *Sci. Am.* 254, No. 10 (1986) 179.

### 1.3.1 Crystal Structures

To date, seven crystal structures describe all the crystals that have been found. By translating the unit cell along the three crystallographic orientations, it is possible to construct a three-dimensional array. The translation of each unit cell along the three principal directions by distances that are multiples of the corresponding unit cell size produces the crystalline lattice.

Up to this point, we have not talked about atoms or molecules; we are just dealing with the mathematical operations of filling space with different shapes of blocks. We now introduce atoms and molecules, or "repeatable structural units." The unit cell is the smallest repetitive unit that will, by translation, produce the atomic or molecular arrangement. Bravais established that there are 14 space lattices. These lattices are based on the seven crystal structures. The points shown in Figure 1.7 correspond to atoms or groups of atoms. The 14 Bravais lattices can represent the

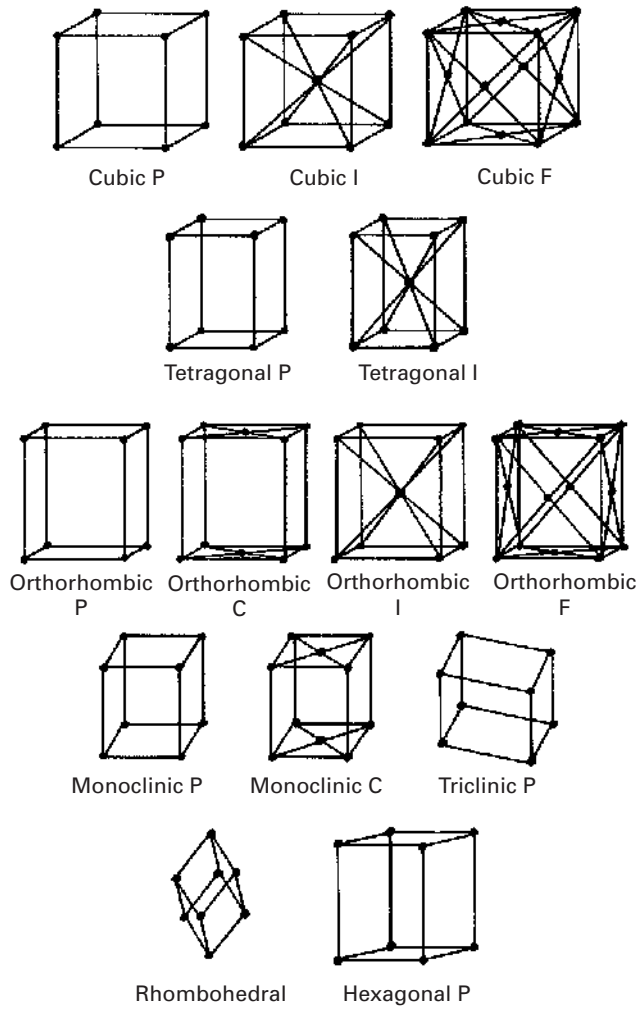


**Figure 1.7** The 14 Bravais space lattices ($P$ = primitive or simple; $I$ = body-centered cubic; $F$ = face-centered cubic; C = base-centered cubic).

**Table 1.3 Seven crystal systems and fourteen Bravais lattices**

| Name | Number of Bravais lattices | © Bart van Zeghbroeck 2007 Conditions | Primitive | Base-centered | Body-centered | Face-centered |
|---|---|---|---|---|---|---|
| Triclinic | 1 | $a_1 \neq a_2 \neq a_3, \alpha \neq \beta \neq \gamma$ | ✓ | | | |
| Monoclinic | 2 | $a_1 \neq a_2 \neq a_3, \alpha = \beta = 90^\circ \neq \gamma$ | ✓ | ✓ | | |
| Orthorhombic | 4 | $a_1 \neq a_2 \neq a_3, \alpha = \beta = \gamma = 90^\circ$ | ✓ | ✓ | ✓ | ✓ |
| Tetragonal | 2 | $a_1 = a_2 \neq a_3, \alpha = \beta = \gamma = 90^\circ$ | ✓ | | ✓ | |
| Cubic | 3 | $a_1 = a_2 = a_3, \alpha = \beta = \gamma = 90^\circ$ | ✓ | | ✓ | ✓ |
| Rhombohedral | 1 | $a_1 = a_2 = a_3, \alpha = \beta = \gamma < 120^\circ \neq 90^\circ$ | ✓ | | | |
| Hexagonal | 1 | $a_1 = a_2 \neq a_3, \alpha = \beta = 90^\circ, \gamma = 120^\circ$ | ✓ | | | |

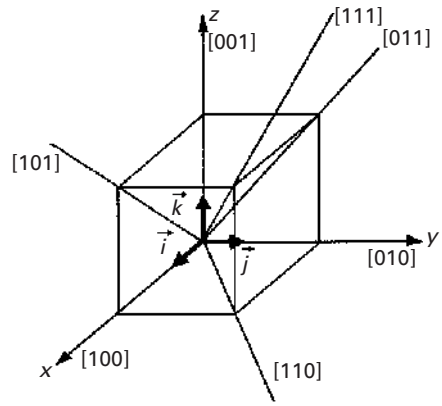


**Figure 1.8** Directions in a cubic unit cell.

unit cells for all crystals. Table 1.3 lists the 14 Bravais lattices as well as the respective lattice parameters. Figure 1.8 shows the indices used for directions in the cubic system. The same symbols are employed for different structures. We simply use the vector passing through the origin and a point ($m$, $n$, $o$):

$$\mathbf{V} = m\mathbf{i} + n\mathbf{j} + o\mathbf{k}.$$

If:

$$\mathbf{u} = u_1\mathbf{i} + u_2\mathbf{j} + u_3\mathbf{k}$$

and:

$$\mathbf{v} = v_1\mathbf{i} + v_2\mathbf{j} + v_3\mathbf{k}$$

we have:

$$\cos\ \alpha = \frac{u_1v_1 + u_2v_2 + u_3v_3}{\sqrt{u_1^2 + u_2^2 + u_3^2}\sqrt{v_1^2 + v_2^2 + v_3^2}}.$$

The angle between two directions **u** and **v** can be calculated through the cross product of the vectors:

$$\cos\alpha = \frac{\mathbf{u}\cdot\mathbf{v}}{|\mathbf{u}|\cdot|\mathbf{v}|}.$$

The notation used for a direction is

[m n o].

When we deal with a family of directions, we use the symbol $<mno>$.

The following family encompasses all equivalent directions:

$$< mno > \Rightarrow [mno], [mon], [omn], [onm], [nmo], [m\overline{n}o]$$
$$[mo\overline{n}], [om\overline{n}], [o\overline{n}m], [\overline{n}mo], \ldots$$

where an overbar indicates a negative sign in front of the variable. When the direction does not pass through the origin, and we have the head of the vector at $(m, n, o)$ and the tail at $(p, q, r)$, the vector **V** is given by

$$\mathbf{V} = (m-p)\mathbf{i} + (n-q)\mathbf{j} + (o-r)\mathbf{k}.$$

A direction not passing through the origin can be represented by

$$[(m-p)(n-q)(o-r)].$$

We can clear fractions, to reach smallest integer. Note that for the negative, we use a bar on top. For planes, we use the Miller indices, obtained from the intersection of a plane with the coordinate axes. Figure 1.9 shows a plane and its intercepts. We take

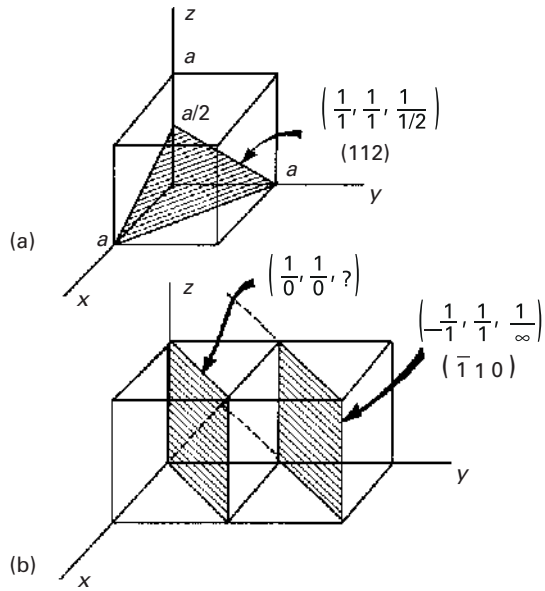


**Figure 1.9** Indexing of planes by Miller rules in the cubic unit cell; (a) (112); (b) $(\overline{1}10)$.

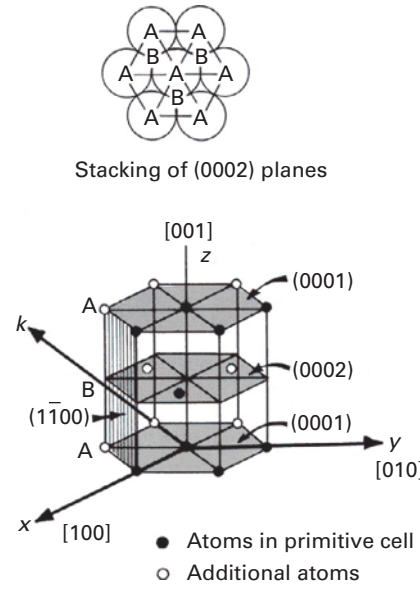


**Figure 1.10** Hexagonal structure consisting of a three-unit cell.

the inverse of the intercepts and multiply them by their common denominator so that we end up with integers. In Figure 1.9(a), we have

$$\frac{1}{1}, \frac{1}{1}, \frac{1}{1/2} \Rightarrow (112).$$

Figure 1.9 (b) shows an indeterminate situation. Thus, we have to translate the plane to the next cell, or else translate the origin. The indeterminate situation arises because the plane passes through the origin. After translation, we obtain intercepts (–1, 1, ∞). By inverting them, we get (110). The symbol for a family of planes is {m n o}. We do not reach to smallest integer. We use round parentheses ( ). For a family, we use { }. If the plane contains one of the axes, we move the origin to the next cell. If the plane is parallel to an axis, it intersects it at infinity. For instance, the spacing between (222) and (111) planes is different.

For hexagonal structures, we have a slightly more complicated situation. We represent the hexagonal structure by the arrangement shown in Figure 1.10. The atomic arrangement in the basal plane is shown in the top portion of the figure. Often, we use four axes ($x$, $y$, $k$, $z$) with unit vectors ($i$, $j$, $k$, $I$) to represent the structure. This is mathematically unnecessary, because three indices are sufficient to represent a direction in space from a known origin. Still, the redundancy is found by some people to have its advantages and is described here. We use the intercepts to designate the planes. The hatched plane (prism plane) has indices

$$\frac{1}{1}, \frac{1}{-1}, \frac{1}{\infty}, \frac{1}{\infty}.$$

After determining the indices of many planes, we learn that one always has

$$h + k = -i.$$

Thus, we do not have to determine the index for the third horizontal axis. If we use only three indices, we can use a dot to designate the fourth index, as follows:

$$(1\bar{1}\cdot 0).$$

For the directions, we can use either the three-index notation or a four-index notation. However, with four indices, the $h + k = -i$ rule will not apply in general, and one has to use special "tricks" to make the vector coordinates obey the rule.

If the indices in the three-index notation are $h'$, $k'$, and $\ell'$, the four index notation of directions can be obtained by the following simple equations:

$$h = \frac{1}{3}(2h' - k')$$
$$k = \frac{1}{3}(2k' - h')$$
$$i = -\frac{1}{3}(h' + k')$$
$$\ell = \ell'.$$

It can be easily verified that $h + k = -i$. Thus, the student is equipped to express the directions in the four-index notation.

### 1.3.2 Metals

The metallic bond can be visualized, in a very simplified way, as an array of positive ions held together by a "glue" consisting of electrons. These positive ions, which repel each other, are attracted to the "glue," which is known as an electron gas. Ionic and covalent bonding, on the other hand, can be visualized as direct attractions between atoms. Hence, these types of bonding, especially covalent bonding, are strongly directional and determine the number of neighbors that one atom will have, as well as their positions.

The bonding and the sizes of the atoms in turn determine the type of structure a material has. Often, the structure is very complicated for ionic and covalent bonding. On the other hand, the directionality of bonding is not very important for metals, and atoms pack into the simplest and most compact forms; indeed, they can be visualized as spheres. The structures favored by metals are the face-centered cubic (FCC), body-centered cubic (BCC), and hexagonal close packed (HCP) structures. In the periodic table, of the 81 elements to the left of the Zindl line, 53 have either the FCC or the HCP structure, and 21 have the BCC structure; the remaining 8 have other structures. The Zindl line defines the boundary of the elements with metallic character in the table. Some of them have several structures, depending on temperature. Perhaps the most complex of the metals is plutonium, which undergoes six polymorphic transformations.

Transmission electron microscopy can reveal the positions of the individual atoms of a metal, as shown in Figure 1.11 for molybdenum. The regular atomic array along a [001] plane can be seen. Molybdenum has a BCC structure.

## Example 1.1

Write the indices for the directions and planes marked in Figure E1.1.

**Figure E1.1**

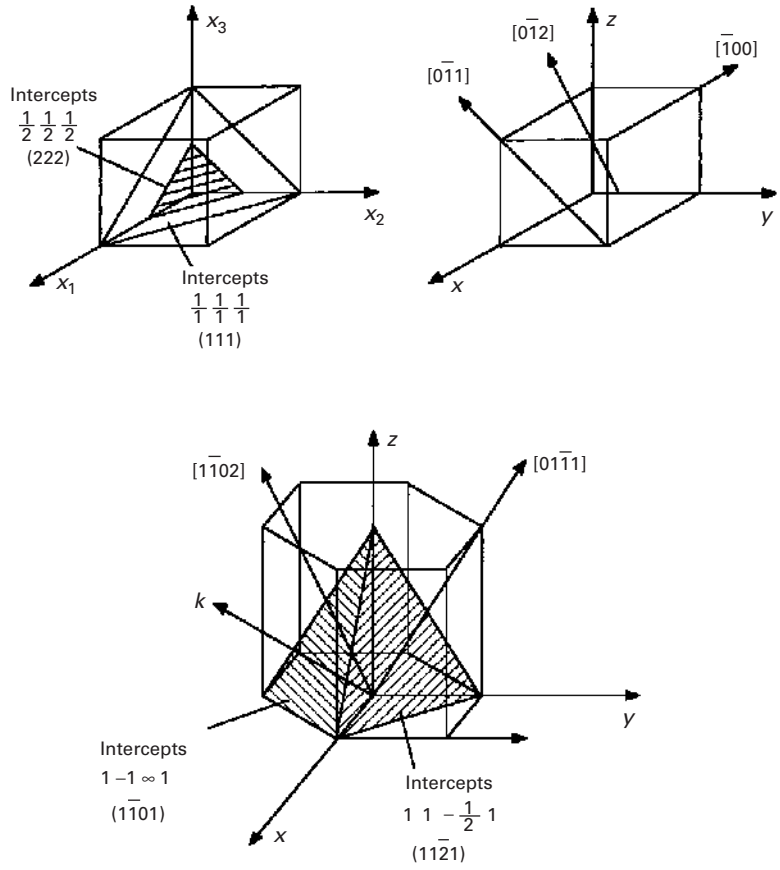


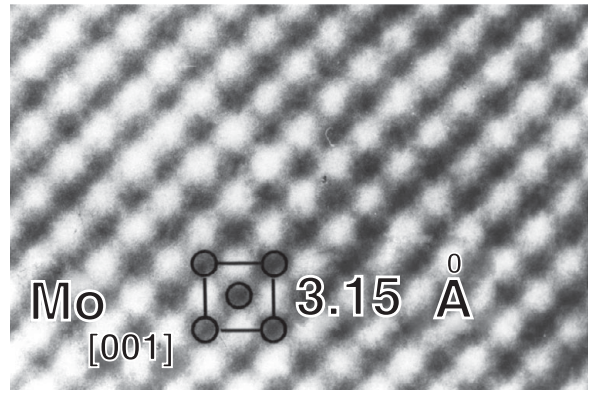


**Figure 1.11** Transmission electron micrograph at atomic resolution of (001) plane in molybdenum showing body-centered cubic arrangement of atoms.
(Figure courtesy of R. Gronsky.)

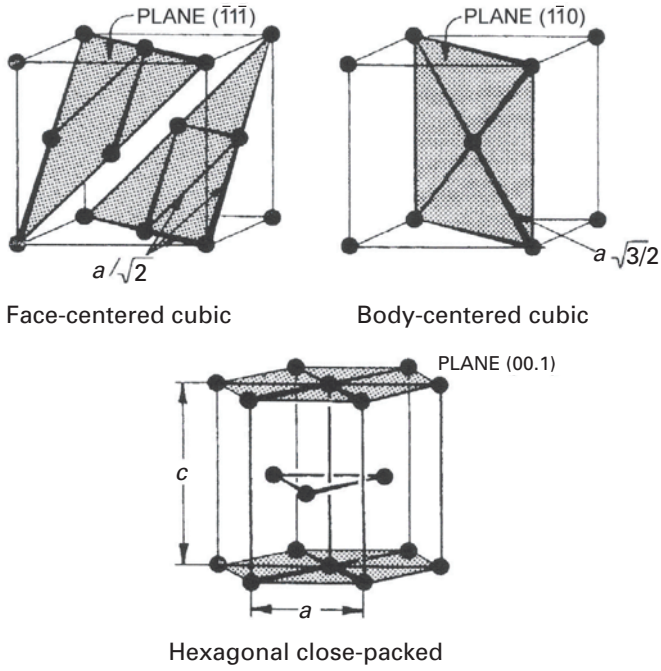


**Figure 1.12** Most closely packed planes in (a) FCC; (b) BCC; (c) HCP.

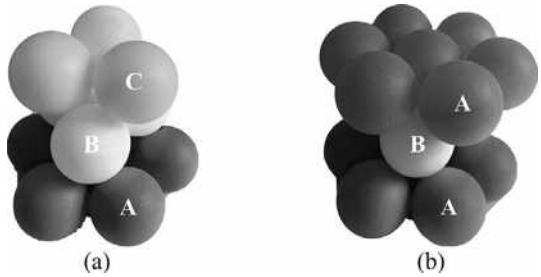


**Figure 1.13** Ball models showing stacking sequence in FCC and HCP structures. (© Sheron Tavares.)
(a) Layers of most closely packed atoms corresponding to (111) in FCC, forming ABC sequence.
(b) Corresponding layers for basal planes in HCP structure, forming ABAB sequence.

Figure 1.12 shows the three main metallic structures. The positions of the atoms are marked by small spheres and the atomic planes by dark sections. The small spheres do not correspond to the scaled-up size of the atoms, which would almost completely fill the available space, touching each other. For the FCC and HCP structures, the coordination number (the number of nearest neighbors of an atom) is 12; for the BCC structure, it is 8.

The ABC sequence of the FCC structure is also revealed in the three-layer model of Figure 1.13(a). The bottom layer (A) is formed of close-packed atoms. The middle layer (B) is also formed of close-packed atoms, whereas the top layer sits on top of three atoms of the B layer. The position of this atom does not correspond to a position in the A or B layers and therefore forms a separate layer C. This is the signature of the FCC structure. On the other hand, the HCP structure can be represented by the ABAB sequence. The third layer is in exact correspondence to the first layer (Figure 1.13(b)).

The planes with the densest packing are $(1\bar{1}1)$, $(1\bar{1}0)$, and (001) for the FCC, BCC, and HCP structures, respectively. These planes have an important effect on the directionality of deformation of the metal, as will be seen in Chapters 4 and 6. The distances between the nearest neighbors are also indicated in the figure. The reader should try to calculate them as an exercise. These distances are $a\sqrt{2}$, $(a\sqrt{3}/2)$, and $a$ for the FCC, BCC, and HCP structures, respectively.

The similarity between the FCC and HCP structures is much greater than might be expected from looking at the unit cells. Planes (111) for FCC and (001) for HCP have the same packing, as may be seen in Figure 1.13. The packing of a second plane similar to, and on top of, the first one (called *A*) can be made in two different ways; Figure 1.13 (a) indicates these two planes by the letters *B* and *C*. Hence, either alternative can be used. A third plane, when placed on top of plane *B*, would have two options: *A* or *C*. If the second plane is *C*, the third plane can be either *A* or *B*. If only the first and second layers are considered, the FCC and HCP structures are identical. If the position of the third layer coincides with that of the first (the *ABA* or *ACA* sequence), we have the HCP structure. Since this packing has to be systematically maintained in the lattice, one would have *ABABAB*... or *ACACAC*... If the third plane does not coincide with the first, we have one of two alternatives *ABC* or *ACB*. Since this sequence has to be systematically maintained, we have *ABCABCABC*... or *ACBACBACB*... This stacking sequence corresponds to the FCC structure. We thus conclude that the only difference between the FCC and HCP structures (the latter with a theoretical *c*/*a* ratio of 1.633) is the stacking sequence of the most densely packed planes. The difference resides in the next neighbors and in the greater symmetry of the FCC structure.

In addition to the metallic elements, intermediate phases and intermetallic compounds exist in great numbers, with a variety of structures. For instance, the beta phase in the copper-manganese-tin (Cu-Mn-Sn) system exhibits a special ordering for the composition $Cu_2MnSn$. The unit cell (BCC) is shown in Figure 1.14. However, the ordering of the Cu, Mn, and Sn atoms creates a super lattice composed of four BCC cells. This super lattice is FCC; hence, the unit cell for the ordered phase is FCC, whereas that for the disordered phase has a BCC unit cell. This ordering has important effects on the functional and structural (mechanical) properties and is discussed in Chapter 11. Although they are composed of three

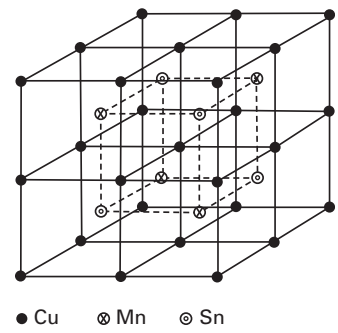


**Figure 1.14** $\beta$-ordered phase in Heusler alloys ($Cu_2MnSn$). (Reprinted from Observations on the ferromagnetic [beta] phase of the Cu-Mn-Sn system, *J. Appl. Cryst.* (1973). 6, 39–41, https://doi.org/10.1107/S0021889873008022, Copyright © International Union of Crystallography (1973).)

**Table 1.4 Some Important Intermetallic Compounds and Their Structures**

| Compound | Melting Point (°C) | Type of Structure |
|---|---|---|
| $Ni_3Al$ | 1,390 | $Ll_2$ (ordered FCC) |
| $Ti_3Al$ | 1,600 | $DO_{19}$ (ordered hexagonal) |
| TiAl | 1,460 | $Ll_0$ (ordered tetragonal) |
| Ni-Ti | 1,310 | CsCl |
| $Cu_3Au$ | 1,640 | $B_2$ (ordered BCC) |
| FeAl | 1,250–1,400 | $B_2$ (ordered BCC) |
| NiAl | 1,380–1,638 | $B_2$ (ordered BCC) |
| $MoSi_2$ | 2,025 | $C11_b$ (tetragonal) |
| $Al_3Ti$ | 1,300 | $DO_{22}$ (tetragonal) |
| $Nb_3Sn$ | 2,134 | $A1_5$ |
| $Nb_5Si_3$ | 2,500 | (tetragonal) |

nonferromagnetic elements, they are ferromagnetic. Heusler alloys were a scientific curiosity until 1984. It was discovered that they have spintronic properties and may lead the way to more efficient computers where information is stored by the spin of the electron. So, Moore's law, which states that the number of transistors in a certain size of computers doubles every two years, can continue for a few more years.

Table 1.4 lists some of the most important intermetallic compounds and their structures. Intermetallic compounds have a bonding that is somewhat intermediate between metallic and ionic/covalent bonding, and have properties that are most desirable for high-temperature applications. Nickel and titanium aluminides are candidates for high-temperature applications in jet turbines and aircraft applications.

## Example 1.2

Determine the ideal $c/a$ ratio for the hexagonal structure.

***Solution:*** The atoms in the basal $A$ plane form a closely packed array, as do the atoms in the $B$ plane going through the mid plane. If we take three atoms in the basal plane, with an atom in the $B$ plane resting among them, we have constructed a tetrahedron. The sides of the tetrahedron are $2r = a$, where $r$ is the atomic radius. The height of this tetrahedron is $c/2$, since the distance between planes is $c$. Hence, the problem is now reduced to finding the height, $c/2$, of a regular tetrahedron. In Figure E1.2, we have

$$DF = \frac{C}{2}$$

$$AB = AC = BC = AD = DB = DC = a.$$

## Example 1.2 (cont.)

**Figure E1.2**

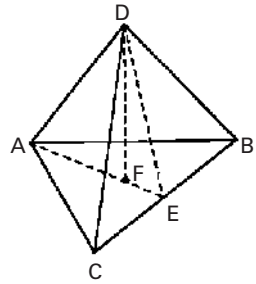


For triangle AEC,

$$AE^2 + EC^2 = AC^2$$

$$AE = \sqrt{a^2 - \frac{a^2}{4}} = \frac{a}{2}\sqrt{3.}$$

For triangle DFE,

$$EF^2 + DF^2 = DE^2.$$

But

$$EF = \frac{1}{3}AE = \frac{a}{6}\sqrt{3,}$$

$$DE = AE = \frac{a}{2}\sqrt{3,}$$

$$DF = \left(\frac{3a^2}{4} - \frac{3a^2}{36}\right)^{1/2},$$

$$\frac{c}{2} = a\left(\frac{2}{3}\right)^{1/2},$$

$$\frac{c}{a} = 2\left(\frac{2}{3}\right)^{1/2}.$$

Thus,

$$\frac{c}{a} = 1.633.$$

## Example 1.3

If the copper atoms have a radius of 0.128 nm, determine the density in FCC and BCC structures.

**(i)** In FCC structures, $4r = \sqrt{2}a_0$

$$a_0 = \frac{4}{\sqrt{2}}r = \frac{4}{\sqrt{2}} \times 0.128 \text{ nm}$$

$$a_0 = 0.362 \text{ nm}.$$

## Example 1.3 (cont.)

There are four atoms per unit cell in FCC. Atomic mass (or weight) of copper is 63.54 g $(g.mol)^{-1}$. So, the density of copper ($\rho$) in FCC structures is

$$\rho = \frac{63.54 \times 4}{\left(0.362 \times 10^{-7}\right)^3 \times \left(6.022 \times 10^{23}\right)} = 8.89 \text{ g cm}^{-3}.$$

↑
Avogadro's Number

**(ii)** In BCC structures, $4r = \sqrt{3}a_0$

$$a_0 = \frac{4}{\sqrt{3}}r = \frac{4}{\sqrt{3}} \times 0.128 \text{ nm}$$
$$a_0 = 0.296 \text{ nm}.$$

There are two atoms per unit cell in BCC structures.

$$\rho = \frac{63.54 \times 2}{\left(0.296 \times 10^{-7}\right)^3 \times \left(6.02 \times 10^{23}\right)} = 8.14 \text{ g cm}^{-3}.$$

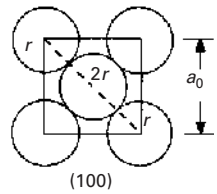


**Figure E1.3** The stable form of Cu is FCC. Only under unique conditions, such as Cu precipitates in iron, is the BCC form stable (because of the constraints of surrounding material).

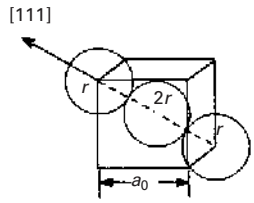


### 1.3.3 Ceramics

The name ceramic comes from the Greek *keramos* (pottery). The production of pottery made of clay dates from 6500 BCE. The production of silicate glass in Egypt dates from 1500 BCE The main ingredient of pottery is a hydrous aluminum silicate that becomes plastic when mixed, in fine powder form, with water. Thus, the early utilization of ceramics included both crystalline and glassy materials. Portland cement is also a silicate ceramic; by far the largest tonnage production of ceramics today – glasses, clay products (brick, etc.), cement – are silicate-based.

However, there have been dramatic changes since the 1970s and a wide range of new ceramics has been developed. These new ceramics are finding applications in

computer memories (due to their unique magnetic applications), in nuclear power stations ($UO_2$ fuel rods), in rocket nose cones and throats, in submarine sonar units (piezoelectric barium titanate), in jet engines (as coatings on metal turbine blades) as electronic packaging components ($Al_2O_3$, SiC substrates), as electrooptical devices (lithium niobate, capable of transforming optical into electrical information and vice versa), as optically transparent materials (ruby and yttrium garnet in lasers, optical fibers), as cutting tools (boron nitride, synthetic diamond, tungsten carbide), as refractories, as military armor ($Al_2O_3$, SiC, $B_4C$), and in a variety of structural applications.

The structure of ceramics is dependent on the character of the bond (ionic, covalent, or partly metallic), on the sizes of the atoms, and on the processing method. We will first discuss the crystalline ceramics.

## Example 1.4

Sketch the 12 members of the <110> family for a cubic crystal. Indicate the four {111} planes. You may use several sketches.

**Figure E1.4**

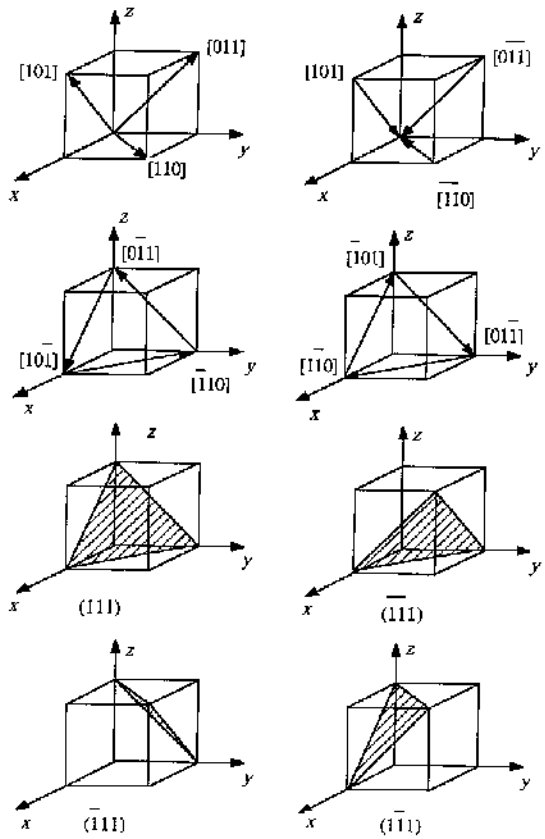

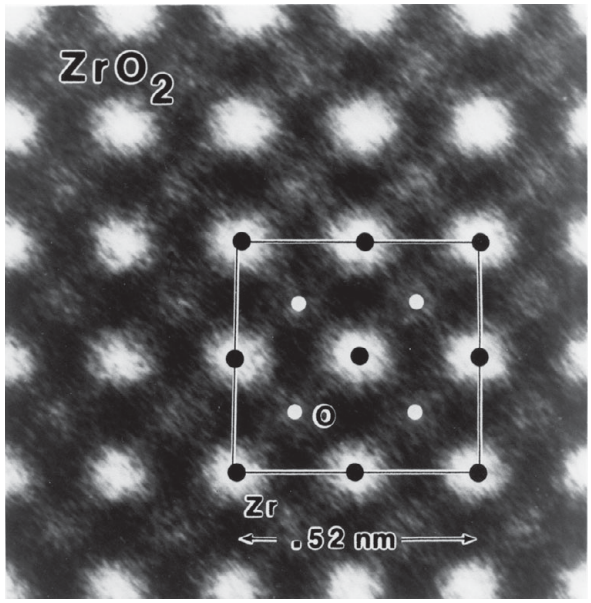


**Figure 1.15** Transmission electron micrograph of $ZrO_2$ at high resolution, showing individual Zr atoms and oxygen sites.
(Figure courtesy of R. Gronsky.)

Transmission electron microscopy has reached the point of development where we can actually image individual atoms, and Figure 1.15 shows a beautiful picture of the zirconium atoms in $ZrO_2$.The much lighter oxygen atoms cannot be seen but their positions are marked in the electron micrograph. By measuring the atomic distances along two orthogonal directions, one can see that the structure is not cubic, but tetragonal. The greater complexity of ceramics, in comparison to metallic structures, is evident from Figure 1.15. Atoms of different sizes have to be accommodated by a structure, and bonding (especially covalent) is highly directional. We will first establish the difference between ionic and covalent bonding.

The electronegativity value is a measure of an atom's ability to attract electrons. Compounds in which the atoms have a large difference in electronegativity are principally ionic, while compounds with the same electronegativity are covalent. In ionic bonding one atom loses electrons and is therefore positively charged (cation). The atom that receives the electrons becomes negatively charged (anion). The bonding is provided by the attraction between positive and negative charges, compensated by the repulsion between charges of equal signs. In covalent bonding the electrons are shared between the neighboring atoms. The quintessential example of covalent bonding is diamond. It has four electrons in the outer shell, which combine with four neighboring carbon atoms, forming a tridimensional regular diamond structure, which is a complex cubic structure. Figure 1.16 shows the diamond structure. The bond angles are fixed and equal to 70° 32'. The covalent bond is the strongest bond, and diamond has the highest hardness of all natural materials. There are synthetic materials that have an even higher hardness, such as graphene and some nanocrystalline structures. Another material that has covalent bonding is SiC.

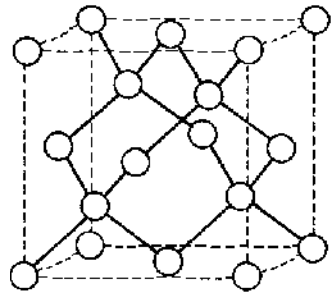

**Figure 1.16** Crystal structure of diamond.

## Example 1.5

(a) Calculate the packing factor of the diamond cubic structure. (b) Calculate the density of diamond. The atomic weight of carbon is 12 g $mol^{-3}$, and the lattice parameter of diamond is 0.357 nm at 300 K.

**Figure E1.5**

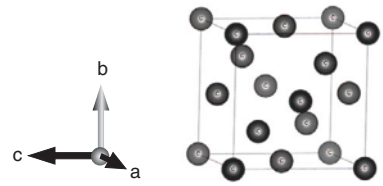


### *Solution:*

**(a)** 8 atoms/cell (4 from FCC + 4 at 1/4, 1/4, 1/4 from FCC atoms).
Nearest neighbor distance:

$$2r = \frac{a\sqrt{3}}{4}$$

$$r = \frac{a\sqrt{3}}{8}.$$

$$\text{Atomic packing factor (APF)} = \frac{\frac{4\pi}{3}\left(\frac{a\sqrt{3}}{8}\right)^{3*}8}{a^3} = \frac{\pi\sqrt{3}}{16} = 0.34.$$

**(b)**

$$\rho\ (\text{g cm}^{-3}) = \frac{m}{V} = \frac{\sum_{i=1}^{N} N_i A_i (\text{g mol}^{-1})}{(a\ \text{nm})^{3*}\left(\frac{1}{1*10^7\,\text{nm}}\right)^{3*}(6.022*10^{23}\,\text{g mol}^{-1})}$$

$$\rho = \frac{(8\ \text{atoms})*(12\ \text{g mol}^{-1})}{(0.357\ \text{nm})^{3*}\left(\frac{1\ \text{cm}}{1*10^7\,\text{nm}}\right)^{3*}(6.022*10^{23}\ \text{g mol}^{-1})} = 3.503\ \text{g cm}^{-3}.$$

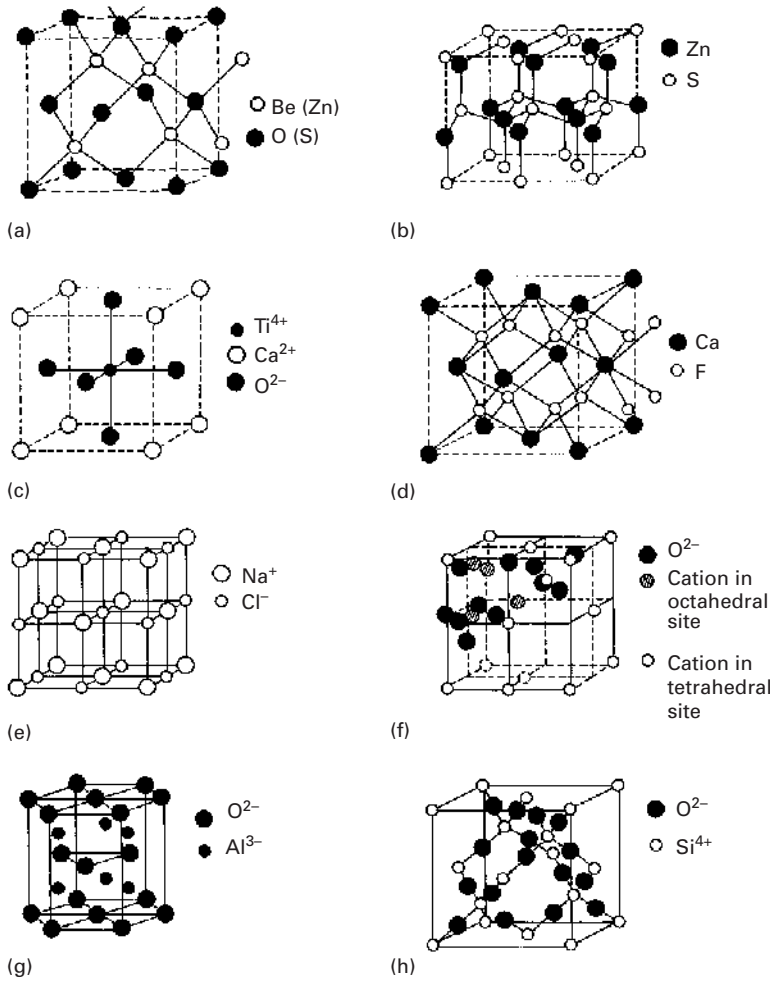


**Figure 1.17** Most common structures for ceramics. (a) Zinc blende (ZnS, BeO, SiC). (b) Wurtzite (ZnS, ZnO, SiC, BN). (c) Perovskite ($CoTiO_3$, $BaTiO_3$, $YCu_2Ba_3O_{7-x}$). (d) Fluorite ($ThO_2$, $UO_2$, $CeO_2$, $ZrO_2$, $PuO_2$). (e) NaCl (KCl, LiF, KBr, MgO, CaO, VO, MnO, NiO). (f) Spinel ($FeAl_2O_4$, $ZnAl_2O_4$, $MoAl_2O_4$). (g) Corundum ($Al_2O_3$, $Fe_2O_3$, $Cr_2O_3$, $Ti_2O_3$, $V_2O_3$). (h) Crystobalite ($SiO_2$-quartz). The CsCl stucture, which has one $Cs^+$ surrounded by four $Cl^-$ ions in cube edges, is not shown.

As the difference of electronegativity is increased, the bonding character changes from pure covalent to covalent-ionic, to purely ionic. Ionic crystals have a structure determined largely by opposite charge surrounding an ion. These structures are therefore established by the maximum packing density of ions. Compounds of metals with oxygen (MgO, $Al_2O_3$, $ZrO_2$, etc.) and with group VII elements (NaCl, LiF, etc.) are largely ionic. The most common structures of ionic crystals are presented in Figure 1.17. Evidently, there are more complex structures in ceramics than in metals because the combinations possible between the elements are so vast.

Ceramics also exist in the glassy state. Silica in this state has the unique optical property of being transparent to light, which is used technologically to great advantage. The building blocks of silica in crystalline and amorphous forms are the silica tetrahedra. Silicon bonds to four oxygen atoms, forming a tetrahedron. The oxygen atoms bond to just two silicon atoms. Numerous structures are possible, with different arrangements of the tetrahedra. Pure silica crystallizes into quartz, crystobalite, and tridymite. Because of these bonding requirements, the structure of silica is fairly open and, consequently, gives the mineral a low density. Quartz has a density of 2.65 g $cm^{-3}$,

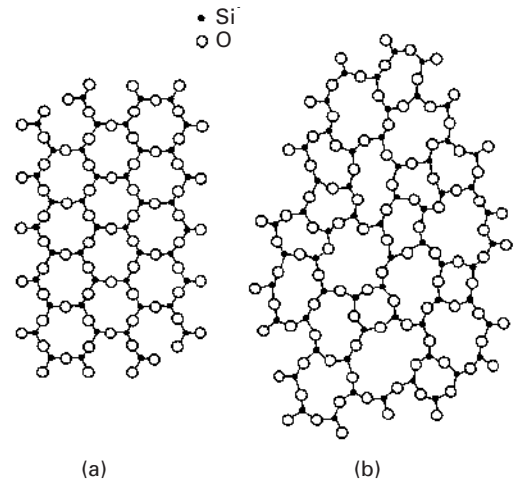


**Figure 1.18** Schematic two-dimensional representation of (a) ordered crystalline and (b) random-network glassy forms of silica.

compared with 3.59 g cm$^{-3}$ and 3.92 g cm$^{-3}$, for MgO and $A1_2O_3$, respectively. The structure of crystobalite (Figure 1.17(h)) shows clearly that each Si atom (open circle) is surrounded by four oxygen atoms (filled circles), while each oxygen atom binds two Si atoms. A complex cubic structure results. However, an amorphous structure in silica is more common when the mineral is cooled from the liquid state. Condensation of vapor on a cold substrate is another method by means of which thin, glassy films are made. One can also obtain glassy materials by electrodeposition, as well as by chemical reaction. Chapter 3 describes glassy metals in greater detail. Figure 1.18 provides a schematic representation of silica in its crystalline and glassy forms in an idealized two-dimensional pattern. The glassy state lacks long-range ordering; the three-dimensional silica tetrahedra arrays lack both symmetry and periodicity.

## Example 1.6

Determine the C–C–C–bonding angle in polyethylene.

***Solution:*** The easiest manner to visualize the bonding angle is to assume that one C atom is in the center of a cube and that it is connected to four other C atoms at the edges of the cube (see Figure E1.6 1) Suppose all angles are equal to $\alpha$.

**Figure E1.6**

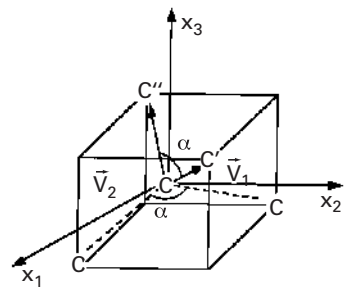

## Example 1.6 (cont.)

The problem is best solved vectorially. We set the origin of the axes at the center of the carbon atom and have two vectors connecting it to neighboring C atoms.

The angle between two vectors is (see Chapter 6 or any calculus text)

$$\cos\alpha = \frac{\frac{1}{2}\left(-\frac{1}{2}\right) + \frac{1}{2}\left(-\frac{1}{2}\right) + \frac{1}{2}\cdot\frac{1}{2}}{\sqrt{\frac{1}{4}+\frac{1}{4}+\frac{1}{4}}\cdot\sqrt{\frac{1}{4}+\frac{1}{4}+\frac{1}{4}}} = -\frac{1}{3}.$$

So

$$\alpha = 109.47^{\circ}.$$

(*Note*: When we have double bonds, the angle is changed.)

### 1.3.4 Glasses

As described earlier, glasses are characterized by a structure in which no long-range ordering exists. There can be short-range ordering, as indicated in the individual tetrahedral arrays of $SiO_4^{-4}$ in Figure 1.18, which shows both the crystalline and glassy forms of silica. Over distances of several atomic spacings, the ordering disappears, leading to the glassy state. It is possible to have glassy ceramics, glassy metals, and glassy polymers.

The structure of glass has been successfully described by the *Zachariasen* model. The *Bernal* model is also a successful one. It consists of drawing lines connecting the centers of adjacent atoms and forming polyhedra. These polyhedra represent the glassy structure of glass. Glassy structures represent a less efficient packing of atoms or molecules than the equivalent crystalline structures. This is very easily understood with the "suitcase" analog. We all know that by throwing clothes randomly into a suitcase, the end result is often a major job of sitting on the suitcase to close it. Neat packing of the same clothes occupies less volume. The same happens in glasses. If we plot the inverse of the density (called *specific volume*) versus temperature, we obtain the plot shown in Figure 1.19. Contraction occurs as the temperature is lowered. If the

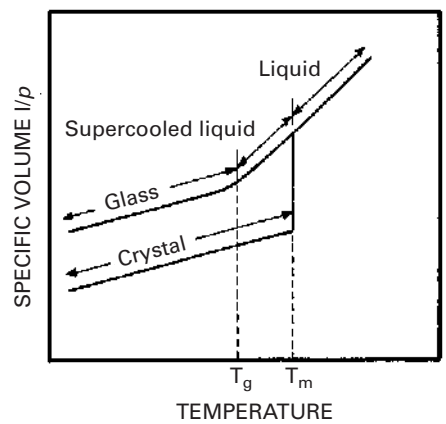


**Figure 1.19** Specific volume (inverse of density) as a function of temperature for glassy and crystalline forms of a material.

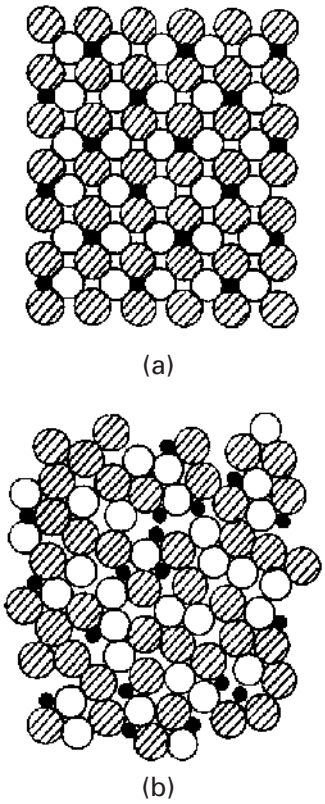


**Figure 1.20** Atomic arrangements in crystalline and glassy metals. (a) Crystalline metal section. (b) Glassy metal section. (Figure courtesy of L. E. Murr.)

material crystallizes, there is a discontinuity in the specific volume at the melting temperature $T_m$. If insufficient time is allowed for crystallization, the material becomes a super-cooled liquid, and contraction follows the liquid line. At a temperature $T_g$, called the *glass transition temperature*, the super-cooled liquid is essentially solid, with very high viscosity. It is then called a glass. This difference in specific volume between the two forms is often referred to as *excess volume*.

In ceramics, reasonably low cooling rates can produce glassy structures. The regular arrangement of the silica tetrahedra in Figure 1.18(a) requires a significant amount of time. The same is true for polymeric chains, which need to organize themselves into regular crystalline arrangements. For metals, this is more difficult. Only under extreme conditions it is possible to obtain solid metals in a noncrystalline structure. Figure 1.20 shows a crystalline and a glassy alloy with the same composition. The liquid state is frozen in, and the structure resembles that of glasses. It is possible to arrive at these special structures by cooling the alloy at such a rate that virtually no reorganization of the atoms into periodic arrays can take place. The required cooling rate is usually on the order of $10^6$ to $10^8$ K $s^{-1}$. It is also possible to arrive at the glassy state by means of solid-state processing (very heavy deformation and reaction) and from the vapor.

The original technique for obtaining metallic glasses was called splat cooling and was pioneered by Duwez and students.[2] An alloy in which the atomic sizes are quite dissimilar, such as Fe-B, is ideal for retaining the "glassy" state upon cooling. This technique consisted of propelling a drop of liquid metal with a high velocity against a heat-conducting surface such as copper. The interest in these alloys was mainly academic at the time. However, the unusual magnetic properties and high strength exhibited by the alloys triggered worldwide interest, and subsequent research has resulted in thousands of papers. The splat-cooling technique has been refined to the point where 0.07 to 0.12 mm-thick wires can be ejected from an orifice. Production rates as high as 1,800 m $min^{-1}$ can be obtained. Sheets and ribbons can be manufactured by the same technique. An alternative technique consists of vapor deposition on a substrate (sputtering). This seems a most promising approach, and samples with a thickness of several millimeters have been successfully produced.

The cooling rates required for the formation of the traditional amorphous metals are in the range of 100–1000 K $s^{-1}$. Thus, a splat-cooling technique must be used and only very thin layers can be produced. However, research at Tohoku University and the California Institute of Technology (Caltech) has yielded alloys based on La, Mg, Zr, Pd, Fe, Cu, and Ti, with critical cooling rates of 1–100 K $s^{-1}$, comparable to oxide glasses. Thus, thicker parts (several cm) can be fabricated. These alloys are known as Bulk Metallic Glasses (BMGs). The Caltech alloys are known as Vitreloy (41.2% Zr, 13.8% Ti, 12.5% Cu, 10% Ni, and 22.5% Be) and have strengths of 1700 MPa. Comparatively, $Ti_6Al_4V$ has a strength of 830 MPa. The bulk metallic glasses (BMGs) have been extensively studied due to their promising application and research value. Due to their glass transition temperature ($T_g$), they exhibit excellent properties such as high strength at low temperatures and appreciable ductility at high temperatures. Examples of applications are golf clubs, which have extraordinarily high coefficient of restitution.

### 1.3.5 Polymers

From a microstructural point of view, polymers are much more complex than metals and ceramics. On the other hand, they are cheap and easily processed. Polymers have lower strengths and moduli and lower temperature use limits than do metals or ceramics. Because of their predominantly covalent bonding, polymers are generally poor conductors of heat and electricity. Polymers are generally more resistant to chemicals than are metals, but prolonged exposure to ultraviolet light and some solvents can cause degradation of a polymer's properties.

#### Chemical Structure

Polymers are giant chain-like molecules (hence, the name *macromolecules*), with covalently bonded atoms forming the backbone of the chain. Polymerization is the

[2] W. Klement, R. H. Willens, and P. Duwez, *Nature*, 187 (1960) 869.

process of joining together many monomers, the basic building blocks of polymers, to form the chains. For example, the ethyl alcohol monomer ($C_2H_3OH$) has the chemical structure:

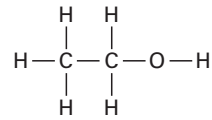

This yields the polymer polyethylene.

The monomer vinyl chloride has the chemical formula $C_2H_3Cl$, which, on polymerization, becomes polyvinyl chloride (PVC). The chemical structure of polyvinyl chloride is represented by:

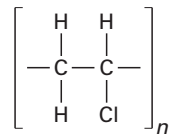

where $n$ is the degree of polymerization. There are numerous polymers with widely different properties: polyvinyl chloride (PVC), polystyrene (PS), poly(propylene) PP, polyether ether ketone (PEEK), etc.

## Types of Polymers

The difference in the behavior of polymers stems from their molecular structure and shape, molecular size and weight, and amount and type of bond (covalent or van der Waals). The different chain configurations are shown in Figure 1.21. A *linear polymer* consists of a long chain of atoms with attached side groups (Figure 1.21(a)). Examples include polyethylene, polyvinyl chloride, and polymethyl methacrylate. Note the coiling and bending of the chain. *Branched polymers* have branches attached to the main chain (Figure 1.21(b)). Branching can occur with linear, cross-linked, or any other types of polymers. A *crossed-linked* polymer has molecules of one chain bonded with those of another (Figure 1.21 (c)). Cross-linking of molecular chains results in a three-dimensional network. It is easy to see that cross-linking makes sliding of molecules past one another difficult, resulting in strong and rigid polymers. *Ladder polymers* have two linear polymers linked in a regular manner (Figure 1.21(d)). Not unexpectedly, ladder polymers are more rigid than linear polymers.

Yet another classification of polymers is based on the type of the repeating unit (see Figure 1.22). When we have one type of repeating unit, for example, *A*, forming the polymer chain, we call it a *homo polymer. Copolymers*, on the other hand, are polymer chains having two different monomers. If the two different monomers, *A* and *B*, are distributed randomly along the chain, then we have a *regular*, or *random, copolymer*. If, however, a long sequence of one monomer *A* is followed by a long sequence of another monomer *B*, we have a *block copolymer*. If we have a chain of one type of monomer *A* and branches of another type *B*, then we have a *graft copolymer*.

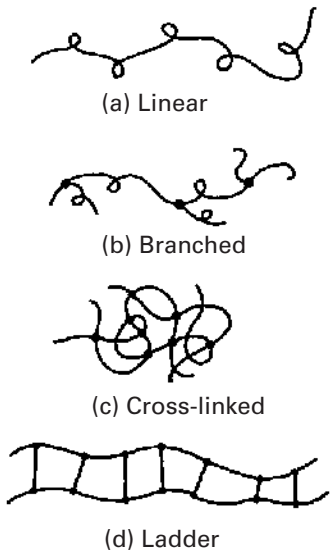


**Figure 1.21** Different types of molecular chain configurations.

(a) Homopolymer −A−A−A−A−A−A−A−

(b) Random copolymer −A−A−B−A−B−B−A−B−B−A−

(c) Block copolymer −A−A−A−A−B−B−B−B−B−

(d) Graft copolymer

```
−A−A−A−A−A−A−A−A−
      |       |
      B       B
      |       |
      B       B
      |       |
      B       B
      |       |
```

**Figure 1.22** (a) Homopolymer: one type of repeating unit. (b) Regular copolymer: two monomers, *A* and *B*, distributed randomly. (c) Block copolymer; a sequence of monomer B. (d) Graft copolymer; monomer *A* forms the main chain, while monomer *B* form the branched chain.

*Tacticity* has to do with the order of placement of side groups on a main chain. It can provide variety in polymers. Consider a polymeric backbone chain having side groups. For example, a methyl group ($CH_3$) can be attached to every second carbon atom in the polypropylene chain. By means of certain catalysts, it is possible to place the methyl groups all on one side of the chain or alternately on both sides, or to randomly distribute them in the chain. Figure 1.23 shows tacticity in polypropylene. When we have all the side groups on one side of the main chain, we have an *isotactic* polymer. If the side groups alternate from one side to another, we have a *syndiotactic* polymer. When the side groups are attached to the main chain in a random fashion, we get an *atactic* polymer.

## Thermosetting Polymers and Thermoplastics

Based on their behavior upon heating, polymers can be divided into two broad categories:

**(i)** thermosetting polymers,
**(ii)** thermoplastics.

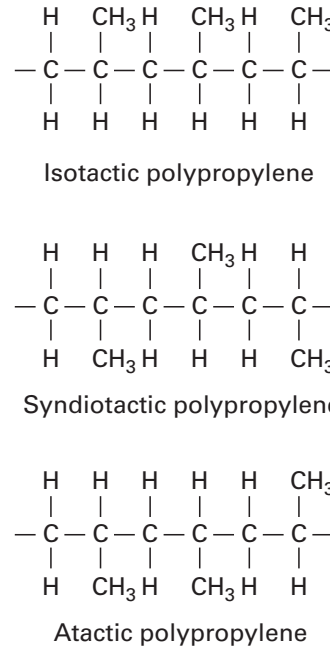


**Figure 1.23** Tacticity, or the order of placement of side groups.

When the molecules in a polymer are cross-linked in the form of a network, they do not soften on heating. We call these cross-linked polymers *thermosetting* polymers. Thermosetting polymers decompose upon heating. As mentioned earlier, cross-linking makes sliding of molecules past one another difficult, which produces a strong and rigid polymer. A typical example is rubber cross-linked with sulfur, i.e., vulcanized rubber. Vulcanized rubber has 10 times the strength of natural rubber. Common examples of thermosetting polymers include phenolic, polyester, polyurethane, and silicone. Polymers that soften or melt upon heating are called *thermoplastics*. Suitable for liquid flow processing, they are mostly linear polymers, for example, low and high-density polyethylene and polymethyl methacrylate (PMMA).

Polymers can have an amorphous or partially crystalline structure. When the structure is amorphous, the molecular chains are arranged randomly, i.e., without any apparent order. Thermosetting polymers, such as epoxy, phenolic, and unsaturated polyester, have an amorphous structure. Semicrystalline polymers can be obtained by using special processing conditions. For example, by precipitating a polymer from an appropriate dilute solution, we can obtain small, plate-like crystalline lamellae, or crystallites. Such solution-grown polymer crystals are characteristically small. Figure 1.24 shows a transmission electron micrograph of a lamellar crystal of poly ($\varepsilon$-caprolactone). Note the formation of new layers of growth spirals around screw dislocations. The screw dislocations responsible for crystal growth are perpendicular to the plane of the micrograph. Polymeric crystals involve molecular chain packing, rather than the atomic packing characteristic of metals. Molecular

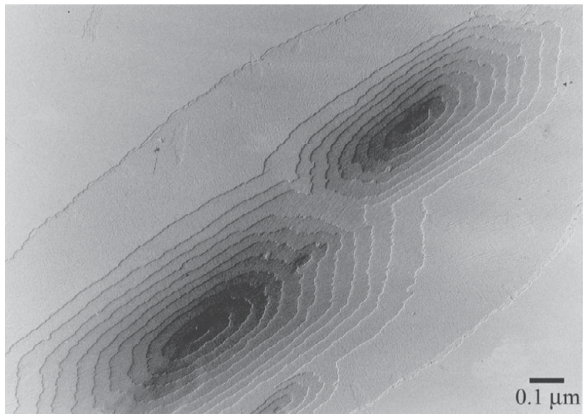


**Figure 1.24** Electron micrograph of a lamellar crystal showing growth spirals around screw dislocations.
(Figure courtesy of H. D. Keith.)

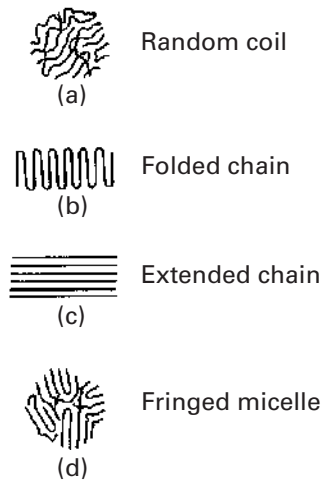


**Figure 1.25** Some important chain configurations.
(a) A flexible coiled chain structure. (b) A folding chain structure. (c) An extended and aligned chain structure.
(d) A fringed micelle chain structure.

chain packing requires a sufficiently stereographic regular chemical structure. Solution-grown polymeric crystals generally have a lamellar form, and the long molecular chains crystallize by folding back and forth in a regular manner. Lamellar polymeric crystals have straight segments of molecules oriented normal to the lamellar panes. Figure 1.25 depicts some important chain configurations in a schematic manner. The flexible, coiled structure is shown in Figure 1.25(a), while the chain-folding configuration that results in crystalline polymers is shown in Figure 1.25(b). Under certain circumstances, one can obtain an extended and aligned chain structure, shown in Figure 1.25(c). Such a structure, typically obtained in fibrous form, has very high strength and stiffness. A semi-crystalline configuration called a fringed micelle structure is shown in Figure 1.25(d). Almost all so-called semicrystalline polymers are, in reality, mixtures of crystalline and amorphous regions. Only by using very special techniques, such as solid-state polymerization, is it possible to prepare a 100% crystalline polymer. Polydiacetylene single crystals in the form of lozenges and fibers have been prepared by solid-state polymerization.

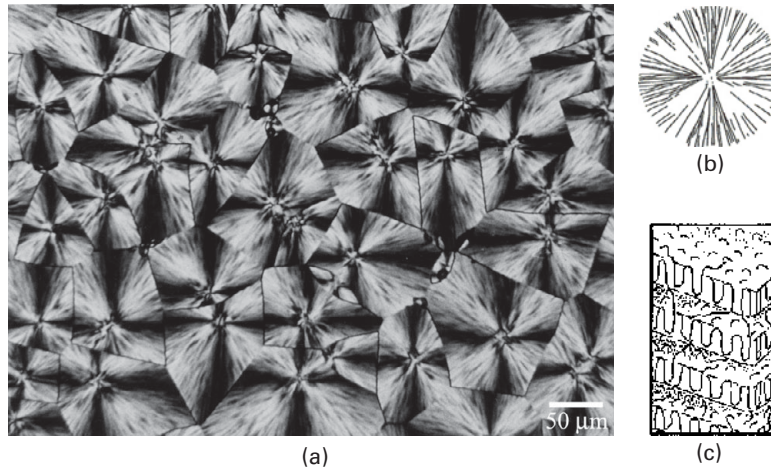


**Figure 1.26** Spherulitic structures.(a) A typical spherulitic structure in a melt-formed polymer film. (Figure courtesy of H. D. Keith.) (b) Schematic of a spherulite. Each spherulite consists of an assembly of radially arranged narrow crystalline lamellae. (c) Each lamella has tightly packed polymer chains folding back and forth. Amorphous regions fill the spaces between the crystalline lamellae.

Partially crystallized, or semicrystalline, polymers can also be obtained from melts. Generally, because of molecular chain entanglement, the melt-formed crystals are more irregular than those obtained from dilute solutions. A characteristic feature of melt-formed polymers is the formation of spherulites. When seen under cross-polarized light in an optical microscope, the classical spherulitic structure shows a Maltese cross pattern (see Figure 1.26(a). Figure 1.26(b) presents a schematic representation of a spherulite whose diameter can vary between a few tens to a few hundreds of micrometers. Spherulites can nucleate at a variety of points, as, for example, with dust or catalyst particles, in a quiescent melt and then grow as spheres. Their growth stops when the neighboring spherulites impinge upon each other. Superficially, the spherulites look like grains in a metal. There are, however, differences between the two. Each grain in a metal is a single crystal, whereas each spherulite in a polymer is an assembly of radially arranged, narrow crystalline lamellae. The fine-scale structure of these lamellae, consisting of tightly packed chains folding back and forth, is shown in Figure 1.26(c). Amorphous regions containing tangled masses of molecules fill the spaces between the crystalline lamellae.

## Degree of Crystallinity

The *degree of crystallinity* of a material can be defined as the fraction of the material that is fully crystalline. This is an important parameter for semicrystalline polymers. Depending on their degree of crystallinity, such polymers can show a range of densities, melting points, etc. It is worth repeating that a 100% crystalline polymer is very difficult to obtain in practice. The reason for the difficulty is the long chain

structure of polymers: some twisted and entangled segments of chains that get trapped between crystalline regions never undergo the conformational reorganization necessary to achieve a fully crystalline state. Molecular architecture also has an important bearing on a polymer's crystallization behavior. Linear molecules with small or no side groups crystallize easily. Branched chain molecules with bulky side groups do not crystallize as easily. For example, linear, high-density polyethylene can be crystallized to 90%, while branched polyethylene can be crystallized only to about 65%. Generally, the stiffness and strength of a polymer increase with the degree of crystallinity.

Like crystalline metals, crystalline polymers have imperfections. It is, however, not easy to analyze these defects, because the topological connectivity of polymer chains leads to large amounts and numerous types of disorder. Polymers are also very sensitive to damage by the electron beam in transmission electron microscopy (TEM), making it difficult to image them. Generally, polymer crystals are highly anisotropic. Because of covalent bonding along the backbone chain, polymeric crystals show low-symmetry structures, such as orthorhombic, monoclinic, or triclinic. Deformation processes such as slipping and twinning, as well as phase transformations that take place in monomeric crystalline solids, may also occur in polymeric crystals.

## Molecular Weight and Distribution

Molecular weight is a very important attribute of polymers, especially because it is not so important in the treatment of nonpolymeric materials. Many mechanical properties increase with molecular weight. In particular, resistance to deformation does so. Of course, concomitant with increasing molecular weight, the processing of polymers becomes more difficult.

The molecular weight of a polymer is given by the product of the molecular weight of the repeat unit (the ""mer") and the number of repeat units. The molecular weight of the ethylene repeat unit ($-CH_2-CH_2-$) is 28. We write the chemical formula: $H(-CH_2-CH_2-)_nH$. If $n$, the number of repeat units, is 10,000, the high-density polyethylene will have a molecular weight of 280,002. In almost all polymers, the chain lengths are not equal, but rather, there is a distribution of chain lengths. In addition, there may be more than one species of chain in the polymer. This makes for different parameters describing the molecular weight.

The number-averaged molecular weight ($M_n$) of a polymer is the total weight of all of the polymer's chains divided by the total number of chains:

$$M_n = \sum N_i, M_i / \sum N_i$$

where $N_i$ is the number of chains of molecular weight $M_i$.

The weight-averaged molecular weight ($M_w$) is the sum of the square of the total molecular weight divided by the total molecular weight. Thus,

$$M_w = \sum N_i M_i^2 / \sum M_i N_i.$$

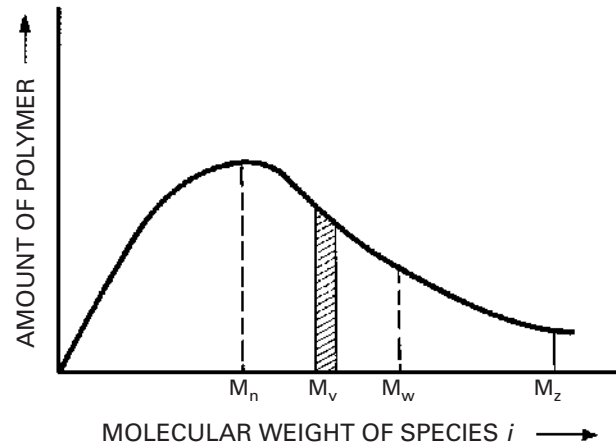


**Figure 1.27** A schematic molecular weight distribution curve. Various molecular weight parameters are indicated.

Two other molecular weight parameters are

$$M_z = \sum N_i M_i^3 / \sum N_i M_i^2$$

and

$$M_v = \left[ \sum N_i M_i^{(1+a)} / \sum N_i M_i \right]^{1/a},$$

where $a$ has a value between 0.5 and 0.8.

Typically, $M_n$:$M_w$:$M_z$ = 1:2:3. Figure 1.27 shows a schematic molecular weight distribution curve with various molecular weight parameters indicated. Molecular weight distributions of the same polymer obtained from two different sources can be very different. Also, molecular weight distributions are not necessarily single peaked. For single-peaked distributions, $M_n$ is generally near the peak that is, the most probable molecular weight. The weight-averaged molecular weight, $M_w$, is always larger than $M_n$. The molecular weight characterization of a polymer is very important. The existence of a very high molecular-weight tail can make processing very difficult because of the enormous contribution of the tail to the melt viscosity of a polymer. The low end of the molecular-weight distribution, however, can be used as a plasticizer.

It is instructive to compare some monomers with low- and high-molecular-weight polymers. A very common monomer is a molecule of water, $H_2O$, with a molecular weight of 18. Benzene, on the other hand, is a low-molecular-weight organic solvent; its molecular weight is 78. By contrast, natural rubber has a molecular weight of about $10^4$, and polyethylene, a common synthetic polymer, can have a molecular weights greater than this. Polymers having such large molecular weights are sometimes called *high polymers*. Their molecular size is also very great.

It is interesting that the acetabular cup in total hip replacement, usually made of PE, has a performance that is highly dependent on its molecular weight. The life expectancy in high-molecular-weight polyethylene (HMWPE) is increased significantly for UHMWPE.

## Example 1.7

A polymer has three species of molecular weights: $3\times10^6$, $4\times10^6$, and $5\times10^6$. Compute its number-averaged molecular weight $M_n$ and weight-averaged molecular weight $M_w$.

***Solution:*** For the number-averaged molecular weight, we have

$$M_n = \frac{\sum N_i M_i}{\sum N_i} = \frac{3\times10^6 + 4\times10^6 + 5\times10^6}{3} = 4\times10^6.$$

The weight-averaged molecular weight is

$$M_w = \frac{\sum N_i M_i^2}{\sum N_i M_i} = \frac{(3\times10^6)^2 + (4\times10^6)^2 + (5\times10^6)^2}{3\times10^6 + 4\times10^6 + 5\times10^6} = \frac{50\times10^{12}}{12\times10^6} = 4.17\times10^6.$$

## Example 1.8

Estimate the molecular weight of polyvinyl chloride with degree of polymerization, $n$, equal to 800.

***Solution:*** The molecular weight of each "mer" of polyvinyl chloride ($C_2H_3Cl$) is

$$2(12) + 3(1) + 35.5 = 62.5.$$

For $n = 800$, the molecular weight is $800 \times 62.5 = 50{,}000$ g mol$^{-1}$.

## Example 1.9

Discuss how a polymer's density changes as crystallization proceeds from the melt.

***Answer:***

The density increases and the volume decreases as crystallization proceeds. This is because the molecular chains are more tightly packed in the crystal than in the molten or noncrystalline polymer. This phenomenon is, in fact, exploited in the so-called *density* method to determine the degree of crystallinity.

## Quasi Crystals

Quasi crystals represent a new state of solid matter. In a crystal, the unit cells are identical, and a single unit cell is repeated in a periodic manner to form the crystalline structure. Thus, the atomic arrangement in crystals has positional and orientational order. Orientational order is characterized by a rotational symmetry; that is, certain rotations leave the orientations of the unit cell unchanged. The theory of crystallography holds that crystals can have twofold, threefold, fourfold, or sixfold axes of rotational symmetry; a fivefold rotational symmetry is not allowed. A two-dimensional analogy of this is that one can tile a bathroom wall using a single shape of tile *if and only if* the tiles are rectangles (or squares), triangles, or hexagons, but not if the tiles are pentagons. One may obtain a glassy structure by rapidly cooling a vapor or liquid well below its melting point, until the disordered atomic arrangement characteristic of the vapor or liquid state gets frozen in. The atomic packing in the glassy state is dense but random. This can be likened to a mosaic formed by taking an infinite number of different shapes of tile and randomly joining them together. Clearly, the concept of a unit cell will not be valid in such a case. The atomic structure in the glassy state will have neither positional nor orientational order.

Quasi crystals are not perfectly periodic, but they do follow the rigorous theorems of crystallography. They can have any rotational symmetry axes which are prohibited in crystals. It is worth reminding the reader that a glassy structure shows an electron diffraction pattern consisting of diffuse rings for all orientations. A crystalline structure has an electron diffraction pattern that depends on the crystal symmetry.

Schectman et al. discovered that a rapidly solidified (melt-spun) aluminum-manganese alloy showed fivefold symmetry axis.[3] They observed a metastable phase that showed a sharp electron diffraction pattern with a perfect icosahedral symmetry. (Remember that sharp electron diffraction patterns are associated with the orderly atomic arrangement in crystals and icosahedral symmetry is forbidden in crystals.) At first, this was thought to be a paradox. However, some very careful and sophisticated electron microscopy work showed conclusively that it was indeed an icosahedral (20-fold) symmetry. Al-Mn alloys containing 18 to 25.3 wt% Mn examined by transmission electron microscopy showed the same anomalous diffraction. In particular, Al-25.3 wt% Mn alloy consisted almost entirely of one phase which has a composition close to $Al_6Mn$. The selected area diffraction pattern of $Al_6Mn$ showed a fivefold symmetry. This new kind of structure is neither amorphous nor crystalline; rather, the new phase in this alloy had a three-dimensional icosahedral symmetry.

Perhaps, it would be in order for us to digress a bit and explain this icosahedral symmetry. *Icosahedral* means 20 faces. An icosahedron has 20 triangular faces, 30 edges, and 12 vertices. Consider the two-dimensional case. As pointed out earlier,

[3] D. Schectman, I. A. Blech, D. Gratias, and J. W. Cahn, *Phys. Rev. Lett.*, 53 (1984) 1951.

one can tile a bathroom wall without leaving an open space (a *crack*) with hexagons. Three hexagons can be tightly packed without leaving a crack. Three pentagons, however, cannot be tightly packed. The reader may try this out. In three dimensions, four spheres pack tightly to form a tetrahedron; 20 tetrahedrons can, with small distortions, fit tightly into an icosahedron. Icosahedrons have fivefold symmetry (five triangular faces meet at each vertex) and they *cannot* fit together tightly, i.e., complete space filling is not possible with them. An icosahedron, therefore, cannot serve as a unit cell for a crystalline structure. Therefore, such structures are known as quasi crystals.

### 1.3.6 Liquid Crystals

A liquid crystal is a state of matter that shares some properties of liquids and crystals. Like all liquids, liquid crystals are fluids; however, unlike ordinary liquids, which are isotropic, liquid crystals can be anisotropic. Liquid crystals are also called *mesophases*. The liquid crystalline state exists in a specific temperature range, below which the solid crystalline state prevails and above which the isotropic liquid state prevails. That is, the liquid crystal has an order between that of a liquid and a crystalline solid. In a crystalline solid, the atoms, ions, or molecules are arranged in an orderly manner. This very regular three-dimensional order is best described in terms of a crystal lattice. Because of a different periodic arrangement in different directions, most crystals are anisotropic. Now consider a crystal lattice with rod-shaped molecules at the lattice points. In this case, we now have, in addition to a positional order, an orientational order. An analogy that is used to qualitatively describe the order in a liquid crystal is as follows. If a random pile of pencils is subjected to an external force, it will undergo an ordering process very much akin to that seen in liquid crystals. The pencils, long and rigid, tend to align themselves, with their long axes approximately parallel. By far the most important characteristic of liquid crystals is that their long molecules tend to organize according to certain patterns. The order of orientation is described by a directed line segment called the *director*. This order is the source of the rather large anisotropic effect in liquid crystals, a characteristic that is exploited in electrooptical displays or so-called liquid-crystal displays. Another important application of liquid crystals is the production of strong and stiff organic fibers such as aramid fiber, in which a rigid, rod-like molecular arrangement is provided by an appropriate polymer solution in the liquid crystalline state.[4] When a polymer manifests the liquid-crystalline order in a solution, we call it a *lyotropic* liquid crystal, and when the polymer shows the liquid crystalline state in the melt, it is called a *thermotropic* liquid crystal. The three types of order in the liquid crystalline state are nematic, smectic, and cholesteric, shown schematically in Figure 1.30. A nematic order is an approximately parallel array of polymer chains that remains disordered with regard to end groups or chain

[4] See K. K. Chawla, *Fibrous Materials* (Cambridge, U.K.: Cambridge University Press, 1998).

units; that is, there is no positional order along the molecular axis. Figure 1.30(a) shows this type of order, with the director vector *n* as indicated. In smectic order, we have one-dimensional, long-range positional order. Figure 1.30(b) shows smectic-A order, which has a layered structure with long-range order in the direction perpendicular to the layers. In this case, the director is perpendicular to the layer. Other more complex smectics are B, C, D, F, and G. The director in these may not be perpendicular to the layer, or there may exist some positional order as well. Cholesteric-type liquid crystals, shown in Figure 1.30(c), have nematic order with a superimposed spiral arrangement of nematic layers; that is, the director *n*, pointed along the molecular axis, has a helical twist.

## 1.3.7 Biological Materials and Biomaterials

### Biological Materials: Unique Characteristics

Seven unique aspects of biological materials distinguish them from their synthetic counterparts. It is through the understanding of each of them that we are advancing our knowledge with the goal of generating novel bioinspired materials and designs. These defining aspects comprise the Arzt heptahedron, presented in Figure 1.28. They are:

- *Evolution and environmental constraints*. Biological materials developed through a multimillion year process of evolution, driven by natural selection.

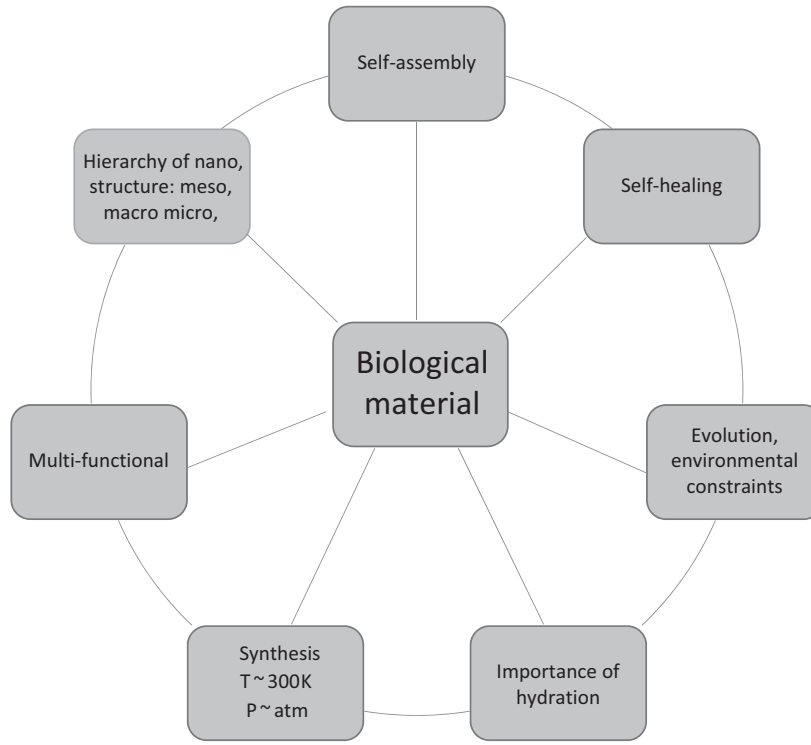


**Figure 1.28** Seven unique characteristics of biological materials: the Artz heptahedron.

- *Importance of hydration*. With notable exceptions, enamel and a few minerals, the level of hydration determines the mechanical properties.
- *Multifunctional.* Many tissues have more than one function, and this provides economy of space and mass.
- *Self-organization.* Nature uses a bottom-up approach to synthesize materials, whereas many of our processing methods are top-down. This bottom-up approach engenders self-organization and self-assembly.
- *Hierarchy of structure.* This is an aspect of utmost importance because it has direct relevance to mechanical properties. The structures at the nano, micro, meso, and ultra levels have different characteristics and work together synergistically.
- *Self-healing*. Many biological materials have a self-healing capability enabled by the cells and vascularity embedded in the extracellular matrix. Only a minute minority of synthetic materials have this capability.
- *Synthesis at ambient temperature and pressure.* Nature does not have at its disposal furnaces for high-temperature or autoclaves for high-pressure processing. Nor does she need them, since organisms exist mostly in a narrow range (–50 to +500 °C) of temperatures. There are isolated cases such as extremophiles and organisms living close to deep-sea vents, but they represent the exception. On the other hand, synthetic materials are designed to resist a variety of environments.

These unique characteristics render them intrinsically different from synthetic materials. Although there is a daunting variety of organisms (~8 million species), there are few recurring motifs in biological materials which have been identified.[5] This consists of seeking common structural designs in biological materials. Eight have been identified and are collectively named "structural design elements." They are amenable to analytical treatment and occur in different species through convergence and parallelism processes.

In spite of millions species of plants and animals on Earth, there is remarkable commonality in the structures observed among the diversity of biological materials. This is due to the fact that many different organisms have developed similar solutions to natural challenges. Our recent research has identified these common designs and named them *structural design elements*.

This new system new system of eight structural design elements enables a quantitative analytical treatment which can explain the mechanical properties, namely strength, stiffness, flexibility, fracture toughness, and energy absorption, of different biological materials for specific multifunctions (e.g. body support, joint movement, impact protection, mobility, flying). These structural design elements (visually displayed in Figure 1.29) are:

- *Fibrous* structures; offering high tensile strength when aligned in a single direction, with limited to nil compressive strength.

[5] M. A. Meyers, J. McKittrick, and P. Y. Chen, *Science*, 339 (2013) 773.

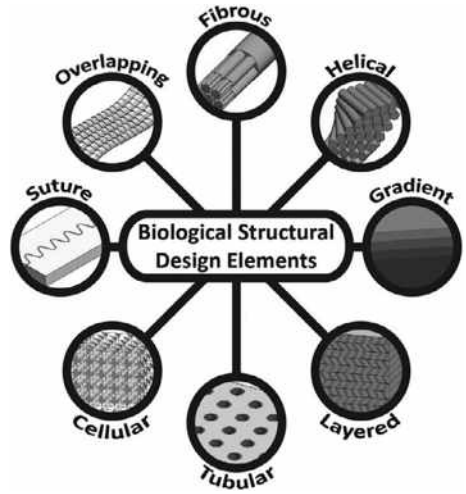


**Figure 1.29** The eight most common biological structural design elements.
(Reproduced from Marc A. Meyers, Joanna McKittrick, Michael M. Porter, et al, Structural Design Elements in Biological Materials: Application to Bioinspiration, *Advanced Materials*, Vol. 27, issue 37 (2015). With permission from John Wiley & Sons.)

- *Helical* structures; common to fibrous or composite materials, offering toughness in multiple directions and in-plane isotropy.
- *Gradient* structures; materials and interfaces that accommodate property mismatch (e.g. elastic modulus) through a gradual transition in order to avoid interfacial mismatch stress buildup, resulting in an increased toughness.
- *Layered* structures; complex composites that increase the toughness of (most commonly) brittle materials through the introduction of interfaces.
- *Tubular* structures; organized porosity that allows for energy absorption and crack deflection.
- *Cellular* structures; lightweight porous or foam architectures that provide directed stress distribution and energy absorption. These are often surrounded by dense layers to form sandwich structures.
- *Suture* structures; interfaces comprising wavy and interdigitating patterns that control the strength and flexibility.
- *Articulating* structures; featuring multiple plates or scutes that overlap to form flexible and often armored surfaces without interfaces.

As with all biological materials, these structural design elements are composed of biopolymers (e.g. collagen, chitin, keratin, cellulose) and biominerals (e.g. calcium carbonate, calcium phosphates, silica) that are hierarchically assembled from the nano to meso scales. However, the extraordinary mechanical properties observed in these natural materials are often a product of the intricate structural organization at higher spatial scales (micro, meso, and macro). As a result, in many cases organisms with different base materials will employ the same structure for the same purpose (e.g. tubules found in human dentin composed of hydroxyapatite/collagen and in a ram horns composed of keratin[6] can both absorb energy).

[6] S. E. Naleway, et al. *Adv Mat* 27.37 (2015) 5455–5476.

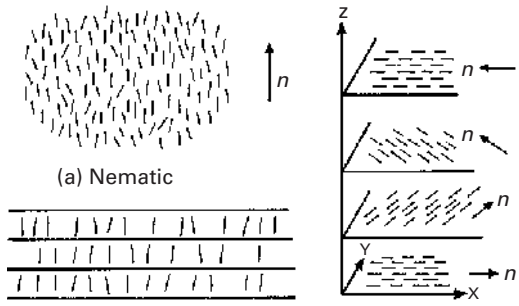


**Figure 1.30** Different types of order in the liquid crystalline state.

This is a new paradigm in the field of biological materials science: the structural design elements can serve as a toolbox for rationalizing the complex response of structural biological materials and for systematizing the development of bioinspired designs for structural applications. The ingenious manner by which these biocomposite structures are engineered is responsible for a mechanical response that is superior to that of synthetic materials

The mechanical properties of biological materials are, of course, of great importance, and the design of all living organisms is optimized for the use of these properties. Biological materials cover a very broad range of structures. The common feature is the hierarchical organization of the structure, so that failure at one level does not generate catastrophic fracture; the other levels in the hierarchy "take up" the load. Figure 1.31 demonstrates this fact. Figure 1.31(a) shows the response of the urether of three animals: guinea pig, dog, and rabbit. This muscle is a thick-walled cylindrical tube that has the ability to contract until the closure of the inner hole is complete. With a nonlinear elastic mechanical response, the urether is not unlike other soft tissues in that regard: its stiffness increases with loading, and the muscle becomes very stiff after a certain strain is reached. The unloading and loading responses are different, as shown in the figure, and this causes a hysteresis. Increases in length of 50% can be produced. Bone, on the other hand, is a material with drastically different properties: its strength and stiffness are much higher, and its maximum elongation is much lower. The structure of bones is quite complex, and they can be considered composite materials. Figure 1.31(b) illustrates the strength (in tension) of dry and wet bone. The maximum tensile strength is approximately 80 MPa, and Young's modulus is about 20 GPa.

The abalone shell and the shells of bivalve mollusks are often used as examples of a naturally occurring laminated composite material. These shells are composed of layers of calcium carbonate, glued together by a viscoplastic organic material. The calcium carbonate is hard and brittle. The effect of the viscoplastic glue is to provide a crack-deflection layer so that cracks have difficulty propagating through the composite. Figure 1.32 shows cracks that are deflected at each soft layer. The toughness of this laminated composite is vastly superior to that of a monolithic material, in which the crack would be able to propagate freely, without barriers.

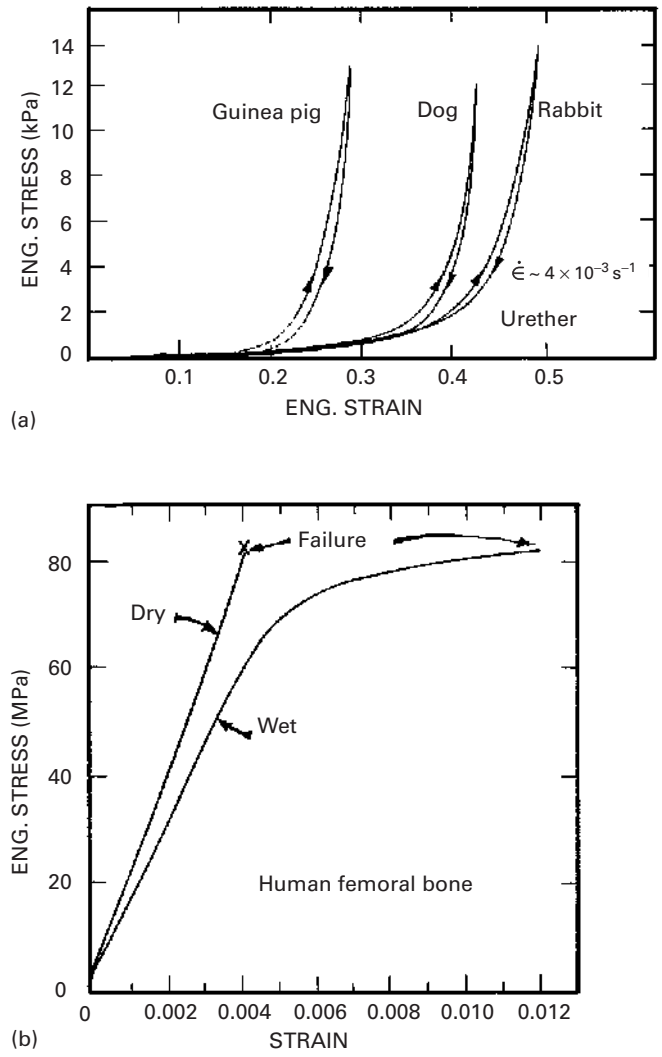


**Figure 1.31** Stress–strain curves for biological materials. (a) Urether. (Reproduced from the *American Journal of Physiology, Consolidated*, FC Yin, YC Fung, Vol. 221, 1971. © The American Physiological Society (APS).) (b) Human femur bone. (Reproduced from the *Journal of Applied Phisiology*, F. Gaynor Evans, Milton Lebow, Vol. 3, 1951, Pages 563–572. © The American Physiological Society (APS).)

The effect is shown at two scales: the mesoscale and the microscale. At the mesoscale, layers of calcium carbonate have a thickness of approximately 500 μm. At the microscale, each calcium carbonate layer is made up of small brick-shaped units (about $0.5 \times 7.5$ μm longitudinal section), glued together with the organic matter. The formation of this laminated composite results in a fracture toughness and strength (about 4 MPa $m^{-1/2}$ and approximately 150 MPa, respectively) that are much superior to those of the monolithic $CaCO_3$. The composite also exhibits a hierarchical structure; that is, the layers of $CaCO_3$ and organic glue exist at more

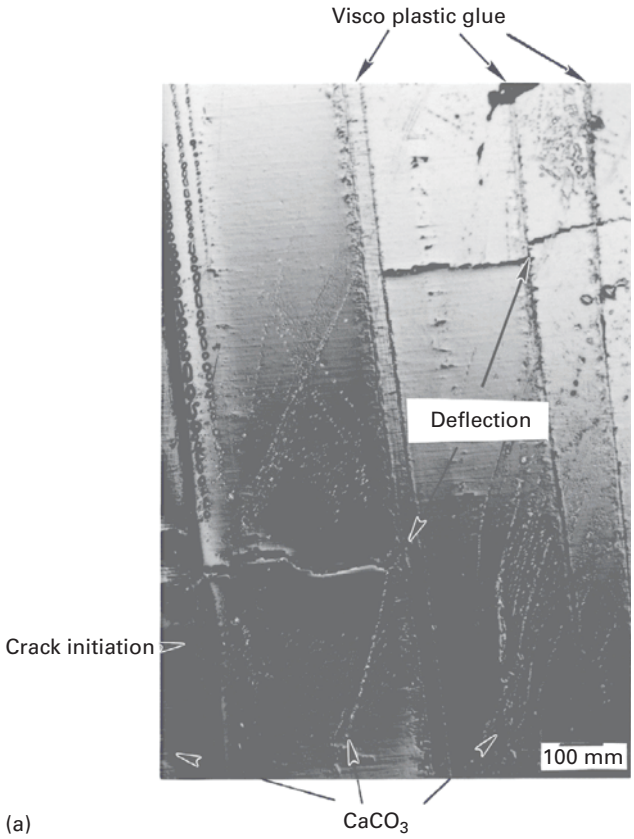


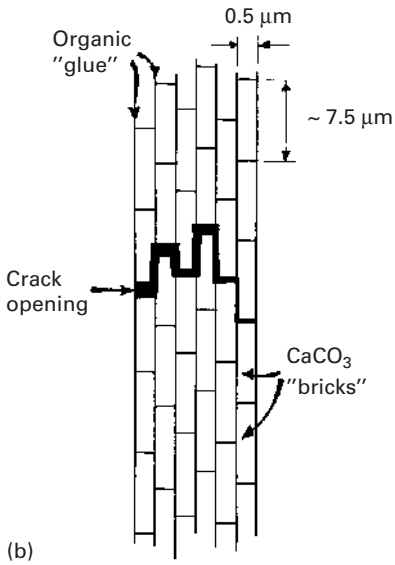


**Figure 1.32** (a) Cross-section of abalone shell showing how a crack, starting on the left, is deflected by a viscoplastic layer between calcium carbonate lamellae (mesoscale). (b) Schematic drawing showing the arrangement of calcium carbonate in nacre, forming a miniature "brick and mortar" structure (micro scale).

than one level (at the micro and meso levels). This naturally occurring composite has served as inspiration for the synthesis of $B_4C$-Al laminate composites, which exhibit superior fracture toughness.[7] In these synthetic composites, there is a 40% increase in both fracture toughness and strength over monolithic $B_4C$-Al cermets. (A cermet is a composite material consisting of ceramic (cer) and sintered metallic (met) materials.) *Biomimetics* is the field of materials science in which inspiration is sought from biological systems for the design of novel materials.

Another area of biomaterials in which mechanical properties have great importance is bioimplants. Complex interactions between the musculoskeletal system and these implants occur in applications where metals and ceramics are used as replacements for hips, knees, teeth, tendons, and ligaments. The matching of material and bone stiffness is important, as are the mechanisms of bonding tissue to these materials. The number of scientific and technological issues is immense, and the field of bioengineering focuses on these.

### 1.3.8 Porous and Cellular Materials

Wood, cancellous bone, Styrofoam, cork, and the insulating tiles of the Space Shuttle are examples of materials that are not compact; their structure has air as a major component. The great advantage of cellular structures is their low density. Techniques for making foam metals, ceramics, and polymers have been developed, and these cellular materials have found a wide range of applications, in insulation, in cushioning, as energy-absorbing elements, in sandwich panels for aircraft, as marine buoyancy components, in skis, and more.

The mechanical response of cellular materials is quite different from that of bulk materials. The elastic loading region is usually followed by a plateau that corresponds to the collapse of the pores, either by elastic, plastic buckling of the membranes or by their fracture. The third stage is an increase in the slope, corresponding to final densification. Figure 1.33(a) shows representative curves for polyethylene with different initial densities. The plateau occurs at different stress levels and extends to different strains for different initial densities. The bulk (fully dense) polyethylene is shown for comparison purposes. Cellular mullite, an alumina-silica solid solution, exhibits a plateau marked by numerous spikes, corresponding to the breakup of the individual cells (Figure 1.33(b)). Materials with initial densities as low as 5% of the bulk density are available as foams. Figure 1.33(c) shows a very important use of foams: sandwich structures, composed of end sheets of solid material in which a foam forms the core region, have numerous applications in the aerospace industry. The foam between the two panels makes them more rigid; this is accomplished without a significant increase in weight.

There are many biological examples of sandwich structures. The toucan beak (Figure 1.34(a)) is a structure with very low density (0.04 g $cm^{-3}$) that consists of an external layer of compact keratin. Figure 1.34(b) shows the keratin layer. It is

[7] M. Sarikaya, K. E. Gunnison, M. Yasrebi, and I. A. Aksay, *Mater. Soc. Symp. Proc.*, 174 (1990) 109.

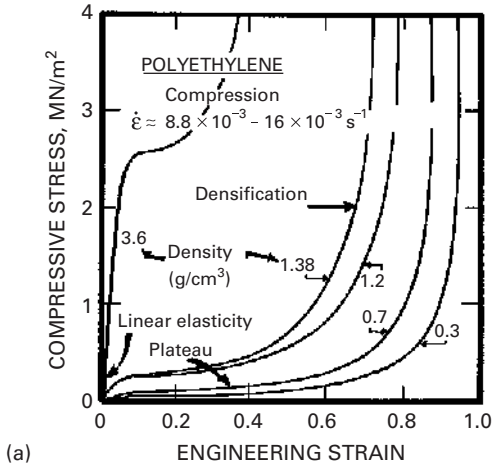


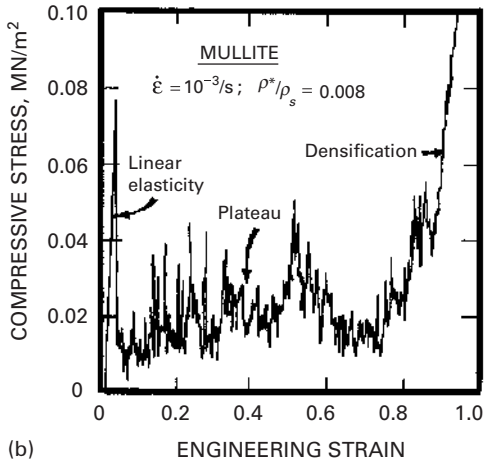


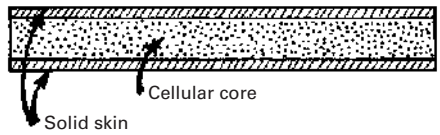


**Figure 1.33** Compressive stress–strain curves for foams. (a) Polyethylene with different initial densities. (b) Mullite with relative density $\rho^*/\rho s = 0.08$. (Adapted from L. J. Gibson and M. F. Ashby, *Cellular Solids: Structure and Properties* (Oxford, U.K.: Pergamon Press, 1988), pp. 124, 125.) (c) Schematic of a sandwich structure. (Adapted from L.J. Gibson and M.F. Ashby, Cellular solids: Structure and properties. *Advances in Polymer Technology*, 9, issue 2 (1989). With permission from John Wiley & Sons.)

composed of superimposed scales. The extremely low density of the inside of the toucan beak is due to a foam-like (cellular) bone structure. The function of the cellular material is to provide structural rigidity to the system. In the absence of this foam, the external shell would buckle easily. Hence the toucan can fly without taking a nose dive.

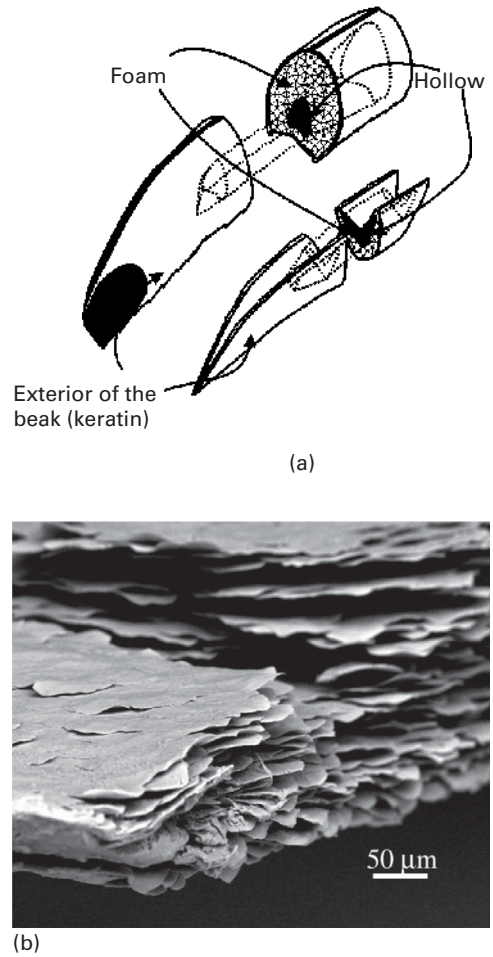


**Figure 1.34** (a) Toucan beak; (b) external shell made of keratin scales. (Figure courtesy of Y. Seki.)

As examples of foams in synthetic and naturally occurring materials, we show in Figure 1.35 two structures. Figure 1.35(a) shows an open-celled aluminum foam. We sectioned the beak of the toucan and observed that the inside is composed of a foam with similar length scale Figure 1.34(b). Nature uses foams for the same purposes we do: to provide rigidity to structures with the addition of minimal weight. In Chapter 12 we give a detailed analysis of stresses involved in foams.

### 1.3.9 Nano- and Microstructures of Biological Materials

Biological materials are more complex than synthetic materials. They form complex arrays, hierarchical structures, and are often multifunctional, i.e., one material has more than one function. For example, bone has a structural function and serves as a producer of red blood cells (in marrow). We classify biological materials, from the mechanical property viewpoint, into soft and hard. Hard materials provide the skeleton, teeth, and nails in vertebrates and the exoskeleton in arthropods.

**Table 1.5 Occurrence of Different Biological Materials in the Body**

| Biological Material | Weight Percentage in Human Body |
|---|---|
| Proteins | 17 |
| Lipids | 15 |
| Carbohydrates | 1 |
| Minerals | 7 |
| DNA, RNA | 2 |
| Water | 58 |

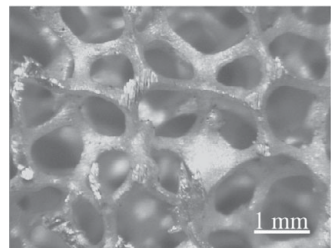


(a)

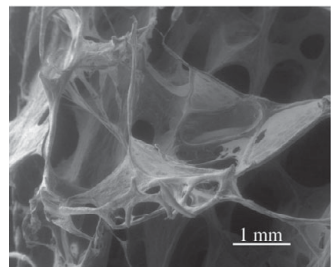


(b)

**Figure 1.35** Cellular materials: (a) synthetic aluminum foam. (Figure courtesy of K. S. Vecchio.) (b) Foam found in the inside of toucan beak. (Figure courtesy of M. S. Schneider.)

Soft biological materials build skin, muscle, internal organs, etc. Table 1.4 provides the distribution (on a weight percentage) of different constituents of the body.

Here are some examples of "hard" biological materials:

- Calcium phosphate (hydroxyapatite-$Ca_{10}(PO_4)_6(OH)_2$): teeth, bone.
- Chitin: nails.
- Keratin: bird beaks, horn, hair.
- Calcium carbonate (aragonite): mollusk shells, some reptile eggs (calcite): bird's eggs, crustaceans, mollusks.
- Amorphous silica ($SiO_2(H_2O)_n$): spicules in sponges.
- Iron oxide (magnetite – $Fe_3O_4$): teeth in chitons (a weird-looking marine worm), bacteria.

Of the above, iron oxide, calcium phosphate, silica, and iron oxide are minerals. Chitin is a polysaccharide and keratin is a protein.

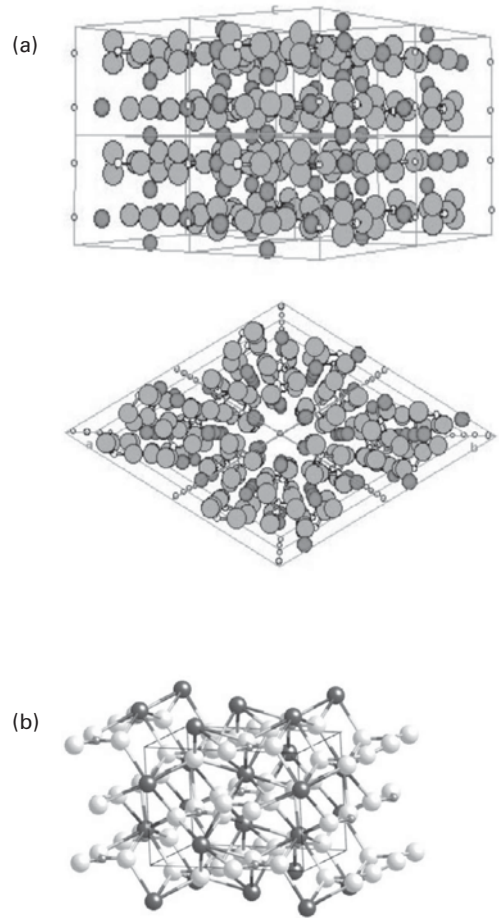


**Figure 1.36** Atomic structure of hydroxyapatite: (a) small white atoms (P), large gray atoms (O), black atoms (Ca). (b) Atomic structure of aragonite: large dark toms (Ca), small gray atoms (C), large white atoms (O).

Figure 1.36(a) shows the atomic arrangement of the calcium, phosphorus, and oxygen atoms in hydroxyapatite. The unit cell is quite complex and consists of four primitive hexagonal cells juxtaposed. We should remember that the hexagonal cell is composed of three primitive cells, brought together at their 120° angles ($3 \times 120 = 360$). In the case of the hydroxyapatite unit cell, there are four unit cells: two at the 60° angle and two at the 120° ($2 \times 60 + 2 \times 120 = 360$).

Figure 1.36(b) shows the aragonitic form of calcium carbonate. Aragonite has the orthorhombic structure. However, it is important to recognize that the minerals do not occur in isolation in living organisms. They are invariably intimately connected with organic materials, forming complex hierarchically structured composites. The resulting composite has mechanical properties that far surpass those of the monolithic minerals. Although we think of bone as a cellular mineral, it is actually composed of 60% collagen (on a volume percentage basis) and 30–40%

hydroxyapatite (on a weight basis). If the mineral is dissolved away, the entire collagen framework is retained.

The principal organic building blocks in living organisms are the proteins. The word comes from Greek (*Proteios*) which means "of first rank" and indeed proteins play a key role in most physiological processes. The soft tissues in the body are made of proteins. As seen above, they are also an important component of biominerals. In order to fully understand proteins, we have to start at the atomic/molecular level, as we did for polymers.

Actually, proteins can be conceived of as polymers with a greater level of complexity. We start with amino acids, which are compounds containing both an amine ($–NH_2$) and a carboxyl (–COOH) group. Most of them have the following structure, shown where R stands for a side chain (Table 1.6 shows some of them):

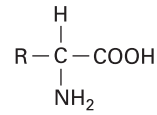

There are nine essential amino acids: histidine, isoleucine, leucine, lysine, methionine, phenylalanine, threonine, tryptophan, and valine. There are currently 20 amino acids found in proteins. In addition to these nine, we have the following: alanine, arginine, asparagine, aspartic acid, cysteine, glutamic acid, glutamine, glycine, proline, serine, and tyrosine.

In proteins, these amino acids combine themselves by forming links between the carboxyl group of one amino acid and the amino group of another. These linear chains, similar to polymer chains, are called polypeptide chains. The polypeptide chains acquire special configurations because of the formation of bonds (hydrogen, van der Waals, and covalent bonds) between amino acids on the same or different chains. The two most common configurations are the alpha helix and the beta sheet. Figure 1.37(a) shows how an alpha helix is formed. The NH and CO groups form hydrogen bonds between them in a regular pattern, and this creates the particular conformation of the chain that is of helical shape. One such bond is shown in Figure 1.37(a). In Figure 1.37(b) several hydrogen bonds are shown, causing the polypeptide chain to fold. The side chains stick out. The amino acid chain with the peptide group is shown in Figure 1.38(a). The amino acid chain with the peptide groups in a straight line is shown in Figure 1.38(b). Figure 1.38(c) shows the alpha helix conformation produced by the coiling of the amino acid chain. The peptide groups face each other and hydrogen bonds form. This keeps the helix stable.

Another common conformation of polypeptide chains is the beta sheet. In this conformation, separate chains are bonded. We can see that the radicals (large grey balls) of two adjacent chains stick out of the sheet plane on opposite sides. Successive chains can bond in such a fashion, creating pleated sheets.

We describe below the most important proteins: collagen, actin, myosin, elastin, resilin, abductin, keratin and silk, as well as cellulose and chitin, which are polysaccharides.

**Table 1.6 Eight amino acids found in proteins**

| Name | Chemical Structure |
|---|---|
| Alanine | 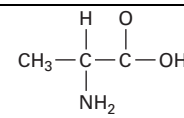 |
| Leucine | 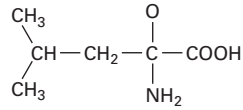 |
| Phenylalanine | 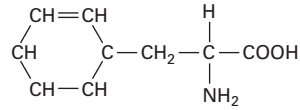 |
| Proline | 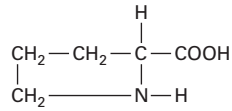 |
| Serine | 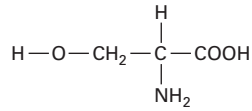 |
| Cysteine | 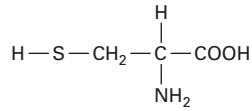 |
| Glutamate | 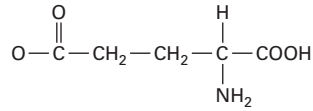 |
| Lysine | 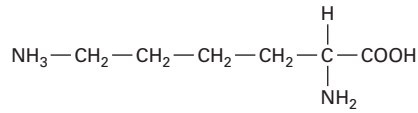 |

**Collagen** Collagen is a rather stiff and hard protein. It is a basic structural material for soft and hard bodies; it is present in different organs and tissues and provides structural integrity. Fung[8] compares it to steel, which is the principal load-carrying component in structures. In living organisms, collagen plays the same role: it is the main load-carrying component of blood vessels, tendons, bone, muscle, etc. In rats, 20% of the proteins are collagen. Humans are similar to rats in physiology and the same proportion should apply. Figure 1.39 shows the structure of collagen. It is a triple helix, each strand being made up of sequences of amino acids. Each strand is itself a left-handed helix with approximately 0.87 nm per turn. The triple helix has a right-handed twist with a period of 8.6 nm. The dots shown in a strand in

[8] Y. C. Fung, *Biomechanics: Mechanical Properties of Living Tissues* (Berlin: Springer, 1993).

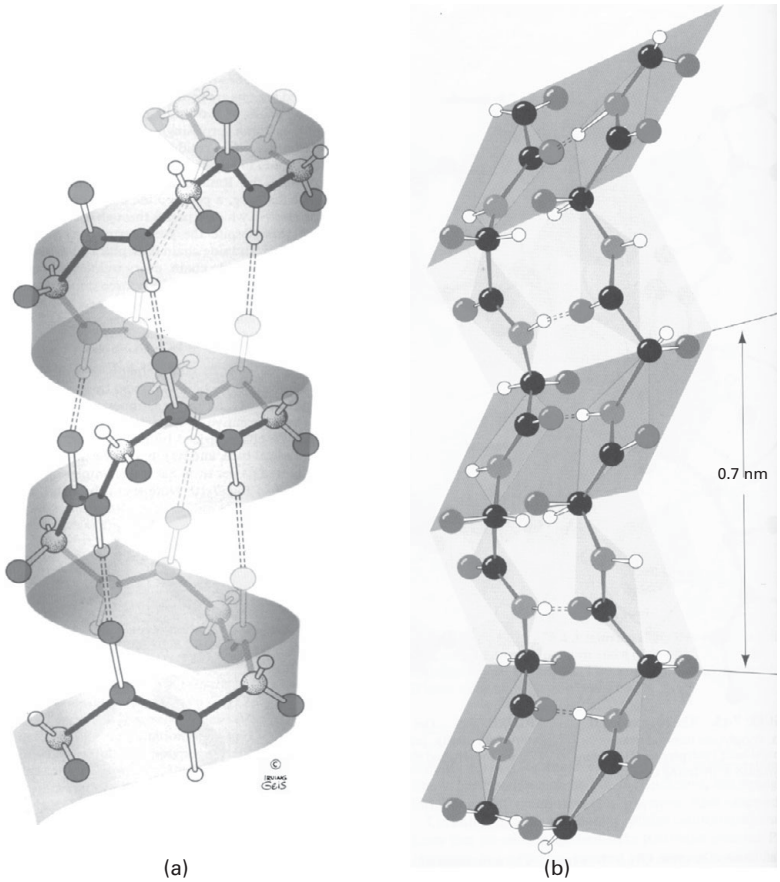


**Figure 1.37** (a) Structure of alpha helix; dotted double lines indicate hydrogen bonds. (b) Structure of beta sheet with two antiparallel polypeptide chains connected by hydrogen bonds (double-dotted lines).

Figure 1.39 represent glycine and different amino acids. There are over 10 types of collagen, called Type I, II, X, etc. Fiber-forming collagens organize themselves into fibrils.

Figure 1.40 shows the structural hierarchy of fibrillar collagen. In collagen formations, helical left-handed procollagen chains form a right-handed triple helix of roughly 300 nm in length. (b) Schematic representation of triple helix formed by three procollagen chains. Figure 1.40(c) shows the arrangement of triple helices into fibrils. Triple helices are arranged in a staggered manner, leading to a gap (0.54 d) and an overlap (0.46 d) region. The gap region has fewer triple helices across the section, and the overlap region has more. This gap and overlap has a periodicity, or d-period, of 67 nm, and is the cause of the visible banding in collagen fibrils. Figure 1.40 shows layers of collagen fibrils in a cross-section of skin. Figure 1.40(d) shows collagen fibrils of 100 nm diameter imaged by TEM. Fibrils clearly display the characteristic banding feature. Due to the viewing angle of the fibrils, d-period measurements decrease proportionally to the cosine of the viewing angle. A 90° viewing angle would lead to perfectly accurate measurements. (f) Atomic force microscopy (AFM) of hydrated collagen fibrils in an arapaima scale. 67nm d-period is measured.

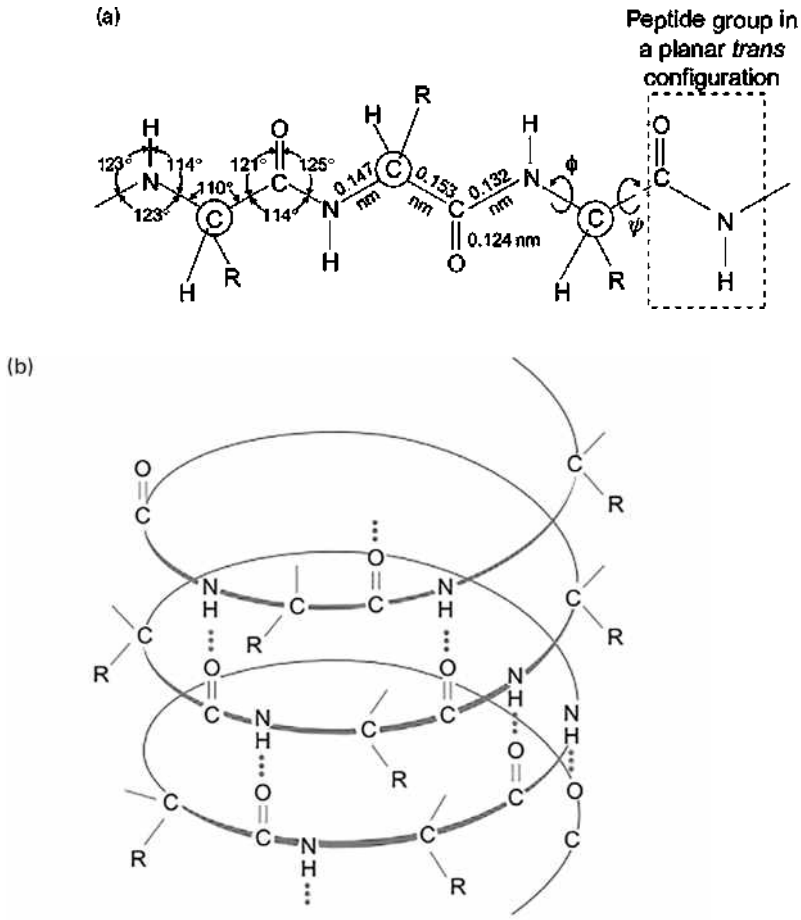


**Figure 1.38** (a) Geometry of a peptide (amide) linkage. (b) Hydrogen bonds in the alpha-helix. Coiling of an amino-acid chain brings peptide groups into juxtaposition so that the hydrogen bonds form and ensure the helical configuration. (Adapted from Journal of the Mechanical Behavior of Biomedical Materials, Vol 52, Vincent R. Sherman, Wen Yang, Marc A. Meyers, The materials science of collagen, 22–50, Copyright (2015), with permission from Elsevier.)

Fibrils, in turn, arrange themselves into fibers. Fibers are bundles of fibrils with diameters between 0.2 and 12 μm. In tendons, these fibers can be as long as the entire tendon. In tendons and ligaments, the collagen fibers form primarily one-dimensional networks. In skin, blood vessels, intestinal mucosa, and the female vaginal tract, the fibers organize themselves into more complex patterns leading to two- and three-dimensional networks.

The hierarchical organization of a tendon starts with tropocollagen (a form of collagen), and moves up, in length scale, to fascicles. There is a crimped, or wavy structure shown in the fascicles that has an important bearing on the mechanical properties. Figure 1.41 shows an idealized representation of a wavy fiber.

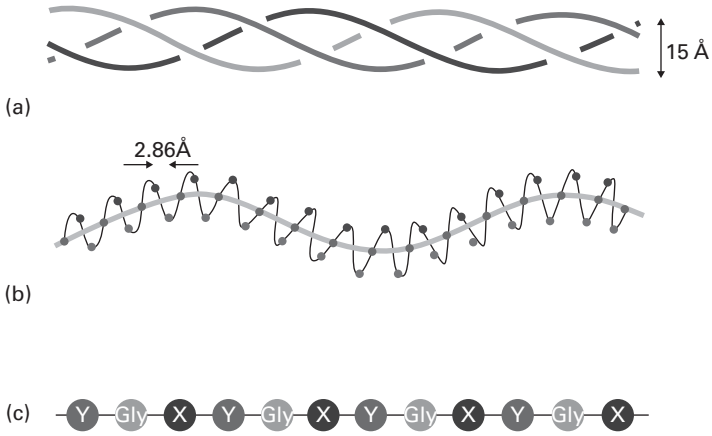


**Figure 1.39** Triple helix structure of collagen. (From Carlo Knupp, John M. Squire, Molecular Packing in Network-Forming Collagens, The Scientific World Journal, vol. 3, Article ID 157031, 20 pages, 2003. https://doi.org/10.1100/tsw.2003.40. Copyright © 2003 Carlo Knupp and John M. Squire.)

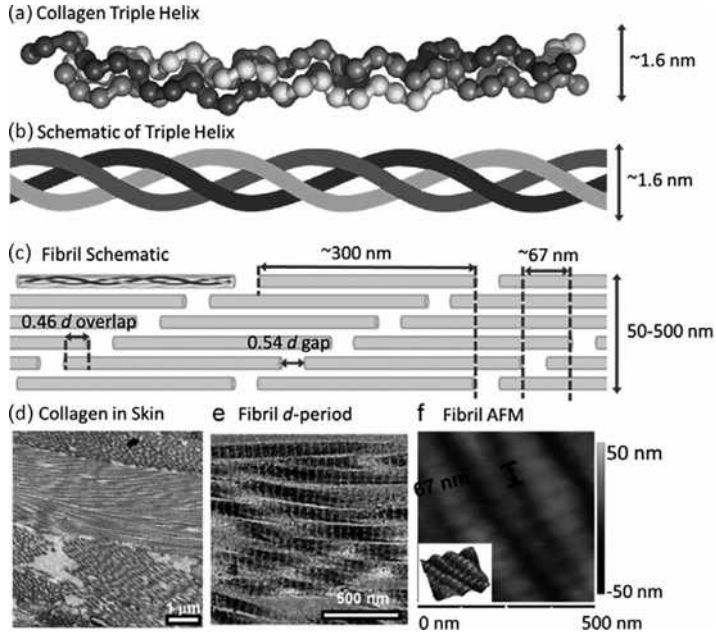


**Figure 1.40** Organization of collagen, starting with triple helix, and going to fibrils: (a) helical left-handed procollagen chains forming a right-handed triple helix of roughly 300 nm in length, (b) triple helix formed by three procollagen chains, (c) triple helices arranged in a staggered manner, leading to a gap (0.54 d) and an overlap (0.46 d) region; gap and overlap has a d-period, of 67 nm, (d) layers of collagen fibrils in a cross-section of skin; collagen fibrils of 100 nm diameter imaged by transmission electron microscopy, (f) atomic force microscopy of hydrated collagen fibrils in an arapaima scale. 67 nm d-period is measured.
(Reprinted from Journal of the Mechanical Behavior of Biomedical Materials, Vol 52, Vincent R. Sherman, Wen Yang, Marc A. Meyers, The materials science of collagen, 22–50, Copyright (2015), with permission from Elsevier.)

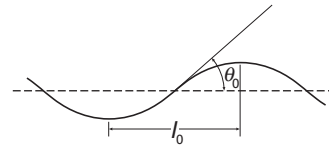


**Figure 1.41** Idealized configuration of a wavy collagen fiber.

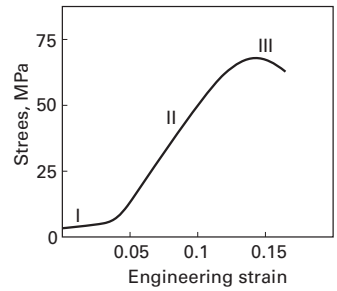


**Figure 1.42** Stress–strain curve of collagen with three characteristic stages.

Two parameters define it: the wavelength $2l_0$ and the angle $\theta_0$. Typical values for the Achilles tendon of a mature human are $l_0 = 20$–$50$ μm and $\theta_0 = 6$–$8°$. These bent collagen fibers stretch out in tension. When the load is removed, the waviness returns. When the tendon is stretched beyond the straightening of the waviness, damage starts to occur. Figure 1.42 shows a schematic stress–strain curve for tendons. The tendon was stretched until rupture. There are essentially three stages:

- Region I: toe part, in which the slope rises rapidly. This is the physiological range in which the tendon operates under normal conditions.
- Region II: linear part, with a constant slope.
- Region III: slope decreases with strain and leads to failure.

The elastic modulus of collagen is approximately 1 GPa and the maximum strain is in the 10–20% range. Cross-linking increases with age, and collagen becomes less flexible.

**Actin and Myosin** These are the principal proteins of muscles, leukocytes (white blood cells), and endothelial cells. Muscles contract and stretch through the controlled gliding/grabbing of the myosin with respect to the actin fibers. Figure 1.43(a) shows an actin fiber. It is composed of two polypeptides in a helical arrangement. Figure 1.43(b) shows the myosin protein. It has little heart-shaped "grapplers" called cross-bridges. The tips of the cross-bridges bind and unbind to the actin filaments. Figure 1.43(c) shows the myosin and actin filaments, and the cross-bridges at different positions. The cross-bridges are hinged to the myosin and can attach themselves to different positions along the actin filaments as the actin is displaced to the left. Thus, the muscles operate by a micro-telescoping action of these two proteins.

Figure 1.44 shows how the filaments organize themselves into myofibrils. Bundles of myofibrils form a muscle fiber. The $Z$ line represents the periodicity

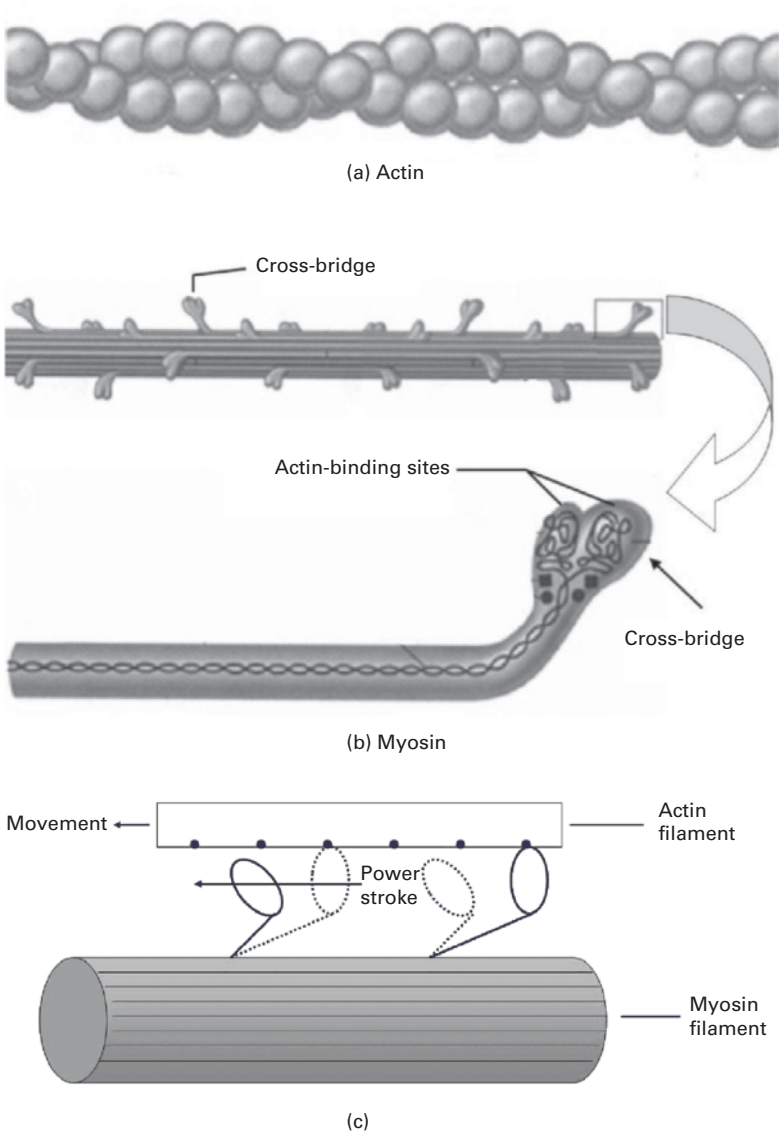


**Figure 1.43** Molecular structure of (a) actin and (b) myosin; (c) action of cross-bridges when actin filament is moved to the left with respect to the myosin filament; notice how cross-bridges detach themselves, then reattach themselves to the actin.

in the myosin-actin units (called sarcomeres) and is approximately equal to 3 μm in the stretched configuration. It shortens when the muscle is contracted. This gives the muscle a striated pattern when observed at high magnification. They resemble a coral snake in the microscope. Myofibrils have a diameter of approximately 1–2 μm.

**Elastin** Elastin is found in skin, walls of arteries and veins, and lung tissue. A prominent place is in the "*ligamentum nuchae*, a long ligament that runs along the top of the neck in horses and is constantly under tension. Other vertebrates have it too, but it is less pronounced. In this manner, the horse can keep its head up

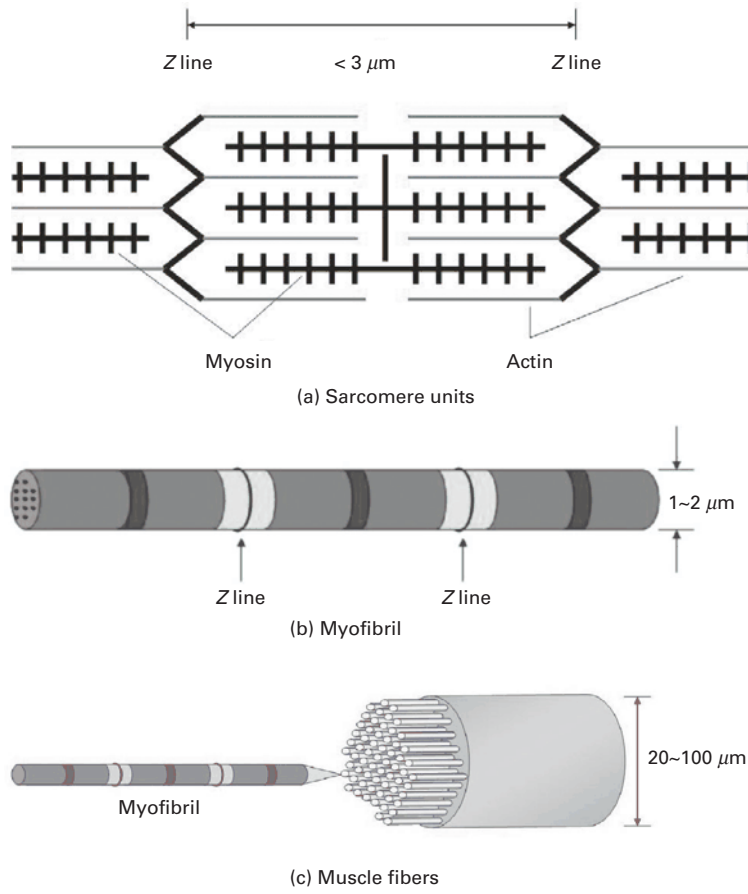


**Figure 1.44** Structure of muscle from (a) the sarcomere units, to (b) myofibril, and finally to (c) muscle fibers.

without using muscles. The "ligamentum nuchae plays a role similar to the cables in a suspension bridge. It is a rather robust cylinder.

**Resilin and Abductin** These are found in arthropods. They have properties similar to those of elastin, but occur in totally different animals and have a different structure.

**Keratin** Keratin is found in hair, horn, bird beaks and feathers, and whale baleen. The toucan beak presented in Section 1.3.8 is made of keratin. It has a structure similar to collagen (three interwoven helices). These helices combine themselves to form micro fibrils with a diameter of 8 nm. Interestingly, it undergoes a phase transformation under tensile load, which increases its elongation.

**Cellulose** Cellulose is the most abundant biological structural material, and is present in wood (which is a composite of cellulose and lignin) and cotton (almost pure cellulose). Cellulose is a cross-linked crystalline polymer. Its basic building block is a fibril with 3.5 nm diameter and 4 nm periodicity.

**Chitin** Chitin is a polysaccharide found in many invertebrates. The exoskeleton of insects is made of chitin.

**Silk** Silk is composed of two proteins: fibroin (tough strands) and sericin, a gummy glue. The mechanical properties (strength and maximum elongation) can vary widely, depending on the application intended by the animal. For instance, among the silks produced by spiders are dragline and spiral. Dragline, used in the radial components of the web, is the structural component, and has high tensile strength (600 mPa) and a strain at failure of about 6%. The spiral tangential components are intended to capture prey, and are "soft" and "sticky." The strain at failure in this case can exceed 16, i.e. 1,600%.

## Example 1.10

Determine the maximum strain that the collagen fibers can experience without damage if their shape is as given in Figure 1.41 with a ratio between amplitude and wavelength of 0.2.

We can assume a sine function of the form:

$$y = k \sin 2\pi x/\lambda.$$

The maximum of $y$ is reached when $x = \pi/4$.

Hence:

$$y_{\max} = k = \lambda/5.$$

We can integrate over the length of the sine wave from 0 to $2\pi$ . However, this will lead to an elliptical integral of difficult solution. A simple approximation is to consider the shape of the wavy protein as an ellipse with major axis $2a$ and minor axis $2b$. The circumference is given by the approximate expression (students should consult a mathematics text to obtain this expression)

$$L \approx \pi\left[\frac{3}{2}(a+b) - (ab)^{1/2}\right].$$

In the sine function, we have two arms, one positive and one negative. Their sum corresponds, in an approximate manner, to the circumference of the ellipse. The strain is equal to

$$\varepsilon = \frac{L - 4a}{4a} = \frac{\pi\left[\frac{3}{2}(a+b) - (ab)^{1/2}\right] - 4a}{4a}.$$

Thus:

$$\varepsilon = \frac{\pi}{4}\left[\frac{3}{2}\left(1 + \frac{b}{a}\right) - \left(\frac{b}{a}\right)^{1/2}\right] - 1.$$

## Example 1.10 (cont.)

The following ratio is given:

$$\frac{b}{2a} = 0.2 \quad \text{and} \quad \frac{b}{a} = 0.4.$$

The corresponding strain is:

$$\varepsilon = 0.53.$$

Beyond this strain, the collagen will break.

### 1.3.10 The Sponge Spicule: An Example of a Biological Material

Marine sponges have long tentacles that are called spicules. These spicules act as antennas, which are subjected to marine currents and other stresses. These long silica rods have properties that dramatically exceed the strength of synthetic silica. Figure 1.43 shows the flexure strength of both spicule and synthetic silica. The difference in flexure strength between sponge spicule and synthetic silica is remarkable. The synthetic silica fractures at a relatively low stress of 200 mPa compared to the yield stress of the spicule at 870 mPa. The area under the stress–strain curve gives a reasonable idea of the toughness. Clearly the toughness of the spicule is many times higher than that of synthetic silica. As evidenced by Figure 1.45, failure

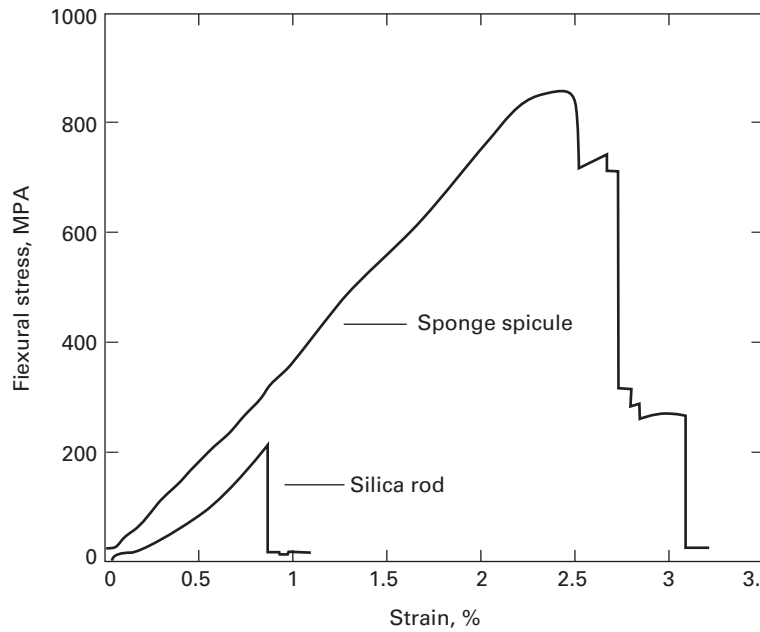


**Figure 1.45** stress deflection responses of synthetic silica rod and sponge spicule in flexure testing. (Figure courtesy of George Mayer.)

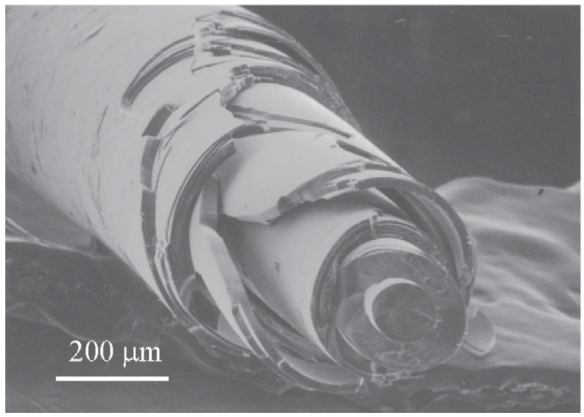


**Figure 1.46** SEM of fractured sponge spicule showing two-dimensional onion-skin structure of concentric layers.
(Figure courtesy of George Mayer.)

does not occur catastrophically in the spicule. Instead, the spicule fails "gracefully," which is a considerable advantage.

Figure 1.46 shows the microstructure of a fracture surface. The spicule consists of many concentric layers. This onion-like structure is responsible for the strengthening effect observed. When stress is applied to a silica rod, a crack will initiate at the weakest point in the material and propagate through the silica rod in a catastrophic manner. In contrast, crack propagation in the spicule will be arrested at each interface. This type of "graceful" failure is extremely useful. We can truly learn and apply this lesson from nature to modern material applications.

### 1.3.11 Active (or Smart) Materials

Technology puts greater and greater demand on materials and there is a constant push to develop materials with enhanced capabilities. The term *multifunctional materials* has been coined to describe materials with more than one capability. This is inspired by nature, where materials often have more than one function. For example, the trunk of a tree is at the same time a structural component and a carrier for the sap. Bones have a structural as well as a blood-cell-producing function.

Another category of advanced materials are *active materials*. They are also called "smart" materials. Active materials have responses that can be used in all kinds of devices. Given below are the main classes of active materials.

- Shape memory alloys: The most common is a NiTi alloy known as Nitinol. It can undergo strains of 1–5% through a martensitic transformation that is reversible. There are numerous applications through two effects: the shape memory effect and the super elastic (or pseudoelastic) effect: dental braces, stents, etc. A detailed description of these alloys is given in Chapter 11.
- Magnetorheological materials: These materials exhibit a viscosity that depends on an externally applied magnetic field. The suspension system of a US-made luxury

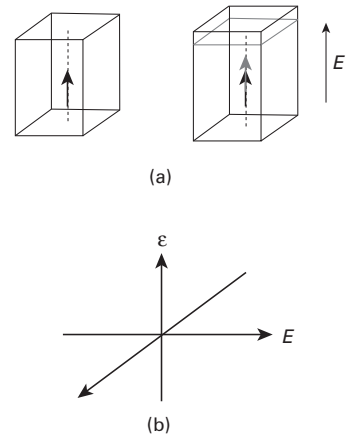


**Figure 1.47** (a) Effect of applied field $E$ on dimension of ferroelectric material. (b) Linear relationship between strain and electric field.
(Figure courtesy of G. Ravichandran.)

automobile uses this material. The stiffness can be adjusted by varying the magnetic field.

- Piezoelectric ceramics and ferroelectricity[9]: These materials generate an electric field when strained. Conversely, if an electric current is passed through them, they change their dimensions. Barium titanate and lead zirconate titanate (Pb(Zr, Ti)$O_3$) are examples. They have the perovskite structure with composition $ABO_3$, where A and B are metals. They are characterized by a linear strain–electric-field response. The maximum strain is on the order of 0.2%. Applications include vibration control, micropositioning devices, ultrasonics, and nondestructive evaluation.

It is a property of ferroelectrics to exhibit polarization in the absence of an electric field. Polarization is defined as dipole moment per unit volume or charge per unit area on the surface. The material is divided into domains, which are regions with uniformly oriented polarization. Ferroelectrics are characterized by a linear relationship between stress $\sigma$ and polarization $P$:

$$P = d\sigma.$$

There is a converse relationship between strain $\varepsilon$ and electric field, $E$:

$$\varepsilon = dE,$$

where $d$ is called the polarizability tensor. Figure 1.47(a) shows how the application of an externally applied electric field $E$ results in a change in length of the specimen. Figure 1.47(b) shows the linear relationship between the strain and the field. This is a property of ferroelectric crystals, certain noncentrosymmetric crystals (e.g. quartz, ZnO), textured polycrystals, and polycrystals with a net spontaneous polarization. Applications include adaptive optics, active rotors and control surfaces, robotics,

[9] K. Bhattacharya and G. Ravichandran, *Acta Mater.*, 51 (2003) 5941.

and MEMS/NEMS (microelectromechanical system/nanoelectromechanical system) actuators.

### 1.3.12 Electronic Materials

Electronic materials are composed, for the most part, of thin films arranged in several layers and deposited on a substrate. The most common substrate is monocrystalline silicon (the silicon wafer). Integrated circuits form the heart of modern computers and the silicon chip is a primary example. Figure 1.48 shows a schematic of the materials and structure used in a CMOS (complementary metal oxide semiconductor) transistor device. The *pn* junctions form transistors. The substrate is silicon, which in this case is *n* doped. The thin film layers are vapor-deposited and there are a number of mechanical aspects that are of considerable importance. In Figure 1.48 we have monocrystalline and polycrystalline silicon, oxide, glass, metal, and a dielectric passivation layer.

The thin films deposited on the substrate have dimensions of a few nanometers to a few micrometers. These films may be under residual stresses as high as 500 MPa. These stresses are due to:

- Thermal expansion coefficient effects: When the film cools it contracts. The thermal expansion coefficients of the different layer scan be different, creating internal stresses.
- Phase transformations: The phases in thin films are often nonequilibrium phases.

There are a number of mechanical problems associated with these stresses. Dislocations at the interface between substrate and thin film, cracking of the

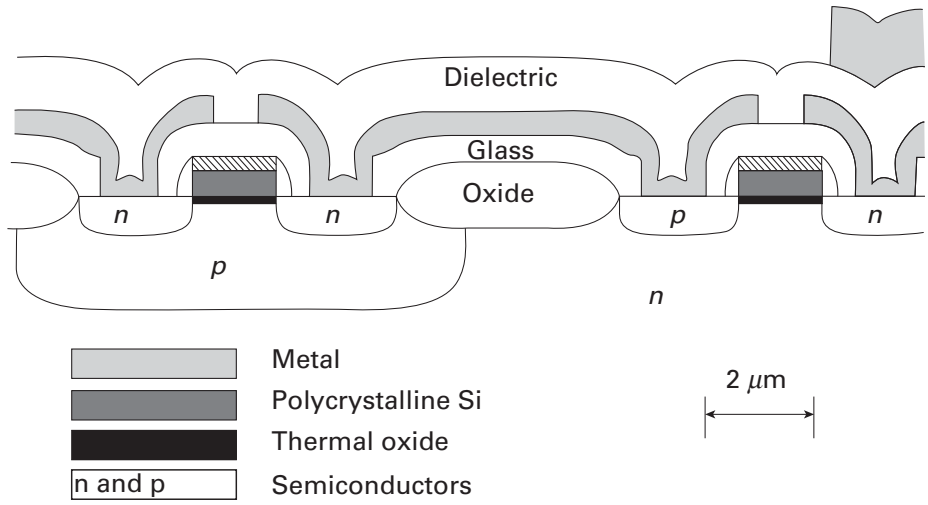


**Figure 1.48** Cross-section of a complementary metal-oxide semiconductor (CMOS). (Adapted by permission of Springer Nature: *Metallurgical Transactions, A, Physical Metallurgy and Materials Science*, Mechanical properties of thin films, William D. Nix, Copyright (1989).)

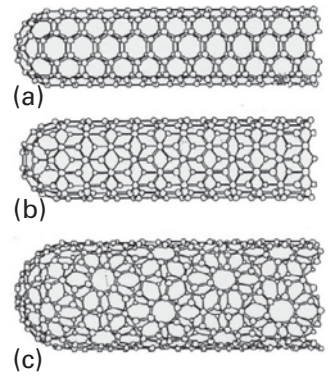


**Figure 1.49** Three configurations for single-wall carbon nanotubes: (a) armchair, (b) "zig-zag", (c) chiral.
(Adapted from *Carbon*, Vol. 33, M.S. Dresselhaus, G. Dresselhaus, R. Saito, Physics of carbon nanotubes, Pages 883–891. Copyright 1995, with permission from Elsevier.)

passivation layer, and bending of the substrate/thin-film system are a few examples. We will briefly describe these effects in Chapters 2, 6, 9, and 13.

Magnetic hard disks are also made of thin films. The aluminum disk, upon which a thin layer of magnetic material is deposited, rotates at surface velocities approaching 80 km $h^{-1}$, while the "head" flies aerodynamically over it. The distance between head and disk is as low as 0.3 μm. Some of the mechanical problems are friction, wear, and the unavoidable collisions between disk and head.

### 1.3.13 Nanotechnology

Nanotechnology[10, 11] refers to the structure and properties of materials and devices at the nanometer level. Developments in synthesis and characterization methods have resulted in materials that are designed from the "bottom up," rather than from the "top down." These terms were first used by the famous physicist Richard Feynman. The traditional method used in the design of new materials is to develop synthesis and processing techniques at the macro scale, and then to carry out detailed characterization at the micrometer and nanometer scale. The new approach is to start with atoms, then assemble them into small arrays and characterize their structure and properties at that level. This approach was led by the semiconductor revolution. As the sizes of devices become smaller, we approach atomic dimensions. At that level, it is being found that many materials possess unique properties. Many biological processes also use the bottom-up approach. Atoms aggregate themselves into molecules and complex arrays through genetic messages. The atoms come together and self-organize themselves into complex arrays of amino acids, which in their turn form proteins. It is hoped that we will be able to fully harness this approach in the future. There are already applications of nanotechnology in the marketplace.

A material that is showing great potential because of unique characteristics is the carbon nanotube. The first nanotube was produced in Japan by S. Iijima. One can

[10] C. P. Poole and F. J. Owens, *Introduction to Nanotechnology* (Hoboken, NJ: Wiley-Interscience, 2003).
[11] M. Ratner and D. Ratner, *Nanotechnology* (Englewood Cliffs, NJ: Prentice Hall, 2003).

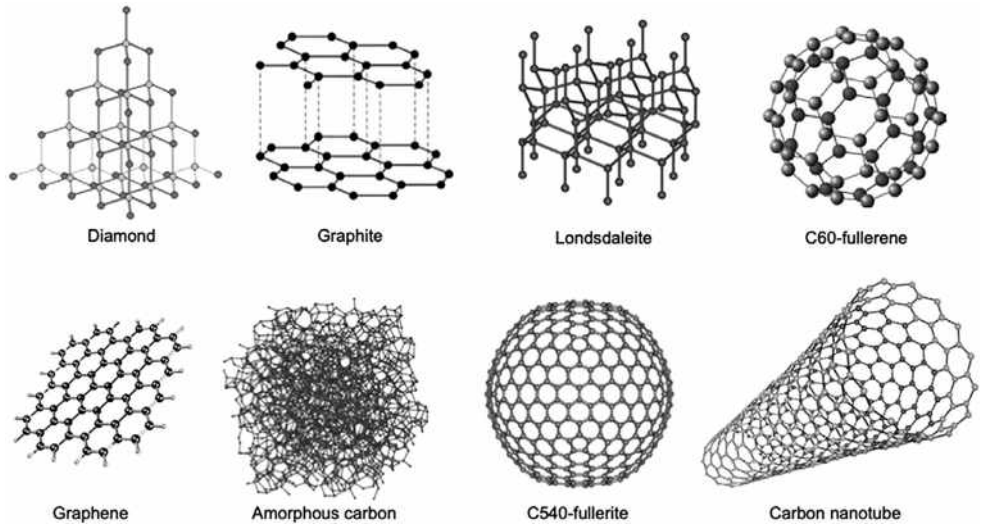


**Figure 1.50** Different arrangements of carbon atoms.
(Reprinted by permission from Springer Nature: Topics in Current Chemistry, Carbon nanotubes in biomedicine, Viviana Negri et al, Copyright (2020).)

envisage a carbon nanotube by rolling a single layer of carbon atoms into a hollow cylinder. The ends can be semispherical caps (one half of a "Bucky ball"). There are three morphologies for carbon nanotubes, shown in Figure 1.47: armchair, zig-zag, and chiral. They differ in the following:

- Armchair: the hexagons have the "pointy" side perpendicular to cylinder axis.
- Zig-zag: the hexagons have the pointy side aligned with the cylinder axis.
- Chiral: The hexagons are inclined with respect to the cylinder axis, and the carbon sheet wraps itself helically around the cylinder.

These carbon nanotubes have typically a diameter between 5 and 20 nm and length between 1 and 100 μm. They have outstanding mechanical properties, since they are based on the C–C bond, the strongest in nature. There are varying estimates of their strength, and values between 45 and 200 GPa are quoted. This would make them the strongest material known, ranking with diamond. Although the nanotubes are very short, one can envisage a day where continuous nanotubes are manufactured. Their incorporation as reinforcements in composites presents a bright prospect.

Figure 1.50 shows several carbon allotropes: diamond, graphite, lonsdaleite, C60-fullerene, graphene, amorphous carbon, C540-fullerite, and single-walled carbon nanotube. Outstanding properties can be achieved by the different configurations of the carbon atoms. This topic, nanostructured materials, is treated in Chapter 5.

Two-dimensional structures, especially graphene and $MoSi_2$, are becoming increasingly important.

## 1.4 Strength of Real Materials

Materials deform and fail through defects. These defects (cracks, point defects, dislocations, twins, martensitic phase transformations, etc.) are discussed in Chapters 4 through 8. The two principal mechanisms are crack growth, and dislocations and plastic flow:

- Crack growth: Real materials can have small internal cracks, at whose extremities high-stress concentrations are set up. Hence, the theoretical cleavage strength can be achieved at the tip of the crack at applied loads that are only a fraction of that stress. Griffith's theory (see Chapter 7) explains this situation very clearly. These stress concentrations are much lower in ductile materials, since plastic flow can take place at the tip of a crack, blunting the crack's tendency to grow.
- Dislocations and plastic flow: Before the theoretical shear stress is reached, dislocations are generated and move in the material; if they are already present, they start moving and multiply. These dislocations are elementary carriers of plastic deformation and can move at stresses that are a small fraction of the theoretical shear stress. They will be discussed in detail in Chapter 4.

In sum, cracks prevent brittle materials from obtaining their theoretical cleavage stress, while dislocations prevent ductile materials from obtaining their theoretical shear stress.

To achieve the theoretical strength of a crystalline lattice, there are two possible methods: (1) eliminating all defects and (2) creating so many defects, that their interactions render them inoperative. The first approach has yielded some materials with extremely high strength. Unfortunately, this has been possible only in special configurations called "whiskers." The second approach is the one more commonly pursued, because of the obvious dimensional limitations of the first; the strength levels achieved in bulk metals have steadily increased by an ingenious combination of strengthening mechanisms, but are still much lower than the theoretical strength. Maraging steels with useful strengths up to 2 GPa have been produced, as have patented steel wires with strengths of up to 4.2 GPa; the latter are the highest strength steels.

Figure 1.51 compares the ambient-temperature strength of tridimensional, filamentary, and whisker materials. The whiskers have a cross-sectional diameter of only a few micrometers and are usually monocrystalline (although polycrystalline whiskers have also been developed). Whiskers are one of the strongest materials developed by human beings. The dramatic effect of the elimination of two dimensions is shown clearly in Figure 1.51 and in Table 1.7. The strongest whiskers are ceramics. Figure 1.51 provides some illustrative examples. Iron whiskers with a strength of 12.6 GPa have been produced, compared with 2 GPa for the strongest bulk steels. The value of 12.6 GPa is essentially identical to the theoretical shear stress, because the normal stress is twice the shear stress. In general, FCC whiskers tend to be much weaker than BCC whiskers and ceramics. For instance, Cu whiskers have a strength of about 2 GPa. This is consistent with the much lower

**Table 1.7 Room Temperature Strength of Some Whiskers**

| Material | Diameter | Maximum tensile strength (GPa) | Source |
|---|---|---|---|
| Cu | 1.2 to 15 μm | 2–6 | [a] |
| Ag | 1.2 to 15 μm | 1.5–4 | [a] |
| Fe | 1.2 to 15 μm | 3–9 | [a] |
| SiC | 4–6 μm | 8.4 | [b] |
| $Al_2O_3$ | 82–320 nm | 49 | [c] |
| $Si_3N_4$ | 40–800 nm | 17–59 | [d] |
| Graphite | 1–5 μm | 20 | [e] |

[a] S. Brenner, *J. Appl. Phys.*, 27(1956)1484–1497.
[b] J. J. Petrovic, J. V. Milewski, D. L. Rohr, F. D. Gac, *J. Matls. Sci.*, 20(1985) 1167–1177.
[c] S. Wang, Y. He, H. Huang, J. Zhou, G. J. Auchterlonie, B. Huang, *Nanotechnology*, 24(2013) 285703.
[d] H. Iwanaga, C, Kawai, *JACS*, 81(1998) 773–776.
[e] R. Bacon, *J. Appl. Phys.*, 31(1960) 283–290.
Adapted with permission from A. Kelly, *Strong Solids* (Oxford, U.K.: Clarendon Press, 1973), p. 263s.

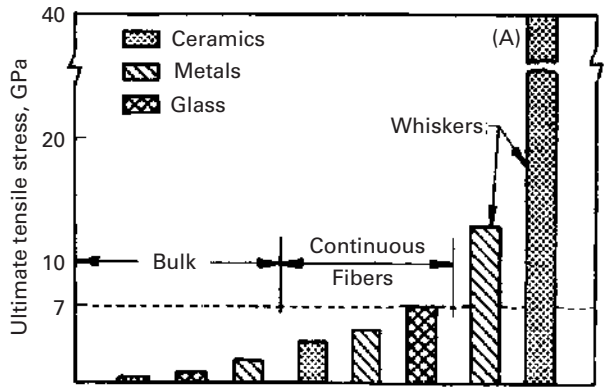


**Figure 1.51** Theoretical strength of continuous fibers and whiskers. The strength of the SiC whisker produced by the Philips Eindhoven Laboratory is indicated by (A).

theoretical shear strength exhibited by copper whiskers. It turns out that silver, gold, and copper have $\tau_{max}/G$ ratios of 0.039 (see Chapter 4). Hence, they are not good whisker materials. Figure 1.52 shows a stress–strain curve for a tin whisker. The stress drops vertically after the yield point. In contrast, the stress–strain curve for the polycrystal is barely different from the abscissa axis. This demonstrates, for a real material, the dramatic effect that a small lateral dimension can have on the strength and ductility.

In the elastic range, the curve deviates slightly from Hooke's law and exhibits some temporary inflections and drops (not shown in the figure). In many cases, for both metals and nonmetals, failure occurs at the elastic line, without appreciable plastic strain. When plastic deformation occurs, as, for example, in copper and zinc, a very large yield drop is observed. Although the strength of whiskers is not completely understood, it is connected to the absence of dislocations. This is also exemplified in Figure 1.52, which compares the strength of single crystalline tin in the form of whiskers with the bulk polycrystalline form. The whiskers have a strength around

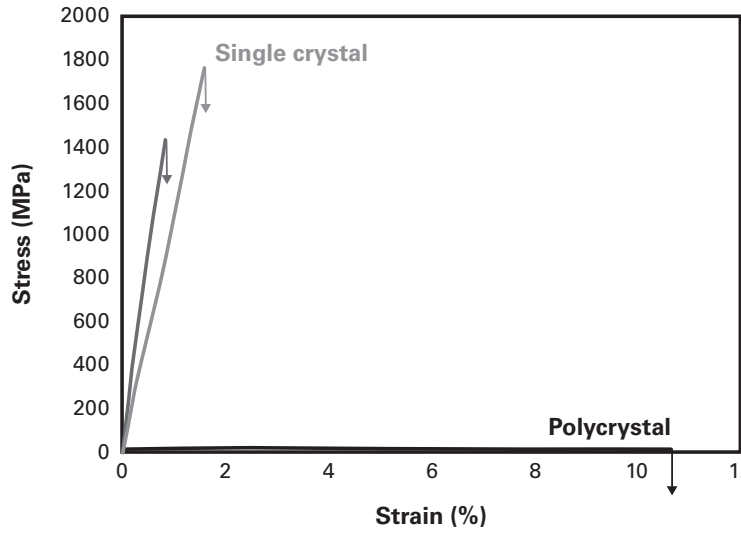


**Figure 1.52** Stress–strain curve of tin whisker and comparison with strength of polycrystal. (Reprinted by permission from Springer Nature: Journal of Electronic Materials, Tensile Behavior of Single-Crystal Tin Whiskers, S.S. Singh et al., Copyright (2014).)

1.6 GPa, whereas the polycrystal strength is in the low MPa range. It is impossible to produce a material virtually free of dislocations, in other words, perfect. However, for whiskers, dislocations can easily escape out of the material during elastic loading. Their density and mean free path are such that they will not interact and produce other sources of dislocation. Hence, the yield point is the stress required to generate dislocations from surface sources. The irregularities often observed in the elastic range indicate that existing dislocations move and escape out of the whisker. At a certain stress, the whisker becomes essentially free of dislocations. When the stress required to activate surface sources is reached, the material yields plastically, or fails.

## Example 1.11

Calculate the stresses generated in a turbine blade if its cross-sectional area is 10 $cm^2$ and the mass of each blade is 0.2 kg.

***Solution:*** This is an example of a rather severe environment where the material properties must be predicted with considerable detail. For example the blade may be in a jet engine. Figure E 1.11 shows a section of the compressor stage of a jet. The individual blades are fixed by a dovetail arrangement to the turbine vanes. Assume a rotational velocity $\omega$ =10,000 rpm and a mean radius $R$ = 0.5 m. The centripetal acceleration in the bottom of each turbine blade is

$$a_c = \omega^2 R = \left[10,000 \times \frac{1}{60} \times 2\pi\right]^2 \times 0.5 = 5.4 \times 10^5 \text{m s}^{-2}.$$

## Example 1.11 (cont.)

The stress that is generated is

$$\sigma = \frac{F}{A} = \frac{ma_c}{A} = \frac{0.2 \times 5.4 \times 10^5}{10 \times 10^{-4}} = 100 \text{ MPa},$$

where $F$ is the centripetal force and $A$ is the cross-sectional area. This stress of 100 MPa is significantly below the flow stress of nickel-based superalloys at room temperature, but can be quite significant at higher temperatures.

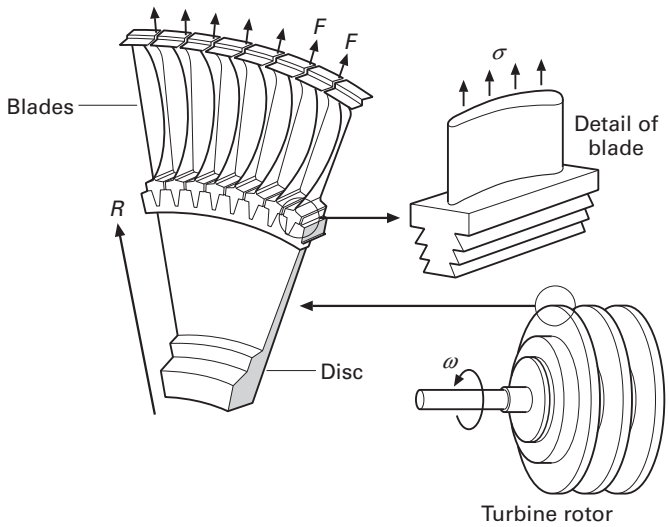


**Figure E1.11** Turbine blade subjected to centripetal force during operation.

## SUGGESTED READING

### Materials in General

J. F. Shackelford. *Introduction to Materials Science for Engineers*, 4th edn. Upper Saddle River, NJ: Prentice Hall, 1996.

W. F. Smith. *Principles of Materials Science and Engineering*, 3rd edn. New York, NY: McGraw Hill, 1996.

D. R. Askeland and P. Phule. *The Science and Engineering of Materials*, 4th edn. Pacific Grove, CA: Thomson, 2003.

W. D. Callister. Jr. *Materials Science and Engineering*, 4th edn. New York, NY: Wiley, 2003.

### Metals

C. S. Barrett and T. B. Massalski. *Structure of Metals*, 3rd rev. edn. Oxford, U.K: Pergamon, 1980.

M. A. Meyers and K. K. Chawla. *Mechanical Metallurgy*. Englewood Cliffs, NJ: Prentice-Hall, 1984.

### Ceramics

W. D. Kingery, H. K. Bowen, and D. R. Uhlmann. *Introduction to Ceramics*, 2nd edn. New York, NY, Wiley, 1976.
Y.-M. Chiang, D. Birnie III, and W. D. Kingery, *Physical Ceramics*, New York, NY: Wiley, 1997.

### Polymers

D. C. Bassett. *Principles of Polymer Morphology*. Cambridge, U.K.: Cambridge University Press, 1981.
Hiltner (ed.) *Structure-Property Relationships of Polymeric Solids*. New York, NY: Plenum Press, 1983.
R. J. Young. *Introduction to Polymers*. London: Chapman & Hall, 1986.
B. Wunderlich. *Macromolecular Physics, Vol. 1: Crystal Structure*. New York, NY: Academic Press, 1973.
B. Wunderlich. *Macromolecular Physics, Vol. 2: Crystal Nucleation*. New York, NY: Academic Press, 1976.

### Composite Materials

K. Chawla. *Composite Materials: Science & Engineering*. 2nd edn. New York, NY: Springer, 1998.
K. Chawla. *Ceramic Matrix Composites*, 2nd edn. Boston, MA: Kluwer, 2003.
N. Chawla and K. K. Chawla. *Metal Matrix Composites*, New York, NY: Springer, 2006.

### Liquid Crystals

A Ciferri, W. R. Krigbaum, and R. B. Meyer (eds.). *Polymer Liquid Crystals*. New York, NY: Academic Press, 1982.

### Biomaterials

M. Elices (ed.). *Structural Biological Materials*, Amsterdam, the Netherlands: Pergamon, 2000.
J. F. V. Vincent. *Structural Biomaterials*. Princeton, NJ: Princeton University Press, 1991.
Y.C. Fung. *Biomechanics: Mechanical Properties of Living Tissues*. New York, NY: Springer, 1981.

### Cellular Materials

J. Gibson and M. F. Ashby. *Cellular Solids: Structure and Properties*. Oxford, U.K.: Pergamon Press, 1988.

### Electronic Materials

W. D. Nix. Mechanical Properties of Thin Films, *Met. Trans.*, 20A (1989) 2217.
L.B. Freund and S. Suresh. *Thin Film Materials: Stress, Defect Formation and Surface Evolution*. Cambridge, U.K.: Cambridge University Press, 2003.

## EXERCISES

**1.1** A jet turbine rotates at a velocity of 7,500 rpm. Calculate the stress acting on the turbine blades if the turbine disc radius is 70 cm and the cross-sectional area is 15 $cm^2$. Take the length to be 10 cm and the alloy density to be 8.5 g $cm^{-3}$.

**1.2** The material of the jet turbine blade in Problem 1.1, Super alloy IN 718, has a room-temperature yield strength equal to 1.2 G Pa; it decreases with temperature as

$$\sigma = \sigma_0 \left(1 - \frac{T - T_0}{T_m - T_0}\right)$$

where $T_0$ is the room temperature and $T_m$ is the melting temperature in K ($T_m = 1{,}700$ K). At what temperature will the turbine flow plastically under the influence of centripetal forces?

**1.3** **(a)** Describe the mechanical properties that are desired in a tennis racket, and recommend different materials for the different parts of the racket.

**(b)** Describe the mechanical properties that are desired in a golf club, and recommend different materials for the different parts of the club.

**1.4** On eight cubes that have one common vertex, corresponding to the origin of axes, draw the family of {111} planes. Show that they form an octahedron and indicate all <110> directions.

**1.5** The frequency of loading is an important parameter in fatigue. Estimate the frequency of loading (in cycles per second, or Hz) of an automobile tire in the radial direction when the car speed is 100 km $h^{-1}$ and the wheel diameter is 0.5 m.

**1.6** Indicate, by their indices and in a drawing, six directions of the <112> family.

**1.7** The density of Cu is 8.9 g $cm^{-3}$ and its atomic weight (or mass) is 63.546. It has the FCC structure. Determine the lattice parameter and the radius of atoms.

**1.8** The lattice parameter for W(BCC) is $a = 0.32$ nm. Calculate the density, knowing that the atomic weight (or mass) of W is 183.85.

**1.9** Consider the unit cell of CsCl which has NaCl structure. The radius of $Cs^+$ is 0.169 nm and that of $Cl^-$ is 0.181 nm. (a) Determine the packing factor of the structure, assuming that $Cs^+$ and $Cl^-$ ions touch each other along the diagonals of the cube. (b) Determine the density of CsCl if the atomic weight of Cs is 132.905 and that of Cl is 35.453.

**1.10** MgO has the same structure as NaCl (simple cubic). If the radii of $O^{2-}$ and $Mg^{2+}$ ions are 0.14 nm and 0.070 nm, respectively, determine (a) the packing factor and (b) the density of the material. The atomic weight of $O_2$ is 16 and that of Mg is 24.3.

**1.11** Germanium has the diamond cubic structure with interatomic spacing of 0.245 nm. Calculate the packing factor and density. (The atomic weight of germanium is 72.6.)

**1.12** The basic unit (or mer) of polytetrafluoroethylene (PTFE) or Teflon is $C_2F_4$. If the mass of the PTFE molecule is 45,000 amu, what is the degree of polymerization?

**1.13** Using the representation of the orthorhombic unit cell of polyethylene (see Figure E1.13), calculate the theoretical density. How does this value compare with the density values of polyethylene obtained in practice?

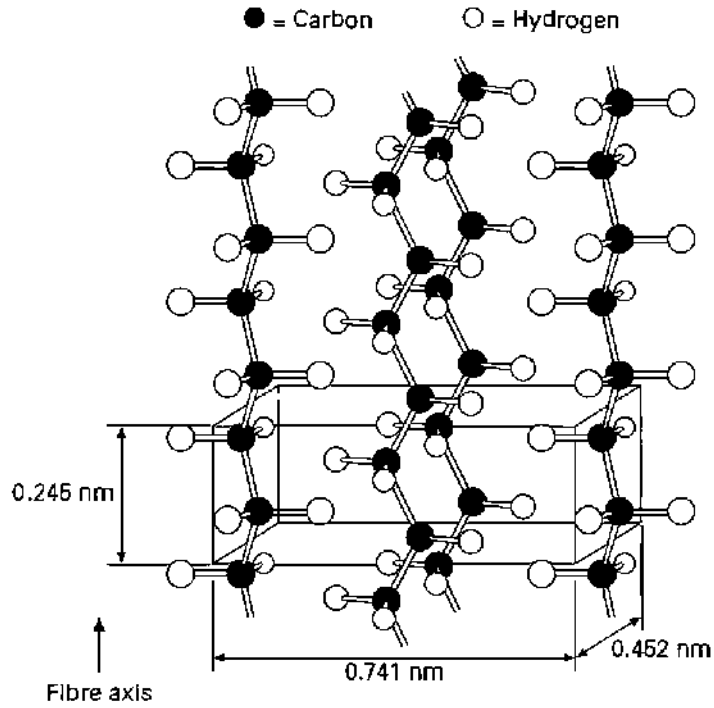


**Figure E1.13** Crystalline form of polyethylene with orthorhombic unit cell.

**1.14** A pitch blend sample has five different molecular species with molecular masses of $0.5 \times 10^6$, $0.5 \times 10^7$, $1 \times 10^7$, $4 \times 10^7$, and $6 \times 10^7$. Compute the number-averaged molecular weight and weight-averaged molecular weight of the sample.

**1.15** Different polymorphs of a material can have different mechanical properties. Give some examples.

**1.16** What are smart materials? Give some examples.

**1.17** What are glass-ceramics? Explain their structure and properties. (Hint: think of Corning ware.)

**1.18** Explain how the scale of microstructure can affect the properties of a material. Use steel, an alloy of iron and carbon, as an example.

**1.19** For a cubic system, calculate the angle between (a) [100] and [111], (b) [111] and [112], (c) [112] and [221].

**1.20** Recalculate the bicycle stiffness ratio for a titanium frame. (See Examples 1.1 and 1.2.) Find the stiffness and weight of the bicycle if the radius of the tube is 25 mm. Use the following information:

$$\begin{aligned} \text{Alloy} &: \text{Ti} - 6\%\text{Al} - 4\%\text{V}, \\ \sigma_y &= 1,150 \text{ MPa}, \\ \text{Density} &= 4.5 \text{ g cm}^{-3}, \\ E &= 106\text{GPa}, \\ G &= 40\text{GPa}. \end{aligned}$$

**1.21** Calculate the packing factor for NaCl, given that $r_{\text{Na}} = 0.186$ nm and $R_{\text{Cl}} = 0.107$ nm.

**1.22** Determine the density of BCC iron structure if the iron atom has a radius of 0.124 nm.

**1.23** Draw the following direction vectors in a cubic unit cell:

(a) [100] and [110], (b) [112], (c) $[\bar{1}10]$, (d) $[\bar{3}2\bar{1}]$.

**1.24** Calculate the stress generated in a turbine blade if its cross-sectional area is 0.002 $m^2$ and the mass of each blade is 0.5 kg. Assume that the rotational velocity $\omega = 15{,}000$ rpm and the turbine disk radius is 1 m.

**1.25** Suppose that the turbine blade from the last problem is part of a jet turbine. The material of the jet turbine is a nickel-based superalloy with yield strength, $\sigma_y = 1.5$ G Pa; it decreases with temperature as:

$$\sigma_y = \sigma_0[(1 - (T - T_0)/(T_m - T_0)],$$

where $T_0 = 293$ K is room temperature and $T_m = 1{,}550$ K is the melting temperature. Find the temperature at which the turbine will flow plastically under the influence of centripetal forces.

**1.26** Calculate the lattice parameter of Ni (FCC) knowing that the atomic diameter of nickel is 0.249 nm.

**1.27** A jet turbine blade, made of MARM 200 (a nickel-based superalloy) rotates at 10,000 rpm. The radius of the disk is 50 mm. The cross-sectional area is 20 $cm^2$ and the length of the blade is equal to 12 cm. The density of MARM 200 is 8.5 g $cm^{-3}$.

**(a)** What is the stress acting on the turbine blade in MPa?

**(b)** If the room temperature strength of MARM 200 is equal to 800 MPa, what is the maximum operational temperature in kelvin?

The yield stress varies with temperature as:

$$\sigma = \sigma_0 \left[ 1 - \left( \frac{(T - T_0)}{(T_m - T_0)} \right)^m \right],$$

where $T_m$ is the melting temperature ($T_m = 1{,}700$ K) and $T_0$ is the room temperature; $m = 0.5$.

**1.28** Generate a three-dimensional unit cell for the intermetallic compound $AuCu_3$ that has a cubic structure. The Au atoms are at the cube corners and the Cu atoms at the center of the faces. Given:

**Figure Ex 1.28**

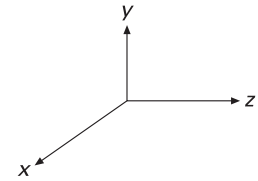


$r_{Cu} = 0.128$ nm $AN_{Cu}$ (atomic number) $= 63.55$ amu
$r_{Au} = 0.144$ nm $AN_{Au} = 196.97$ amu.
(a) Find the lattice parameter in nanometers.
(b) What is the atomic mass of the unit cell in grams?
(c) What is the density of the compound in g $cm^{-3}$?

**1.29** Draw the following unit cells with the planes (one plane per cube with the coordinate axes): (a) $(\bar{1}01)$, (b) $(1\bar{1}1)$, (c) $(0\bar{1}2)$, (d) (301).

**1.30** Show how the atoms pack in the following planes by drawing circles (atoms) in the appropriate spots: (a) (111) in FCC, (b) (110) in FCC, (c) (111) in BCC, (d) (110) in BCC.

**1.31** BET is a technique for measuring the surface area of particles, which is of obvious importance in nanomaterials. Describe this technique. Don't forget to mention what the acronym BET stands for.

**1.32** "Tin plate" is one of the largest tonnage steel products. It is commonly used for making containers. If it is a steel product why is it called tin plate?

**1.33** Using Figure 1.7, list the important symmetry operations in the following crystal systems: (a) triclinic, (b) monoclinic, (c) orthorhombic.

**1.34** The only possible rotation operations that can be used to define crystal systems are rotations of the type $n = 1, 2, 3, 4$, and 6. Using other values of $n$ will result in unit cells which, when joined together, will not fill all space. Demonstrate this by giving a simple mathematical proof. (*Hint*: consider two lattice points separated by a unit translation vector.)

**1.35** Calculate the APF (atomic packing factor) for BCC and FCC unit cells, assuming the atoms are represented as hard spheres. Do the same for the diamond cubic structure.

**1.36** Draw the following crystallographic planes in BCC and FCC unit cells along with their atoms that intersect the planes: (a) (101), (b) (110), (c) (441), (d) (111), (e) (312).

**1.37** A block copolymer has macromolecules of each polymer attached to the other as can be seen in Figure 1.22(c). The total molecular weight is 100,000 g $mol^{-1}$. If 140 g of A and 60 g of B were added, determine the degree of polymerization for each polymer. A: 56 g $mol^{-1}$; B: 70 g $mol^{-1}$.

**1.38** Sketch the following planes within the unit cell. Draw one cell for each solution. Show new origin and ALL necessary calculations.
(a) $(0\bar{1}\bar{1})$, (b) (102), (c) (002), (d) $(1\bar{3}0)$, (e) $(\bar{2}12)$, (f) $(3\bar{1}\bar{2})$.

**1.39** Sketch the following directions within the unit cell. Draw one cell for each solution. Show new origin and ALL necessary calculations.
(a) [101], (b) $[0\bar{1}0]$, (c) $[12\bar{2}]$, (d) [301], (e) $[\bar{2}01]$, (f) $[2\bar{1}3]$.

**1.40** Suppose we introduce one carbon atom for every 100 iron atoms in an interstitial position in BCC iron, giving a lattice parameter of 0.2867 nm. For the Fe-C alloy, find the density and the packing factor.
Given:
Atomic mass of C = 12,
Atomic mass of Fe = 55.89,
$a_{Fe} = 0.2867$ nm,
Avogadro's number, $N = 6.02 \times 10^{23}$.

**1.41** Determine the maximum length of a polymer chain made with 1,500 molecules of ethylene, knowing that the carbon bond length is 0.13 nm.

**1.42** Calculate the atomic packing factor (APF) of diamond cubic.

**1.43** SiC has the diamond cubic structure. Calculate the APF of SiC ($r_{Si} = 0.11$ nm and $r_C = 0.07$ nm).

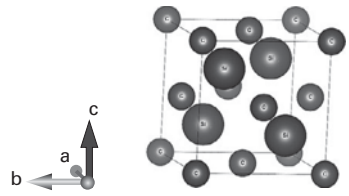


**Figure Ex 1.43**

**1.44** **(a)** How can the development of composites influence future aircraft?
**(b)** What are the principal features of composites?

**1.45** If steel is as strong as aluminum alloys in terms of strength, why are planes built with aluminum alloys?

**1.46** What composite materials are used in the Boeing 787?

**1.47** Draw the direction vectors in a cubic unit cell: [111], [201] and $[\bar{2}31]$.

**1.48** (a) Determine the interplanar spacing of (110) planes in a tetragonal unit cell ($a = b \neq c$, $\alpha = \beta = \gamma = 90^\circ$) with lattice parameters of $a = 0.3963$ nm and $c = 0.3671$ nm. (b) Determine the areas of the following planes $(\bar{1}10)$, $(1\bar{2}0)$ and $(00\bar{1})$.

**1.49** There are face-centered and body-centered structures in cubic systems, but no base-centered cubic. Show that the base-centered cubic structure is equivalent to another structure of the Bravais lattices.

**1.50** Explain the concept of free volume in glass transition in condensed matter. Why we can easily make a polymer which is composed of small molecules like metals in a glassy state but not in a crystalline state (though certain metallic glasses can be made easily).

**1.51** Stress–strain diagrams for three different polymers can be found in the following plot. It is known that one of the polymers is in a rubbery state, one is in a glassy state and the third is in a semicrystalline state. Please indicate the corresponding curves for the rubber, glassy, and semicrystalline polymers.

**1.52** Why is the percentage of composite materials increasing as time goes by? What are the advantages of using composite materials over traditional metallic materials?

**1.53** If gold atoms have a radius of 0.144 nm, determine the density and APF (atomic packing factor) in FCC and BCC structures. (Atoms are in contact along the face diagonal and body diagonal directions; $a = 0.407$ nm.)

**1.54** Find the indices of planes and directions in the HCP crystal structure.

**Figure Ex 1.54**

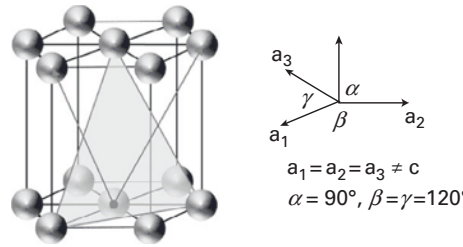


**1.55** How many major types of composite materials are there? What is the main component of composite materials?

**1.56** Draw three types of composite material.

**1.57** It is known that FCC and HCP possess relatively high APFs (atomic packing factors). Determine (a) the stacking pattern of FCC, HCP and BCC, (b) the closest packing plane of the FCC and BCC structures.

**1.58** Explain the difference between homopolymer, copolymer and block polymer by drawing them.

**1.59** Dental implant surgery is a procedure to replace the tooth roots with man-made materials. After the surgery, the artificial teeth will function as real ones. Stainless steel used to be the primary choice for implants. However, titanium is chosen over stainless steel nowadays. What is the advantage of titanium over stainless steel in this case?

**1.60** A continuous and aligned glass-fiber-reinforced composite consists of 25 vol% glass fibers with an elastic modulus of 80 GPa and 75 vol% of a polymer with an elastic modulus of 4.2 GPa.

**(a)** Compute the elastic modulus of this material in the longitudinal direction.

**(b)** If the cross-sectional area is 300 $mm^2$ and a stress of 40 MPa is applied along longitudinal direction, determine the load on the reinforcement and matrix phases respectively.

**(c)** What is the displacement and strain of the matrix and reinforcement phases under these conditions?

**1.61** Given that the lattice parameter of Ti is $a = 0.2950$nm and $c/a = 1.588$, determine the atomic packing factor and density of Ti. (The atomic weight of Ti is 48 g $mol^{-1}$ and the radius of a Ti atom is 147 pm.)

# Chapter 2 Elasticity and Viscoelasticity

## 2.1 Introduction

Elasticity deals with elastic stresses and strains, their relationship, and the external forces that cause them. An *elastic strain* is defined as a strain that disappears instantaneously once the forces that cause it are removed. The theory of elasticity for Hookean solids in which stress is proportional to strain is rather complex in its more rigorous treatment. However, it is essential to the understanding of micro- and macromechanical problems. Examples of the former are stress fields around dislocations, incompatibilities of stresses at the interface between grains, and dislocation interactions in work hardening; examples of the latter are the stresses developed in drawing and rolling wire, and the analysis of specimen machine interactions interesting for tensile strength. This chapter is structured in such a way as to satisfy the needs of both the undergraduate and the graduate student. A simplified treatment of elasticity is presented, in a manner so as to treat problems in an undergraduate course. Stresses and strains are calculated for a few simplified cases; the tridimensional treatment is kept at a minimum. A graphical method for the solution of two-dimensional stress problems (the Mohr circle) is described. On the other hand, the graduate student needs more powerful tools to handle problems that are somewhat more involved. In most cases, the stress and strain systems in tridimensional bodies can be better treated as tensors, with the indicial notation. Once this tensor approach is understood, the student will have acquired a very helpful visualization of stresses and strains as tridimensional entities. Important problems whose solutions require this kind of treatment involve stresses around dislocations, interactions between dislocations and solute atoms, fracture mechanics, plastic waves in solids, stress concentrations caused by precipitates, the anisotropy of individual grains and the stress state in a composite material.

## 2.2 Longitudinal Stress and Strain

Figure 2.1 shows a cylindrical specimen being stressed in a machine that tests materials for tensile strength. The upper part of the specimen is screwed to the crosshead of the machine. The coupled rotation of the two lateral screws causes the crosshead to move.

MARC A. MEYERS AND KRISHAN K. CHAWLA

# Mechanical Behavior of Materials

THIRD EDITION

# Mechanical Behavior of Materials

## Third Edition

Fully revised and updated, the new edition of this classic textbook provides a balanced mechanics-materials approach to understanding the mechanical behavior of materials.

It presents fundamental mechanisms operating at micro- and nanometer scales across a wide range of materials, in a way that is mathematically simple and requires no extensive knowledge of materials, and demonstrates how the microstructures and mesostructures of these materials determine their mechanical behavior.

Accompanied online by further resources for instructors, this is the ideal introduction for senior undergraduate and graduate students in materials science and engineering.

### New to this edition

New coverage of biomaterials, electronic materials, and cellular materials alongside established coverage of metals, polymers, ceramics, and composites.

New testing techniques such as micropillar compression and electron back-scattered diffraction.

Important new materials, such as high-entropy alloys, are introduced.

A stronger emphasis on real-world test data and tables, to train students in practical materials applications.

Over 40 new figures, over 100 worked examples, and over 740 exercises, including over 280 new exercises, to help cement student understanding.

**Marc A. Meyers** is a Distinguished Professor of Materials Science and Engineering at the University of California, San Diego, known for his expertise on the dynamic behavior of materials. He is a recipient of the TMS Educator Award (2013), the ASM International Albert Easton White Distinguished Teacher Award (2015), and the APS George Duvall Shock Compression Science Award (2017). He is a coauthor of *Biological Materials Science* (2014), and is a Fellow of TMS, ASM International, and the APS.

**Krishan K. Chawla** is an Emeritus Professor at the University of Alabama at Birmingham, and a former Program Director for Metals and Ceramics in the US NSF Division of Materials Research. He is the editor and chairman of the ASM Editorial Board for *International Materials Reviews*, the author of *Fibrous Materials*, 2nd edn. (2016), and a Fellow of ASM International.

# Mechanical Behavior of Materials

THIRD EDITION

**Marc A. Meyers**
University of California, San Diego

**Krishan K. Chawla**
University of Alabama at Birmingham

CAMBRIDGE
UNIVERSITY PRESS

CAMBRIDGE
UNIVERSITY PRESS

Shaftesbury Road, Cambridge CB2 8EA, United Kingdom

One Liberty Plaza, 20th Floor, New York, NY 10006, USA

477 Williamstown Road, Port Melbourne, VIC 3207, Australia

314–321, 3rd Floor, Plot 3, Splendor Forum, Jasola District Centre, New Delhi – 110025, India

103 Penang Road, #05–06/07, Visioncrest Commercial, Singapore 238467

Cambridge University Press is part of Cambridge University Press & Assessment,
a department of the University of Cambridge.

We share the University's mission to contribute to society through the pursuit of
education, learning and research at the highest international levels of excellence.

www.cambridge.org
Information on this title: www.cambridge.org/highereducation/isbn/9781108837903

DOI: 10.1017/9781108943383



First published in 1998 by Prentice-Hall
Second edition 2009 Cambridge University Press
6th printing 2013
Third edition 2025

*A catalogue record for this publication is available from the British Library.*

*Library of Congress Cataloging-in-Publication Data*
Names: Meyers, Marc A., author. | Chawla, Krishan Kumar, 1942– author.
Title: Mechanical behavior of materials / Marc A. Meyers, University of California, San Diego,
Krishan K. Chawla, University of Alabama, Birmingham.
Description: Third edition. | Cambridge ; New York, NY, USA : Cambridge University Press, [2025] |
Includes bibliographical references and index.
Identifiers: LCCN 2024014471 (print) | LCCN 2024014472 (ebook) | ISBN 9781108837903 (hardback) |
ISBN 9781108943383 (epub)
Subjects: LCSH: Strength of materials.
Classification: LCC TA403 .M554 2025 (print) | LCC TA403 (ebook) | DDC 620.1/12–dc23/eng/20240531
LC record available at https://lccn.loc.gov/2024014471
LC ebook record available at https://lccn.loc.gov/2024014472

ISBN 978-1-108-83790-3 Hardback

Additional resources for this publication at www.cambridge.org/mbm3

**Lovingly dedicated to the memory of my parents, Henri and Marie-Anne.**

**Marc André Meyers**

**Lovingly dedicated to the memory of my parents, Manohar L. and Sumitra Chawla.**

**Krishan Kumar Chawla**

# Contents

# Preface to the Third Edition

We are very pleased to offer this third edition of *Mechanical Behavior of Materials*. The first edition was published by Prentice-Hall in 1998. The second edition, a Cambridge University Press imprint, came out in 2009. The third edition is now seeing the light of the day in 2025. Needless to say, we have maintained the same fundamental theme of the book, viz., the fundamental mechanisms responsible for the mechanical properties of different materials under a variety of environmental conditions. The unique feature of the book is the presentation in a unified manner of important principles responsible for mechanical behavior of materials, metals, polymers, ceramics, composites, biological materials, electronic materials. The underlying theme is that structure (at the micro or nanometer level) of the material controls the properties of the material.

Although the basic theme of the book remains unchanged, the third edition has been updated with:

- State-of-the-art coverage of the major developments in materials, such as steels, ceramics, polymers, composites, biologic materials. Specifically, we discuss: unique characteristics of biological materials including the Arzt heptahedron and structural design elements which enable a quantitative engineering treatment in Chapter 1; the Euler equation, elasticity averaging methods of isostress and isostrain (Voigt and Reuss), and anisotropic effects to matrix formulation of stiffness in Chapter 2; High-Entropy Alloys in Chapter 10; Micropillar mechanical testing, EBSD (electron back-scattered diffraction), a powerful characterization method, and coincidence site lattice update in Chapter 5; fracture toughness of biological materials in Chapter 7.
- Many new figures to improve the presentation and to clarify the concepts presented.
- Fresh worked examples and exercises that help the students test their understanding.

The book is principally meant for use in the upper division and graduate level courses of mechanical engineering, and materials science and engineering departments. However, it will also be a great source of reference material to the practicing engineer, scientist, and researcher. We have kept the level of mathematics quite simple, and suggest the reader to refer back to Chapter 1 if needed, as it provides the basic materials-level information necessary to study this subject.

MAM would like to thank Sheron Tavares and Aomin Huang for their competent and dedicated work in the revision and permissions. This third edition would never have seen the day if it were not for them. He also thanks Boya Li for

contributing with exercises. He is grateful to his children Marc Meyers and Cristina Windsor, his granddaughters Claire, Isabelle, and Abigail, his brothers Pedro, Jacques, and Carlos for supporting him through this process. A special thanks is due to Linda Homayoun.

KKC is grateful to K. Carlisle, N. Chawla, A. Goel, M. Koopman, R. Kulkarni, A Mortensen, B. R. Patterson, P.D. Portella, and U. Vaidya, for their innumerable discussions and counsels. He is especially grateful to Kanika Chawla and M. Armstrong for their help with figures. As always, he is thankful to his family members, Anita, Kanika, Nikhil, Nimeesh, and Nivi for their forbearance.

# Preface to the Second Edition

The second edition of Mechanical Behavior of Materials has revised and updated material in every chapter to reflect the changes occurring in the field. In view of the increasing importance of bioengineering, a special emphasis is given to the mechanical behavior of biological materials and biomaterials throughout this second edition. A new chapter on environmental effects has been added. Professors Fine and Voorhees[1] make a cogent case for integrating biological materials into materials science and engineering curricula. This trend is already in progress at many US and European universities. Our second edition takes due recognition of this important trend. We have resisted the temptation to make a separate chapter on biological and biomaterials. Instead, we treat these materials together with traditional materials, viz., metals, ceramics, polymers, etc. In addition, taking due cognizance of the importance of electronic materials, we have emphasized the distinctive features of these materials from a mechanical behavior point of view.

The underlying theme in the second edition is the same as in the first edition. The text connects the fundamental mechanisms to the wide range of mechanical properties of different materials under a variety of environments. This book is unique in that it presents, in a unified manner, important principles involved in the mechanical behavior of different materials: metals, polymers, ceramics, composites, electronic materials, and biomaterials. The unifying thread running throughout is that the nano/microstructure of a material controls its mechanical behavior. A wealth of micrographs and line diagrams are provided to clarify the concepts. Solved examples and chapter-end exercise problems are provided throughout the text.

This text is designed for use in mechanical engineering and materials science and engineering courses by upper division and graduate students. It is also a useful reference tool for the practicing engineers involved with mechanical behavior of materials. The book does not presuppose any extensive knowledge of materials and is mathematically simple. Indeed, Chapter 1 provides the background necessary. We invite the reader to consult this chapter off and on because it contains very general material.

In addition to the major changes discussed above, the mechanical behavior of cellular and electronic materials was incorporated. Major reorganization of material has been made in the following parts: elasticity; Mohr circle treatment; elastic constants of fiber reinforced composites; elastic properties of biological and of biomaterials; failure criteria of composite materials; nanoindentation technique

[1] M. E. Fine and P. Voorhees, "On the evolving curriculum in materials science & engineering," *Daedalus*, Spring 2005, 134.

and its use in extracting material properties; etc. New solved and chapter-end exercises are added. New micrographs and line diagrams are provided to clarify the concepts.

We are grateful to many faculty members who adopted the first edition for classroom use and were kind enough to provide us with very useful feedback. We also appreciate the feedback we received from a number of students. MAM would like to thank Kanika Chawla and Jennifer Ko for help in the biomaterials area. The help provided by Marc H. Meyers and M. Cristina Meyers in teaching him the rudiments of biology has been invaluable. KKC would like thank K. B. Carlisle, N. Chawla, A. Goel, M. Koopman, R. Kulkarni, and B. R. Patterson for their help. KKC acknowledges the hospitality of Dr. P. D. Portella at Federal Institute for Materials Research and Testing (BAM), Berlin, Germany, where he spent a part of his sabbatical. As always, he is grateful to his family members, Anita, Kanika, Nikhil, and Nivi for their patience and understanding.

# A Note to the Reader

Our goal in writing *Mechanical Behavior of Materials* has been to produce a book that will be the pre-eminent source of fundamental knowledge about the subject. We expect this to be a guide to the student beyond his or her college years. There is, of course, a lot more material than can be covered in a normal semester-long course. We make no apologies for that in addition to being a classroom text, we want this volume to act as a useful reference work on the subject for the practicing scientist, researcher, and engineer.

Specifically, we have an introductory Chapter 1 (Materials: Structure, Properties, and Performance) dwelling on the themes of the book: structure, mechanical properties, and performance. This section introduces some key terms and concepts that are covered in detail in later chapters. We advise the reader to use this chapter as a handy reference tool, and consult it as and when required. We strongly suggest that the instructor use this first chapter as a self-study resource. Of course, individual sections, examples, and exercises can be added to the subsequent material as and when desired.

Enjoy!

# Chapter 1 Materials: Structure, Properties, and Performance

## 1.1 Introduction

Everything that surrounds us is matter. The origin of the word matter is *mater* (Latin) or *matri* (Sanskrit), for *mother*. In this sense, human beings anthropomorphized that which made them possible – that which gave them nourishment. Every scientific discipline concerns itself with matter. Of all matter surrounding us, a portion comprises materials. What are materials? They have been variously defined. One acceptable definition is "matter that human beings use and/or process." Another definition is "all matter used to produce manufactured or consumer goods." In this sense, a rock is not a material, intrinsically; however, if it is used in aggregate (concrete) by humans, it becomes a material. The same applies to all matter found on Earth: a tree becomes a material when it is processed and used by people, and a skin becomes a material once it is removed from its host and shaped into an artifact.

The successful utilization of materials requires that they satisfy a set of properties. These properties can be classified into thermal, optical, mechanical, physical, chemical, and nuclear, and they are intimately connected to the structure of materials. The structure, in its turn, is the result of synthesis and processing. A schematic framework that explains the complex relationships in the field of the mechanical behavior of materials, shown in Figure 1.1, is Thomas's iterative tetrahedron, which contains four principal elements: mechanical properties, characterization, theory, and processing. These elements are related, and changes in one are inseparably linked to changes in the others. For example, changes may be introduced by the synthesis and processing of, for instance, steel. The most common metal, steel has a wide range of strengths and ductilities (*mechanical properties*), which makes it the material of choice for numerous applications. While low-carbon steel is used as reinforcing bars in concrete and in the body of automobiles, quenched and tempered high-carbon steel is used in more critical applications such as axles and gears. Cast iron, much more brittle, is used in a variety of applications, including automobile engine blocks. These different applications require, obviously, different mechanical properties of the material. The different properties of the three materials, resulting in differences in performance, are attributed to differences in the internal structure of the materials.

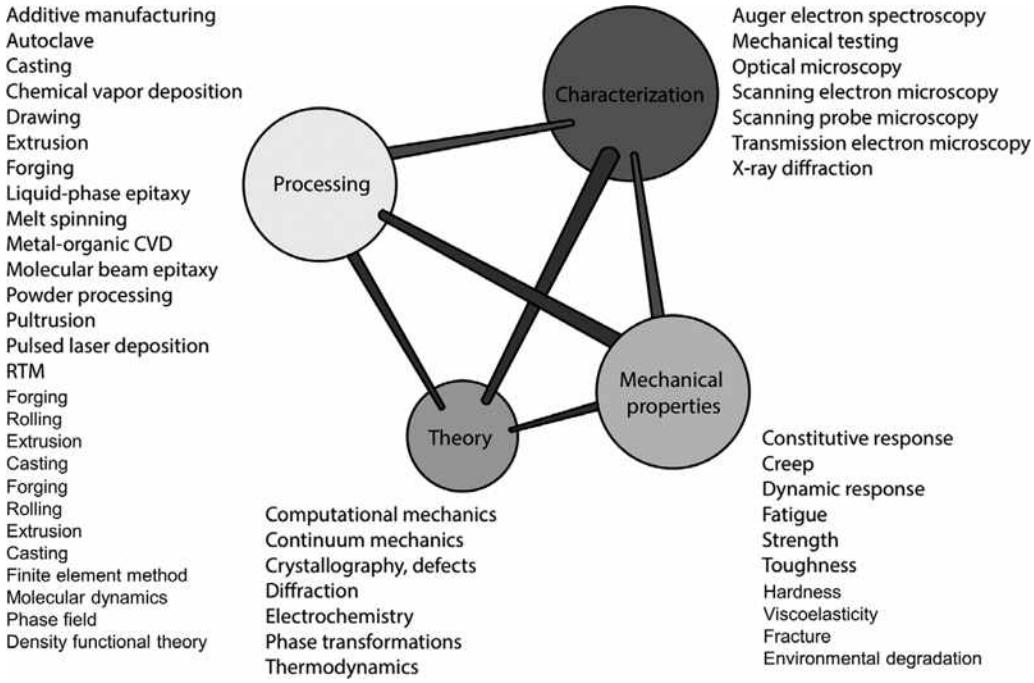


**Figure 1.1** Thomas's iterative materials tetrahedron applied to mechanical behavior of materials. (Figure courtesy of Annelies Zeeman.)

The understanding of the structure comes from *theory*. The determination of the many aspects of the micro-, meso-, and macrostructure of materials is obtained by *characterization*. Low-carbon steel has a primarily ferritic structure (body-centered cubic; see Section 1.3.1), with some interspersed pearlite (a ferrite–cementite mixture). The high hardness of the quenched and tempered high-carbon steel is due to its martensitic structure (body-centered tetragonal). The relatively brittle cast iron has a structure resulting directly from solidification, without subsequent mechanical working such as hot rolling. How does one obtain low-carbon steel, quenched and tempered high-carbon steel, and cast iron? By different *synthesis and processing* routes. The low carbon steel is processed from the melt by a sequence of mechanical working operations. The high-carbon steel is synthesized with a greater concentration of carbon (>0.5%) than the low-carbon steel (0.1%). Additionally, after mechanical processing, the high-carbon steel is rapidly cooled from a temperature of approximately 1,000 °C by throwing it into water or oil; it is then reheated to an intermediate temperature (tempering). The cast iron is synthesized with even higher carbon contents (~2%). It is poured directly into the molds and allowed to solidify in them. Thus, no mechanical working, except for some minor machining, is needed. These interrelationships among structure, properties, and performance, and their modification by synthesis and processing, constitute the central theme of materials science and engineering. The tetrahedron of

Figure 1.1 lists the principal processing methods, the most important theoretical approaches, and the most-used characterization techniques in materials science today.

The selection, processing, and utilization of materials have been part of human culture since its beginnings. Anthropologists refer to humans as "the toolmakers," and this is indeed a very realistic description of a key aspect of human beings responsible for their ascent and domination over other animals. It is the ability of humans to manufacture and use tools, and the ability to produce manufactured goods, that has allowed technological, cultural, and artistic progress and that has led to civilization and its development. Materials were as important to a Neolithic tribe in the year 10,000 BCE as they are to us today. The only difference is that today more complex synthetic materials are available in our society, while Neolithic tribes had only natural materials at their disposal: wood, minerals, bones, hides, and fibers from plants and animals. Although these naturally occurring materials are still used today, they are vastly inferior in properties to synthetic materials.

## 1.2 Monolithic, Composite, and Hierarchical Materials

The early materials used by humans were natural, and their structure varied widely. Rocks are crystalline, pottery is a mixture of glassy and crystalline components, wood is a fibrous organic material with a cellular structure, and leather is a complex organic material. Human beings started to synthesize their own materials in the Neolithic period: ceramics first, then metals, and later, polymers. In the twentieth century, simple monolithic structures were used first. The term *monolithic* comes from the Greek *mono* (one) and *lithos* (stone). It means that the material has essentially uniform properties throughout. Microstructurally, monolithic materials can have two or more phases. Nevertheless, they have properties (electrical, mechanical, optical, and chemical) that are constant throughout. Table 1.1 presents some of the important properties of metals, ceramics, and polymers. Their detailed structures will be described in Section 1.3. The differences in their structure are responsible for differences in properties. Metals have densities ranging from 2 to 19 g $cm^{-3}$; iron, nickel, chromium, and niobium have densities ranging from to 7 to 9 g $cm^{-3}$ aluminum has a density of 2.7 g $cm^{-3}$; and titanium has a density of 4.5 g $cm^{-3}$. Ceramics tend to have lower densities, ranging from 5 g $cm^{-3}$ (titanium carbide; TiC = 4.9) to 3 g $cm^{-3}$(alumina; $Al_2O_3$ = 3.95; silicon carbide; SiC = 3.2). Polymers have the lowest densities, fluctuating around 1 g $cm^{-3}$. Another marked difference among these three classes of materials is their ductility (ability to undergo plastic deformation). At room temperature, metals can undergo significant plastic deformation. Thus, metals tend to be ductile, although there are a number of exceptions. Ceramics, on the other hand, are very brittle, and the most ductile ceramics will be more brittle than most metals. Polymers have a behavior ranging from brittle (at temperatures below their glass transition temperature) to very deformable (in a nonlinear elastic material, such as rubber). The fracture toughness

**Table 1.1 Summary of Properties of Main Classes of Materials**

| Property | Metals | Ceramics | Polymers |
|---|---|---|---|
| Density (g $cm^{-3}$) | 2–20 | 1–14 | 1–2.5 |
| Electrical conductivity | high | low | low |
| Thermal conductivity | high | low | low |
| Ductility or strain-to-fracture (%) | 4–40 | <1 | 2–4 |
| Tensile strength (MPa) | 100–1,500 | 100–400 | – |
| Compressive strength (MPa) | 100–1,500 | 1,000–5,000 | – |
| Fracture toughness ($MNm^{-3/2}$) | 10–30 | 1–10 | 2–8 |
| Maximum service temperature (°C) | 1,000 | 1,800 | 250 |
| Corrosion resistance | low to medium | superior | medium |
| Bonding | metallic (free-electron cloud) | ionic or covalent | covalent |
| Structure | mostly crystalline (face-centered cubic, FCC; body-centered cubic, BCC; hexagonal close packed, HCP) | complex crystalline structure | amorphous or semicrystalline polymer |

is a good measure of the resistance of a material to failure and is generally quite high for metals and low for ceramics and polymers. Ceramics far outperform metals and polymers in high-temperature applications, since many ceramics do not oxidize even at very high temperatures (the oxide ceramics are already oxidized) and retain their strength to such temperatures. One can compare the mechanical, thermal, optical, electrical, and electronic properties of the different classes of materials and see that there is a very wide range of properties. Thus, monolithic structures built from primarily one class of material cannot provide all desired properties.

In the field of biomaterials (materials used in implants and life support systems), developments have also had far-reaching effects. The mechanical performance of implants is critical in many applications, including hipbone implants, which are subjected to high stresses, and endosseous implants in the jaw designed to serve as the base for teeth. Figure 1.2(a) shows the most successful design for endosseous implants in the jawbone. With this design, a titanium post is first screwed into the jawbone and allowed to heal. The tooth is fixed to the post and is effectively rooted into the jaw. The insertion of endosseous implants into the mandibles or maxillae, which was initiated in the 1980s, has been a revolution in dentistry. There is a little story associated with this discovery. Researchers were investigating the bone marrow of rabbits. They routinely used stainless steel hollow cylinders screwed into the bone. Through the hole, they could observe the bone marrow. It so happened that one of these cylinders was made of titanium. Since these cylinders were expensive, the researchers removed them periodically, in order to reuse them. When they tried to remove the titanium cylinder, it was tightly fused to the bone.

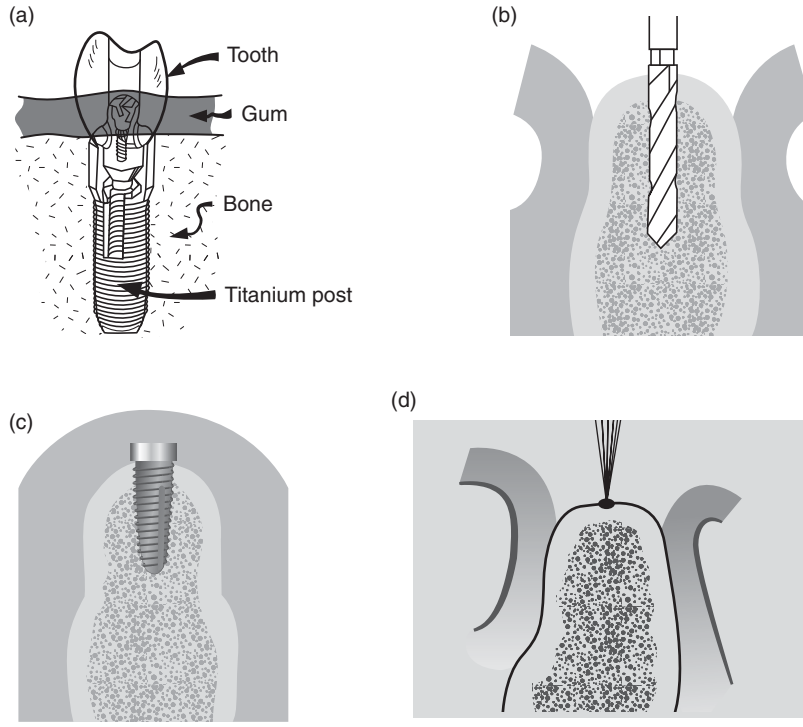


**Figure 1.2** (a) Complete endosseous implant, (b) a hole is drilled, and (c) a titanium post is screwed into jawbone. (d) Marking of site with small drill. (Figure courtesy of J. Mahooti.)

This triggered the creative intuition of one of the researchers, who said "What if. . .?".

Figure 1.2 shows the procedure used to insert the titanium implant. The site is first marked with a small drill that penetrates the cortical bone (Figure 1.2(d)). Then successive drills are used to create an orifice of the desired diameter (Figure 1.2(b)). The implant is screwed into the bone and the tissue is closed (Figure 1.2(c)). This implant is allowed to heal and fuse with the bone for approximately six months. Chances are that most readers will have these devices installed sometime in their lives.

Hip- and knee-replacement surgery is becoming commonplace. In the USA alone between 250,000 and 300,000 of each procedure are carried out annually. The materials of the prostheses have an important bearing on survival probability. Typical hip and knee prostheses are shown in Figure 1.3.

The hip prosthesis is made up of two parts: the acetabular component, or socket portion, which replaces the acetabulum, and the femoral component, or stem portion, which replaces the femoral head.

The femoral component is made of a metal stem with a metal ball on the extremity. In some prostheses a ceramic ball is attached to the metal stem. The acetabular component is a metal shell with a plastic inner socket liner made of

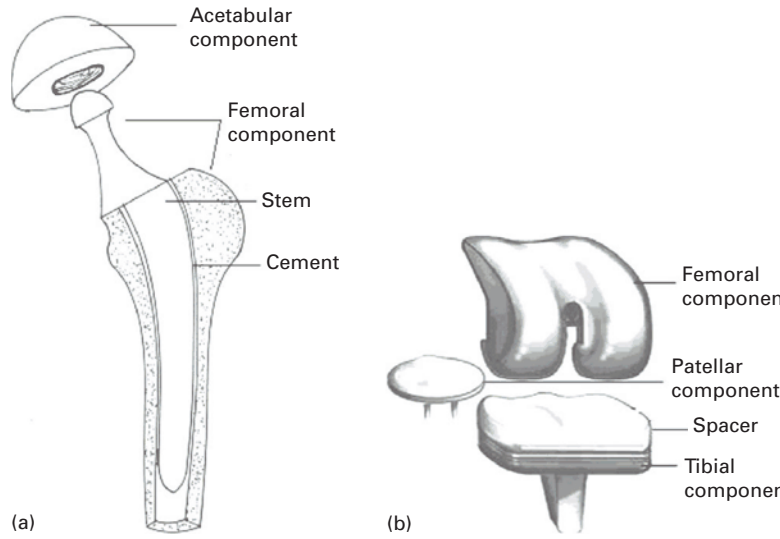


**Figure 1.3** (a) Total hip replacement prosthesis (b) total knee replacement prosthesis.

metal, ceramic, or a plastic called ultra-high-molecular-weight polyethylene (UHMWPE) that acts like a bearing. A *cemented* prosthesis is held in place by a type of epoxy cement that attaches the metal to the bone. An *uncemented* prosthesis has a fine mesh of holes on the surface area that touches the bone. The mesh allows the bone to grow into the mesh and become part of the bone. Biomaterial advances have allowed experimentation with new bearing surfaces, and there are now several different options when hip-replacement surgery is considered.

The metal has to be inert in the body environment. The preferred materials for the prostheses are Co–Cr alloys (Vitalium®) and titanium alloys. However, there are problems that have not yet been resolved: the metallic components have elastic moduli that far surpass those of bone. Therefore, they "carry" a disproportionate fraction of the load, and the bone is therefore unloaded. Since the health and growth of bone is closely connected to the loads applied to it, this unloading tends to lead to bone loss.

The most common cause of joint replacement failure is wear of the implant surfaces. This is especially critical for the polymeric components of the prosthesis. This wear produces debris which leads to tissue irritation. Another important cause of failure is loosening of the implant due to weakening of the surrounding bone. A third source of failure is fatigue.

*Biocompatibility* is a major concern for all implants, and ceramics are especially attractive because of their (relative) chemical inertness. Metallic alloys such as Vitalium® and titanium alloys have also proved to be successful, as have polymers such as polyethylene. A titanium alloy with a solid core surrounded by a porous periphery (produced by sintering of powders) has shown considerable potential. The porous periphery allows bone to grow and affords very effective fixation. Two new classes of materials that appear to present the best biocompatibility with bones are the Bioglass® and calcium phosphate ceramics. Bones contain calcium and

phosphorus, and Bioglass® is a glass in which the silicon has been replaced by those two elements. Thus, the bone "perceives" these materials as being another bone and actually bonds with it. Biomechanical properties are of great importance in bone implants, as are the elastic properties of materials. If the stiffness of a material is too high, then when implanted the material will carry more of the load placed on it than the adjacent bone. This could in turn lead to a weakening of the bone, since bone growth and strength depend on the stresses that the bone is subjected to. Thus, the elastic properties of bone and implant should be similar. Polymers reinforced with strong carbon fibers are also candidates for such applications. Metals, on the other hand, are stiffer than bones and tend to carry most of the load. With metals, the bones would be shielded from stress, which could lead to bone resorption and loosening of the implant.

Although new materials are being developed continuously, monolithic materials, with their uniform properties, cannot deliver the range of performance needed in any critical applications. *Composites* are a mixture of two classes of materials: metal–ceramic, metal–polymer, or polymer–ceramic. They have unique mechanical properties that are dependent on the amount and manner in which their constituents are arranged. Figure 1.4(a) shows schematically how different composites can be formed. Composites consist of a matrix and a reinforcing material. In making them, the modern materials engineer has at his or her disposal a very wide range of possibilities. However, the technological problems involved in producing some of them are immense, although there is a great deal of research addressing these problems. Figure 1.4(b) shows three principal kinds of reinforcement in composites: particles, continuous fibers, and discontinuous (short) fibers. The reinforcement usually has a higher strength than the matrix, which provides the ductility of the material. In ceramic-based composites, however, the matrix is brittle, and the fibers provide barriers to the propagating cracks, increasing the toughness of the material.

The alignment of the fibers is critical in determining the strength of a composite. The strength is highest along a direction parallel to the fibers and lowest along directions perpendicular to it. For the three kinds of composite shown in Figure 1.4(b), the polymer matrix plus (aramid, carbon, or glass) fiber is the most common combination if no high-temperature capability is needed.

Composites are becoming a major material in the aircraft industry. Carbon/epoxy and aramid/epoxy composites are being introduced in a large number of aircraft parts. These composite parts reduce the weight of the aircraft, increasing its economy and payload. The major mechanical property advantages of advanced composites over metals are better stiffness-to-density and strength-to-density ratios and greater resistance to fatigue. The values given in Table 1.2 apply to a unidirectional composite along the fiber reinforcement orientation. The values along other directions are much lower, and therefore the design of a composite has to incorporate the anisotropy of the materials. It is clear from the table that composites have advantages over monolithic materials. In most applications, the fibers are arranged along different orientations in different layers. For the central composite of Figure 1.4(b), these orientations are 0°, 45° 90°, and 135° to the tensile axis.

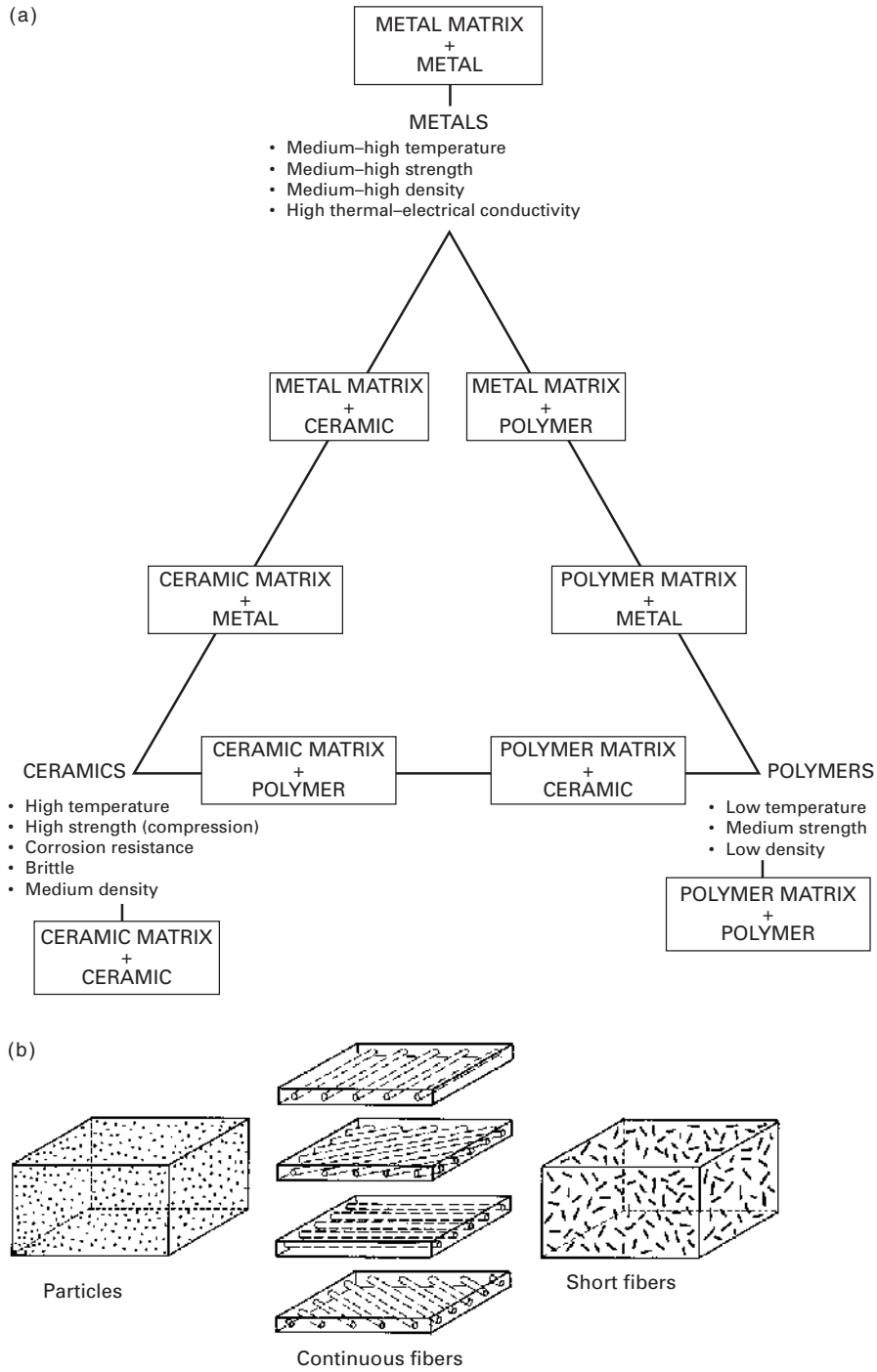


**Figure 1.4** (a) Schematic representations of different classes of composites. (b) Different kinds of reinforcement in composite materials. Composite with continuous fibers with four different orientations (shown separately for clarity).

**Table 1.2 Specific Modulus and Strength of Materials Used in Aircraft**

| Material | Elastic modulus/density (GPa/g cm$^{-3}$) | Tensile strength/density (MPa/g cm$^{-3}$) |
|---|---|---|
| Steel (AISI 4340) | 25 | 230 |
| Al (7075-T6) | 25 | 180 |
| Titanium (Ti-6Al-4V) | 25 | 250 |
| E glass/epoxy composite | 21 | 490 |
| S glass/epoxy composite | 47 | 790 |
| *Aramid/epoxy composite | 55 | 890 |
| HS (high tensile strength) carbon/epoxy composite | 92 | 780 |
| HM (high modulus) carbon/epoxy composite | 134 | 460 |

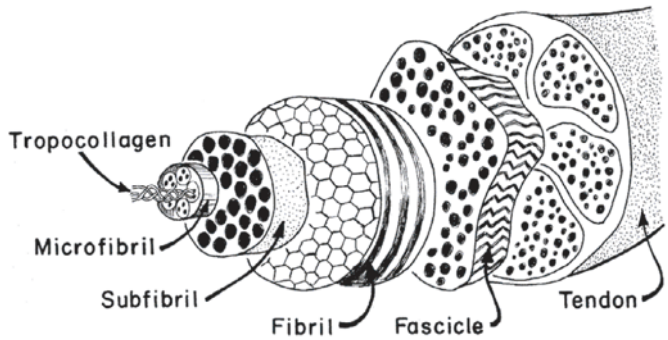


**Figure 1.5** A model of a hierarchical structure occurring in the human body. (Figure courtesy of E. Baer.)

Can we look beyond composites in order to obtain even higher mechanical performance? Indeed, we can: Nature is infinitely imaginative.

Our body is a complex arrangement of parts, designed, as a whole, to perform all the tasks needed to keep us alive. Scientists are looking into the make-up of soft tissue (skin, tendon, intestine, etc.), which is a very complex structure with different units active at different levels complementing each other. The structure of soft tissue has been called a *hierarchical* structure, because there seems to be a relationship between the ways in which it operates at different levels. Figure 1.5 shows the structure of a tendon. This structure begins with the tropocollagen molecule, a triple helix of polymeric protein chains. The tropocollagen molecule has a diameter of approximately 1.5 mm. The tropocollagen organizes itself into microfibrils, subfibrils, and fibrils. The fibrils, a critical component of the structure, are crimped when there is no stress on them. When stressed, they stretch out and then transfer their load to the fascicles, which compose the tendon. The fascicles have a diameter of approximately 150–300 μm and constitute the basic unit of the tendon. The hierarchical organization of the tendon is responsible for its toughness. Separate structural units can fail independently and thus absorb energy locally, without causing the failure of the entire tendon. Both experimental and analytical studies have been done, modeling the tendon as a composite of elastic, wavy fibers in a

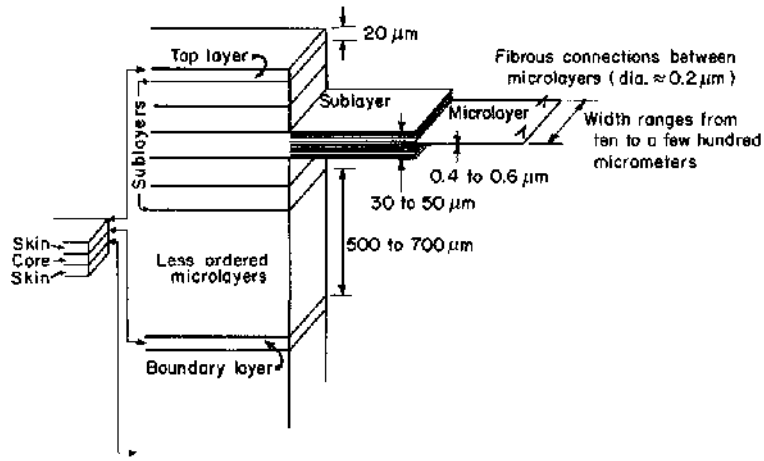


**Figure 1.6** Schematic illustration of a proposed hierarchical model for a composite (not drawn to scale).
(Figure courtesy of E. Baer.)

viscoelastic matrix. Local failures, absorbing energy, will prevent catastrophic failure of the entire tendon until enormous damage is produced.

Materials engineers are beginning to look beyond simple two component composites, imitating nature in organizing different levels of materials in a hierarchical manner. Baer[1] suggests that the study of biological materials could lead to new hierarchical designs for composites. One such example is shown in Figure 1.6, a layered structure of liquid-crystalline polymers consisting of alternating core and skin layers. Each layer is composed of sublayers which, in their turn, are composed of microlayers. The molecules are arranged in different arrays in different layers. The lesson that can be learned from this arrangement is that we appear to be moving toward composites of increasing complexity.

## 1.3 Structure of Materials

The *crystallinity*, or periodicity, of a structure, does not exist in gases or liquids. Among solids, the metals, ceramics, and polymers may or may not exhibit it, depending on a series of processing and composition parameters. Metals are normally crystalline. However, a metal cooled at a superfast rate from its liquid state called *splat cooling* can have an amorphous structure. (This subject is treated in greater detail in Section 1.3.4.) Silicon dioxide ($SiO_2$) can exist as amorphous (fused silica) or as crystalline (cristobalite or tridymite). Polymers consisting of molecular chains can exist in various degrees of crystallinity.

Readers not familiar with structures, lattices, crystal systems, and Miller indices should study these subjects before proceeding with the text. Most books on materials science, physical metallurgy, or X-rays treat the subjects completely. A brief introduction is presented next.

[1] E. Baer, *Sci. Am.* 254, No. 10 (1986) 179.

### 1.3.1 Crystal Structures

To date, seven crystal structures describe all the crystals that have been found. By translating the unit cell along the three crystallographic orientations, it is possible to construct a three-dimensional array. The translation of each unit cell along the three principal directions by distances that are multiples of the corresponding unit cell size produces the crystalline lattice.

Up to this point, we have not talked about atoms or molecules; we are just dealing with the mathematical operations of filling space with different shapes of blocks. We now introduce atoms and molecules, or "repeatable structural units." The unit cell is the smallest repetitive unit that will, by translation, produce the atomic or molecular arrangement. Bravais established that there are 14 space lattices. These lattices are based on the seven crystal structures. The points shown in Figure 1.7 correspond to atoms or groups of atoms. The 14 Bravais lattices can represent the

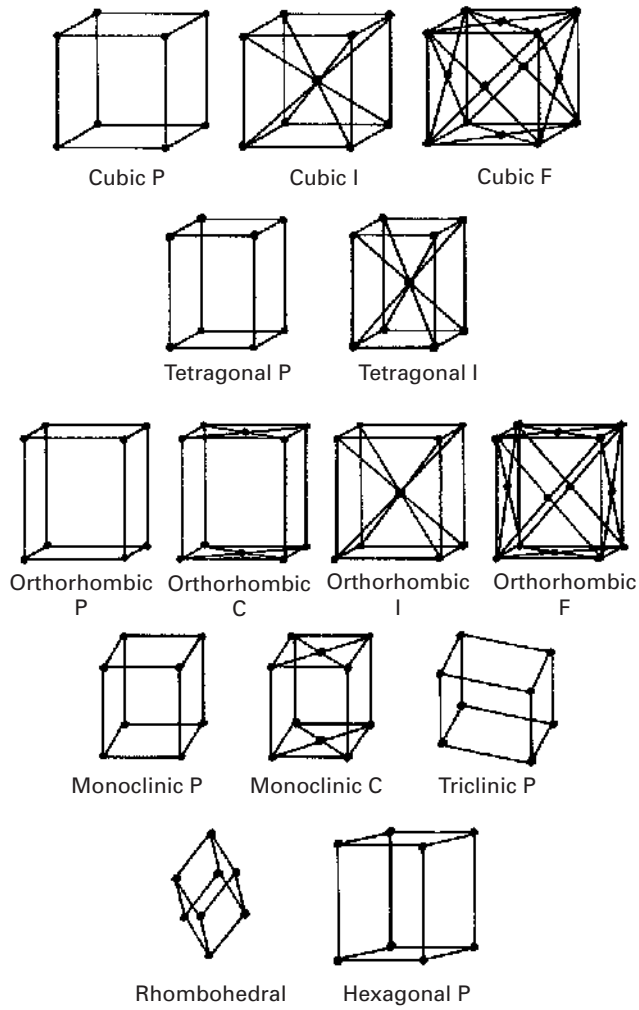


**Figure 1.7** The 14 Bravais space lattices ($P$ = primitive or simple; $I$ = body-centered cubic; $F$ = face-centered cubic; C = base-centered cubic).

**Table 1.3 Seven crystal systems and fourteen Bravais lattices**

| Name | Number of Bravais lattices | © Bart van Zeghbroeck 2007 Conditions | Primitive | Base-centered | Body-centered | Face-centered |
|---|---|---|---|---|---|---|
| Triclinic | 1 | $a_1 \neq a_2 \neq a_3, \alpha \neq \beta \neq \gamma$ | ✓ | | | |
| Monoclinic | 2 | $a_1 \neq a_2 \neq a_3, \alpha = \beta = 90^\circ \neq \gamma$ | ✓ | ✓ | | |
| Orthorhombic | 4 | $a_1 \neq a_2 \neq a_3, \alpha = \beta = \gamma = 90^\circ$ | ✓ | ✓ | ✓ | ✓ |
| Tetragonal | 2 | $a_1 = a_2 \neq a_3, \alpha = \beta = \gamma = 90^\circ$ | ✓ | | ✓ | |
| Cubic | 3 | $a_1 = a_2 = a_3, \alpha = \beta = \gamma = 90^\circ$ | ✓ | | ✓ | ✓ |
| Rhombohedral | 1 | $a_1 = a_2 = a_3, \alpha = \beta = \gamma < 120^\circ \neq 90^\circ$ | ✓ | | | |
| Hexagonal | 1 | $a_1 = a_2 \neq a_3, \alpha = \beta = 90^\circ, \gamma = 120^\circ$ | ✓ | | | |

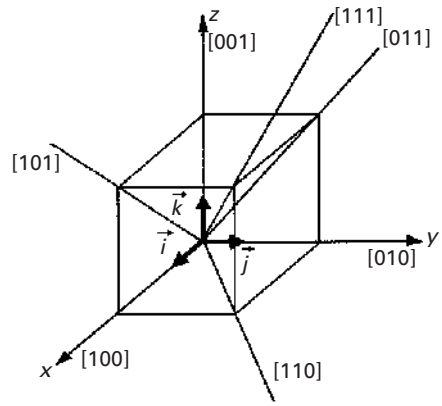


**Figure 1.8** Directions in a cubic unit cell.

unit cells for all crystals. Table 1.3 lists the 14 Bravais lattices as well as the respective lattice parameters. Figure 1.8 shows the indices used for directions in the cubic system. The same symbols are employed for different structures. We simply use the vector passing through the origin and a point ($m$, $n$, $o$):

$$\mathbf{V} = m\mathbf{i} + n\mathbf{j} + o\mathbf{k}.$$

If:

$$\mathbf{u} = u_1\mathbf{i} + u_2\mathbf{j} + u_3\mathbf{k}$$

and:

$$\mathbf{v} = v_1\mathbf{i} + v_2\mathbf{j} + v_3\mathbf{k}$$

we have:

$$\cos\ \alpha = \frac{u_1v_1 + u_2v_2 + u_3v_3}{\sqrt{u_1^2 + u_2^2 + u_3^2}\sqrt{v_1^2 + v_2^2 + v_3^2}}.$$

The angle between two directions **u** and **v** can be calculated through the cross product of the vectors:

$$\cos\alpha = \frac{\mathbf{u}\cdot\mathbf{v}}{|\mathbf{u}|\cdot|\mathbf{v}|}.$$

The notation used for a direction is

[m n o].

When we deal with a family of directions, we use the symbol $<mno>$.

The following family encompasses all equivalent directions:

$$< mno > \Rightarrow [mno], [mon], [omn], [onm], [nmo], [m\overline{n}o]$$
$$[mo\overline{n}], [om\overline{n}], [o\overline{n}m], [\overline{n}mo], \ldots$$

where an overbar indicates a negative sign in front of the variable. When the direction does not pass through the origin, and we have the head of the vector at $(m, n, o)$ and the tail at $(p, q, r)$, the vector **V** is given by

$$\mathbf{V} = (m-p)\mathbf{i} + (n-q)\mathbf{j} + (o-r)\mathbf{k}.$$

A direction not passing through the origin can be represented by

$$[(m-p)(n-q)(o-r)].$$

We can clear fractions, to reach smallest integer. Note that for the negative, we use a bar on top. For planes, we use the Miller indices, obtained from the intersection of a plane with the coordinate axes. Figure 1.9 shows a plane and its intercepts. We take

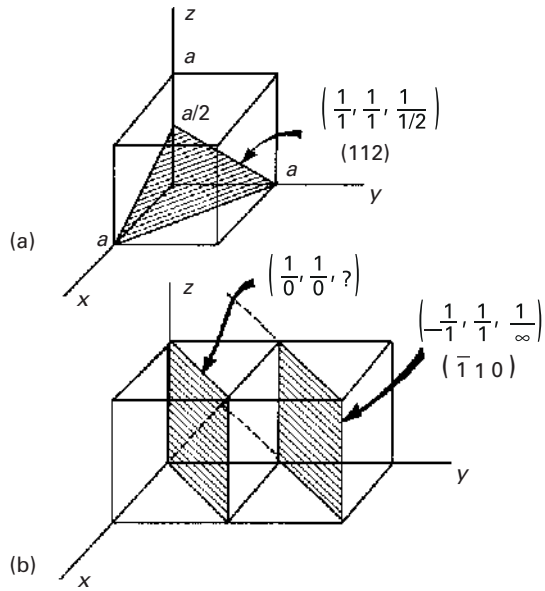


**Figure 1.9** Indexing of planes by Miller rules in the cubic unit cell; (a) (112); (b) $(\overline{1}10)$.

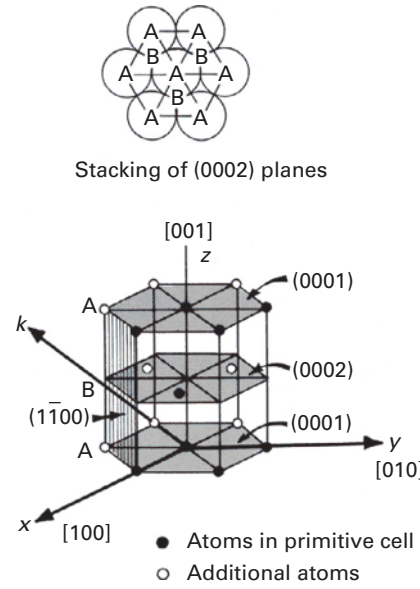


**Figure 1.10** Hexagonal structure consisting of a three-unit cell.

the inverse of the intercepts and multiply them by their common denominator so that we end up with integers. In Figure 1.9(a), we have

$$\frac{1}{1}, \frac{1}{1}, \frac{1}{1/2} \Rightarrow (112).$$

Figure 1.9 (b) shows an indeterminate situation. Thus, we have to translate the plane to the next cell, or else translate the origin. The indeterminate situation arises because the plane passes through the origin. After translation, we obtain intercepts (–1, 1, ∞). By inverting them, we get (110). The symbol for a family of planes is {m n o}. We do not reach to smallest integer. We use round parentheses ( ). For a family, we use { }. If the plane contains one of the axes, we move the origin to the next cell. If the plane is parallel to an axis, it intersects it at infinity. For instance, the spacing between (222) and (111) planes is different.

For hexagonal structures, we have a slightly more complicated situation. We represent the hexagonal structure by the arrangement shown in Figure 1.10. The atomic arrangement in the basal plane is shown in the top portion of the figure. Often, we use four axes ($x$, $y$, $k$, $z$) with unit vectors ($i$, $j$, $k$, $I$) to represent the structure. This is mathematically unnecessary, because three indices are sufficient to represent a direction in space from a known origin. Still, the redundancy is found by some people to have its advantages and is described here. We use the intercepts to designate the planes. The hatched plane (prism plane) has indices

$$\frac{1}{1}, \frac{1}{-1}, \frac{1}{\infty}, \frac{1}{\infty}.$$

After determining the indices of many planes, we learn that one always has

$$h + k = -i.$$

Thus, we do not have to determine the index for the third horizontal axis. If we use only three indices, we can use a dot to designate the fourth index, as follows:

$$(1\bar{1}\cdot 0).$$

For the directions, we can use either the three-index notation or a four-index notation. However, with four indices, the $h + k = -i$ rule will not apply in general, and one has to use special "tricks" to make the vector coordinates obey the rule.

If the indices in the three-index notation are $h'$, $k'$, and $\ell'$, the four index notation of directions can be obtained by the following simple equations:

$$h = \frac{1}{3}(2h' - k')$$
$$k = \frac{1}{3}(2k' - h')$$
$$i = -\frac{1}{3}(h' + k')$$
$$\ell = \ell'.$$

It can be easily verified that $h + k = -i$. Thus, the student is equipped to express the directions in the four-index notation.

### 1.3.2 Metals

The metallic bond can be visualized, in a very simplified way, as an array of positive ions held together by a "glue" consisting of electrons. These positive ions, which repel each other, are attracted to the "glue," which is known as an electron gas. Ionic and covalent bonding, on the other hand, can be visualized as direct attractions between atoms. Hence, these types of bonding, especially covalent bonding, are strongly directional and determine the number of neighbors that one atom will have, as well as their positions.

The bonding and the sizes of the atoms in turn determine the type of structure a material has. Often, the structure is very complicated for ionic and covalent bonding. On the other hand, the directionality of bonding is not very important for metals, and atoms pack into the simplest and most compact forms; indeed, they can be visualized as spheres. The structures favored by metals are the face-centered cubic (FCC), body-centered cubic (BCC), and hexagonal close packed (HCP) structures. In the periodic table, of the 81 elements to the left of the Zindl line, 53 have either the FCC or the HCP structure, and 21 have the BCC structure; the remaining 8 have other structures. The Zindl line defines the boundary of the elements with metallic character in the table. Some of them have several structures, depending on temperature. Perhaps the most complex of the metals is plutonium, which undergoes six polymorphic transformations.

Transmission electron microscopy can reveal the positions of the individual atoms of a metal, as shown in Figure 1.11 for molybdenum. The regular atomic array along a [001] plane can be seen. Molybdenum has a BCC structure.

## Example 1.1

Write the indices for the directions and planes marked in Figure E1.1.

**Figure E1.1**

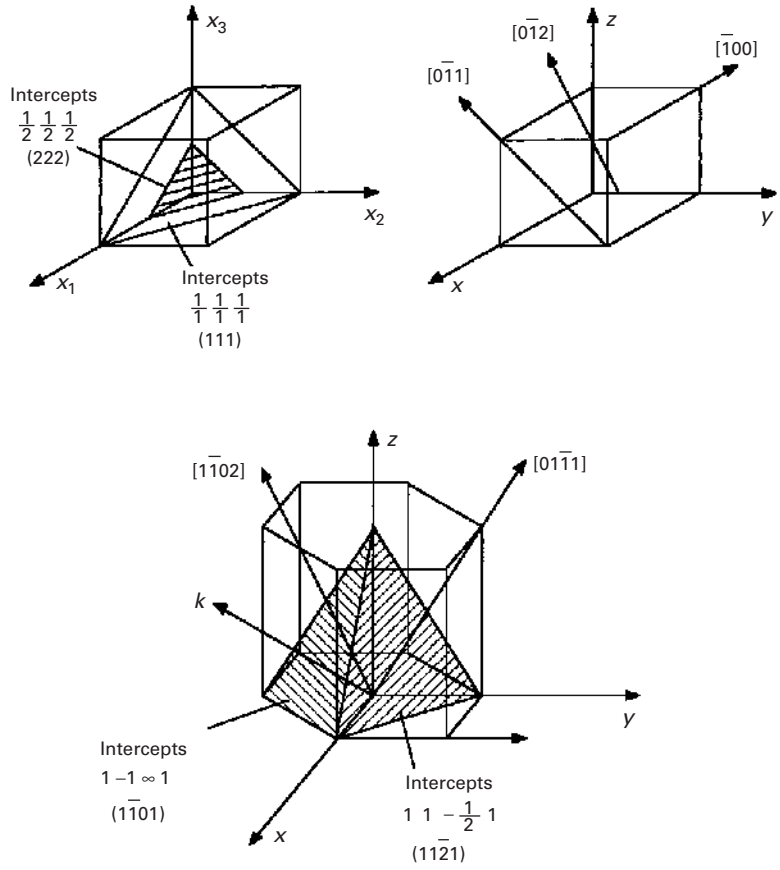


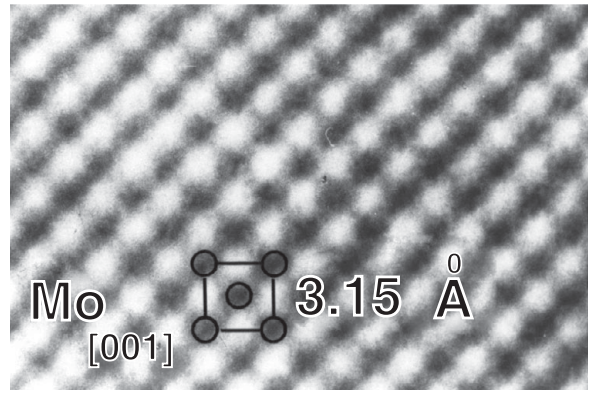


**Figure 1.11** Transmission electron micrograph at atomic resolution of (001) plane in molybdenum showing body-centered cubic arrangement of atoms.
(Figure courtesy of R. Gronsky.)

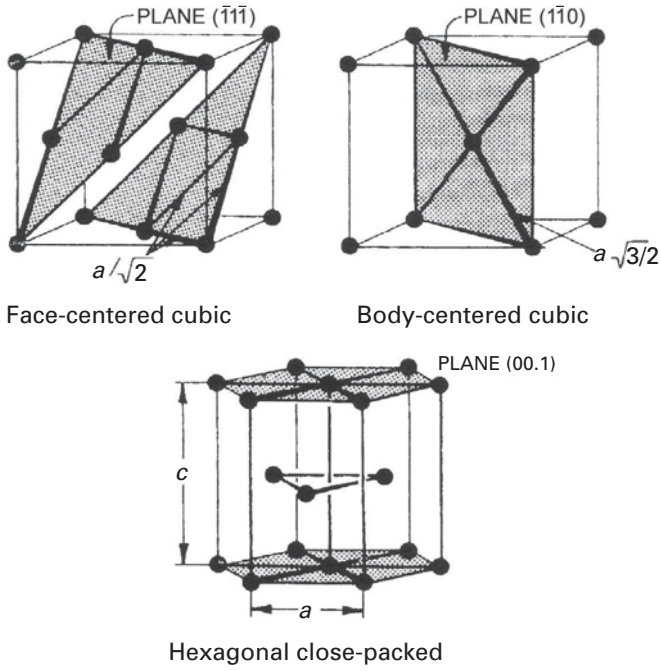


**Figure 1.12** Most closely packed planes in (a) FCC; (b) BCC; (c) HCP.

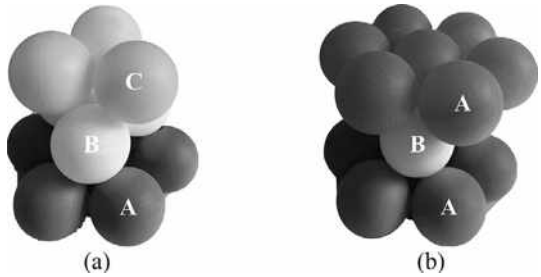


**Figure 1.13** Ball models showing stacking sequence in FCC and HCP structures. (© Sheron Tavares.)
(a) Layers of most closely packed atoms corresponding to (111) in FCC, forming ABC sequence.
(b) Corresponding layers for basal planes in HCP structure, forming ABAB sequence.

Figure 1.12 shows the three main metallic structures. The positions of the atoms are marked by small spheres and the atomic planes by dark sections. The small spheres do not correspond to the scaled-up size of the atoms, which would almost completely fill the available space, touching each other. For the FCC and HCP structures, the coordination number (the number of nearest neighbors of an atom) is 12; for the BCC structure, it is 8.

The ABC sequence of the FCC structure is also revealed in the three-layer model of Figure 1.13(a). The bottom layer (A) is formed of close-packed atoms. The middle layer (B) is also formed of close-packed atoms, whereas the top layer sits on top of three atoms of the B layer. The position of this atom does not correspond to a position in the A or B layers and therefore forms a separate layer C. This is the signature of the FCC structure. On the other hand, the HCP structure can be represented by the ABAB sequence. The third layer is in exact correspondence to the first layer (Figure 1.13(b)).

The planes with the densest packing are $(1\bar{1}1)$, $(1\bar{1}0)$, and (001) for the FCC, BCC, and HCP structures, respectively. These planes have an important effect on the directionality of deformation of the metal, as will be seen in Chapters 4 and 6. The distances between the nearest neighbors are also indicated in the figure. The reader should try to calculate them as an exercise. These distances are $a\sqrt{2}$, $(a\sqrt{3}/2)$, and $a$ for the FCC, BCC, and HCP structures, respectively.

The similarity between the FCC and HCP structures is much greater than might be expected from looking at the unit cells. Planes (111) for FCC and (001) for HCP have the same packing, as may be seen in Figure 1.13. The packing of a second plane similar to, and on top of, the first one (called *A*) can be made in two different ways; Figure 1.13 (a) indicates these two planes by the letters *B* and *C*. Hence, either alternative can be used. A third plane, when placed on top of plane *B*, would have two options: *A* or *C*. If the second plane is *C*, the third plane can be either *A* or *B*. If only the first and second layers are considered, the FCC and HCP structures are identical. If the position of the third layer coincides with that of the first (the *ABA* or *ACA* sequence), we have the HCP structure. Since this packing has to be systematically maintained in the lattice, one would have *ABABAB*... or *ACACAC*... If the third plane does not coincide with the first, we have one of two alternatives *ABC* or *ACB*. Since this sequence has to be systematically maintained, we have *ABCABCABC*... or *ACBACBACB*... This stacking sequence corresponds to the FCC structure. We thus conclude that the only difference between the FCC and HCP structures (the latter with a theoretical *c*/*a* ratio of 1.633) is the stacking sequence of the most densely packed planes. The difference resides in the next neighbors and in the greater symmetry of the FCC structure.

In addition to the metallic elements, intermediate phases and intermetallic compounds exist in great numbers, with a variety of structures. For instance, the beta phase in the copper-manganese-tin (Cu-Mn-Sn) system exhibits a special ordering for the composition $Cu_2MnSn$. The unit cell (BCC) is shown in Figure 1.14. However, the ordering of the Cu, Mn, and Sn atoms creates a super lattice composed of four BCC cells. This super lattice is FCC; hence, the unit cell for the ordered phase is FCC, whereas that for the disordered phase has a BCC unit cell. This ordering has important effects on the functional and structural (mechanical) properties and is discussed in Chapter 11. Although they are composed of three

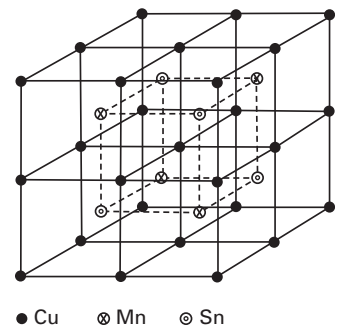


**Figure 1.14** $\beta$-ordered phase in Heusler alloys ($Cu_2MnSn$). (Reprinted from Observations on the ferromagnetic [beta] phase of the Cu-Mn-Sn system, *J. Appl. Cryst.* (1973). 6, 39–41, https://doi.org/10.1107/S0021889873008022, Copyright © International Union of Crystallography (1973).)

**Table 1.4 Some Important Intermetallic Compounds and Their Structures**

| Compound | Melting Point (°C) | Type of Structure |
|---|---|---|
| $Ni_3Al$ | 1,390 | $Ll_2$ (ordered FCC) |
| $Ti_3Al$ | 1,600 | $DO_{19}$ (ordered hexagonal) |
| TiAl | 1,460 | $Ll_0$ (ordered tetragonal) |
| Ni-Ti | 1,310 | CsCl |
| $Cu_3Au$ | 1,640 | $B_2$ (ordered BCC) |
| FeAl | 1,250–1,400 | $B_2$ (ordered BCC) |
| NiAl | 1,380–1,638 | $B_2$ (ordered BCC) |
| $MoSi_2$ | 2,025 | $C11_b$ (tetragonal) |
| $Al_3Ti$ | 1,300 | $DO_{22}$ (tetragonal) |
| $Nb_3Sn$ | 2,134 | $A1_5$ |
| $Nb_5Si_3$ | 2,500 | (tetragonal) |

nonferromagnetic elements, they are ferromagnetic. Heusler alloys were a scientific curiosity until 1984. It was discovered that they have spintronic properties and may lead the way to more efficient computers where information is stored by the spin of the electron. So, Moore's law, which states that the number of transistors in a certain size of computers doubles every two years, can continue for a few more years.

Table 1.4 lists some of the most important intermetallic compounds and their structures. Intermetallic compounds have a bonding that is somewhat intermediate between metallic and ionic/covalent bonding, and have properties that are most desirable for high-temperature applications. Nickel and titanium aluminides are candidates for high-temperature applications in jet turbines and aircraft applications.

## Example 1.2

Determine the ideal $c/a$ ratio for the hexagonal structure.

***Solution:*** The atoms in the basal $A$ plane form a closely packed array, as do the atoms in the $B$ plane going through the mid plane. If we take three atoms in the basal plane, with an atom in the $B$ plane resting among them, we have constructed a tetrahedron. The sides of the tetrahedron are $2r = a$, where $r$ is the atomic radius. The height of this tetrahedron is $c/2$, since the distance between planes is $c$. Hence, the problem is now reduced to finding the height, $c/2$, of a regular tetrahedron. In Figure E1.2, we have

$$DF = \frac{C}{2}$$

$$AB = AC = BC = AD = DB = DC = a.$$

## Example 1.2 (cont.)

**Figure E1.2**

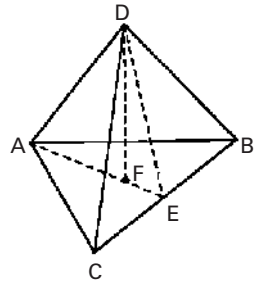


For triangle AEC,

$$AE^2 + EC^2 = AC^2$$

$$AE = \sqrt{a^2 - \frac{a^2}{4}} = \frac{a}{2}\sqrt{3.}$$

For triangle DFE,

$$EF^2 + DF^2 = DE^2.$$

But

$$EF = \frac{1}{3}AE = \frac{a}{6}\sqrt{3,}$$

$$DE = AE = \frac{a}{2}\sqrt{3,}$$

$$DF = \left(\frac{3a^2}{4} - \frac{3a^2}{36}\right)^{1/2},$$

$$\frac{c}{2} = a\left(\frac{2}{3}\right)^{1/2},$$

$$\frac{c}{a} = 2\left(\frac{2}{3}\right)^{1/2}.$$

Thus,

$$\frac{c}{a} = 1.633.$$

## Example 1.3

If the copper atoms have a radius of 0.128 nm, determine the density in FCC and BCC structures.

**(i)** In FCC structures, $4r = \sqrt{2}a_0$

$$a_0 = \frac{4}{\sqrt{2}}r = \frac{4}{\sqrt{2}} \times 0.128 \text{ nm}$$

$$a_0 = 0.362 \text{ nm}.$$

## Example 1.3 (cont.)

There are four atoms per unit cell in FCC. Atomic mass (or weight) of copper is 63.54 g $(g.mol)^{-1}$. So, the density of copper ($\rho$) in FCC structures is

$$\rho = \frac{63.54 \times 4}{\left(0.362 \times 10^{-7}\right)^3 \times \left(6.022 \times 10^{23}\right)} = 8.89 \text{ g cm}^{-3}.$$

↑
Avogadro's Number

**(ii)** In BCC structures, $4r = \sqrt{3}a_0$

$$a_0 = \frac{4}{\sqrt{3}}r = \frac{4}{\sqrt{3}} \times 0.128 \text{ nm}$$
$$a_0 = 0.296 \text{ nm}.$$

There are two atoms per unit cell in BCC structures.

$$\rho = \frac{63.54 \times 2}{\left(0.296 \times 10^{-7}\right)^3 \times \left(6.02 \times 10^{23}\right)} = 8.14 \text{ g cm}^{-3}.$$

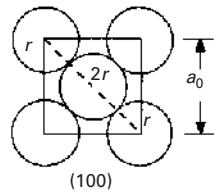


**Figure E1.3** The stable form of Cu is FCC. Only under unique conditions, such as Cu precipitates in iron, is the BCC form stable (because of the constraints of surrounding material).

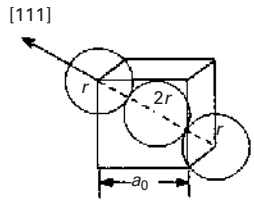


### 1.3.3 Ceramics

The name ceramic comes from the Greek *keramos* (pottery). The production of pottery made of clay dates from 6500 BCE. The production of silicate glass in Egypt dates from 1500 BCE The main ingredient of pottery is a hydrous aluminum silicate that becomes plastic when mixed, in fine powder form, with water. Thus, the early utilization of ceramics included both crystalline and glassy materials. Portland cement is also a silicate ceramic; by far the largest tonnage production of ceramics today – glasses, clay products (brick, etc.), cement – are silicate-based.

However, there have been dramatic changes since the 1970s and a wide range of new ceramics has been developed. These new ceramics are finding applications in

computer memories (due to their unique magnetic applications), in nuclear power stations ($UO_2$ fuel rods), in rocket nose cones and throats, in submarine sonar units (piezoelectric barium titanate), in jet engines (as coatings on metal turbine blades) as electronic packaging components ($Al_2O_3$, SiC substrates), as electrooptical devices (lithium niobate, capable of transforming optical into electrical information and vice versa), as optically transparent materials (ruby and yttrium garnet in lasers, optical fibers), as cutting tools (boron nitride, synthetic diamond, tungsten carbide), as refractories, as military armor ($Al_2O_3$, SiC, $B_4C$), and in a variety of structural applications.

The structure of ceramics is dependent on the character of the bond (ionic, covalent, or partly metallic), on the sizes of the atoms, and on the processing method. We will first discuss the crystalline ceramics.

## Example 1.4

Sketch the 12 members of the <110> family for a cubic crystal. Indicate the four {111} planes. You may use several sketches.

**Figure E1.4**

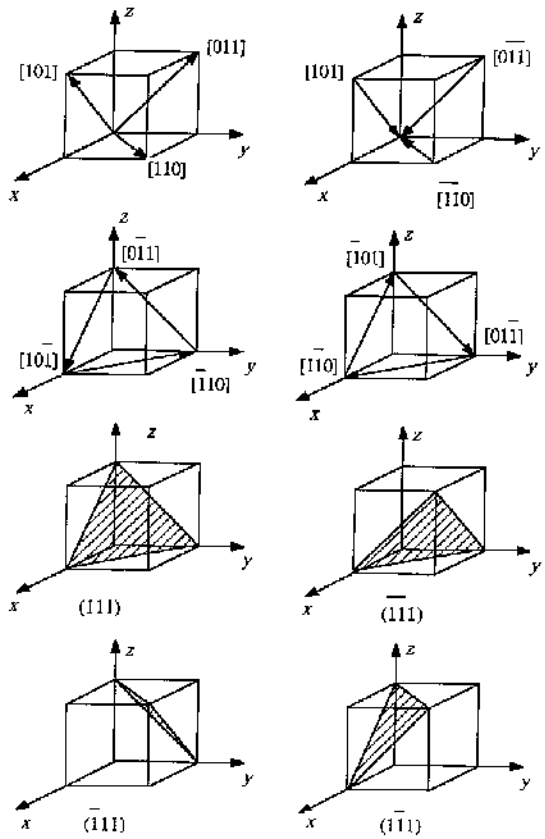

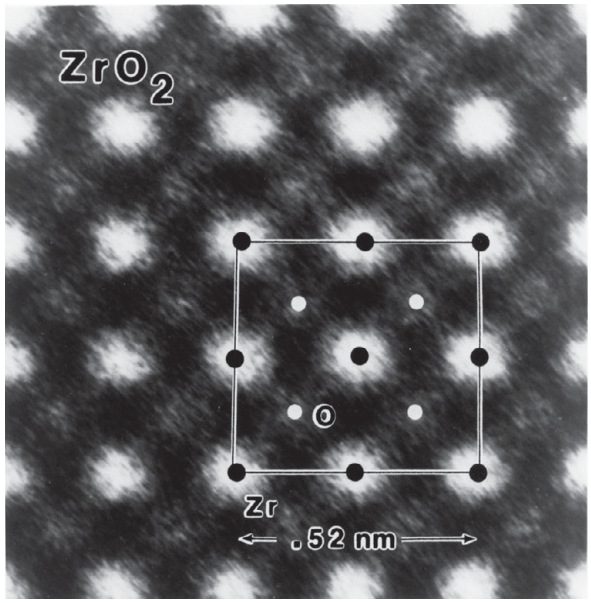


**Figure 1.15** Transmission electron micrograph of $ZrO_2$ at high resolution, showing individual Zr atoms and oxygen sites.
(Figure courtesy of R. Gronsky.)

Transmission electron microscopy has reached the point of development where we can actually image individual atoms, and Figure 1.15 shows a beautiful picture of the zirconium atoms in $ZrO_2$.The much lighter oxygen atoms cannot be seen but their positions are marked in the electron micrograph. By measuring the atomic distances along two orthogonal directions, one can see that the structure is not cubic, but tetragonal. The greater complexity of ceramics, in comparison to metallic structures, is evident from Figure 1.15. Atoms of different sizes have to be accommodated by a structure, and bonding (especially covalent) is highly directional. We will first establish the difference between ionic and covalent bonding.

The electronegativity value is a measure of an atom's ability to attract electrons. Compounds in which the atoms have a large difference in electronegativity are principally ionic, while compounds with the same electronegativity are covalent. In ionic bonding one atom loses electrons and is therefore positively charged (cation). The atom that receives the electrons becomes negatively charged (anion). The bonding is provided by the attraction between positive and negative charges, compensated by the repulsion between charges of equal signs. In covalent bonding the electrons are shared between the neighboring atoms. The quintessential example of covalent bonding is diamond. It has four electrons in the outer shell, which combine with four neighboring carbon atoms, forming a tridimensional regular diamond structure, which is a complex cubic structure. Figure 1.16 shows the diamond structure. The bond angles are fixed and equal to 70° 32'. The covalent bond is the strongest bond, and diamond has the highest hardness of all natural materials. There are synthetic materials that have an even higher hardness, such as graphene and some nanocrystalline structures. Another material that has covalent bonding is SiC.

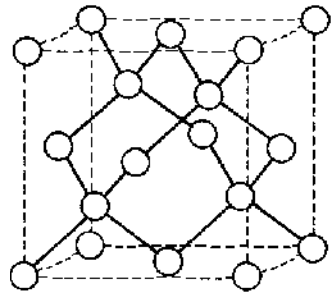

**Figure 1.16** Crystal structure of diamond.

## Example 1.5

(a) Calculate the packing factor of the diamond cubic structure. (b) Calculate the density of diamond. The atomic weight of carbon is 12 g $mol^{-3}$, and the lattice parameter of diamond is 0.357 nm at 300 K.

**Figure E1.5**

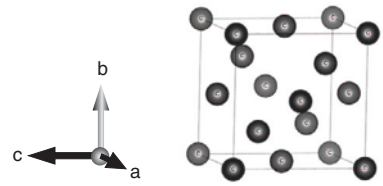


### *Solution:*

**(a)** 8 atoms/cell (4 from FCC + 4 at 1/4, 1/4, 1/4 from FCC atoms).
Nearest neighbor distance:

$$2r = \frac{a\sqrt{3}}{4}$$

$$r = \frac{a\sqrt{3}}{8}.$$

$$\text{Atomic packing factor (APF)} = \frac{\frac{4\pi}{3}\left(\frac{a\sqrt{3}}{8}\right)^{3*}8}{a^3} = \frac{\pi\sqrt{3}}{16} = 0.34.$$

**(b)**

$$\rho\ (\text{g cm}^{-3}) = \frac{m}{V} = \frac{\sum_{i=1}^{N} N_i A_i (\text{g mol}^{-1})}{(a\ \text{nm})^{3*}\left(\frac{1}{1*10^7\,\text{nm}}\right)^{3*}(6.022*10^{23}\,\text{g mol}^{-1})}$$

$$\rho = \frac{(8\ \text{atoms})*(12\ \text{g mol}^{-1})}{(0.357\ \text{nm})^{3*}\left(\frac{1\ \text{cm}}{1*10^7\,\text{nm}}\right)^{3*}(6.022*10^{23}\ \text{g mol}^{-1})} = 3.503\ \text{g cm}^{-3}.$$

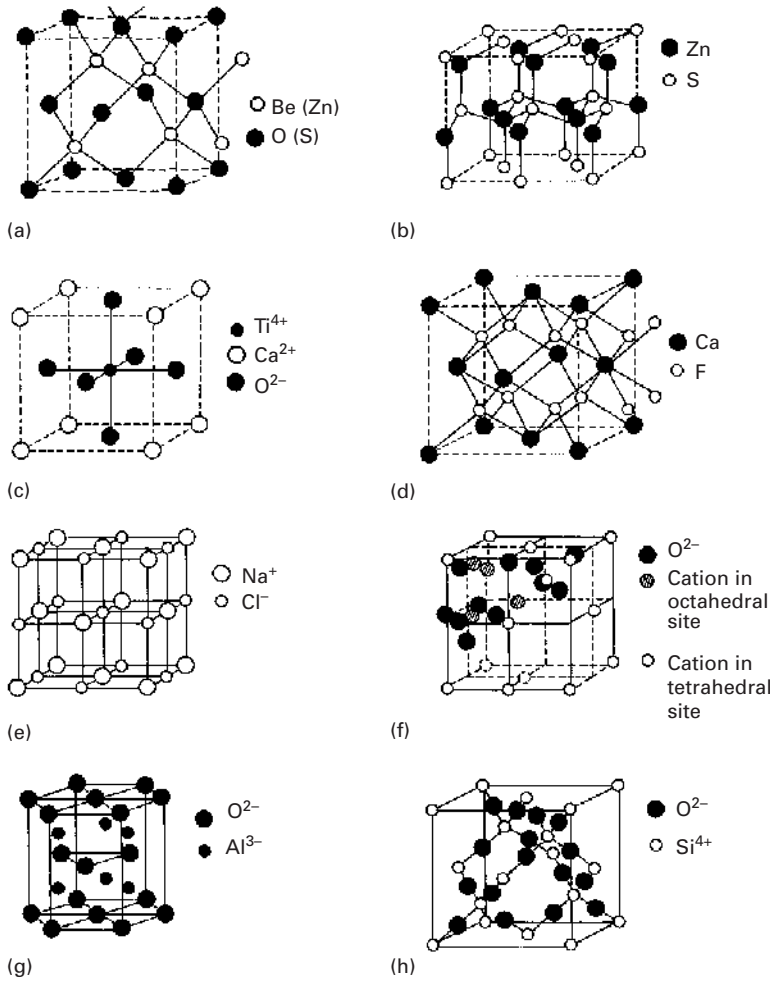


**Figure 1.17** Most common structures for ceramics. (a) Zinc blende (ZnS, BeO, SiC). (b) Wurtzite (ZnS, ZnO, SiC, BN). (c) Perovskite ($CoTiO_3$, $BaTiO_3$, $YCu_2Ba_3O_{7-x}$). (d) Fluorite ($ThO_2$, $UO_2$, $CeO_2$, $ZrO_2$, $PuO_2$). (e) NaCl (KCl, LiF, KBr, MgO, CaO, VO, MnO, NiO). (f) Spinel ($FeAl_2O_4$, $ZnAl_2O_4$, $MoAl_2O_4$). (g) Corundum ($Al_2O_3$, $Fe_2O_3$, $Cr_2O_3$, $Ti_2O_3$, $V_2O_3$). (h) Crystobalite ($SiO_2$-quartz). The CsCl stucture, which has one $Cs^+$ surrounded by four $Cl^-$ ions in cube edges, is not shown.

As the difference of electronegativity is increased, the bonding character changes from pure covalent to covalent-ionic, to purely ionic. Ionic crystals have a structure determined largely by opposite charge surrounding an ion. These structures are therefore established by the maximum packing density of ions. Compounds of metals with oxygen (MgO, $Al_2O_3$, $ZrO_2$, etc.) and with group VII elements (NaCl, LiF, etc.) are largely ionic. The most common structures of ionic crystals are presented in Figure 1.17. Evidently, there are more complex structures in ceramics than in metals because the combinations possible between the elements are so vast.

Ceramics also exist in the glassy state. Silica in this state has the unique optical property of being transparent to light, which is used technologically to great advantage. The building blocks of silica in crystalline and amorphous forms are the silica tetrahedra. Silicon bonds to four oxygen atoms, forming a tetrahedron. The oxygen atoms bond to just two silicon atoms. Numerous structures are possible, with different arrangements of the tetrahedra. Pure silica crystallizes into quartz, crystobalite, and tridymite. Because of these bonding requirements, the structure of silica is fairly open and, consequently, gives the mineral a low density. Quartz has a density of 2.65 g $cm^{-3}$,

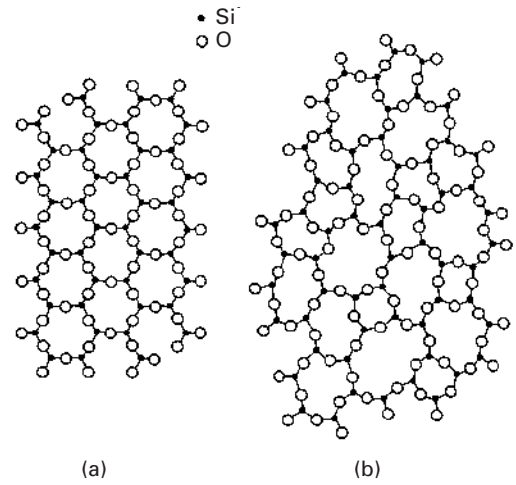


**Figure 1.18** Schematic two-dimensional representation of (a) ordered crystalline and (b) random-network glassy forms of silica.

compared with 3.59 g cm$^{-3}$ and 3.92 g cm$^{-3}$, for MgO and $A1_2O_3$, respectively. The structure of crystobalite (Figure 1.17(h)) shows clearly that each Si atom (open circle) is surrounded by four oxygen atoms (filled circles), while each oxygen atom binds two Si atoms. A complex cubic structure results. However, an amorphous structure in silica is more common when the mineral is cooled from the liquid state. Condensation of vapor on a cold substrate is another method by means of which thin, glassy films are made. One can also obtain glassy materials by electrodeposition, as well as by chemical reaction. Chapter 3 describes glassy metals in greater detail. Figure 1.18 provides a schematic representation of silica in its crystalline and glassy forms in an idealized two-dimensional pattern. The glassy state lacks long-range ordering; the three-dimensional silica tetrahedra arrays lack both symmetry and periodicity.

## Example 1.6

Determine the C–C–C–bonding angle in polyethylene.

***Solution:*** The easiest manner to visualize the bonding angle is to assume that one C atom is in the center of a cube and that it is connected to four other C atoms at the edges of the cube (see Figure E1.6 1) Suppose all angles are equal to $\alpha$.

**Figure E1.6**

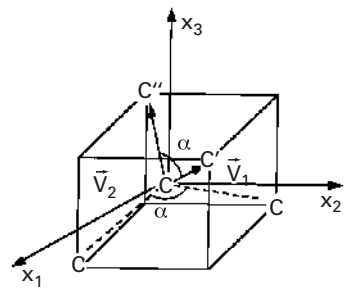

## Example 1.6 (cont.)

The problem is best solved vectorially. We set the origin of the axes at the center of the carbon atom and have two vectors connecting it to neighboring C atoms.

The angle between two vectors is (see Chapter 6 or any calculus text)

$$\cos\alpha = \frac{\frac{1}{2}\left(-\frac{1}{2}\right) + \frac{1}{2}\left(-\frac{1}{2}\right) + \frac{1}{2}\cdot\frac{1}{2}}{\sqrt{\frac{1}{4}+\frac{1}{4}+\frac{1}{4}}\cdot\sqrt{\frac{1}{4}+\frac{1}{4}+\frac{1}{4}}} = -\frac{1}{3}.$$

So

$$\alpha = 109.47^{\circ}.$$

(*Note*: When we have double bonds, the angle is changed.)

### 1.3.4 Glasses

As described earlier, glasses are characterized by a structure in which no long-range ordering exists. There can be short-range ordering, as indicated in the individual tetrahedral arrays of $SiO_4^{-4}$ in Figure 1.18, which shows both the crystalline and glassy forms of silica. Over distances of several atomic spacings, the ordering disappears, leading to the glassy state. It is possible to have glassy ceramics, glassy metals, and glassy polymers.

The structure of glass has been successfully described by the *Zachariasen* model. The *Bernal* model is also a successful one. It consists of drawing lines connecting the centers of adjacent atoms and forming polyhedra. These polyhedra represent the glassy structure of glass. Glassy structures represent a less efficient packing of atoms or molecules than the equivalent crystalline structures. This is very easily understood with the "suitcase" analog. We all know that by throwing clothes randomly into a suitcase, the end result is often a major job of sitting on the suitcase to close it. Neat packing of the same clothes occupies less volume. The same happens in glasses. If we plot the inverse of the density (called *specific volume*) versus temperature, we obtain the plot shown in Figure 1.19. Contraction occurs as the temperature is lowered. If the

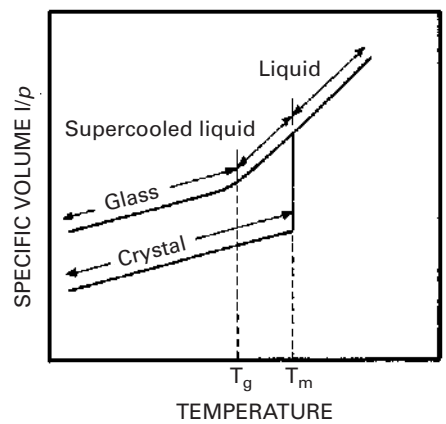


**Figure 1.19** Specific volume (inverse of density) as a function of temperature for glassy and crystalline forms of a material.

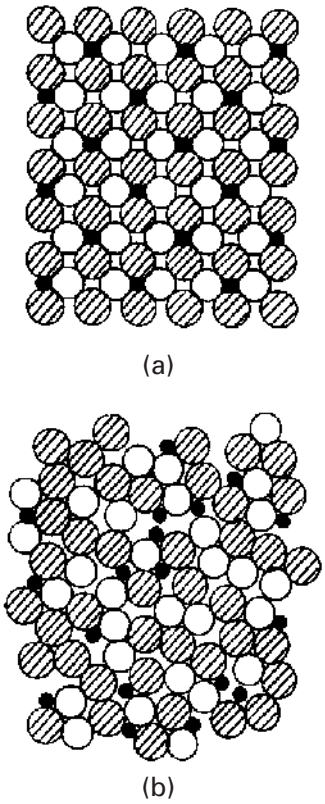


**Figure 1.20** Atomic arrangements in crystalline and glassy metals. (a) Crystalline metal section. (b) Glassy metal section. (Figure courtesy of L. E. Murr.)

material crystallizes, there is a discontinuity in the specific volume at the melting temperature $T_m$. If insufficient time is allowed for crystallization, the material becomes a super-cooled liquid, and contraction follows the liquid line. At a temperature $T_g$, called the *glass transition temperature*, the super-cooled liquid is essentially solid, with very high viscosity. It is then called a glass. This difference in specific volume between the two forms is often referred to as *excess volume*.

In ceramics, reasonably low cooling rates can produce glassy structures. The regular arrangement of the silica tetrahedra in Figure 1.18(a) requires a significant amount of time. The same is true for polymeric chains, which need to organize themselves into regular crystalline arrangements. For metals, this is more difficult. Only under extreme conditions it is possible to obtain solid metals in a noncrystalline structure. Figure 1.20 shows a crystalline and a glassy alloy with the same composition. The liquid state is frozen in, and the structure resembles that of glasses. It is possible to arrive at these special structures by cooling the alloy at such a rate that virtually no reorganization of the atoms into periodic arrays can take place. The required cooling rate is usually on the order of $10^6$ to $10^8$ K $s^{-1}$. It is also possible to arrive at the glassy state by means of solid-state processing (very heavy deformation and reaction) and from the vapor.

The original technique for obtaining metallic glasses was called splat cooling and was pioneered by Duwez and students.[2] An alloy in which the atomic sizes are quite dissimilar, such as Fe-B, is ideal for retaining the "glassy" state upon cooling. This technique consisted of propelling a drop of liquid metal with a high velocity against a heat-conducting surface such as copper. The interest in these alloys was mainly academic at the time. However, the unusual magnetic properties and high strength exhibited by the alloys triggered worldwide interest, and subsequent research has resulted in thousands of papers. The splat-cooling technique has been refined to the point where 0.07 to 0.12 mm-thick wires can be ejected from an orifice. Production rates as high as 1,800 m $min^{-1}$ can be obtained. Sheets and ribbons can be manufactured by the same technique. An alternative technique consists of vapor deposition on a substrate (sputtering). This seems a most promising approach, and samples with a thickness of several millimeters have been successfully produced.

The cooling rates required for the formation of the traditional amorphous metals are in the range of 100–1000 K $s^{-1}$. Thus, a splat-cooling technique must be used and only very thin layers can be produced. However, research at Tohoku University and the California Institute of Technology (Caltech) has yielded alloys based on La, Mg, Zr, Pd, Fe, Cu, and Ti, with critical cooling rates of 1–100 K $s^{-1}$, comparable to oxide glasses. Thus, thicker parts (several cm) can be fabricated. These alloys are known as Bulk Metallic Glasses (BMGs). The Caltech alloys are known as Vitreloy (41.2% Zr, 13.8% Ti, 12.5% Cu, 10% Ni, and 22.5% Be) and have strengths of 1700 MPa. Comparatively, $Ti_6Al_4V$ has a strength of 830 MPa. The bulk metallic glasses (BMGs) have been extensively studied due to their promising application and research value. Due to their glass transition temperature ($T_g$), they exhibit excellent properties such as high strength at low temperatures and appreciable ductility at high temperatures. Examples of applications are golf clubs, which have extraordinarily high coefficient of restitution.

### 1.3.5 Polymers

From a microstructural point of view, polymers are much more complex than metals and ceramics. On the other hand, they are cheap and easily processed. Polymers have lower strengths and moduli and lower temperature use limits than do metals or ceramics. Because of their predominantly covalent bonding, polymers are generally poor conductors of heat and electricity. Polymers are generally more resistant to chemicals than are metals, but prolonged exposure to ultraviolet light and some solvents can cause degradation of a polymer's properties.

#### Chemical Structure

Polymers are giant chain-like molecules (hence, the name *macromolecules*), with covalently bonded atoms forming the backbone of the chain. Polymerization is the

[2] W. Klement, R. H. Willens, and P. Duwez, *Nature*, 187 (1960) 869.

process of joining together many monomers, the basic building blocks of polymers, to form the chains. For example, the ethyl alcohol monomer ($C_2H_3OH$) has the chemical structure:

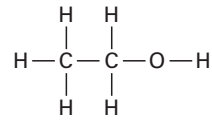

This yields the polymer polyethylene.

The monomer vinyl chloride has the chemical formula $C_2H_3Cl$, which, on polymerization, becomes polyvinyl chloride (PVC). The chemical structure of polyvinyl chloride is represented by:

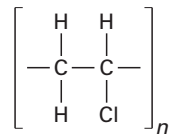

where $n$ is the degree of polymerization. There are numerous polymers with widely different properties: polyvinyl chloride (PVC), polystyrene (PS), poly(propylene) PP, polyether ether ketone (PEEK), etc.

## Types of Polymers

The difference in the behavior of polymers stems from their molecular structure and shape, molecular size and weight, and amount and type of bond (covalent or van der Waals). The different chain configurations are shown in Figure 1.21. A *linear polymer* consists of a long chain of atoms with attached side groups (Figure 1.21(a)). Examples include polyethylene, polyvinyl chloride, and polymethyl methacrylate. Note the coiling and bending of the chain. *Branched polymers* have branches attached to the main chain (Figure 1.21(b)). Branching can occur with linear, cross-linked, or any other types of polymers. A *crossed-linked* polymer has molecules of one chain bonded with those of another (Figure 1.21 (c)). Cross-linking of molecular chains results in a three-dimensional network. It is easy to see that cross-linking makes sliding of molecules past one another difficult, resulting in strong and rigid polymers. *Ladder polymers* have two linear polymers linked in a regular manner (Figure 1.21(d)). Not unexpectedly, ladder polymers are more rigid than linear polymers.

Yet another classification of polymers is based on the type of the repeating unit (see Figure 1.22). When we have one type of repeating unit, for example, *A*, forming the polymer chain, we call it a *homo polymer. Copolymers*, on the other hand, are polymer chains having two different monomers. If the two different monomers, *A* and *B*, are distributed randomly along the chain, then we have a *regular*, or *random, copolymer*. If, however, a long sequence of one monomer *A* is followed by a long sequence of another monomer *B*, we have a *block copolymer*. If we have a chain of one type of monomer *A* and branches of another type *B*, then we have a *graft copolymer*.

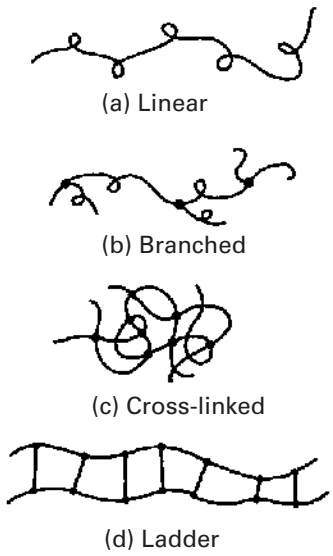


**Figure 1.21** Different types of molecular chain configurations.

(a) Homopolymer −A−A−A−A−A−A−A−

(b) Random copolymer −A−A−B−A−B−B−A−B−B−A−

(c) Block copolymer −A−A−A−A−B−B−B−B−B−

(d) Graft copolymer

```
−A−A−A−A−A−A−A−A−
      |       |
      B       B
      |       |
      B       B
      |       |
      B       B
      |       |
```

**Figure 1.22** (a) Homopolymer: one type of repeating unit. (b) Regular copolymer: two monomers, *A* and *B*, distributed randomly. (c) Block copolymer; a sequence of monomer B. (d) Graft copolymer; monomer *A* forms the main chain, while monomer *B* form the branched chain.

*Tacticity* has to do with the order of placement of side groups on a main chain. It can provide variety in polymers. Consider a polymeric backbone chain having side groups. For example, a methyl group ($CH_3$) can be attached to every second carbon atom in the polypropylene chain. By means of certain catalysts, it is possible to place the methyl groups all on one side of the chain or alternately on both sides, or to randomly distribute them in the chain. Figure 1.23 shows tacticity in polypropylene. When we have all the side groups on one side of the main chain, we have an *isotactic* polymer. If the side groups alternate from one side to another, we have a *syndiotactic* polymer. When the side groups are attached to the main chain in a random fashion, we get an *atactic* polymer.

## Thermosetting Polymers and Thermoplastics

Based on their behavior upon heating, polymers can be divided into two broad categories:

**(i)** thermosetting polymers,
**(ii)** thermoplastics.

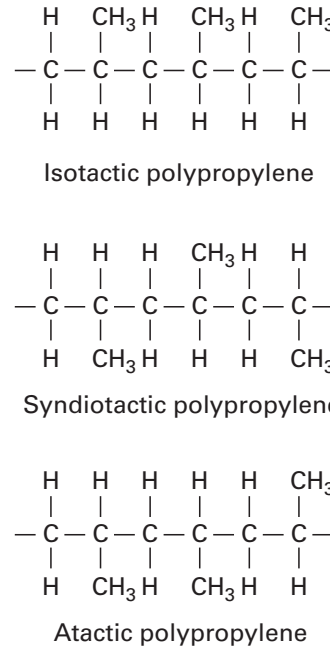


**Figure 1.23** Tacticity, or the order of placement of side groups.

When the molecules in a polymer are cross-linked in the form of a network, they do not soften on heating. We call these cross-linked polymers *thermosetting* polymers. Thermosetting polymers decompose upon heating. As mentioned earlier, cross-linking makes sliding of molecules past one another difficult, which produces a strong and rigid polymer. A typical example is rubber cross-linked with sulfur, i.e., vulcanized rubber. Vulcanized rubber has 10 times the strength of natural rubber. Common examples of thermosetting polymers include phenolic, polyester, polyurethane, and silicone. Polymers that soften or melt upon heating are called *thermoplastics*. Suitable for liquid flow processing, they are mostly linear polymers, for example, low and high-density polyethylene and polymethyl methacrylate (PMMA).

Polymers can have an amorphous or partially crystalline structure. When the structure is amorphous, the molecular chains are arranged randomly, i.e., without any apparent order. Thermosetting polymers, such as epoxy, phenolic, and unsaturated polyester, have an amorphous structure. Semicrystalline polymers can be obtained by using special processing conditions. For example, by precipitating a polymer from an appropriate dilute solution, we can obtain small, plate-like crystalline lamellae, or crystallites. Such solution-grown polymer crystals are characteristically small. Figure 1.24 shows a transmission electron micrograph of a lamellar crystal of poly ($\varepsilon$-caprolactone). Note the formation of new layers of growth spirals around screw dislocations. The screw dislocations responsible for crystal growth are perpendicular to the plane of the micrograph. Polymeric crystals involve molecular chain packing, rather than the atomic packing characteristic of metals. Molecular

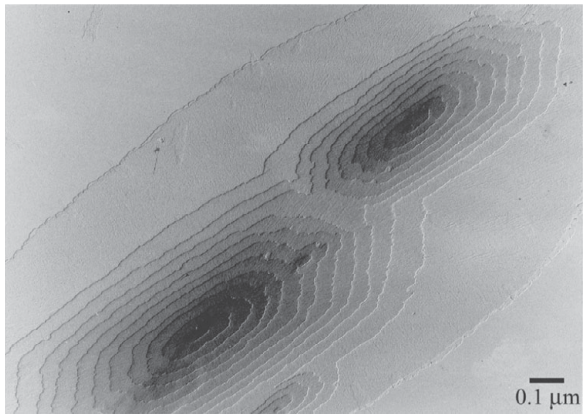


**Figure 1.24** Electron micrograph of a lamellar crystal showing growth spirals around screw dislocations.
(Figure courtesy of H. D. Keith.)

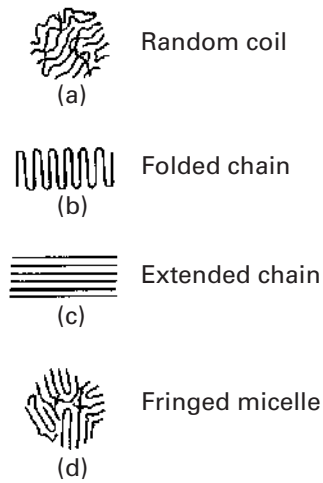


**Figure 1.25** Some important chain configurations.
(a) A flexible coiled chain structure. (b) A folding chain structure. (c) An extended and aligned chain structure.
(d) A fringed micelle chain structure.

chain packing requires a sufficiently stereographic regular chemical structure. Solution-grown polymeric crystals generally have a lamellar form, and the long molecular chains crystallize by folding back and forth in a regular manner. Lamellar polymeric crystals have straight segments of molecules oriented normal to the lamellar panes. Figure 1.25 depicts some important chain configurations in a schematic manner. The flexible, coiled structure is shown in Figure 1.25(a), while the chain-folding configuration that results in crystalline polymers is shown in Figure 1.25(b). Under certain circumstances, one can obtain an extended and aligned chain structure, shown in Figure 1.25(c). Such a structure, typically obtained in fibrous form, has very high strength and stiffness. A semi-crystalline configuration called a fringed micelle structure is shown in Figure 1.25(d). Almost all so-called semicrystalline polymers are, in reality, mixtures of crystalline and amorphous regions. Only by using very special techniques, such as solid-state polymerization, is it possible to prepare a 100% crystalline polymer. Polydiacetylene single crystals in the form of lozenges and fibers have been prepared by solid-state polymerization.

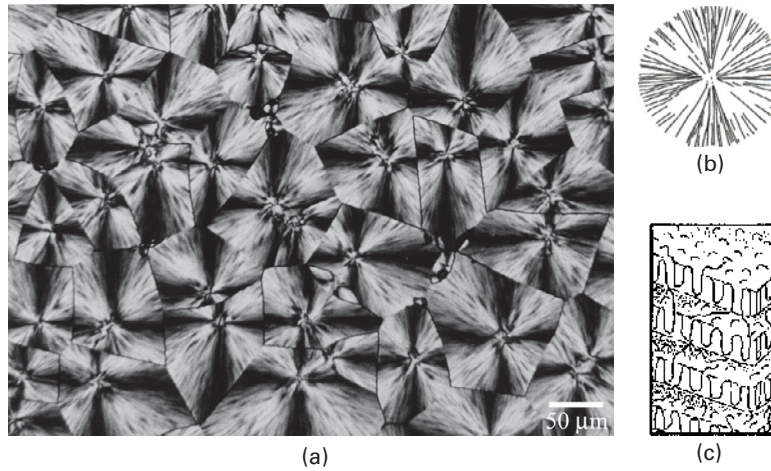


**Figure 1.26** Spherulitic structures.(a) A typical spherulitic structure in a melt-formed polymer film. (Figure courtesy of H. D. Keith.) (b) Schematic of a spherulite. Each spherulite consists of an assembly of radially arranged narrow crystalline lamellae. (c) Each lamella has tightly packed polymer chains folding back and forth. Amorphous regions fill the spaces between the crystalline lamellae.

Partially crystallized, or semicrystalline, polymers can also be obtained from melts. Generally, because of molecular chain entanglement, the melt-formed crystals are more irregular than those obtained from dilute solutions. A characteristic feature of melt-formed polymers is the formation of spherulites. When seen under cross-polarized light in an optical microscope, the classical spherulitic structure shows a Maltese cross pattern (see Figure 1.26(a). Figure 1.26(b) presents a schematic representation of a spherulite whose diameter can vary between a few tens to a few hundreds of micrometers. Spherulites can nucleate at a variety of points, as, for example, with dust or catalyst particles, in a quiescent melt and then grow as spheres. Their growth stops when the neighboring spherulites impinge upon each other. Superficially, the spherulites look like grains in a metal. There are, however, differences between the two. Each grain in a metal is a single crystal, whereas each spherulite in a polymer is an assembly of radially arranged, narrow crystalline lamellae. The fine-scale structure of these lamellae, consisting of tightly packed chains folding back and forth, is shown in Figure 1.26(c). Amorphous regions containing tangled masses of molecules fill the spaces between the crystalline lamellae.

## Degree of Crystallinity

The *degree of crystallinity* of a material can be defined as the fraction of the material that is fully crystalline. This is an important parameter for semicrystalline polymers. Depending on their degree of crystallinity, such polymers can show a range of densities, melting points, etc. It is worth repeating that a 100% crystalline polymer is very difficult to obtain in practice. The reason for the difficulty is the long chain

structure of polymers: some twisted and entangled segments of chains that get trapped between crystalline regions never undergo the conformational reorganization necessary to achieve a fully crystalline state. Molecular architecture also has an important bearing on a polymer's crystallization behavior. Linear molecules with small or no side groups crystallize easily. Branched chain molecules with bulky side groups do not crystallize as easily. For example, linear, high-density polyethylene can be crystallized to 90%, while branched polyethylene can be crystallized only to about 65%. Generally, the stiffness and strength of a polymer increase with the degree of crystallinity.

Like crystalline metals, crystalline polymers have imperfections. It is, however, not easy to analyze these defects, because the topological connectivity of polymer chains leads to large amounts and numerous types of disorder. Polymers are also very sensitive to damage by the electron beam in transmission electron microscopy (TEM), making it difficult to image them. Generally, polymer crystals are highly anisotropic. Because of covalent bonding along the backbone chain, polymeric crystals show low-symmetry structures, such as orthorhombic, monoclinic, or triclinic. Deformation processes such as slipping and twinning, as well as phase transformations that take place in monomeric crystalline solids, may also occur in polymeric crystals.

## Molecular Weight and Distribution

Molecular weight is a very important attribute of polymers, especially because it is not so important in the treatment of nonpolymeric materials. Many mechanical properties increase with molecular weight. In particular, resistance to deformation does so. Of course, concomitant with increasing molecular weight, the processing of polymers becomes more difficult.

The molecular weight of a polymer is given by the product of the molecular weight of the repeat unit (the ""mer") and the number of repeat units. The molecular weight of the ethylene repeat unit ($-CH_2-CH_2-$) is 28. We write the chemical formula: $H(-CH_2-CH_2-)_nH$. If $n$, the number of repeat units, is 10,000, the high-density polyethylene will have a molecular weight of 280,002. In almost all polymers, the chain lengths are not equal, but rather, there is a distribution of chain lengths. In addition, there may be more than one species of chain in the polymer. This makes for different parameters describing the molecular weight.

The number-averaged molecular weight ($M_n$) of a polymer is the total weight of all of the polymer's chains divided by the total number of chains:

$$M_n = \sum N_i, M_i / \sum N_i$$

where $N_i$ is the number of chains of molecular weight $M_i$.

The weight-averaged molecular weight ($M_w$) is the sum of the square of the total molecular weight divided by the total molecular weight. Thus,

$$M_w = \sum N_i M_i^2 / \sum M_i N_i.$$

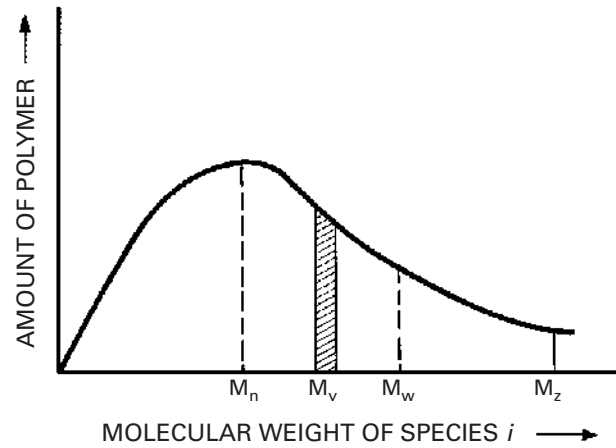


**Figure 1.27** A schematic molecular weight distribution curve. Various molecular weight parameters are indicated.

Two other molecular weight parameters are

$$M_z = \sum N_i M_i^3 / \sum N_i M_i^2$$

and

$$M_v = \left[ \sum N_i M_i^{(1+a)} / \sum N_i M_i \right]^{1/a},$$

where $a$ has a value between 0.5 and 0.8.

Typically, $M_n$:$M_w$:$M_z$ = 1:2:3. Figure 1.27 shows a schematic molecular weight distribution curve with various molecular weight parameters indicated. Molecular weight distributions of the same polymer obtained from two different sources can be very different. Also, molecular weight distributions are not necessarily single peaked. For single-peaked distributions, $M_n$ is generally near the peak that is, the most probable molecular weight. The weight-averaged molecular weight, $M_w$, is always larger than $M_n$. The molecular weight characterization of a polymer is very important. The existence of a very high molecular-weight tail can make processing very difficult because of the enormous contribution of the tail to the melt viscosity of a polymer. The low end of the molecular-weight distribution, however, can be used as a plasticizer.

It is instructive to compare some monomers with low- and high-molecular-weight polymers. A very common monomer is a molecule of water, $H_2O$, with a molecular weight of 18. Benzene, on the other hand, is a low-molecular-weight organic solvent; its molecular weight is 78. By contrast, natural rubber has a molecular weight of about $10^4$, and polyethylene, a common synthetic polymer, can have a molecular weights greater than this. Polymers having such large molecular weights are sometimes called *high polymers*. Their molecular size is also very great.

It is interesting that the acetabular cup in total hip replacement, usually made of PE, has a performance that is highly dependent on its molecular weight. The life expectancy in high-molecular-weight polyethylene (HMWPE) is increased significantly for UHMWPE.

## Example 1.7

A polymer has three species of molecular weights: $3\times10^6$, $4\times10^6$, and $5\times10^6$. Compute its number-averaged molecular weight $M_n$ and weight-averaged molecular weight $M_w$.

***Solution:*** For the number-averaged molecular weight, we have

$$M_n = \frac{\sum N_i M_i}{\sum N_i} = \frac{3\times10^6 + 4\times10^6 + 5\times10^6}{3} = 4\times10^6.$$

The weight-averaged molecular weight is

$$M_w = \frac{\sum N_i M_i^2}{\sum N_i M_i} = \frac{(3\times10^6)^2 + (4\times10^6)^2 + (5\times10^6)^2}{3\times10^6 + 4\times10^6 + 5\times10^6} = \frac{50\times10^{12}}{12\times10^6} = 4.17\times10^6.$$

## Example 1.8

Estimate the molecular weight of polyvinyl chloride with degree of polymerization, $n$, equal to 800.

***Solution:*** The molecular weight of each "mer" of polyvinyl chloride ($C_2H_3Cl$) is

$$2(12) + 3(1) + 35.5 = 62.5.$$

For $n = 800$, the molecular weight is $800 \times 62.5 = 50{,}000$ g mol$^{-1}$.

## Example 1.9

Discuss how a polymer's density changes as crystallization proceeds from the melt.

***Answer:***

The density increases and the volume decreases as crystallization proceeds. This is because the molecular chains are more tightly packed in the crystal than in the molten or noncrystalline polymer. This phenomenon is, in fact, exploited in the so-called *density* method to determine the degree of crystallinity.

## Quasi Crystals

Quasi crystals represent a new state of solid matter. In a crystal, the unit cells are identical, and a single unit cell is repeated in a periodic manner to form the crystalline structure. Thus, the atomic arrangement in crystals has positional and orientational order. Orientational order is characterized by a rotational symmetry; that is, certain rotations leave the orientations of the unit cell unchanged. The theory of crystallography holds that crystals can have twofold, threefold, fourfold, or sixfold axes of rotational symmetry; a fivefold rotational symmetry is not allowed. A two-dimensional analogy of this is that one can tile a bathroom wall using a single shape of tile *if and only if* the tiles are rectangles (or squares), triangles, or hexagons, but not if the tiles are pentagons. One may obtain a glassy structure by rapidly cooling a vapor or liquid well below its melting point, until the disordered atomic arrangement characteristic of the vapor or liquid state gets frozen in. The atomic packing in the glassy state is dense but random. This can be likened to a mosaic formed by taking an infinite number of different shapes of tile and randomly joining them together. Clearly, the concept of a unit cell will not be valid in such a case. The atomic structure in the glassy state will have neither positional nor orientational order.

Quasi crystals are not perfectly periodic, but they do follow the rigorous theorems of crystallography. They can have any rotational symmetry axes which are prohibited in crystals. It is worth reminding the reader that a glassy structure shows an electron diffraction pattern consisting of diffuse rings for all orientations. A crystalline structure has an electron diffraction pattern that depends on the crystal symmetry.

Schectman et al. discovered that a rapidly solidified (melt-spun) aluminum-manganese alloy showed fivefold symmetry axis.[3] They observed a metastable phase that showed a sharp electron diffraction pattern with a perfect icosahedral symmetry. (Remember that sharp electron diffraction patterns are associated with the orderly atomic arrangement in crystals and icosahedral symmetry is forbidden in crystals.) At first, this was thought to be a paradox. However, some very careful and sophisticated electron microscopy work showed conclusively that it was indeed an icosahedral (20-fold) symmetry. Al-Mn alloys containing 18 to 25.3 wt% Mn examined by transmission electron microscopy showed the same anomalous diffraction. In particular, Al-25.3 wt% Mn alloy consisted almost entirely of one phase which has a composition close to $Al_6Mn$. The selected area diffraction pattern of $Al_6Mn$ showed a fivefold symmetry. This new kind of structure is neither amorphous nor crystalline; rather, the new phase in this alloy had a three-dimensional icosahedral symmetry.

Perhaps, it would be in order for us to digress a bit and explain this icosahedral symmetry. *Icosahedral* means 20 faces. An icosahedron has 20 triangular faces, 30 edges, and 12 vertices. Consider the two-dimensional case. As pointed out earlier,

[3] D. Schectman, I. A. Blech, D. Gratias, and J. W. Cahn, *Phys. Rev. Lett.*, 53 (1984) 1951.

one can tile a bathroom wall without leaving an open space (a *crack*) with hexagons. Three hexagons can be tightly packed without leaving a crack. Three pentagons, however, cannot be tightly packed. The reader may try this out. In three dimensions, four spheres pack tightly to form a tetrahedron; 20 tetrahedrons can, with small distortions, fit tightly into an icosahedron. Icosahedrons have fivefold symmetry (five triangular faces meet at each vertex) and they *cannot* fit together tightly, i.e., complete space filling is not possible with them. An icosahedron, therefore, cannot serve as a unit cell for a crystalline structure. Therefore, such structures are known as quasi crystals.

### 1.3.6 Liquid Crystals

A liquid crystal is a state of matter that shares some properties of liquids and crystals. Like all liquids, liquid crystals are fluids; however, unlike ordinary liquids, which are isotropic, liquid crystals can be anisotropic. Liquid crystals are also called *mesophases*. The liquid crystalline state exists in a specific temperature range, below which the solid crystalline state prevails and above which the isotropic liquid state prevails. That is, the liquid crystal has an order between that of a liquid and a crystalline solid. In a crystalline solid, the atoms, ions, or molecules are arranged in an orderly manner. This very regular three-dimensional order is best described in terms of a crystal lattice. Because of a different periodic arrangement in different directions, most crystals are anisotropic. Now consider a crystal lattice with rod-shaped molecules at the lattice points. In this case, we now have, in addition to a positional order, an orientational order. An analogy that is used to qualitatively describe the order in a liquid crystal is as follows. If a random pile of pencils is subjected to an external force, it will undergo an ordering process very much akin to that seen in liquid crystals. The pencils, long and rigid, tend to align themselves, with their long axes approximately parallel. By far the most important characteristic of liquid crystals is that their long molecules tend to organize according to certain patterns. The order of orientation is described by a directed line segment called the *director*. This order is the source of the rather large anisotropic effect in liquid crystals, a characteristic that is exploited in electrooptical displays or so-called liquid-crystal displays. Another important application of liquid crystals is the production of strong and stiff organic fibers such as aramid fiber, in which a rigid, rod-like molecular arrangement is provided by an appropriate polymer solution in the liquid crystalline state.[4] When a polymer manifests the liquid-crystalline order in a solution, we call it a *lyotropic* liquid crystal, and when the polymer shows the liquid crystalline state in the melt, it is called a *thermotropic* liquid crystal. The three types of order in the liquid crystalline state are nematic, smectic, and cholesteric, shown schematically in Figure 1.30. A nematic order is an approximately parallel array of polymer chains that remains disordered with regard to end groups or chain

[4] See K. K. Chawla, *Fibrous Materials* (Cambridge, U.K.: Cambridge University Press, 1998).

units; that is, there is no positional order along the molecular axis. Figure 1.30(a) shows this type of order, with the director vector *n* as indicated. In smectic order, we have one-dimensional, long-range positional order. Figure 1.30(b) shows smectic-A order, which has a layered structure with long-range order in the direction perpendicular to the layers. In this case, the director is perpendicular to the layer. Other more complex smectics are B, C, D, F, and G. The director in these may not be perpendicular to the layer, or there may exist some positional order as well. Cholesteric-type liquid crystals, shown in Figure 1.30(c), have nematic order with a superimposed spiral arrangement of nematic layers; that is, the director *n*, pointed along the molecular axis, has a helical twist.

## 1.3.7 Biological Materials and Biomaterials

### Biological Materials: Unique Characteristics

Seven unique aspects of biological materials distinguish them from their synthetic counterparts. It is through the understanding of each of them that we are advancing our knowledge with the goal of generating novel bioinspired materials and designs. These defining aspects comprise the Arzt heptahedron, presented in Figure 1.28. They are:

- *Evolution and environmental constraints*. Biological materials developed through a multimillion year process of evolution, driven by natural selection.

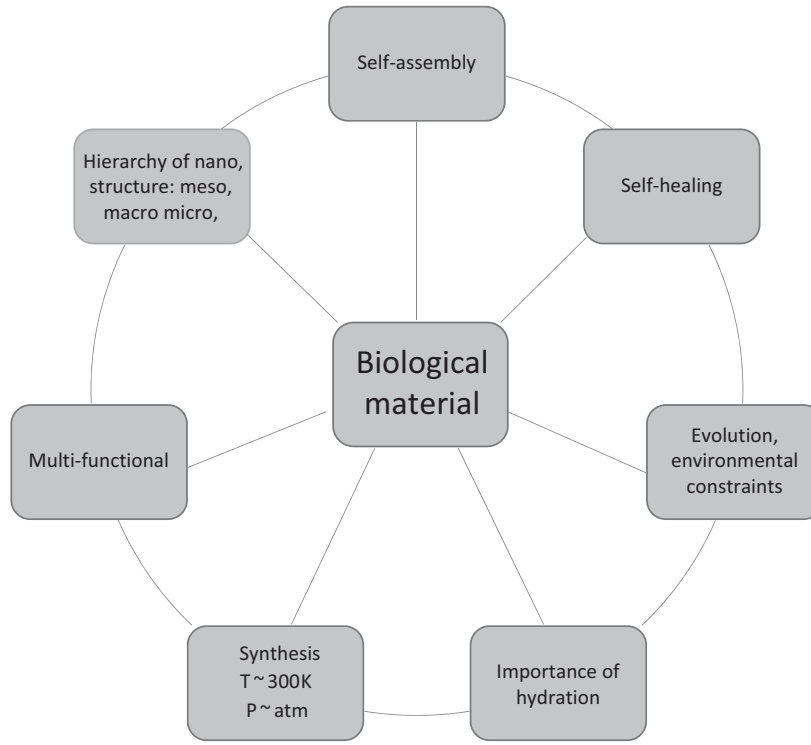


**Figure 1.28** Seven unique characteristics of biological materials: the Artz heptahedron.

- *Importance of hydration*. With notable exceptions, enamel and a few minerals, the level of hydration determines the mechanical properties.
- *Multifunctional.* Many tissues have more than one function, and this provides economy of space and mass.
- *Self-organization.* Nature uses a bottom-up approach to synthesize materials, whereas many of our processing methods are top-down. This bottom-up approach engenders self-organization and self-assembly.
- *Hierarchy of structure.* This is an aspect of utmost importance because it has direct relevance to mechanical properties. The structures at the nano, micro, meso, and ultra levels have different characteristics and work together synergistically.
- *Self-healing*. Many biological materials have a self-healing capability enabled by the cells and vascularity embedded in the extracellular matrix. Only a minute minority of synthetic materials have this capability.
- *Synthesis at ambient temperature and pressure.* Nature does not have at its disposal furnaces for high-temperature or autoclaves for high-pressure processing. Nor does she need them, since organisms exist mostly in a narrow range (–50 to +500 °C) of temperatures. There are isolated cases such as extremophiles and organisms living close to deep-sea vents, but they represent the exception. On the other hand, synthetic materials are designed to resist a variety of environments.

These unique characteristics render them intrinsically different from synthetic materials. Although there is a daunting variety of organisms (~8 million species), there are few recurring motifs in biological materials which have been identified.[5] This consists of seeking common structural designs in biological materials. Eight have been identified and are collectively named "structural design elements." They are amenable to analytical treatment and occur in different species through convergence and parallelism processes.

In spite of millions species of plants and animals on Earth, there is remarkable commonality in the structures observed among the diversity of biological materials. This is due to the fact that many different organisms have developed similar solutions to natural challenges. Our recent research has identified these common designs and named them *structural design elements*.

This new system new system of eight structural design elements enables a quantitative analytical treatment which can explain the mechanical properties, namely strength, stiffness, flexibility, fracture toughness, and energy absorption, of different biological materials for specific multifunctions (e.g. body support, joint movement, impact protection, mobility, flying). These structural design elements (visually displayed in Figure 1.29) are:

- *Fibrous* structures; offering high tensile strength when aligned in a single direction, with limited to nil compressive strength.

[5] M. A. Meyers, J. McKittrick, and P. Y. Chen, *Science*, 339 (2013) 773.

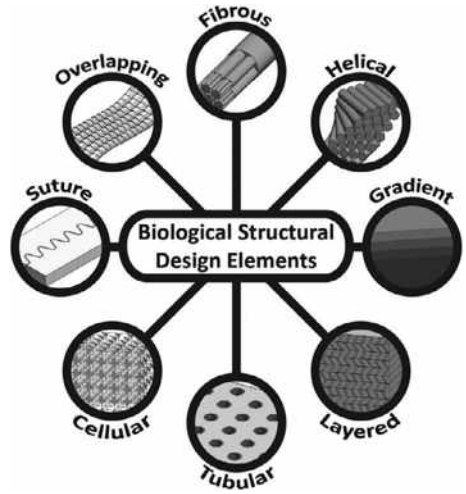


**Figure 1.29** The eight most common biological structural design elements.
(Reproduced from Marc A. Meyers, Joanna McKittrick, Michael M. Porter, et al, Structural Design Elements in Biological Materials: Application to Bioinspiration, *Advanced Materials*, Vol. 27, issue 37 (2015). With permission from John Wiley & Sons.)

- *Helical* structures; common to fibrous or composite materials, offering toughness in multiple directions and in-plane isotropy.
- *Gradient* structures; materials and interfaces that accommodate property mismatch (e.g. elastic modulus) through a gradual transition in order to avoid interfacial mismatch stress buildup, resulting in an increased toughness.
- *Layered* structures; complex composites that increase the toughness of (most commonly) brittle materials through the introduction of interfaces.
- *Tubular* structures; organized porosity that allows for energy absorption and crack deflection.
- *Cellular* structures; lightweight porous or foam architectures that provide directed stress distribution and energy absorption. These are often surrounded by dense layers to form sandwich structures.
- *Suture* structures; interfaces comprising wavy and interdigitating patterns that control the strength and flexibility.
- *Articulating* structures; featuring multiple plates or scutes that overlap to form flexible and often armored surfaces without interfaces.

As with all biological materials, these structural design elements are composed of biopolymers (e.g. collagen, chitin, keratin, cellulose) and biominerals (e.g. calcium carbonate, calcium phosphates, silica) that are hierarchically assembled from the nano to meso scales. However, the extraordinary mechanical properties observed in these natural materials are often a product of the intricate structural organization at higher spatial scales (micro, meso, and macro). As a result, in many cases organisms with different base materials will employ the same structure for the same purpose (e.g. tubules found in human dentin composed of hydroxyapatite/collagen and in a ram horns composed of keratin[6] can both absorb energy).

[6] S. E. Naleway, et al. *Adv Mat* 27.37 (2015) 5455–5476.

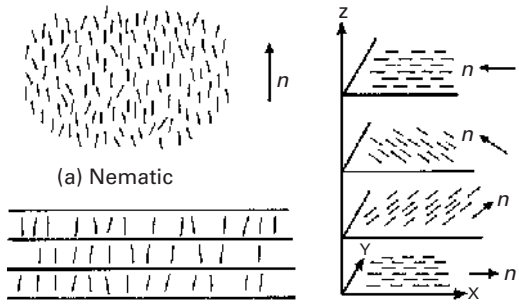


**Figure 1.30** Different types of order in the liquid crystalline state.

This is a new paradigm in the field of biological materials science: the structural design elements can serve as a toolbox for rationalizing the complex response of structural biological materials and for systematizing the development of bioinspired designs for structural applications. The ingenious manner by which these biocomposite structures are engineered is responsible for a mechanical response that is superior to that of synthetic materials

The mechanical properties of biological materials are, of course, of great importance, and the design of all living organisms is optimized for the use of these properties. Biological materials cover a very broad range of structures. The common feature is the hierarchical organization of the structure, so that failure at one level does not generate catastrophic fracture; the other levels in the hierarchy "take up" the load. Figure 1.31 demonstrates this fact. Figure 1.31(a) shows the response of the urether of three animals: guinea pig, dog, and rabbit. This muscle is a thick-walled cylindrical tube that has the ability to contract until the closure of the inner hole is complete. With a nonlinear elastic mechanical response, the urether is not unlike other soft tissues in that regard: its stiffness increases with loading, and the muscle becomes very stiff after a certain strain is reached. The unloading and loading responses are different, as shown in the figure, and this causes a hysteresis. Increases in length of 50% can be produced. Bone, on the other hand, is a material with drastically different properties: its strength and stiffness are much higher, and its maximum elongation is much lower. The structure of bones is quite complex, and they can be considered composite materials. Figure 1.31(b) illustrates the strength (in tension) of dry and wet bone. The maximum tensile strength is approximately 80 MPa, and Young's modulus is about 20 GPa.

The abalone shell and the shells of bivalve mollusks are often used as examples of a naturally occurring laminated composite material. These shells are composed of layers of calcium carbonate, glued together by a viscoplastic organic material. The calcium carbonate is hard and brittle. The effect of the viscoplastic glue is to provide a crack-deflection layer so that cracks have difficulty propagating through the composite. Figure 1.32 shows cracks that are deflected at each soft layer. The toughness of this laminated composite is vastly superior to that of a monolithic material, in which the crack would be able to propagate freely, without barriers.

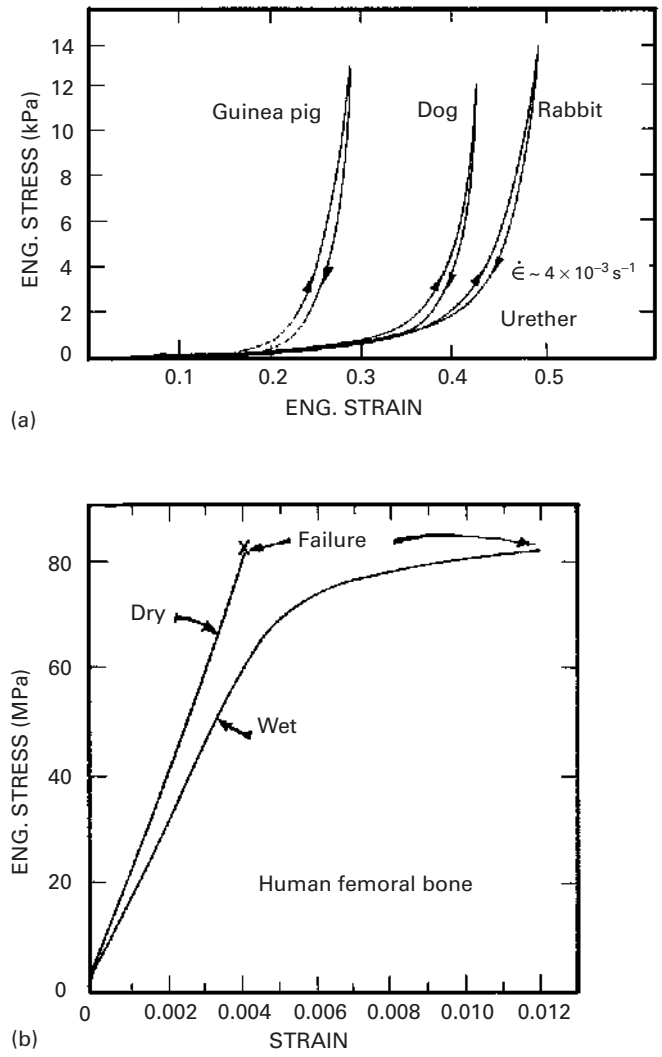


**Figure 1.31** Stress–strain curves for biological materials. (a) Urether. (Reproduced from the *American Journal of Physiology, Consolidated*, FC Yin, YC Fung, Vol. 221, 1971. © The American Physiological Society (APS).) (b) Human femur bone. (Reproduced from the *Journal of Applied Phisiology*, F. Gaynor Evans, Milton Lebow, Vol. 3, 1951, Pages 563–572. © The American Physiological Society (APS).)

The effect is shown at two scales: the mesoscale and the microscale. At the mesoscale, layers of calcium carbonate have a thickness of approximately 500 μm. At the microscale, each calcium carbonate layer is made up of small brick-shaped units (about $0.5 \times 7.5$ μm longitudinal section), glued together with the organic matter. The formation of this laminated composite results in a fracture toughness and strength (about 4 MPa $m^{-1/2}$ and approximately 150 MPa, respectively) that are much superior to those of the monolithic $CaCO_3$. The composite also exhibits a hierarchical structure; that is, the layers of $CaCO_3$ and organic glue exist at more

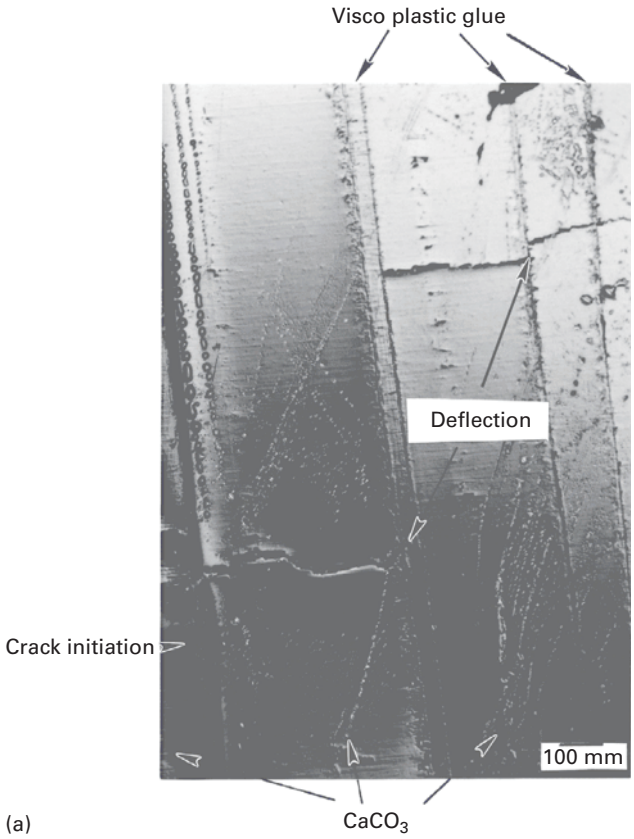


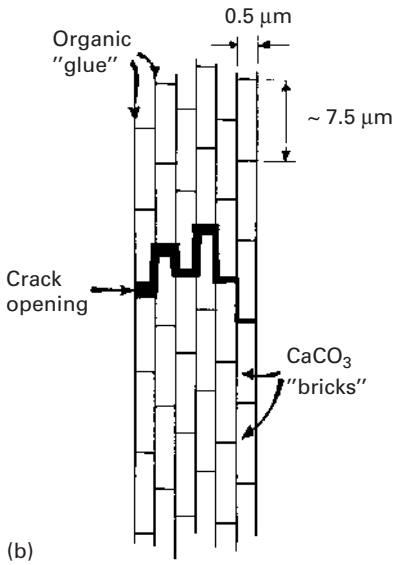


**Figure 1.32** (a) Cross-section of abalone shell showing how a crack, starting on the left, is deflected by a viscoplastic layer between calcium carbonate lamellae (mesoscale). (b) Schematic drawing showing the arrangement of calcium carbonate in nacre, forming a miniature "brick and mortar" structure (micro scale).

than one level (at the micro and meso levels). This naturally occurring composite has served as inspiration for the synthesis of $B_4C$-Al laminate composites, which exhibit superior fracture toughness.[7] In these synthetic composites, there is a 40% increase in both fracture toughness and strength over monolithic $B_4C$-Al cermets. (A cermet is a composite material consisting of ceramic (cer) and sintered metallic (met) materials.) *Biomimetics* is the field of materials science in which inspiration is sought from biological systems for the design of novel materials.

Another area of biomaterials in which mechanical properties have great importance is bioimplants. Complex interactions between the musculoskeletal system and these implants occur in applications where metals and ceramics are used as replacements for hips, knees, teeth, tendons, and ligaments. The matching of material and bone stiffness is important, as are the mechanisms of bonding tissue to these materials. The number of scientific and technological issues is immense, and the field of bioengineering focuses on these.

### 1.3.8 Porous and Cellular Materials

Wood, cancellous bone, Styrofoam, cork, and the insulating tiles of the Space Shuttle are examples of materials that are not compact; their structure has air as a major component. The great advantage of cellular structures is their low density. Techniques for making foam metals, ceramics, and polymers have been developed, and these cellular materials have found a wide range of applications, in insulation, in cushioning, as energy-absorbing elements, in sandwich panels for aircraft, as marine buoyancy components, in skis, and more.

The mechanical response of cellular materials is quite different from that of bulk materials. The elastic loading region is usually followed by a plateau that corresponds to the collapse of the pores, either by elastic, plastic buckling of the membranes or by their fracture. The third stage is an increase in the slope, corresponding to final densification. Figure 1.33(a) shows representative curves for polyethylene with different initial densities. The plateau occurs at different stress levels and extends to different strains for different initial densities. The bulk (fully dense) polyethylene is shown for comparison purposes. Cellular mullite, an alumina-silica solid solution, exhibits a plateau marked by numerous spikes, corresponding to the breakup of the individual cells (Figure 1.33(b)). Materials with initial densities as low as 5% of the bulk density are available as foams. Figure 1.33(c) shows a very important use of foams: sandwich structures, composed of end sheets of solid material in which a foam forms the core region, have numerous applications in the aerospace industry. The foam between the two panels makes them more rigid; this is accomplished without a significant increase in weight.

There are many biological examples of sandwich structures. The toucan beak (Figure 1.34(a)) is a structure with very low density (0.04 g $cm^{-3}$) that consists of an external layer of compact keratin. Figure 1.34(b) shows the keratin layer. It is

[7] M. Sarikaya, K. E. Gunnison, M. Yasrebi, and I. A. Aksay, *Mater. Soc. Symp. Proc.*, 174 (1990) 109.

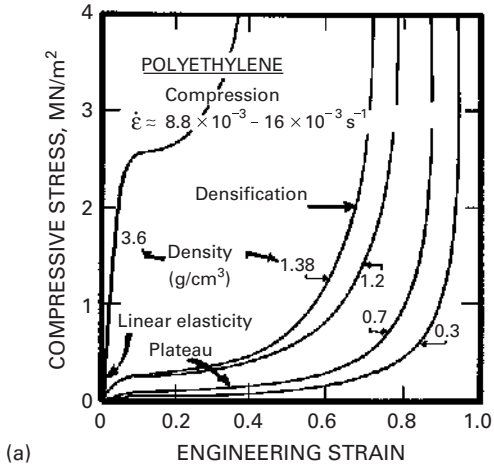


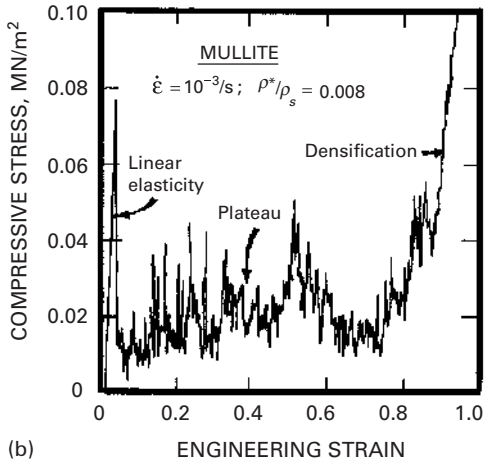


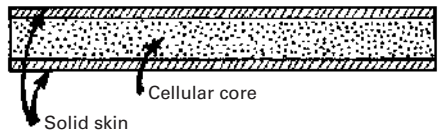


**Figure 1.33** Compressive stress–strain curves for foams. (a) Polyethylene with different initial densities. (b) Mullite with relative density $\rho^*/\rho s = 0.08$. (Adapted from L. J. Gibson and M. F. Ashby, *Cellular Solids: Structure and Properties* (Oxford, U.K.: Pergamon Press, 1988), pp. 124, 125.) (c) Schematic of a sandwich structure. (Adapted from L.J. Gibson and M.F. Ashby, Cellular solids: Structure and properties. *Advances in Polymer Technology*, 9, issue 2 (1989). With permission from John Wiley & Sons.)

composed of superimposed scales. The extremely low density of the inside of the toucan beak is due to a foam-like (cellular) bone structure. The function of the cellular material is to provide structural rigidity to the system. In the absence of this foam, the external shell would buckle easily. Hence the toucan can fly without taking a nose dive.

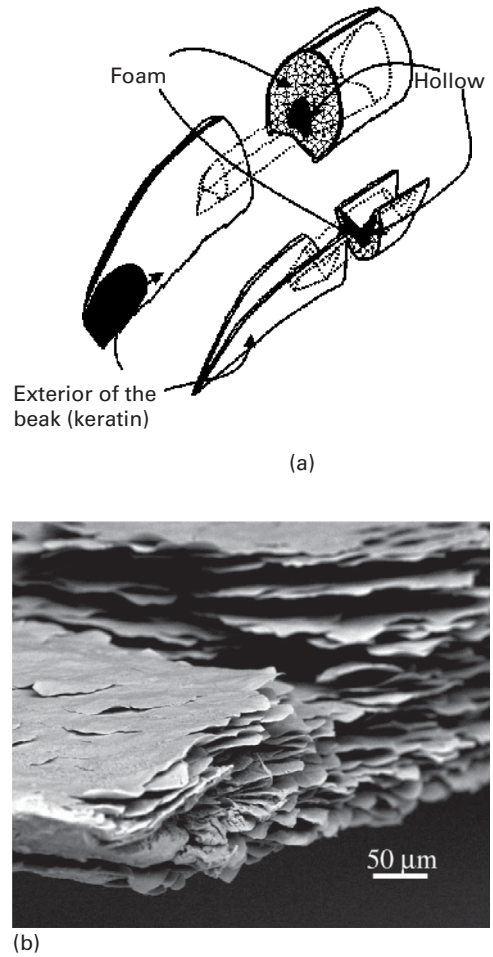


**Figure 1.34** (a) Toucan beak; (b) external shell made of keratin scales. (Figure courtesy of Y. Seki.)

As examples of foams in synthetic and naturally occurring materials, we show in Figure 1.35 two structures. Figure 1.35(a) shows an open-celled aluminum foam. We sectioned the beak of the toucan and observed that the inside is composed of a foam with similar length scale Figure 1.34(b). Nature uses foams for the same purposes we do: to provide rigidity to structures with the addition of minimal weight. In Chapter 12 we give a detailed analysis of stresses involved in foams.

### 1.3.9 Nano- and Microstructures of Biological Materials

Biological materials are more complex than synthetic materials. They form complex arrays, hierarchical structures, and are often multifunctional, i.e., one material has more than one function. For example, bone has a structural function and serves as a producer of red blood cells (in marrow). We classify biological materials, from the mechanical property viewpoint, into soft and hard. Hard materials provide the skeleton, teeth, and nails in vertebrates and the exoskeleton in arthropods.

**Table 1.5 Occurrence of Different Biological Materials in the Body**

| Biological Material | Weight Percentage in Human Body |
|---|---|
| Proteins | 17 |
| Lipids | 15 |
| Carbohydrates | 1 |
| Minerals | 7 |
| DNA, RNA | 2 |
| Water | 58 |

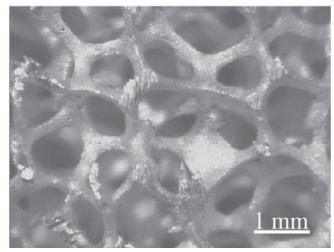


(a)

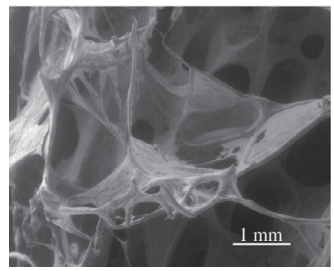


(b)

**Figure 1.35** Cellular materials: (a) synthetic aluminum foam. (Figure courtesy of K. S. Vecchio.) (b) Foam found in the inside of toucan beak. (Figure courtesy of M. S. Schneider.)

Soft biological materials build skin, muscle, internal organs, etc. Table 1.4 provides the distribution (on a weight percentage) of different constituents of the body.

Here are some examples of "hard" biological materials:

- Calcium phosphate (hydroxyapatite-$Ca_{10}(PO_4)_6(OH)_2$): teeth, bone.
- Chitin: nails.
- Keratin: bird beaks, horn, hair.
- Calcium carbonate (aragonite): mollusk shells, some reptile eggs (calcite): bird's eggs, crustaceans, mollusks.
- Amorphous silica ($SiO_2(H_2O)_n$): spicules in sponges.
- Iron oxide (magnetite – $Fe_3O_4$): teeth in chitons (a weird-looking marine worm), bacteria.

Of the above, iron oxide, calcium phosphate, silica, and iron oxide are minerals. Chitin is a polysaccharide and keratin is a protein.

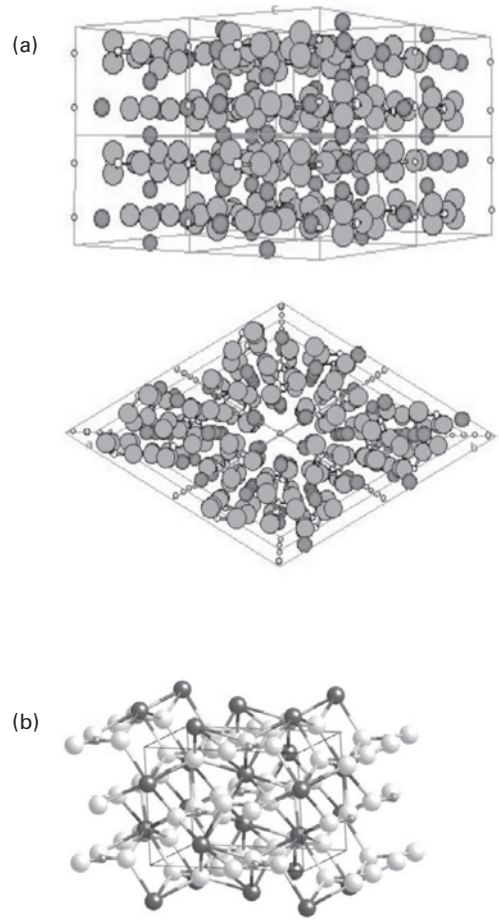


**Figure 1.36** Atomic structure of hydroxyapatite: (a) small white atoms (P), large gray atoms (O), black atoms (Ca). (b) Atomic structure of aragonite: large dark toms (Ca), small gray atoms (C), large white atoms (O).

Figure 1.36(a) shows the atomic arrangement of the calcium, phosphorus, and oxygen atoms in hydroxyapatite. The unit cell is quite complex and consists of four primitive hexagonal cells juxtaposed. We should remember that the hexagonal cell is composed of three primitive cells, brought together at their 120° angles ($3 \times 120 = 360$). In the case of the hydroxyapatite unit cell, there are four unit cells: two at the 60° angle and two at the 120° ($2 \times 60 + 2 \times 120 = 360$).

Figure 1.36(b) shows the aragonitic form of calcium carbonate. Aragonite has the orthorhombic structure. However, it is important to recognize that the minerals do not occur in isolation in living organisms. They are invariably intimately connected with organic materials, forming complex hierarchically structured composites. The resulting composite has mechanical properties that far surpass those of the monolithic minerals. Although we think of bone as a cellular mineral, it is actually composed of 60% collagen (on a volume percentage basis) and 30–40%

hydroxyapatite (on a weight basis). If the mineral is dissolved away, the entire collagen framework is retained.

The principal organic building blocks in living organisms are the proteins. The word comes from Greek (*Proteios*) which means "of first rank" and indeed proteins play a key role in most physiological processes. The soft tissues in the body are made of proteins. As seen above, they are also an important component of biominerals. In order to fully understand proteins, we have to start at the atomic/molecular level, as we did for polymers.

Actually, proteins can be conceived of as polymers with a greater level of complexity. We start with amino acids, which are compounds containing both an amine ($–NH_2$) and a carboxyl (–COOH) group. Most of them have the following structure, shown where R stands for a side chain (Table 1.6 shows some of them):

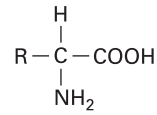

There are nine essential amino acids: histidine, isoleucine, leucine, lysine, methionine, phenylalanine, threonine, tryptophan, and valine. There are currently 20 amino acids found in proteins. In addition to these nine, we have the following: alanine, arginine, asparagine, aspartic acid, cysteine, glutamic acid, glutamine, glycine, proline, serine, and tyrosine.

In proteins, these amino acids combine themselves by forming links between the carboxyl group of one amino acid and the amino group of another. These linear chains, similar to polymer chains, are called polypeptide chains. The polypeptide chains acquire special configurations because of the formation of bonds (hydrogen, van der Waals, and covalent bonds) between amino acids on the same or different chains. The two most common configurations are the alpha helix and the beta sheet. Figure 1.37(a) shows how an alpha helix is formed. The NH and CO groups form hydrogen bonds between them in a regular pattern, and this creates the particular conformation of the chain that is of helical shape. One such bond is shown in Figure 1.37(a). In Figure 1.37(b) several hydrogen bonds are shown, causing the polypeptide chain to fold. The side chains stick out. The amino acid chain with the peptide group is shown in Figure 1.38(a). The amino acid chain with the peptide groups in a straight line is shown in Figure 1.38(b). Figure 1.38(c) shows the alpha helix conformation produced by the coiling of the amino acid chain. The peptide groups face each other and hydrogen bonds form. This keeps the helix stable.

Another common conformation of polypeptide chains is the beta sheet. In this conformation, separate chains are bonded. We can see that the radicals (large grey balls) of two adjacent chains stick out of the sheet plane on opposite sides. Successive chains can bond in such a fashion, creating pleated sheets.

We describe below the most important proteins: collagen, actin, myosin, elastin, resilin, abductin, keratin and silk, as well as cellulose and chitin, which are polysaccharides.

**Table 1.6 Eight amino acids found in proteins**

| Name | Chemical Structure |
|---|---|
| Alanine | 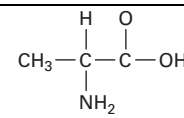 |
| Leucine | 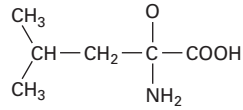 |
| Phenylalanine | 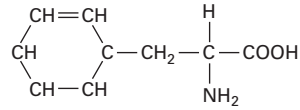 |
| Proline | 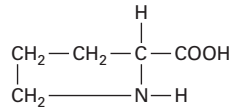 |
| Serine | 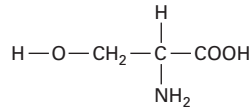 |
| Cysteine | 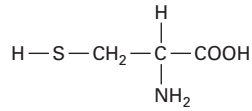 |
| Glutamate | 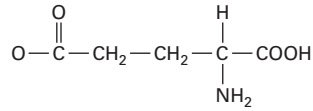 |
| Lysine | 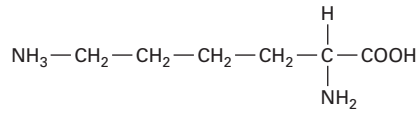 |

**Collagen** Collagen is a rather stiff and hard protein. It is a basic structural material for soft and hard bodies; it is present in different organs and tissues and provides structural integrity. Fung[8] compares it to steel, which is the principal load-carrying component in structures. In living organisms, collagen plays the same role: it is the main load-carrying component of blood vessels, tendons, bone, muscle, etc. In rats, 20% of the proteins are collagen. Humans are similar to rats in physiology and the same proportion should apply. Figure 1.39 shows the structure of collagen. It is a triple helix, each strand being made up of sequences of amino acids. Each strand is itself a left-handed helix with approximately 0.87 nm per turn. The triple helix has a right-handed twist with a period of 8.6 nm. The dots shown in a strand in

[8] Y. C. Fung, *Biomechanics: Mechanical Properties of Living Tissues* (Berlin: Springer, 1993).

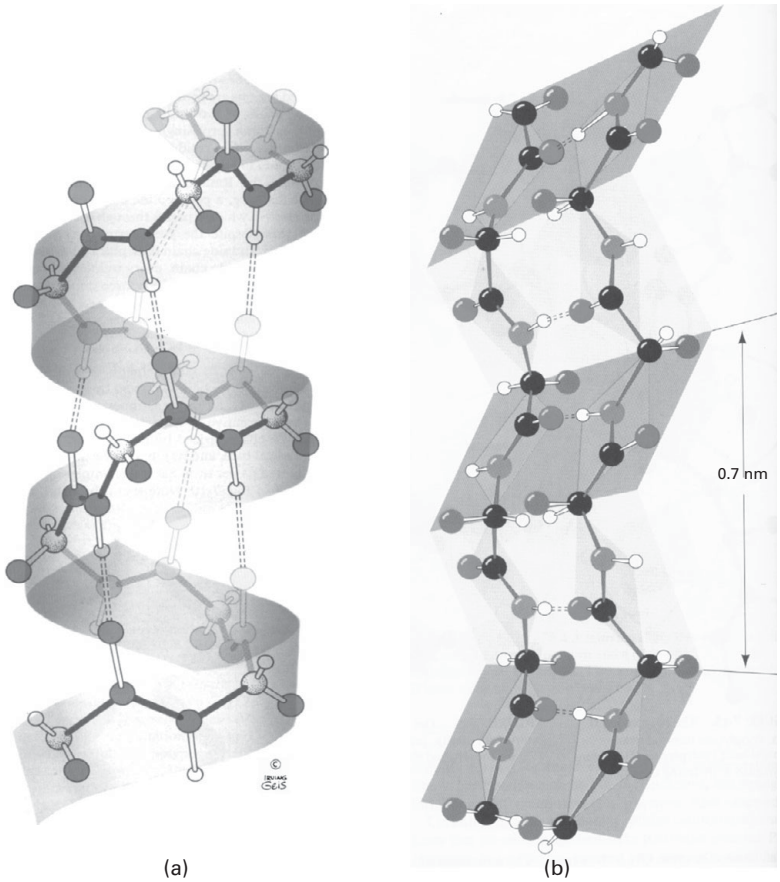


**Figure 1.37** (a) Structure of alpha helix; dotted double lines indicate hydrogen bonds. (b) Structure of beta sheet with two antiparallel polypeptide chains connected by hydrogen bonds (double-dotted lines).

Figure 1.39 represent glycine and different amino acids. There are over 10 types of collagen, called Type I, II, X, etc. Fiber-forming collagens organize themselves into fibrils.

Figure 1.40 shows the structural hierarchy of fibrillar collagen. In collagen formations, helical left-handed procollagen chains form a right-handed triple helix of roughly 300 nm in length. (b) Schematic representation of triple helix formed by three procollagen chains. Figure 1.40(c) shows the arrangement of triple helices into fibrils. Triple helices are arranged in a staggered manner, leading to a gap (0.54 d) and an overlap (0.46 d) region. The gap region has fewer triple helices across the section, and the overlap region has more. This gap and overlap has a periodicity, or d-period, of 67 nm, and is the cause of the visible banding in collagen fibrils. Figure 1.40 shows layers of collagen fibrils in a cross-section of skin. Figure 1.40(d) shows collagen fibrils of 100 nm diameter imaged by TEM. Fibrils clearly display the characteristic banding feature. Due to the viewing angle of the fibrils, d-period measurements decrease proportionally to the cosine of the viewing angle. A 90° viewing angle would lead to perfectly accurate measurements. (f) Atomic force microscopy (AFM) of hydrated collagen fibrils in an arapaima scale. 67nm d-period is measured.

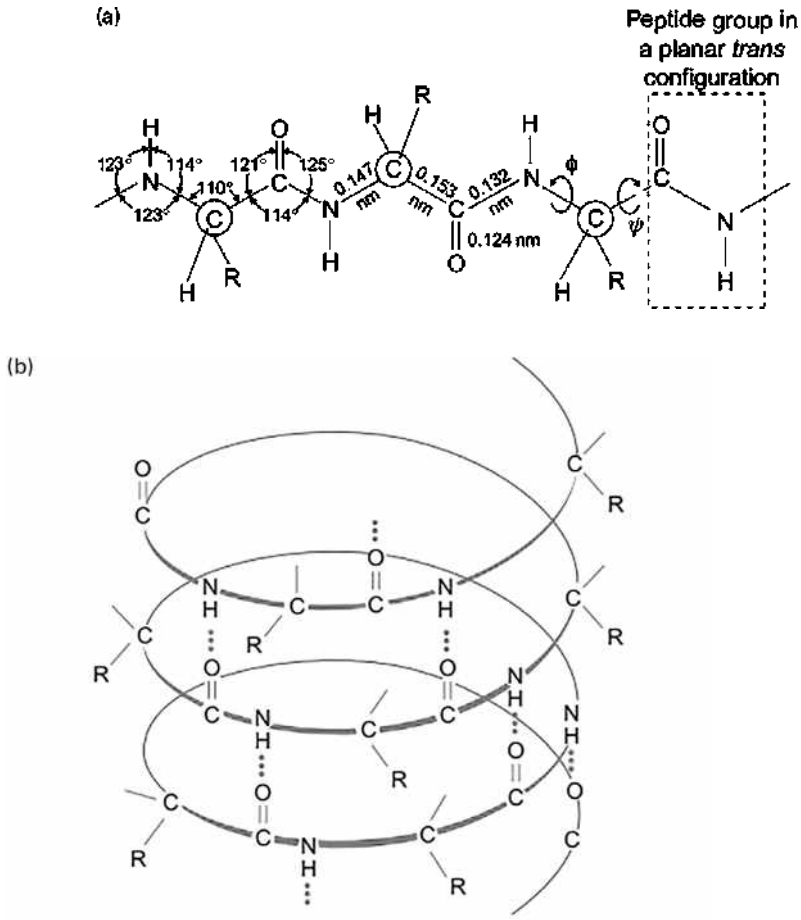


**Figure 1.38** (a) Geometry of a peptide (amide) linkage. (b) Hydrogen bonds in the alpha-helix. Coiling of an amino-acid chain brings peptide groups into juxtaposition so that the hydrogen bonds form and ensure the helical configuration. (Adapted from Journal of the Mechanical Behavior of Biomedical Materials, Vol 52, Vincent R. Sherman, Wen Yang, Marc A. Meyers, The materials science of collagen, 22–50, Copyright (2015), with permission from Elsevier.)

Fibrils, in turn, arrange themselves into fibers. Fibers are bundles of fibrils with diameters between 0.2 and 12 μm. In tendons, these fibers can be as long as the entire tendon. In tendons and ligaments, the collagen fibers form primarily one-dimensional networks. In skin, blood vessels, intestinal mucosa, and the female vaginal tract, the fibers organize themselves into more complex patterns leading to two- and three-dimensional networks.

The hierarchical organization of a tendon starts with tropocollagen (a form of collagen), and moves up, in length scale, to fascicles. There is a crimped, or wavy structure shown in the fascicles that has an important bearing on the mechanical properties. Figure 1.41 shows an idealized representation of a wavy fiber.

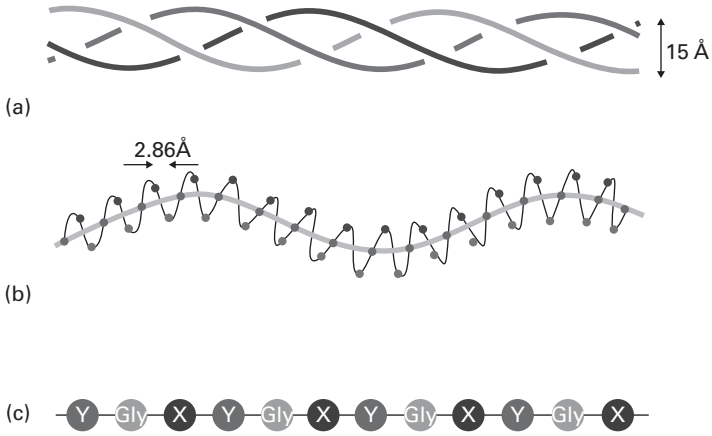


**Figure 1.39** Triple helix structure of collagen. (From Carlo Knupp, John M. Squire, Molecular Packing in Network-Forming Collagens, The Scientific World Journal, vol. 3, Article ID 157031, 20 pages, 2003. https://doi.org/10.1100/tsw.2003.40. Copyright © 2003 Carlo Knupp and John M. Squire.)

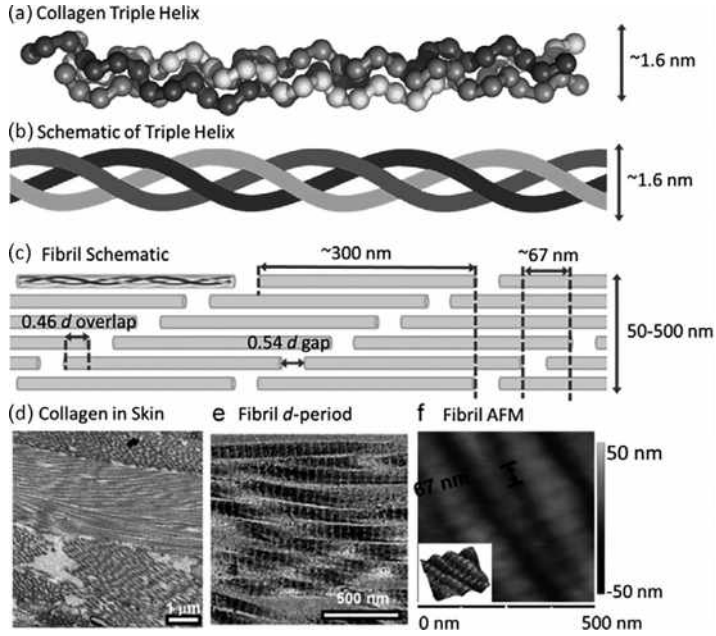


**Figure 1.40** Organization of collagen, starting with triple helix, and going to fibrils: (a) helical left-handed procollagen chains forming a right-handed triple helix of roughly 300 nm in length, (b) triple helix formed by three procollagen chains, (c) triple helices arranged in a staggered manner, leading to a gap (0.54 d) and an overlap (0.46 d) region; gap and overlap has a d-period, of 67 nm, (d) layers of collagen fibrils in a cross-section of skin; collagen fibrils of 100 nm diameter imaged by transmission electron microscopy, (f) atomic force microscopy of hydrated collagen fibrils in an arapaima scale. 67 nm d-period is measured.
(Reprinted from Journal of the Mechanical Behavior of Biomedical Materials, Vol 52, Vincent R. Sherman, Wen Yang, Marc A. Meyers, The materials science of collagen, 22–50, Copyright (2015), with permission from Elsevier.)

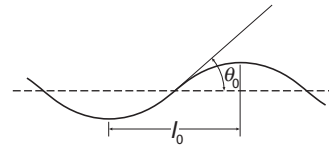


**Figure 1.41** Idealized configuration of a wavy collagen fiber.

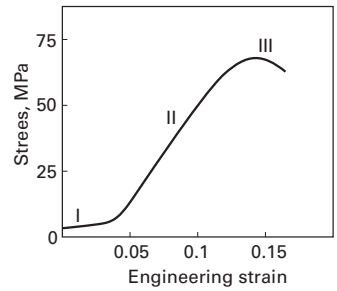


**Figure 1.42** Stress–strain curve of collagen with three characteristic stages.

Two parameters define it: the wavelength $2l_0$ and the angle $\theta_0$. Typical values for the Achilles tendon of a mature human are $l_0 = 20$–$50$ μm and $\theta_0 = 6$–$8°$. These bent collagen fibers stretch out in tension. When the load is removed, the waviness returns. When the tendon is stretched beyond the straightening of the waviness, damage starts to occur. Figure 1.42 shows a schematic stress–strain curve for tendons. The tendon was stretched until rupture. There are essentially three stages:

- Region I: toe part, in which the slope rises rapidly. This is the physiological range in which the tendon operates under normal conditions.
- Region II: linear part, with a constant slope.
- Region III: slope decreases with strain and leads to failure.

The elastic modulus of collagen is approximately 1 GPa and the maximum strain is in the 10–20% range. Cross-linking increases with age, and collagen becomes less flexible.

**Actin and Myosin** These are the principal proteins of muscles, leukocytes (white blood cells), and endothelial cells. Muscles contract and stretch through the controlled gliding/grabbing of the myosin with respect to the actin fibers. Figure 1.43(a) shows an actin fiber. It is composed of two polypeptides in a helical arrangement. Figure 1.43(b) shows the myosin protein. It has little heart-shaped "grapplers" called cross-bridges. The tips of the cross-bridges bind and unbind to the actin filaments. Figure 1.43(c) shows the myosin and actin filaments, and the cross-bridges at different positions. The cross-bridges are hinged to the myosin and can attach themselves to different positions along the actin filaments as the actin is displaced to the left. Thus, the muscles operate by a micro-telescoping action of these two proteins.

Figure 1.44 shows how the filaments organize themselves into myofibrils. Bundles of myofibrils form a muscle fiber. The $Z$ line represents the periodicity

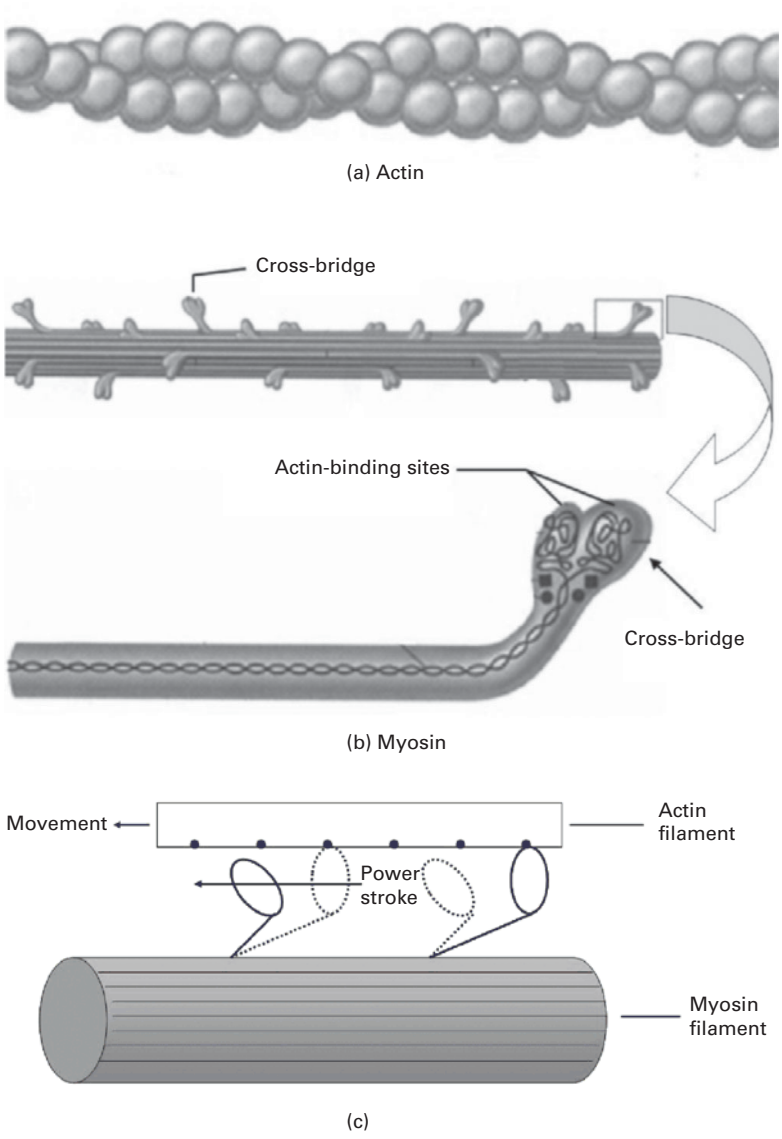


**Figure 1.43** Molecular structure of (a) actin and (b) myosin; (c) action of cross-bridges when actin filament is moved to the left with respect to the myosin filament; notice how cross-bridges detach themselves, then reattach themselves to the actin.

in the myosin-actin units (called sarcomeres) and is approximately equal to 3 μm in the stretched configuration. It shortens when the muscle is contracted. This gives the muscle a striated pattern when observed at high magnification. They resemble a coral snake in the microscope. Myofibrils have a diameter of approximately 1–2 μm.

**Elastin** Elastin is found in skin, walls of arteries and veins, and lung tissue. A prominent place is in the "*ligamentum nuchae*, a long ligament that runs along the top of the neck in horses and is constantly under tension. Other vertebrates have it too, but it is less pronounced. In this manner, the horse can keep its head up

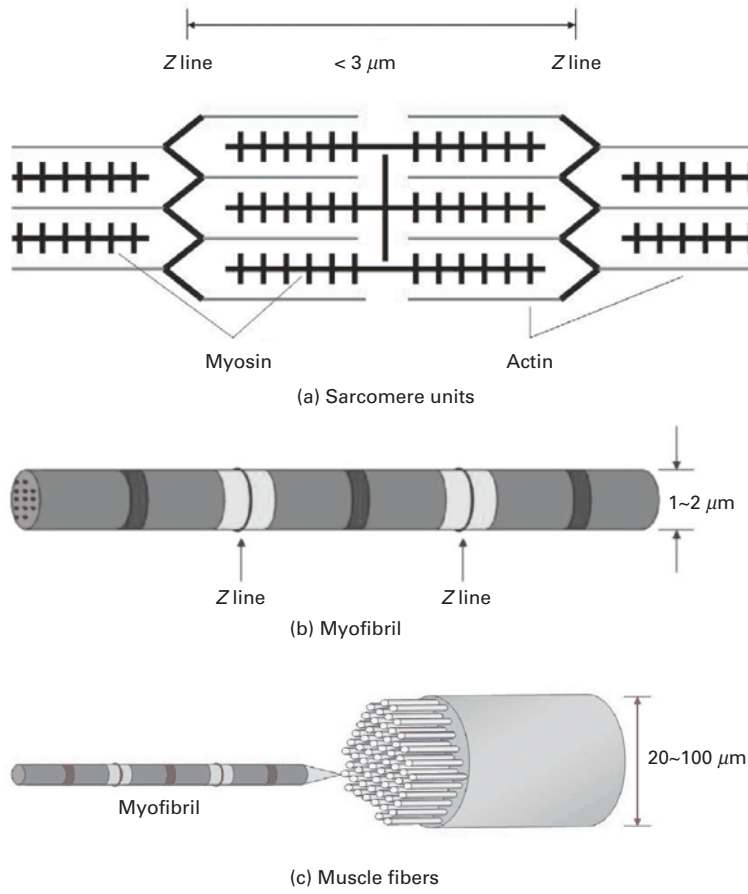


**Figure 1.44** Structure of muscle from (a) the sarcomere units, to (b) myofibril, and finally to (c) muscle fibers.

without using muscles. The "ligamentum nuchae plays a role similar to the cables in a suspension bridge. It is a rather robust cylinder.

**Resilin and Abductin** These are found in arthropods. They have properties similar to those of elastin, but occur in totally different animals and have a different structure.

**Keratin** Keratin is found in hair, horn, bird beaks and feathers, and whale baleen. The toucan beak presented in Section 1.3.8 is made of keratin. It has a structure similar to collagen (three interwoven helices). These helices combine themselves to form micro fibrils with a diameter of 8 nm. Interestingly, it undergoes a phase transformation under tensile load, which increases its elongation.

**Cellulose** Cellulose is the most abundant biological structural material, and is present in wood (which is a composite of cellulose and lignin) and cotton (almost pure cellulose). Cellulose is a cross-linked crystalline polymer. Its basic building block is a fibril with 3.5 nm diameter and 4 nm periodicity.

**Chitin** Chitin is a polysaccharide found in many invertebrates. The exoskeleton of insects is made of chitin.

**Silk** Silk is composed of two proteins: fibroin (tough strands) and sericin, a gummy glue. The mechanical properties (strength and maximum elongation) can vary widely, depending on the application intended by the animal. For instance, among the silks produced by spiders are dragline and spiral. Dragline, used in the radial components of the web, is the structural component, and has high tensile strength (600 mPa) and a strain at failure of about 6%. The spiral tangential components are intended to capture prey, and are "soft" and "sticky." The strain at failure in this case can exceed 16, i.e. 1,600%.

## Example 1.10

Determine the maximum strain that the collagen fibers can experience without damage if their shape is as given in Figure 1.41 with a ratio between amplitude and wavelength of 0.2.

We can assume a sine function of the form:

$$y = k \sin 2\pi x/\lambda.$$

The maximum of $y$ is reached when $x = \pi/4$.

Hence:

$$y_{\max} = k = \lambda/5.$$

We can integrate over the length of the sine wave from 0 to $2\pi$ . However, this will lead to an elliptical integral of difficult solution. A simple approximation is to consider the shape of the wavy protein as an ellipse with major axis $2a$ and minor axis $2b$. The circumference is given by the approximate expression (students should consult a mathematics text to obtain this expression)

$$L \approx \pi\left[\frac{3}{2}(a+b) - (ab)^{1/2}\right].$$

In the sine function, we have two arms, one positive and one negative. Their sum corresponds, in an approximate manner, to the circumference of the ellipse. The strain is equal to

$$\varepsilon = \frac{L - 4a}{4a} = \frac{\pi\left[\frac{3}{2}(a+b) - (ab)^{1/2}\right] - 4a}{4a}.$$

Thus:

$$\varepsilon = \frac{\pi}{4}\left[\frac{3}{2}\left(1 + \frac{b}{a}\right) - \left(\frac{b}{a}\right)^{1/2}\right] - 1.$$

## Example 1.10 (cont.)

The following ratio is given:

$$\frac{b}{2a} = 0.2 \quad \text{and} \quad \frac{b}{a} = 0.4.$$

The corresponding strain is:

$$\varepsilon = 0.53.$$

Beyond this strain, the collagen will break.

### 1.3.10 The Sponge Spicule: An Example of a Biological Material

Marine sponges have long tentacles that are called spicules. These spicules act as antennas, which are subjected to marine currents and other stresses. These long silica rods have properties that dramatically exceed the strength of synthetic silica. Figure 1.43 shows the flexure strength of both spicule and synthetic silica. The difference in flexure strength between sponge spicule and synthetic silica is remarkable. The synthetic silica fractures at a relatively low stress of 200 mPa compared to the yield stress of the spicule at 870 mPa. The area under the stress–strain curve gives a reasonable idea of the toughness. Clearly the toughness of the spicule is many times higher than that of synthetic silica. As evidenced by Figure 1.45, failure

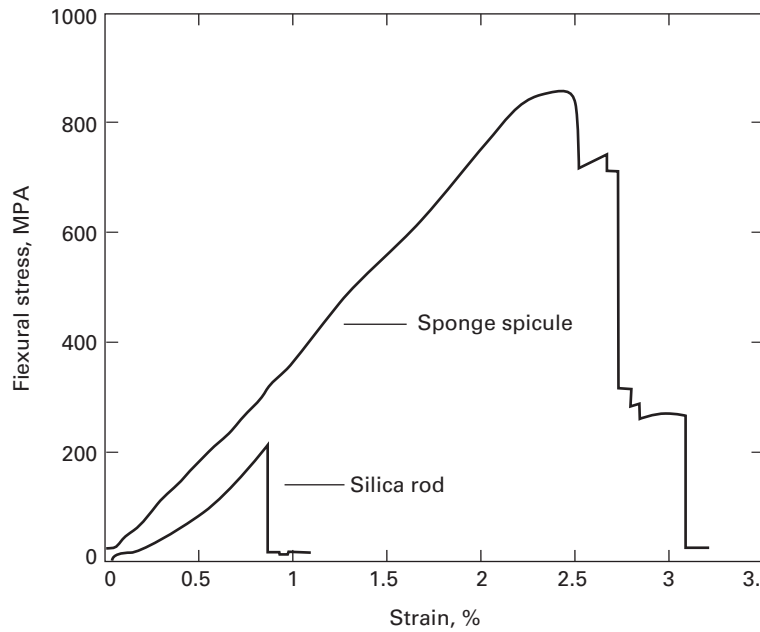


**Figure 1.45** stress deflection responses of synthetic silica rod and sponge spicule in flexure testing. (Figure courtesy of George Mayer.)

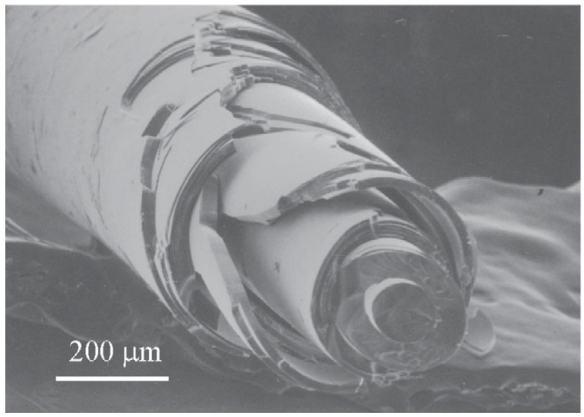


**Figure 1.46** SEM of fractured sponge spicule showing two-dimensional onion-skin structure of concentric layers.
(Figure courtesy of George Mayer.)

does not occur catastrophically in the spicule. Instead, the spicule fails "gracefully," which is a considerable advantage.

Figure 1.46 shows the microstructure of a fracture surface. The spicule consists of many concentric layers. This onion-like structure is responsible for the strengthening effect observed. When stress is applied to a silica rod, a crack will initiate at the weakest point in the material and propagate through the silica rod in a catastrophic manner. In contrast, crack propagation in the spicule will be arrested at each interface. This type of "graceful" failure is extremely useful. We can truly learn and apply this lesson from nature to modern material applications.

### 1.3.11 Active (or Smart) Materials

Technology puts greater and greater demand on materials and there is a constant push to develop materials with enhanced capabilities. The term *multifunctional materials* has been coined to describe materials with more than one capability. This is inspired by nature, where materials often have more than one function. For example, the trunk of a tree is at the same time a structural component and a carrier for the sap. Bones have a structural as well as a blood-cell-producing function.

Another category of advanced materials are *active materials*. They are also called "smart" materials. Active materials have responses that can be used in all kinds of devices. Given below are the main classes of active materials.

- Shape memory alloys: The most common is a NiTi alloy known as Nitinol. It can undergo strains of 1–5% through a martensitic transformation that is reversible. There are numerous applications through two effects: the shape memory effect and the super elastic (or pseudoelastic) effect: dental braces, stents, etc. A detailed description of these alloys is given in Chapter 11.
- Magnetorheological materials: These materials exhibit a viscosity that depends on an externally applied magnetic field. The suspension system of a US-made luxury

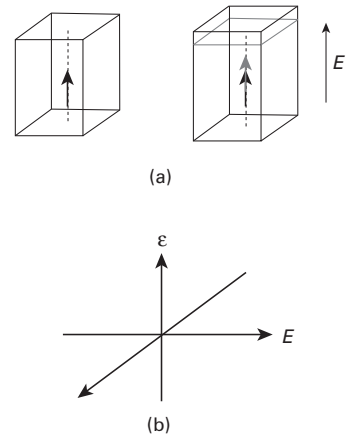


**Figure 1.47** (a) Effect of applied field $E$ on dimension of ferroelectric material. (b) Linear relationship between strain and electric field.
(Figure courtesy of G. Ravichandran.)

automobile uses this material. The stiffness can be adjusted by varying the magnetic field.

- Piezoelectric ceramics and ferroelectricity[9]: These materials generate an electric field when strained. Conversely, if an electric current is passed through them, they change their dimensions. Barium titanate and lead zirconate titanate (Pb(Zr, Ti)$O_3$) are examples. They have the perovskite structure with composition $ABO_3$, where A and B are metals. They are characterized by a linear strain–electric-field response. The maximum strain is on the order of 0.2%. Applications include vibration control, micropositioning devices, ultrasonics, and nondestructive evaluation.

It is a property of ferroelectrics to exhibit polarization in the absence of an electric field. Polarization is defined as dipole moment per unit volume or charge per unit area on the surface. The material is divided into domains, which are regions with uniformly oriented polarization. Ferroelectrics are characterized by a linear relationship between stress $\sigma$ and polarization $P$:

$$P = d\sigma.$$

There is a converse relationship between strain $\varepsilon$ and electric field, $E$:

$$\varepsilon = dE,$$

where $d$ is called the polarizability tensor. Figure 1.47(a) shows how the application of an externally applied electric field $E$ results in a change in length of the specimen. Figure 1.47(b) shows the linear relationship between the strain and the field. This is a property of ferroelectric crystals, certain noncentrosymmetric crystals (e.g. quartz, ZnO), textured polycrystals, and polycrystals with a net spontaneous polarization. Applications include adaptive optics, active rotors and control surfaces, robotics,

[9] K. Bhattacharya and G. Ravichandran, *Acta Mater.*, 51 (2003) 5941.

and MEMS/NEMS (microelectromechanical system/nanoelectromechanical system) actuators.

### 1.3.12 Electronic Materials

Electronic materials are composed, for the most part, of thin films arranged in several layers and deposited on a substrate. The most common substrate is monocrystalline silicon (the silicon wafer). Integrated circuits form the heart of modern computers and the silicon chip is a primary example. Figure 1.48 shows a schematic of the materials and structure used in a CMOS (complementary metal oxide semiconductor) transistor device. The *pn* junctions form transistors. The substrate is silicon, which in this case is *n* doped. The thin film layers are vapor-deposited and there are a number of mechanical aspects that are of considerable importance. In Figure 1.48 we have monocrystalline and polycrystalline silicon, oxide, glass, metal, and a dielectric passivation layer.

The thin films deposited on the substrate have dimensions of a few nanometers to a few micrometers. These films may be under residual stresses as high as 500 MPa. These stresses are due to:

- Thermal expansion coefficient effects: When the film cools it contracts. The thermal expansion coefficients of the different layer scan be different, creating internal stresses.
- Phase transformations: The phases in thin films are often nonequilibrium phases.

There are a number of mechanical problems associated with these stresses. Dislocations at the interface between substrate and thin film, cracking of the

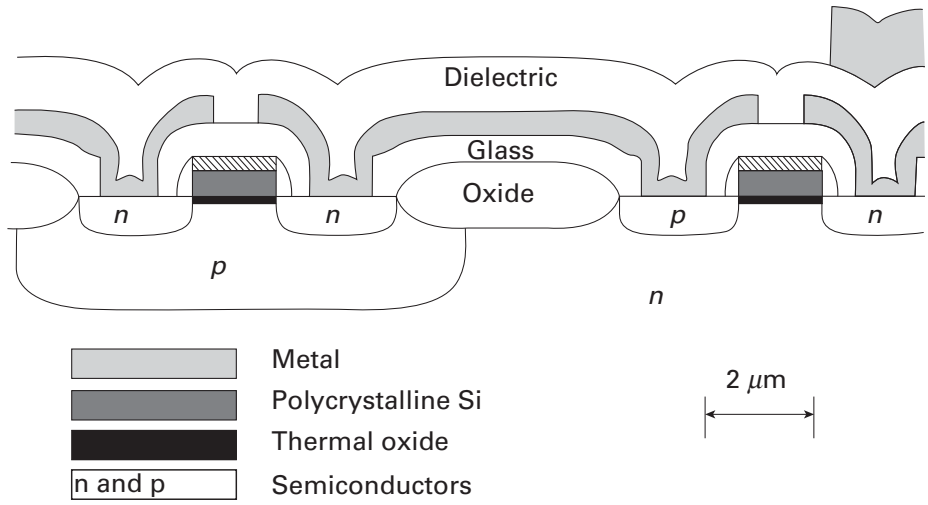


**Figure 1.48** Cross-section of a complementary metal-oxide semiconductor (CMOS). (Adapted by permission of Springer Nature: *Metallurgical Transactions, A, Physical Metallurgy and Materials Science*, Mechanical properties of thin films, William D. Nix, Copyright (1989).)

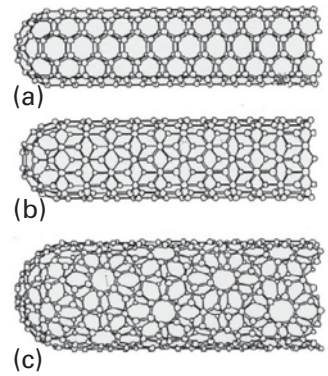


**Figure 1.49** Three configurations for single-wall carbon nanotubes: (a) armchair, (b) "zig-zag", (c) chiral.
(Adapted from *Carbon*, Vol. 33, M.S. Dresselhaus, G. Dresselhaus, R. Saito, Physics of carbon nanotubes, Pages 883–891. Copyright 1995, with permission from Elsevier.)

passivation layer, and bending of the substrate/thin-film system are a few examples. We will briefly describe these effects in Chapters 2, 6, 9, and 13.

Magnetic hard disks are also made of thin films. The aluminum disk, upon which a thin layer of magnetic material is deposited, rotates at surface velocities approaching 80 km $h^{-1}$, while the "head" flies aerodynamically over it. The distance between head and disk is as low as 0.3 μm. Some of the mechanical problems are friction, wear, and the unavoidable collisions between disk and head.

### 1.3.13 Nanotechnology

Nanotechnology[10, 11] refers to the structure and properties of materials and devices at the nanometer level. Developments in synthesis and characterization methods have resulted in materials that are designed from the "bottom up," rather than from the "top down." These terms were first used by the famous physicist Richard Feynman. The traditional method used in the design of new materials is to develop synthesis and processing techniques at the macro scale, and then to carry out detailed characterization at the micrometer and nanometer scale. The new approach is to start with atoms, then assemble them into small arrays and characterize their structure and properties at that level. This approach was led by the semiconductor revolution. As the sizes of devices become smaller, we approach atomic dimensions. At that level, it is being found that many materials possess unique properties. Many biological processes also use the bottom-up approach. Atoms aggregate themselves into molecules and complex arrays through genetic messages. The atoms come together and self-organize themselves into complex arrays of amino acids, which in their turn form proteins. It is hoped that we will be able to fully harness this approach in the future. There are already applications of nanotechnology in the marketplace.

A material that is showing great potential because of unique characteristics is the carbon nanotube. The first nanotube was produced in Japan by S. Iijima. One can

[10] C. P. Poole and F. J. Owens, *Introduction to Nanotechnology* (Hoboken, NJ: Wiley-Interscience, 2003).
[11] M. Ratner and D. Ratner, *Nanotechnology* (Englewood Cliffs, NJ: Prentice Hall, 2003).

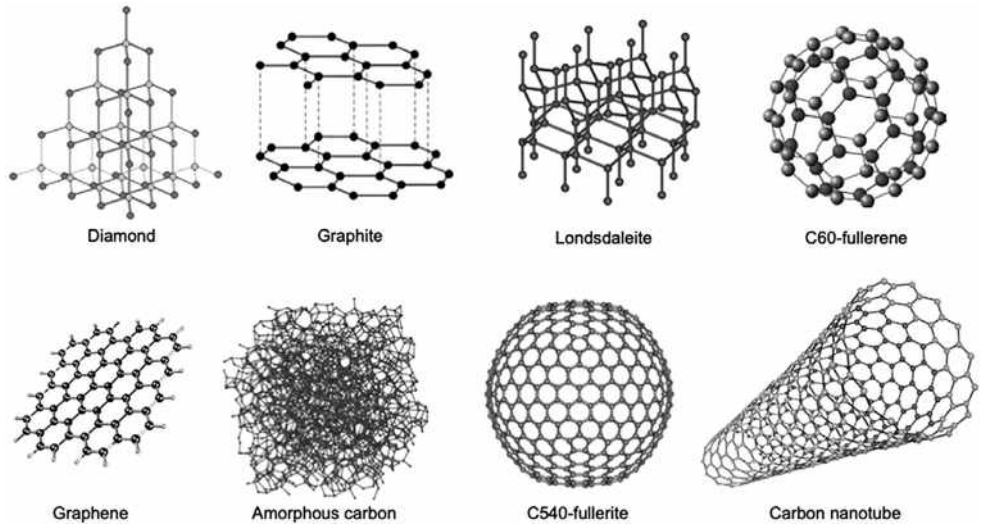


**Figure 1.50** Different arrangements of carbon atoms.
(Reprinted by permission from Springer Nature: Topics in Current Chemistry, Carbon nanotubes in biomedicine, Viviana Negri et al, Copyright (2020).)

envisage a carbon nanotube by rolling a single layer of carbon atoms into a hollow cylinder. The ends can be semispherical caps (one half of a "Bucky ball"). There are three morphologies for carbon nanotubes, shown in Figure 1.47: armchair, zig-zag, and chiral. They differ in the following:

- Armchair: the hexagons have the "pointy" side perpendicular to cylinder axis.
- Zig-zag: the hexagons have the pointy side aligned with the cylinder axis.
- Chiral: The hexagons are inclined with respect to the cylinder axis, and the carbon sheet wraps itself helically around the cylinder.

These carbon nanotubes have typically a diameter between 5 and 20 nm and length between 1 and 100 μm. They have outstanding mechanical properties, since they are based on the C–C bond, the strongest in nature. There are varying estimates of their strength, and values between 45 and 200 GPa are quoted. This would make them the strongest material known, ranking with diamond. Although the nanotubes are very short, one can envisage a day where continuous nanotubes are manufactured. Their incorporation as reinforcements in composites presents a bright prospect.

Figure 1.50 shows several carbon allotropes: diamond, graphite, lonsdaleite, C60-fullerene, graphene, amorphous carbon, C540-fullerite, and single-walled carbon nanotube. Outstanding properties can be achieved by the different configurations of the carbon atoms. This topic, nanostructured materials, is treated in Chapter 5.

Two-dimensional structures, especially graphene and $MoSi_2$, are becoming increasingly important.

## 1.4 Strength of Real Materials

Materials deform and fail through defects. These defects (cracks, point defects, dislocations, twins, martensitic phase transformations, etc.) are discussed in Chapters 4 through 8. The two principal mechanisms are crack growth, and dislocations and plastic flow:

- Crack growth: Real materials can have small internal cracks, at whose extremities high-stress concentrations are set up. Hence, the theoretical cleavage strength can be achieved at the tip of the crack at applied loads that are only a fraction of that stress. Griffith's theory (see Chapter 7) explains this situation very clearly. These stress concentrations are much lower in ductile materials, since plastic flow can take place at the tip of a crack, blunting the crack's tendency to grow.
- Dislocations and plastic flow: Before the theoretical shear stress is reached, dislocations are generated and move in the material; if they are already present, they start moving and multiply. These dislocations are elementary carriers of plastic deformation and can move at stresses that are a small fraction of the theoretical shear stress. They will be discussed in detail in Chapter 4.

In sum, cracks prevent brittle materials from obtaining their theoretical cleavage stress, while dislocations prevent ductile materials from obtaining their theoretical shear stress.

To achieve the theoretical strength of a crystalline lattice, there are two possible methods: (1) eliminating all defects and (2) creating so many defects, that their interactions render them inoperative. The first approach has yielded some materials with extremely high strength. Unfortunately, this has been possible only in special configurations called "whiskers." The second approach is the one more commonly pursued, because of the obvious dimensional limitations of the first; the strength levels achieved in bulk metals have steadily increased by an ingenious combination of strengthening mechanisms, but are still much lower than the theoretical strength. Maraging steels with useful strengths up to 2 GPa have been produced, as have patented steel wires with strengths of up to 4.2 GPa; the latter are the highest strength steels.

Figure 1.51 compares the ambient-temperature strength of tridimensional, filamentary, and whisker materials. The whiskers have a cross-sectional diameter of only a few micrometers and are usually monocrystalline (although polycrystalline whiskers have also been developed). Whiskers are one of the strongest materials developed by human beings. The dramatic effect of the elimination of two dimensions is shown clearly in Figure 1.51 and in Table 1.7. The strongest whiskers are ceramics. Figure 1.51 provides some illustrative examples. Iron whiskers with a strength of 12.6 GPa have been produced, compared with 2 GPa for the strongest bulk steels. The value of 12.6 GPa is essentially identical to the theoretical shear stress, because the normal stress is twice the shear stress. In general, FCC whiskers tend to be much weaker than BCC whiskers and ceramics. For instance, Cu whiskers have a strength of about 2 GPa. This is consistent with the much lower

**Table 1.7 Room Temperature Strength of Some Whiskers**

| Material | Diameter | Maximum tensile strength (GPa) | Source |
|---|---|---|---|
| Cu | 1.2 to 15 μm | 2–6 | [a] |
| Ag | 1.2 to 15 μm | 1.5–4 | [a] |
| Fe | 1.2 to 15 μm | 3–9 | [a] |
| SiC | 4–6 μm | 8.4 | [b] |
| $Al_2O_3$ | 82–320 nm | 49 | [c] |
| $Si_3N_4$ | 40–800 nm | 17–59 | [d] |
| Graphite | 1–5 μm | 20 | [e] |

[a] S. Brenner, *J. Appl. Phys.*, 27(1956)1484–1497.
[b] J. J. Petrovic, J. V. Milewski, D. L. Rohr, F. D. Gac, *J. Matls. Sci.*, 20(1985) 1167–1177.
[c] S. Wang, Y. He, H. Huang, J. Zhou, G. J. Auchterlonie, B. Huang, *Nanotechnology*, 24(2013) 285703.
[d] H. Iwanaga, C, Kawai, *JACS*, 81(1998) 773–776.
[e] R. Bacon, *J. Appl. Phys.*, 31(1960) 283–290.
Adapted with permission from A. Kelly, *Strong Solids* (Oxford, U.K.: Clarendon Press, 1973), p. 263s.

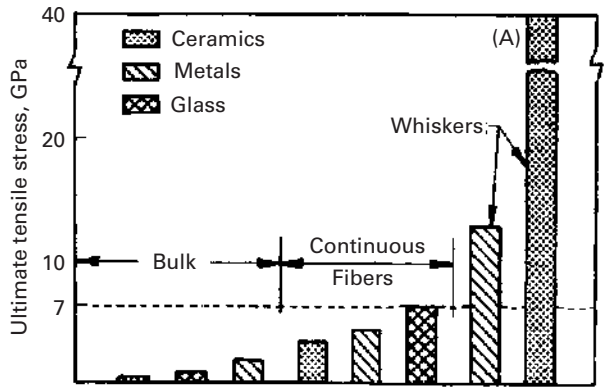


**Figure 1.51** Theoretical strength of continuous fibers and whiskers. The strength of the SiC whisker produced by the Philips Eindhoven Laboratory is indicated by (A).

theoretical shear strength exhibited by copper whiskers. It turns out that silver, gold, and copper have $\tau_{max}/G$ ratios of 0.039 (see Chapter 4). Hence, they are not good whisker materials. Figure 1.52 shows a stress–strain curve for a tin whisker. The stress drops vertically after the yield point. In contrast, the stress–strain curve for the polycrystal is barely different from the abscissa axis. This demonstrates, for a real material, the dramatic effect that a small lateral dimension can have on the strength and ductility.

In the elastic range, the curve deviates slightly from Hooke's law and exhibits some temporary inflections and drops (not shown in the figure). In many cases, for both metals and nonmetals, failure occurs at the elastic line, without appreciable plastic strain. When plastic deformation occurs, as, for example, in copper and zinc, a very large yield drop is observed. Although the strength of whiskers is not completely understood, it is connected to the absence of dislocations. This is also exemplified in Figure 1.52, which compares the strength of single crystalline tin in the form of whiskers with the bulk polycrystalline form. The whiskers have a strength around

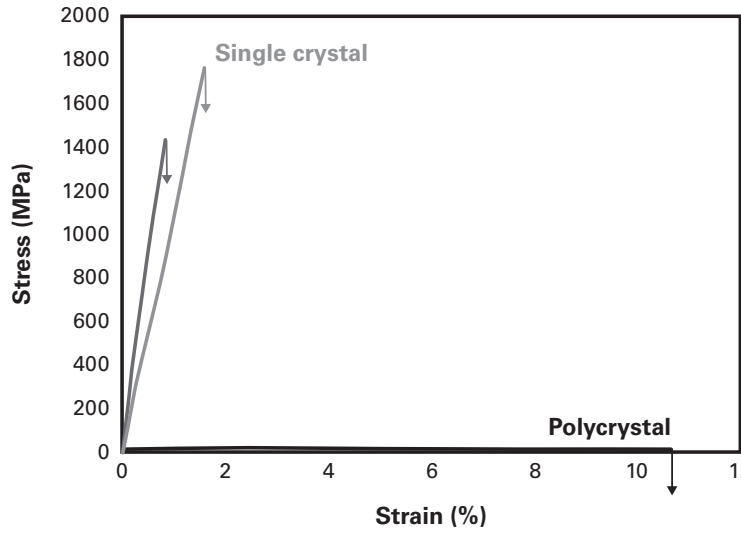


**Figure 1.52** Stress–strain curve of tin whisker and comparison with strength of polycrystal. (Reprinted by permission from Springer Nature: Journal of Electronic Materials, Tensile Behavior of Single-Crystal Tin Whiskers, S.S. Singh et al., Copyright (2014).)

1.6 GPa, whereas the polycrystal strength is in the low MPa range. It is impossible to produce a material virtually free of dislocations, in other words, perfect. However, for whiskers, dislocations can easily escape out of the material during elastic loading. Their density and mean free path are such that they will not interact and produce other sources of dislocation. Hence, the yield point is the stress required to generate dislocations from surface sources. The irregularities often observed in the elastic range indicate that existing dislocations move and escape out of the whisker. At a certain stress, the whisker becomes essentially free of dislocations. When the stress required to activate surface sources is reached, the material yields plastically, or fails.

## Example 1.11

Calculate the stresses generated in a turbine blade if its cross-sectional area is 10 $cm^2$ and the mass of each blade is 0.2 kg.

***Solution:*** This is an example of a rather severe environment where the material properties must be predicted with considerable detail. For example the blade may be in a jet engine. Figure E 1.11 shows a section of the compressor stage of a jet. The individual blades are fixed by a dovetail arrangement to the turbine vanes. Assume a rotational velocity $\omega$ =10,000 rpm and a mean radius $R$ = 0.5 m. The centripetal acceleration in the bottom of each turbine blade is

$$a_c = \omega^2 R = \left[10,000 \times \frac{1}{60} \times 2\pi\right]^2 \times 0.5 = 5.4 \times 10^5 \text{m s}^{-2}.$$

## Example 1.11 (cont.)

The stress that is generated is

$$\sigma = \frac{F}{A} = \frac{ma_c}{A} = \frac{0.2 \times 5.4 \times 10^5}{10 \times 10^{-4}} = 100 \text{ MPa},$$

where $F$ is the centripetal force and $A$ is the cross-sectional area. This stress of 100 MPa is significantly below the flow stress of nickel-based superalloys at room temperature, but can be quite significant at higher temperatures.

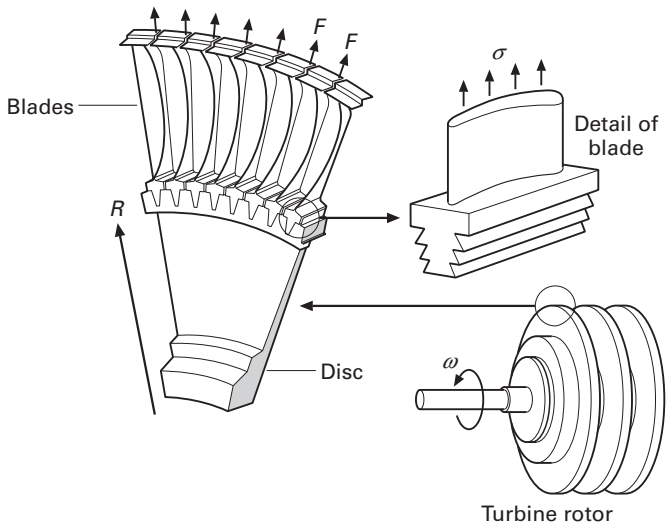


**Figure E1.11** Turbine blade subjected to centripetal force during operation.

## SUGGESTED READING

### Materials in General

J. F. Shackelford. *Introduction to Materials Science for Engineers*, 4th edn. Upper Saddle River, NJ: Prentice Hall, 1996.

W. F. Smith. *Principles of Materials Science and Engineering*, 3rd edn. New York, NY: McGraw Hill, 1996.

D. R. Askeland and P. Phule. *The Science and Engineering of Materials*, 4th edn. Pacific Grove, CA: Thomson, 2003.

W. D. Callister. Jr. *Materials Science and Engineering*, 4th edn. New York, NY: Wiley, 2003.

### Metals

C. S. Barrett and T. B. Massalski. *Structure of Metals*, 3rd rev. edn. Oxford, U.K: Pergamon, 1980.

M. A. Meyers and K. K. Chawla. *Mechanical Metallurgy*. Englewood Cliffs, NJ: Prentice-Hall, 1984.

### Ceramics

W. D. Kingery, H. K. Bowen, and D. R. Uhlmann. *Introduction to Ceramics*, 2nd edn. New York, NY, Wiley, 1976.
Y.-M. Chiang, D. Birnie III, and W. D. Kingery, *Physical Ceramics*, New York, NY: Wiley, 1997.

### Polymers

D. C. Bassett. *Principles of Polymer Morphology*. Cambridge, U.K.: Cambridge University Press, 1981.
Hiltner (ed.) *Structure-Property Relationships of Polymeric Solids*. New York, NY: Plenum Press, 1983.
R. J. Young. *Introduction to Polymers*. London: Chapman & Hall, 1986.
B. Wunderlich. *Macromolecular Physics, Vol. 1: Crystal Structure*. New York, NY: Academic Press, 1973.
B. Wunderlich. *Macromolecular Physics, Vol. 2: Crystal Nucleation*. New York, NY: Academic Press, 1976.

### Composite Materials

K. Chawla. *Composite Materials: Science & Engineering*. 2nd edn. New York, NY: Springer, 1998.
K. Chawla. *Ceramic Matrix Composites*, 2nd edn. Boston, MA: Kluwer, 2003.
N. Chawla and K. K. Chawla. *Metal Matrix Composites*, New York, NY: Springer, 2006.

### Liquid Crystals

A Ciferri, W. R. Krigbaum, and R. B. Meyer (eds.). *Polymer Liquid Crystals*. New York, NY: Academic Press, 1982.

### Biomaterials

M. Elices (ed.). *Structural Biological Materials*, Amsterdam, the Netherlands: Pergamon, 2000.
J. F. V. Vincent. *Structural Biomaterials*. Princeton, NJ: Princeton University Press, 1991.
Y.C. Fung. *Biomechanics: Mechanical Properties of Living Tissues*. New York, NY: Springer, 1981.

### Cellular Materials

J. Gibson and M. F. Ashby. *Cellular Solids: Structure and Properties*. Oxford, U.K.: Pergamon Press, 1988.

### Electronic Materials

W. D. Nix. Mechanical Properties of Thin Films, *Met. Trans.*, 20A (1989) 2217.
L.B. Freund and S. Suresh. *Thin Film Materials: Stress, Defect Formation and Surface Evolution*. Cambridge, U.K.: Cambridge University Press, 2003.

## EXERCISES

**1.1** A jet turbine rotates at a velocity of 7,500 rpm. Calculate the stress acting on the turbine blades if the turbine disc radius is 70 cm and the cross-sectional area is 15 $cm^2$. Take the length to be 10 cm and the alloy density to be 8.5 g $cm^{-3}$.

**1.2** The material of the jet turbine blade in Problem 1.1, Super alloy IN 718, has a room-temperature yield strength equal to 1.2 G Pa; it decreases with temperature as

$$\sigma = \sigma_0 \left(1 - \frac{T - T_0}{T_m - T_0}\right)$$

where $T_0$ is the room temperature and $T_m$ is the melting temperature in K ($T_m = 1{,}700$ K). At what temperature will the turbine flow plastically under the influence of centripetal forces?

**1.3** **(a)** Describe the mechanical properties that are desired in a tennis racket, and recommend different materials for the different parts of the racket.

**(b)** Describe the mechanical properties that are desired in a golf club, and recommend different materials for the different parts of the club.

**1.4** On eight cubes that have one common vertex, corresponding to the origin of axes, draw the family of {111} planes. Show that they form an octahedron and indicate all <110> directions.

**1.5** The frequency of loading is an important parameter in fatigue. Estimate the frequency of loading (in cycles per second, or Hz) of an automobile tire in the radial direction when the car speed is 100 km $h^{-1}$ and the wheel diameter is 0.5 m.

**1.6** Indicate, by their indices and in a drawing, six directions of the <112> family.

**1.7** The density of Cu is 8.9 g $cm^{-3}$ and its atomic weight (or mass) is 63.546. It has the FCC structure. Determine the lattice parameter and the radius of atoms.

**1.8** The lattice parameter for W(BCC) is $a = 0.32$ nm. Calculate the density, knowing that the atomic weight (or mass) of W is 183.85.

**1.9** Consider the unit cell of CsCl which has NaCl structure. The radius of $Cs^+$ is 0.169 nm and that of $Cl^-$ is 0.181 nm. (a) Determine the packing factor of the structure, assuming that $Cs^+$ and $Cl^-$ ions touch each other along the diagonals of the cube. (b) Determine the density of CsCl if the atomic weight of Cs is 132.905 and that of Cl is 35.453.

**1.10** MgO has the same structure as NaCl (simple cubic). If the radii of $O^{2-}$ and $Mg^{2+}$ ions are 0.14 nm and 0.070 nm, respectively, determine (a) the packing factor and (b) the density of the material. The atomic weight of $O_2$ is 16 and that of Mg is 24.3.

**1.11** Germanium has the diamond cubic structure with interatomic spacing of 0.245 nm. Calculate the packing factor and density. (The atomic weight of germanium is 72.6.)

**1.12** The basic unit (or mer) of polytetrafluoroethylene (PTFE) or Teflon is $C_2F_4$. If the mass of the PTFE molecule is 45,000 amu, what is the degree of polymerization?

**1.13** Using the representation of the orthorhombic unit cell of polyethylene (see Figure E1.13), calculate the theoretical density. How does this value compare with the density values of polyethylene obtained in practice?

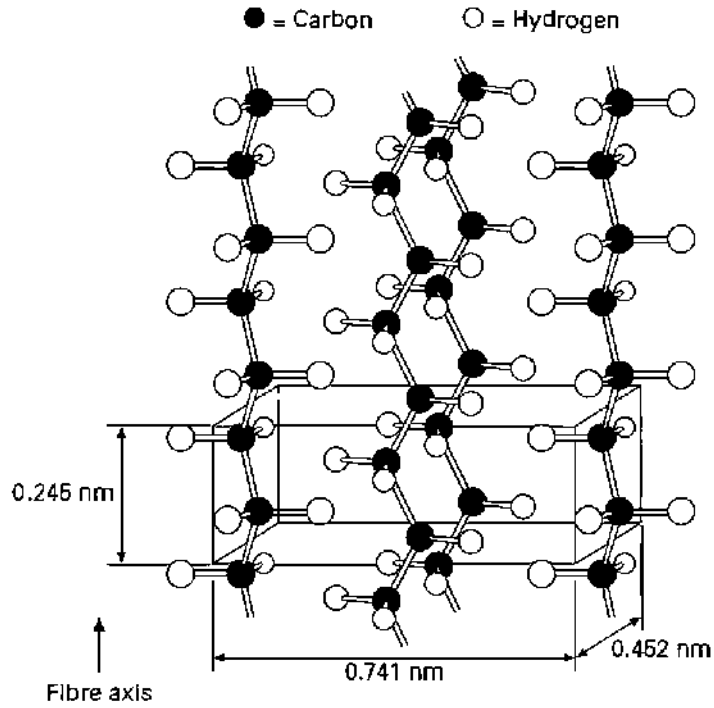


**Figure E1.13** Crystalline form of polyethylene with orthorhombic unit cell.

**1.14** A pitch blend sample has five different molecular species with molecular masses of $0.5 \times 10^6$, $0.5 \times 10^7$, $1 \times 10^7$, $4 \times 10^7$, and $6 \times 10^7$. Compute the number-averaged molecular weight and weight-averaged molecular weight of the sample.

**1.15** Different polymorphs of a material can have different mechanical properties. Give some examples.

**1.16** What are smart materials? Give some examples.

**1.17** What are glass-ceramics? Explain their structure and properties. (Hint: think of Corning ware.)

**1.18** Explain how the scale of microstructure can affect the properties of a material. Use steel, an alloy of iron and carbon, as an example.

**1.19** For a cubic system, calculate the angle between (a) [100] and [111], (b) [111] and [112], (c) [112] and [221].

**1.20** Recalculate the bicycle stiffness ratio for a titanium frame. (See Examples 1.1 and 1.2.) Find the stiffness and weight of the bicycle if the radius of the tube is 25 mm. Use the following information:

$$\begin{aligned} \text{Alloy} &: \text{Ti} - 6\%\text{Al} - 4\%\text{V}, \\ \sigma_y &= 1,150 \text{ MPa}, \\ \text{Density} &= 4.5 \text{ g cm}^{-3}, \\ E &= 106\text{GPa}, \\ G &= 40\text{GPa}. \end{aligned}$$

**1.21** Calculate the packing factor for NaCl, given that $r_{\text{Na}} = 0.186$ nm and $R_{\text{Cl}} = 0.107$ nm.

**1.22** Determine the density of BCC iron structure if the iron atom has a radius of 0.124 nm.

**1.23** Draw the following direction vectors in a cubic unit cell:

(a) [100] and [110], (b) [112], (c) $[\bar{1}10]$, (d) $[\bar{3}2\bar{1}]$.

**1.24** Calculate the stress generated in a turbine blade if its cross-sectional area is 0.002 $m^2$ and the mass of each blade is 0.5 kg. Assume that the rotational velocity $\omega = 15{,}000$ rpm and the turbine disk radius is 1 m.

**1.25** Suppose that the turbine blade from the last problem is part of a jet turbine. The material of the jet turbine is a nickel-based superalloy with yield strength, $\sigma_y = 1.5$ G Pa; it decreases with temperature as:

$$\sigma_y = \sigma_0[(1 - (T - T_0)/(T_m - T_0)],$$

where $T_0 = 293$ K is room temperature and $T_m = 1{,}550$ K is the melting temperature. Find the temperature at which the turbine will flow plastically under the influence of centripetal forces.

**1.26** Calculate the lattice parameter of Ni (FCC) knowing that the atomic diameter of nickel is 0.249 nm.

**1.27** A jet turbine blade, made of MARM 200 (a nickel-based superalloy) rotates at 10,000 rpm. The radius of the disk is 50 mm. The cross-sectional area is 20 $cm^2$ and the length of the blade is equal to 12 cm. The density of MARM 200 is 8.5 g $cm^{-3}$.

**(a)** What is the stress acting on the turbine blade in MPa?

**(b)** If the room temperature strength of MARM 200 is equal to 800 MPa, what is the maximum operational temperature in kelvin?

The yield stress varies with temperature as:

$$\sigma = \sigma_0 \left[ 1 - \left( \frac{(T - T_0)}{(T_m - T_0)} \right)^m \right],$$

where $T_m$ is the melting temperature ($T_m = 1{,}700$ K) and $T_0$ is the room temperature; $m = 0.5$.

**1.28** Generate a three-dimensional unit cell for the intermetallic compound $AuCu_3$ that has a cubic structure. The Au atoms are at the cube corners and the Cu atoms at the center of the faces. Given:

**Figure Ex 1.28**

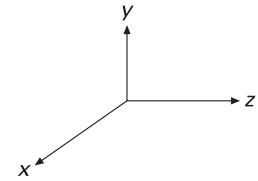


$r_{Cu} = 0.128$ nm $AN_{Cu}$ (atomic number) $= 63.55$ amu
$r_{Au} = 0.144$ nm $AN_{Au} = 196.97$ amu.
(a) Find the lattice parameter in nanometers.
(b) What is the atomic mass of the unit cell in grams?
(c) What is the density of the compound in g $cm^{-3}$?

**1.29** Draw the following unit cells with the planes (one plane per cube with the coordinate axes): (a) $(\bar{1}01)$, (b) $(1\bar{1}1)$, (c) $(0\bar{1}2)$, (d) (301).

**1.30** Show how the atoms pack in the following planes by drawing circles (atoms) in the appropriate spots: (a) (111) in FCC, (b) (110) in FCC, (c) (111) in BCC, (d) (110) in BCC.

**1.31** BET is a technique for measuring the surface area of particles, which is of obvious importance in nanomaterials. Describe this technique. Don't forget to mention what the acronym BET stands for.

**1.32** "Tin plate" is one of the largest tonnage steel products. It is commonly used for making containers. If it is a steel product why is it called tin plate?

**1.33** Using Figure 1.7, list the important symmetry operations in the following crystal systems: (a) triclinic, (b) monoclinic, (c) orthorhombic.

**1.34** The only possible rotation operations that can be used to define crystal systems are rotations of the type $n = 1, 2, 3, 4$, and 6. Using other values of $n$ will result in unit cells which, when joined together, will not fill all space. Demonstrate this by giving a simple mathematical proof. (*Hint*: consider two lattice points separated by a unit translation vector.)

**1.35** Calculate the APF (atomic packing factor) for BCC and FCC unit cells, assuming the atoms are represented as hard spheres. Do the same for the diamond cubic structure.

**1.36** Draw the following crystallographic planes in BCC and FCC unit cells along with their atoms that intersect the planes: (a) (101), (b) (110), (c) (441), (d) (111), (e) (312).

**1.37** A block copolymer has macromolecules of each polymer attached to the other as can be seen in Figure 1.22(c). The total molecular weight is 100,000 g $mol^{-1}$. If 140 g of A and 60 g of B were added, determine the degree of polymerization for each polymer. A: 56 g $mol^{-1}$; B: 70 g $mol^{-1}$.

**1.38** Sketch the following planes within the unit cell. Draw one cell for each solution. Show new origin and ALL necessary calculations.
(a) $(0\bar{1}\bar{1})$, (b) (102), (c) (002), (d) $(1\bar{3}0)$, (e) $(\bar{2}12)$, (f) $(3\bar{1}\bar{2})$.

**1.39** Sketch the following directions within the unit cell. Draw one cell for each solution. Show new origin and ALL necessary calculations.
(a) [101], (b) $[0\bar{1}0]$, (c) $[12\bar{2}]$, (d) [301], (e) $[\bar{2}01]$, (f) $[2\bar{1}3]$.

**1.40** Suppose we introduce one carbon atom for every 100 iron atoms in an interstitial position in BCC iron, giving a lattice parameter of 0.2867 nm. For the Fe-C alloy, find the density and the packing factor.
Given:
Atomic mass of C = 12,
Atomic mass of Fe = 55.89,
$a_{Fe} = 0.2867$ nm,
Avogadro's number, $N = 6.02 \times 10^{23}$.

**1.41** Determine the maximum length of a polymer chain made with 1,500 molecules of ethylene, knowing that the carbon bond length is 0.13 nm.

**1.42** Calculate the atomic packing factor (APF) of diamond cubic.

**1.43** SiC has the diamond cubic structure. Calculate the APF of SiC ($r_{Si} = 0.11$ nm and $r_C = 0.07$ nm).

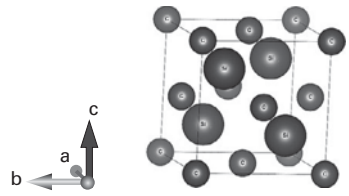


**Figure Ex 1.43**

**1.44** **(a)** How can the development of composites influence future aircraft?
**(b)** What are the principal features of composites?

**1.45** If steel is as strong as aluminum alloys in terms of strength, why are planes built with aluminum alloys?

**1.46** What composite materials are used in the Boeing 787?

**1.47** Draw the direction vectors in a cubic unit cell: $[111]$, $[201]$ and $[\bar{2}31]$.

**1.48** (a) Determine the interplanar spacing of (110) planes in a tetragonal unit cell ($a = b \neq c$, $\alpha = \beta = \gamma = 90^\circ$) with lattice parameters of $a = 0.3963$ nm and $c = 0.3671$ nm. (b) Determine the areas of the following planes $(\bar{1}10)$, $(1\bar{2}0)$ and $(00\bar{1})$.

**1.49** There are face-centered and body-centered structures in cubic systems, but no base-centered cubic. Show that the base-centered cubic structure is equivalent to another structure of the Bravais lattices.

**1.50** Explain the concept of free volume in glass transition in condensed matter. Why we can easily make a polymer which is composed of small molecules like metals in a glassy state but not in a crystalline state (though certain metallic glasses can be made easily).

**1.51** Stress–strain diagrams for three different polymers can be found in the following plot. It is known that one of the polymers is in a rubbery state, one is in a glassy state and the third is in a semicrystalline state. Please indicate the corresponding curves for the rubber, glassy, and semicrystalline polymers.

**1.52** Why is the percentage of composite materials increasing as time goes by? What are the advantages of using composite materials over traditional metallic materials?

**1.53** If gold atoms have a radius of 0.144 nm, determine the density and APF (atomic packing factor) in FCC and BCC structures. (Atoms are in contact along the face diagonal and body diagonal directions; $a = 0.407$ nm.)

**1.54** Find the indices of planes and directions in the HCP crystal structure.

**Figure Ex 1.54**

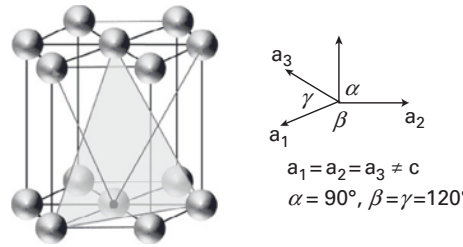


**1.55** How many major types of composite materials are there? What is the main component of composite materials?

**1.56** Draw three types of composite material.

**1.57** It is known that FCC and HCP possess relatively high APFs (atomic packing factors). Determine (a) the stacking pattern of FCC, HCP and BCC, (b) the closest packing plane of the FCC and BCC structures.

**1.58** Explain the difference between homopolymer, copolymer and block polymer by drawing them.

**1.59** Dental implant surgery is a procedure to replace the tooth roots with man-made materials. After the surgery, the artificial teeth will function as real ones. Stainless steel used to be the primary choice for implants. However, titanium is chosen over stainless steel nowadays. What is the advantage of titanium over stainless steel in this case?

**1.60** A continuous and aligned glass-fiber-reinforced composite consists of 25 vol% glass fibers with an elastic modulus of 80 GPa and 75 vol% of a polymer with an elastic modulus of 4.2 GPa.

**(a)** Compute the elastic modulus of this material in the longitudinal direction.

**(b)** If the cross-sectional area is 300 $mm^2$ and a stress of 40 MPa is applied along longitudinal direction, determine the load on the reinforcement and matrix phases respectively.

**(c)** What is the displacement and strain of the matrix and reinforcement phases under these conditions?

**1.61** Given that the lattice parameter of Ti is $a = 0.2950$nm and $c/a = 1.588$, determine the atomic packing factor and density of Ti. (The atomic weight of Ti is 48 g $mol^{-1}$ and the radius of a Ti atom is 147 pm.)

# Chapter 2 Elasticity and Viscoelasticity

## 2.1 Introduction

Elasticity deals with elastic stresses and strains, their relationship, and the external forces that cause them. An *elastic strain* is defined as a strain that disappears instantaneously once the forces that cause it are removed. The theory of elasticity for Hookean solids in which stress is proportional to strain is rather complex in its more rigorous treatment. However, it is essential to the understanding of micro- and macromechanical problems. Examples of the former are stress fields around dislocations, incompatibilities of stresses at the interface between grains, and dislocation interactions in work hardening; examples of the latter are the stresses developed in drawing and rolling wire, and the analysis of specimen machine interactions interesting for tensile strength. This chapter is structured in such a way as to satisfy the needs of both the undergraduate and the graduate student. A simplified treatment of elasticity is presented, in a manner so as to treat problems in an undergraduate course. Stresses and strains are calculated for a few simplified cases; the tridimensional treatment is kept at a minimum. A graphical method for the solution of two-dimensional stress problems (the Mohr circle) is described. On the other hand, the graduate student needs more powerful tools to handle problems that are somewhat more involved. In most cases, the stress and strain systems in tridimensional bodies can be better treated as tensors, with the indicial notation. Once this tensor approach is understood, the student will have acquired a very helpful visualization of stresses and strains as tridimensional entities. Important problems whose solutions require this kind of treatment involve stresses around dislocations, interactions between dislocations and solute atoms, fracture mechanics, plastic waves in solids, stress concentrations caused by precipitates, the anisotropy of individual grains and the stress state in a composite material.

## 2.2 Longitudinal Stress and Strain

Figure 2.1 shows a cylindrical specimen being stressed in a machine that tests materials for tensile strength. The upper part of the specimen is screwed to the crosshead of the machine. The coupled rotation of the two lateral screws causes the crosshead to move.

# Chapter 16 Environmental Effects

## 16.1 Introduction

Environment by its omnipresence, except perhaps in space, affects the behavior of all materials. Such effects can range from swelling in polymers to surface oxidation of metals and nonoxide ceramics to catastrophic failure of some materials under a combined action of stress and environment. Environmental degradation of materials is often referred to as corrosion. Such damage is generally time-dependent, i.e., one is able to predict it. Over time, however, environmental damage can become critical. There is, however, a more insidious corrosion problem which is time-independent. Examples of time-independent corrosion include stress corrosion cracking (SCC), environment-induced embrittlement, etc. Such damage can occur at any time, without much warning. There are many examples of such failures resulting in human and economic loss. Corrosion of structural components in aging aircraft is a serious problem. Just to cite one such example, a Boeing 737 belonging to Aloha Airlines, which flew interisland in Hawaii, lost a large portion of its upper fuselage at 7,500 m (24,000 feet) in the air. It turned out that the fuselage panels joined by rivets had corroded, which resulted in mid-flight failure due to corrosion fatigue.

All materials (metals, ceramics, and polymers) show phenomena of premature failure or mechanical property degradation under certain combinations of stress and environment. We describe below the salient points in regard to environmental effects in different materials. We emphasize the role that the microstructure of a given material plays in this phenomenon, especially in environmentally assisted fracture.

## 16.2 Electrochemical Nature of Corrosion in Metals

Corrosion in metals, i.e., attack by an aggressive environment, is essentially electrochemical in nature. Fundamentally, there are two electrochemical reactions involved in the corrosion of a metal: oxidation and reduction. The reaction at a less noble metal is called oxidation or an anodic reaction (electrons are released in

this reaction). In this case, the metal is the anode and it is oxidized to an ion. We can write the reaction as:

$$\mathrm{M} \rightarrow \mathrm{M}^{n+} + n\mathrm{e}^{-}.$$

At a more noble metal, one or more reduction or cathodic reactions, depending on the environment, can occur. Electrons are consumed in a cathodic reaction as per the following reaction:

$$\mathrm{M}^{n+} + n\mathrm{e}^{-} \rightarrow \mathrm{M}.$$

Both these reactions occur simultaneously and at the same rate. If that were not so, there would occur a charge buildup in the metal.

One can classify the corrosion of metals in the following categories.

### 16.2.1 Galvanic Corrosion

Consider two different metals, say iron and copper, in electrical contact and exposed to an environment (i.e., an electrolyte such as water). The two dissimilar metals are said to form a *galvanic* cell. Metals and alloys can be conveniently ranked in terms of their relative reactivities to each other in an environment. Such a ranking is called the galvanic series.

Table 16.1 lists some metals and alloys in a seawater environment. The metal that is less noble will corrode at the junction while the more noble one will be protected. In the example, iron will corrode when it forms a galvanic cell with copper. The reader should note that the less noble metal is sacrificed.

**Table 16.1 Galvanic series of some metals, alloys, and other materials (in seawater)**

| | |
|---|---|
| Pt | ↑Cathodic |
| Au | |
| Graphite | |
| Ti | |
| Stainless steel (passivated) | |
| Cu-Ni alloys | |
| Bronze (Cu-Sn alloys) | |
| Cu | |
| Sn | |
| Pb | |
| Pb-Sn solders | |
| Stainless steel (activated) | |
| Cast Iron | |
| Steel | |
| Al alloys | |
| Al | |
| Zn | |
| Mg | ↓Anodic |

Examples of such galvanic corrosion include steel screws suffering corrosion when in contact with brass in a marine environment. For example, if we have copper and steel in a water heater, they will form a galvanic couple, and the steel will corrode. It should be pointed out that the rate of the corrosion is proportional to the ratio of the surface areas of the more and less noble metals. Because the currents of the more and less noble metal must be equal, if the less noble metal has a smaller surface area it will corrode very rapidly.

As a practical matter, we list some general recommendations to reduce galvanic corrosion:

- If dissimilar metals must be coupled, choose metals with similar activities.
- Avoid a small anode area.
- Electrically insulate the two metals.
- Use cathodic protection. This involves the use of a third metal that may be deliberately sacrificed. The least noble metal can be used as a sacrificial node to protect pipelines, ships, tanks, etc.

Stainless steels (Fe+Ni+12% or more Cr) owe their corrosion resistance to a protective layer of chromium oxide. Such a coating protects the underlying metal from further corrosion.

### 16.2.2 Uniform Corrosion

This type of corrosion occurs uniformly over the entire surface. Uniform corrosion is the least objectionable corrosion form because it is easy to predict. Examples of uniform corrosion include rusting of steel and tarnishing of silver. When iron is exposed to moist air, it corrodes. This is generally referred to as "rusting." The following chemical reactions are involved in rusting:

$$\mathrm{Fe} + 1/2\mathrm{O_2} + \mathrm{H_2O} \rightarrow \mathrm{Fe(OH)_2},$$

$$2\mathrm{Fe(OH)_2} + 1/2\mathrm{O_2} + \mathrm{H_2O} \rightarrow 2\mathrm{Fe(OH)_3}.$$

The rust consists of $\mathrm{Fe(OH)_3}$, a hydrated oxide, which is cathodic in nature and insoluble in water.

### 16.2.3 Crevice Corrosion

Initially metal corrodes uniformly. However, if there are holes on the surface for any reason, then solution in holes is stagnant so the oxygen concentration in the crevice solution is reduced by the following reactions:

$$\mathrm{O_2} + 4\mathrm{H^+} + 4\mathrm{e^-} \rightarrow 2\mathrm{H_2O},$$

for an acidic solution containing dissolved oxygen and

$$\mathrm{O_2} + 2\mathrm{H_2O} + 4\mathrm{e^-} \rightarrow 4(\mathrm{OH})^-,$$

for neutral or basic solutions with dissolved oxygen.

This generates a potential difference between crevice and noncrevice regions, also called oxygen-concentration cells. The metal in contact with the most concentrated solution is the cathode and the metal in contact with the dilute solution (in the crevice) is the anode. The crevice (crack, depression, or a dent), where the oxygen concentration is relatively low, will corrode preferentially.

To reduce crevice corrosion, one should:

- Avoid crevices in design, for example use welds rather than rivets.
- Flush crevices regularly.

### 16.2.4 Pitting Corrosion

This is another form of localized corrosion that involves the formation of small pits on the surface of a metal. Pits are likely to start at structural and/or compositional heterogeneities.

### 16.2.5 Intergranular Corrosion

This type of corrosion, as suggested by the name, occurs along the grain boundaries. Generally, grain boundaries are energetically more active (i.e., anodic) than the grain interior. Recall that grain boundaries are regions of atomic disorder. Hence when exposed to an electrolyte the anodic grain boundaries dissolve preferentially and form a groove. A well-known example of this is the phenomenon of *sensitization* in austenitic stainless steels. If austenitic stainless steels are heated to 500–800 °C for a long enough period, chromium carbide, $Cr_{23}C_6$, precipitates along the grain boundaries. This leaves the areas adjacent to the grain boundaries depleted in chromium. One needs at least 12% chromium for the stainless steel to be corrosion resistant. If the chromium content in regions adjacent to the boundary falls below 12%, it will corrode preferentially. Some high-strength aluminum alloys also show intergranular corrosion.

### 16.2.6 Selective Leaching

In this case, one element in an alloy dissolves preferentially. For example, zinc can leach out preferentially in a Cu-Zn brass.

### 16.2.7 Erosion-Corrosion

This type of corrosion involves a combination of chemical attack and mechanical abrasion, which is worse than either alone.

### 16.2.8 Radiation Damage

Damage can occur in metals when they are bombarded with energetic particles such as neutrons. Such damage includes formation of point defects, voids, and compositional

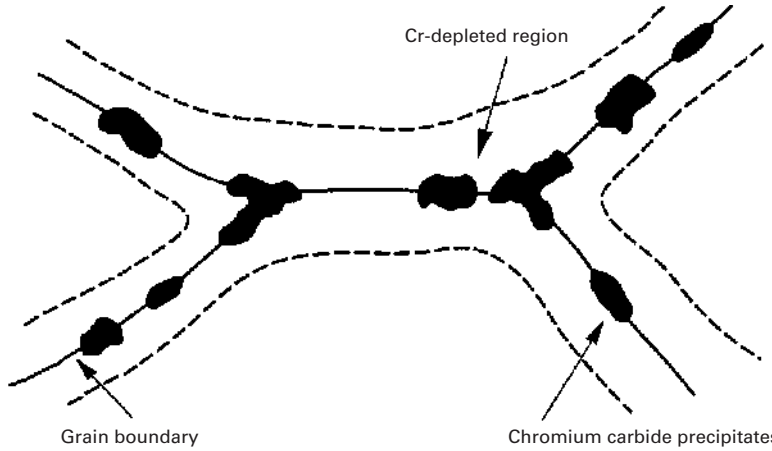


**Figure 16.1** Sensitization of austenitic stainless steel. When austenitic stainless steels are heated to 500–800 °C for a long enough period, chromium carbide, $Cr_{23}C_6$, precipitates along grain boundaries, leaving the areas adjacent to the grain boundaries depleted in chromium and prone to corrosion.

and/or microstructural changes. We discussed this topic in Section 4.3.4. Suffice to reiterate here that among the property changes to which radiation damage can lead are: swelling, because of void formation, embrittlement, because of the generation of defects, and accelerated creep because of the formation of voids and bubbles.

### 16.2.9 Stress Corrosion

This type of degradation of a metal involves the combined action of stress and a specific corrosive medium. Failure occurs at stresses and corrosion levels where typically it would not occur alone. Residual stresses can also cause stress corrosion cracking. We describe the phenomenon of stress corrosion cracking in Section 16.3 in some detail because of its importance.

## 16.3 Oxidation of Metals

The transformation of a metal into an oxide is accompanied by a reduction in energy, i.e., generally there is a thermodynamic driving force for a metal to convert to what might be called its natural state. The natural state of metals (i.e., as they are found in nature) is one of compounds such as oxides, hydroxides, carbonates, silicates, sulfides, sulfates, etc. There are, of course, exceptions such as gold and platinum, which are called noble metals! Oxidation is sometimes referred to as dry corrosion. We can represent oxidation as a chemical reaction in the following manner:

$$n\mathrm{M}_{(\mathrm{s})} + p\mathrm{O}_{2(g)} \rightarrow \mathrm{M}_n\mathrm{O}_{2p(\mathrm{s\ or\ g})}, (\mathrm{s\ or\ g})$$

where M represents a metal such as aluminum or a metalloid such as silicon.

Steel, which in its simplest form is an alloy of iron and carbon, can be decarburized in an oxygen environment as per the following reaction:

$$2\text{C (in steel)} + \text{O}_{2(\text{g})} \rightarrow 2\text{CO}_{(\text{g})}.$$

Some normally active metals become passive, i.e., lose their chemical reactivity and become inert by the formation of a highly adherent, thin oxide film on the surface that protects the metal from further corrosion. This phenomenon is called *passivity*. Examples of metals that passivate include Cr, Ni, Ti, and Al. It is the chromium oxide film on the surface of stainless steel that makes the steel *stainless*, i.e., corrosion resistant. Similarly, aluminum oxide on aluminum provides a protective film. The important factor is whether the oxide scale that forms on the surface is protective or not? This feature can determined by a parameter called the Pilling–Bedworth ratio:

$$\text{Pilling–Bedworth ratio} = A_{\text{o}}\rho_{\text{o}}/A_{\text{m}}\rho_{\text{m}},$$

where $A_{\text{o}}$ is the atomic weight of the oxide, $\rho_{\text{o}}$ is the density of the oxide, $A_{\text{m}}$ is the atomic weight of the metal, and $\rho_{\text{m}}$ is the density of the metal.

- For a protective oxide, the Pilling–Bedworth ratio is approximately 1.
- For a porous oxide, the Pilling–Bedworth ratio is less than 1.
- For a flaking oxide, the Pilling–Bedworth ratio is around 2 to 3.

Thermal mismatch between a metal and its oxide, as represented by the difference in their coefficients of thermal expansion $(\alpha_{\text{oxide}} - \alpha_{\text{metal}})$, is another important parameter.

If $\alpha_{\text{oxide}} > \alpha_{\text{metal}}$, the oxide will contract more than the underlying metal on cooling, putting the oxide layer in tension, which may crack. If $\alpha_{\text{metal}} > \alpha_{\text{oxide}}$, the metal substrate will contract more than the oxide on cooling, putting the oxide in compression, which may cause cracking or buckling of the oxide and possible delamination.

If a continuous and adherent oxide film forms on the surface of a material in sufficient quantity to cover the surface, it may be used to protect the underlying material against further oxidation.

## 16.4 Environmentally Assisted Fracture in Metals

Environmentally assisted fracture in metals can be classified under the following subheadings:

- Stress corrosion cracking.
- Hydrogen damage.
- Liquid and solid metal embrittlement.

### 16.4.1 Stress Corrosion Cracking (SCC)

Generally, SCC is initiated by a rupture of the protective oxide film on the metal. This film rupture may occur because of a mechanical action or a chemical action of

**Table 16.2 Some important alloy–environment combinations for SCC**

| Alloys | Environments |
|---|---|
| Copper alloys | Ammonia, sulfur dioxide, oxygen |
| Austenitic stainless steels, Al alloys, Ti alloys, high-strength steels | Chlorides and moisture |
| Low-carbon steels | Hydrogen sulfide |
| Carbon steels | CO or $CO_2$ and moisture |
| Copper alloys | Oxides of nitrogen |

some species. Possible initiation sites of SCC include microscopic inhomogeneities such as local differences in chemical composition, amount of the corrosive species, and/or thickness of the protective film, and any stress concentration sites such as a preexisting gouge mark on the surface. Corrosion pits form at the rupture sites and cracking starts at the root of the pit. Electrochemical action maintains the sharpness of the crack tip, with corrosion continuing at the tip of a propagating crack. Bare metal under the protective film or passivated layer is exposed by the slip (i.e., plastic deformation) occurring at the crack tip. The new metal surface that is exposed becomes anodic with respect to adjacent areas, which act catholically. The corroding metal gets passivated again and the process of crack growth is repeated. The crack thus propagates in a stepwise manner in a transgranular or intergranular mode depending on the metal and environmental conditions. Characteristically, SCC shows branching, with the main crack growing in a direction perpendicular to the major tensile stress component and a low ductility.

As mentioned above, SCC occurs under the combined action of a tensile stress (applied or residual) and an aggressive environment. However, a specific metal–environment combination is required for SCC to occur. Examples include aluminum-alloys–seawater, brass–ammonia, austenitic-stainless-steel–seawater, titanium–liquid-nitrogen-tetroxide ($N_2O_4$), etc. Table 16.2 summarizes some of the important metal–environment combinations.

The treatment of SCC in terms of linear elastic fracture mechanics (LEFM) analysis involves the use of the crack-tip stress intensity factor as the dominant parameter controlling the crack growth under SCC conditions. Under a specific combination of a material and an aggressive environment, cracks can grow under a constant stress intensity factor $K$ less than $K_{Ic}$, the fracture toughness. We then define $K_{Ic}$ as the threshold stress intensity value below which the crack propagation rate is negligible. One should add here the same warning in regard to the applicability of linear fracture mechanics concepts as in the case of ordinary fracture in the absence of an aggressive environment; that is, the size of the plastic zone at the crack tip must be small compared to the specimen dimensions for the application of LEFM to be valid. Crack growth velocity varies with the stress intensity factor, $K$. A schematic plot of log $da/dt$ versus applied stress intensity is shown in Figure 16.2. There are three regions in this curve:

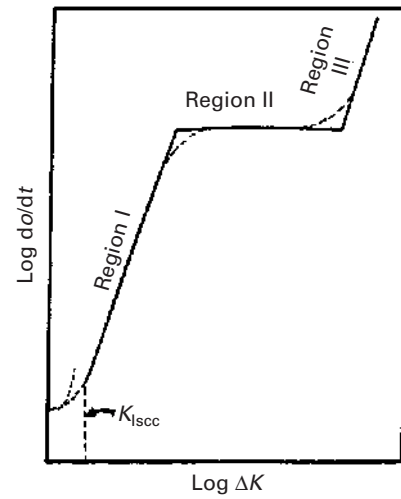


**Figure 16.2** Crack growth rate as a function of the stress intensity factor under conditions of SCC.

*Region I*: In this region the crack velocity depends on the stress intensity factor. The threshold stress intensity $K_{Iscc}$, below which crack growth does not occur, is shown by a dashed line. Quite frequently, a true $K_{Iscc}$ does not exist. In such a case, we can define an operational $K_{Iscc}$ as that corresponding to a crack growth rate of $10^{-9}$ or $10^{-10}$ m $s^{-1}$. Such an arbitrary value can be used to rate different alloys.

*Region II*: The crack velocity in this region is independent of the stress intensity factor. The value at which this plateau region occurs is very specific to the metal–environment combination and test conditions such as temperature.

*Region III*: In this region the crack velocity becomes very fast as the crack-tip stress intensity factor approaches $K_{Ic}$. In this region, the crack velocity is mainly controlled by the stress intensity.

Figure 16.3 shows actual plots of log crack velocity versus stress intensity factor for aluminum 7079 alloy in a potassium iodide solution at different temperatures.[1] Only data from regions I and II are shown in this figure. As the temperature increases, the curves shift upward, i.e., for a given stress intensity, the crack velocity increases with temperature. It should be clear to the reader that a knowledge of the full crack velocity versus stress intensity factor curve for a specific alloy in a specific environment will provide a better evaluation of the SCC resistance of the alloy in that particular environment. Similar three-region curves may be obtained under conditions of hydrogen damage and liquid-metal embrittlement.

## Effect of Material Variables on SCC

In general, high-purity metals are less prone to SCC than alloys or impure metals. In particular, trace amounts of interstitial elements can have a very large effect.

[1] M. O. Speidel, *Met. Trans.*, 6A (1975) 631.

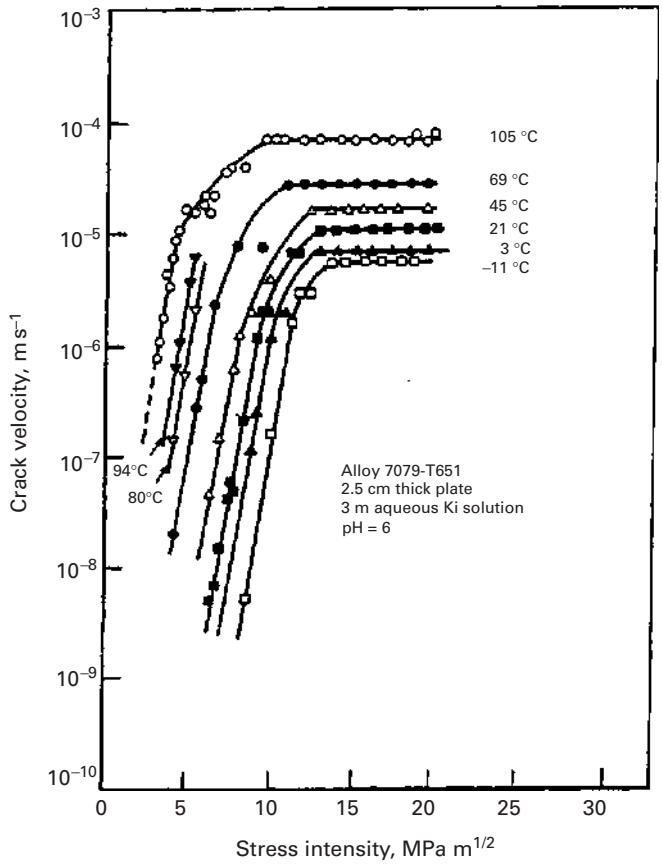


**Figure 16.3** Log crack velocity versus stress intensity factor for two aluminum alloys in a potassium iodide solution. Region III is not shown. (Adapted by permission from Springer Nature, *Metallurgical Transactions, A, Physical Metallurgy and Materials Science*, Stress corrosion cracking of aluminum alloys, Markus O. Speidel, Copyright (1975).)

For example, nitrogen in excess of 500 ppm in austenitic stainless steel in chloride environments can be disastrous. The cracking in austenitic stainless steels is mainly transgranular, indicating that the effect of nitrogen must either be on the process of slip or the stability of the protective film. The grain size of the metal can also have a profound effect on its resistance to SCC. A smaller grain size is more resistant to SCC than a coarse one. Elongated grain structure commonly obtained in wrought aluminum alloys can cause markedly anisotropic SCC behavior. For example, a sheet or plate of Al 7075-T6 shows high resistance against SCC when stressed in the rolling or long transverse direction, but rather poor resistance against SCC in the plate thickness direction. The 7075-T7 temper, which has a lower strength than the T6 temper, can improve resistance against SCC in the through thickness direction. Generally, the aging treatment in aluminum alloys results in increasing their resistance against SCC. The 7XXX series of aluminum alloys (Al-Zn-Mg) show the best resistance against SCC when they are aged beyond the peak hardness, i.e., in the overaged condition.

Aluminum-lithium alloys are now used in the aerospace industry because of their enhanced modulus and low density (see Chapter 10). Generally, ternary or quaternary alloys are used. In particular, Al-Li-Cu-Zr alloys show quite an attractive

combination of properties. It has been observed that the (Li/Cu) ratio can have significant effect on the precipitation sequence and consequently the resultant mechanical properties. The (Li/Cu) ratio also affects the stress corrosion resistance of the alloy. It would appear that the reduction in $K_{Iscc}$ is partly due to the loss of toughness of these alloys with increasing (Li/Cu). Low-Li alloys show transgranular cracking and crack branching while high-Li alloys show intergranular cracking.

An excellent example of SCC is the drastic effect of NaCl in water has on the tensile strength of aluminum alloys. Figure 16.4 shows how the tensile strength in a

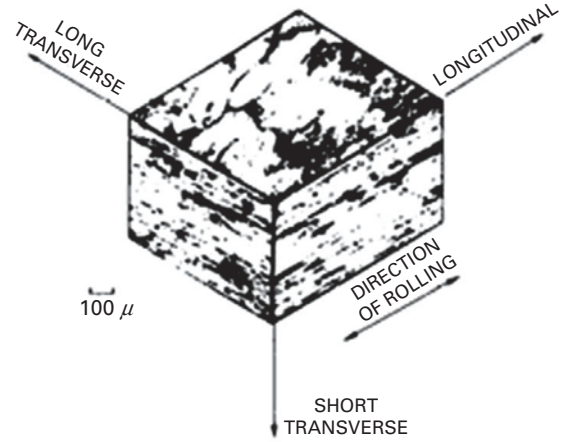


DIRECTIONAL GRAIN STRUCTURE OF 7075-T651 HOT ROLLED PLATE

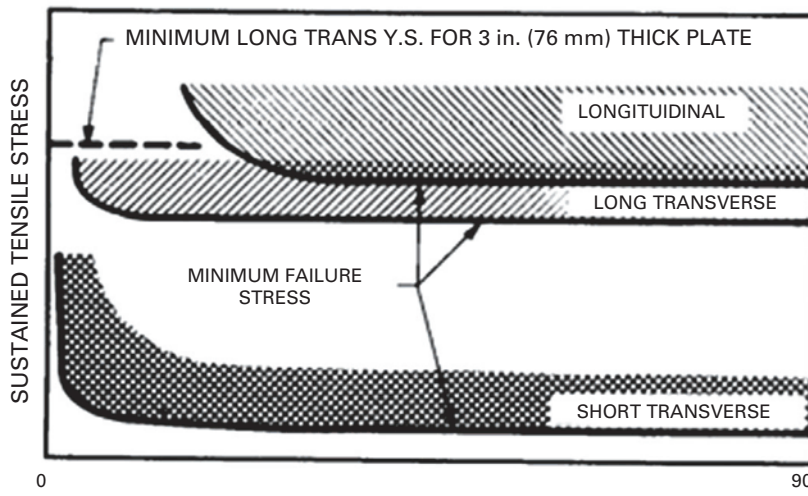


**Figure 16.4** Effect of exposure to a 35% saline solution in water on the tensile strength (in three orientations) of 7075-T651 Al.

(Reprinted from Engineering Fracture Mechanics, Vol. 12, R.J. Bucci, Selecting aluminum alloys to resist failure by fracture mechanisms, 407–441, Copyright (1979), with permission from Elsevier.)

7075 aluminum alloy hot-rolled plate with T651 temper decreases with exposure time in 35% NaCl. Three orientations, marked in the 3D micrograph, are shown. The tensile strength is highest in the longitudinal and long transverse direction and lower in the short transverse direction. The abscissa of the plot reaches 90 days. The short transverse direction is not usually subjected to tension in thin sheets, but thicker sections (extrusions, forgings) might be loaded in tension and this produces a drastic reduction in strength.

### 16.4.2 Hydrogen Damage in Metals

The presence of hydrogen in a material can cause serious damage to its performance. In addition to its great technological importance, the phenomenon of hydrogen damage has been a challenging basic research problem. One main reason for the damage caused by hydrogen in metals and alloys is the extremely small size of the hydrogen atom, which allows it to move very fast within the metallic lattice. It is therefore not surprising that over the years a considerable research effort has gone into obtaining an understanding of the phenomenon, especially in metals and alloys. We provide below a short account of the hydrogen effects in various metals and alloys.

Some of the common sources of hydrogen in metals, as well as some simple and straightforward remedies for the problem are as follows. Metals may absorb hydrogen during processing or service. For example, during melting and casting of metals, the hot metal can react with the raw materials or humidity in the air to form an oxide and hydrogen. The latter can be absorbed by the hot metal. This problem of hydrogen absorption by the liquid metal can be reduced by vacuum degassing processing. Atmospheric humidity can be a source of hydrogen in the arc welding of steels, while the electrode itself may absorb hydrogen during casting. Frequently, during some steps in the processing of a metal into a useful article, a chemical or electrochemical treatment is given. Nascent hydrogen is released due to reaction of metal with acid during such a treatment. Most of it combines to form molecular hydrogen, while the remainder will diffuse into the metal. Certain metals such as titanium, zirconium, etc. dissolve rather large quantities of hydrogen exothermally and form very brittle hydrides.

Quite frequently, in order to improve the corrosion resistance and/or for decorative purposes, electropolishing or plating of materials is carried out. Such finishing processes represent another important source of hydrogen entry into the base metal. In these finishing processes, hydrogen, together with the electroplated species, is deposited at the cathode. In such cases, it is thought by some that baking out at moderate temperatures after plating may help remove hydrogen. Others hold the view that the protective coating serves as a barrier to hydrogen removal during bakeout.

Aqueous corrosion is another common source of hydrogen for metals in service. Metals react with water to form oxides (or hydroxides) and atomic hydrogen, which is easily absorbed by the metal. In pressurized water nuclear reactors (PWR), water

used for heat transfer can be an important source of hydrogen. Hydrogen embrittlement of zirconium alloy fuel cladding or of the pressure vessel itself can be a serious problem.

In the chemical and petrochemical industries, containers of chemicals (used for storage or as reaction chambers) can absorb hydrogen over the period of use. Natural gas containing $H_2S$, called sour gas, can cause hydrogen-induced cracking (HIC) in the pipeline steel. The sulfide ion especially is a problem species because it acts as a "surface poison," retarding the recombination of atomic hydrogen to form molecular hydrogen at the surface, leading to absorption of atomic hydrogen.

## Theories of Hydrogen Damage

No single model or theory is capable of explaining all the effects associated with the presence of hydrogen in different materials. However, almost all theories recognize that one of the most important attributes of hydrogen is that it diffuses very rapidly in almost any material. For example, in steels, hydrogen diffuses at about 10μm per second at room temperature. This fast diffusion characteristic of hydrogen stems partly from its extremely small size; hydrogen has the smallest atomic diameter of all the elements. In general, hydrogen tends to collect at defect sites in any material where it can produce high internal pressure, which can lead to cracking. There are certain special aspects of hydrogen behavior in steels. Hydrogen has a very high mobility in the BCC lattice of Fe at ambient temperature. The comparative values of the diffusivity of hydrogen and nitrogen in the iron lattice at room temperature given below give a good idea of the extraordinarily high mobility of the hydrogen atom[2,3]:

$$D_{\mathrm{H}} \text{ in Fe} \sim 10^{-2}\ \mathrm{m^2\ s^{-1}} \text{ at } 300\ \mathrm{K},$$
$$D_{\mathrm{N}} \text{ in Fe} \sim 10^{-12}\ \mathrm{m^2\ s^{-1}} \text{ at } 300\ \mathrm{K}.$$

One can write for the local concentration of hydrogen in the BCC iron lattice as[4]:

$$\ln \frac{C_{\mathrm{H}}}{C_0} = \frac{\Omega \sigma_{\mathrm{p}}}{RT},$$

where $C_{\mathrm{H}}$ is the local hydrogen concentration, $C_0$ is the equilibrium hydrogen concentration in the unstressed lattice, $\Omega$ is the molar volume of hydrogen in iron, and $\sigma_{\mathrm{p}}$ the hydrostatic stress $(= (\sigma_1 + \sigma_2 + \sigma_3)/3)$. Thus, in any nonuniformly stressed solid, there is a driving force for solute migration, which is a function of the solute atomic volume and the gradient in the hydrostatic tension.

Figure 16.5 shows schematically the transport processes at a crack tip that eventually lead to the embrittlement reaction between hydrogen and the metal, in

[2] C. A. Wert, *Phys. Rev.*, 79 (1959) 601.
[3] R. A. Oriani, in *Fundamental Aspects of Stress Corrosion Cracking*, Houston, TX: NACE, 1969, p. 32.
[4] J. C. M. Li, R. A. Oriani, and L. W. Darken, *Z. Phys. Chem.* 49 (1966) 271.

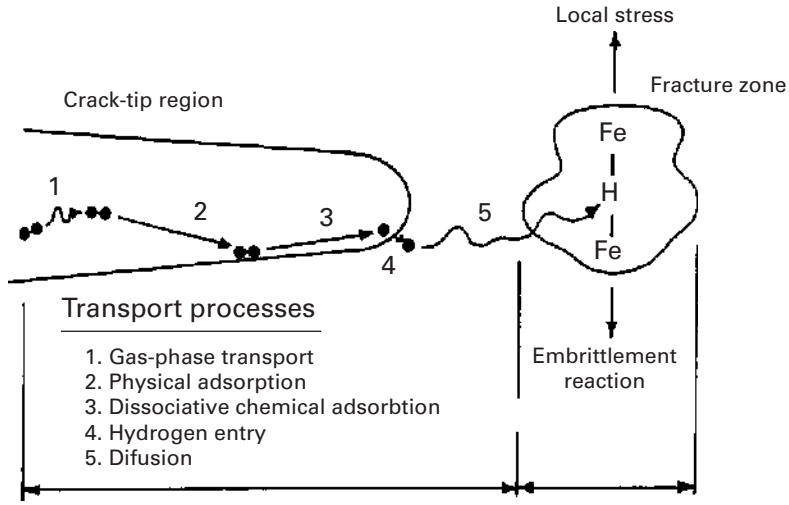


**Figure 16.5** Schematic of the hydrogen transport processes at a crack tip in Fe and the embrittlement reaction. (Adapted by permission from Springer Nature, *Metallurgical Transactions, A, Physical Metallurgy and Materials Science*, Gaseous hydrogen embrittlement of high strength steels, R. P. Gangloff and R. P. Wei, Copyright (1977).)

this case iron.[5] This hydrogen transport process can be divided into the following steps:

- Diffusion of hydrogen to the surface.
- Adsorption on the surface.
- Dissociation in the surface adsorption layer.
- Penetration through the surface.
- Diffusion into the bulk of the metal.

Having given this very general picture of the effects of hydrogen in metals, we review briefly some of the specific theories that have been advanced to explain the phenomenon of hydrogen damage.

## Lattice Decohesion

Hydrogen-induced lattice decohesion can occur as originally proposed by Toriano.[6] Hydrogen diffuses into the triaxial tensile stress region at a crack tip, causing a localized reduction of the lattice cohesive strength. The concept is quite valid in very general terms. The exact mechanisms involved are, however, not clear.

## Pressure Theory

Hydrogen atoms combine and precipitate as molecular hydrogen and cause internal pressure. When this internal pressure exceeds a critical value, HIC occurs. Because of the extremely high mobility of hydrogen in most lattices, segregation of absorbed hydrogen to regions of high expansion in the lattice, for example, internal voids and

[5] R. P. Gangloff and R. P. Wei, *Met. Trans.*, 8A (1977) 1043.
[6] A. R. Toriano, *Trans. ASM*, 52 (1960) 54.

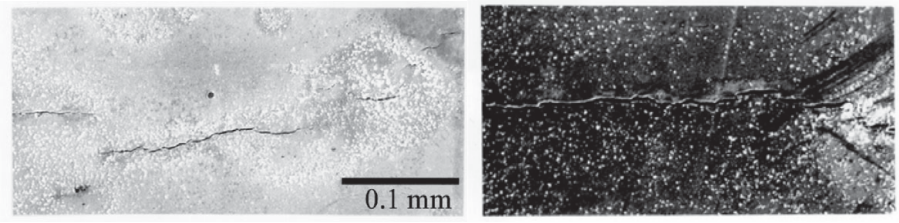


**Figure 16.6** Stepwise cracking in a microalloyed steel after 24 h cathodic charging.
(Reprinted by permission from Springer Nature, *Journal of Materials Science* (full set), Hydrogen-induced cracking in two linepipe steels, K. K. Chawla, J. M. Rigsbee, and J. D. Woodhouse, Copyright (1969).)

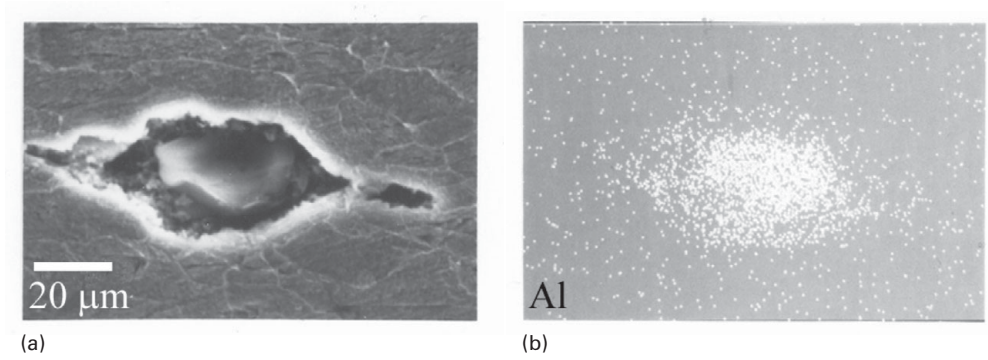


**Figure 16.7** An aluminum-based inclusion in the interior of a void produced by hydrogen charging.
(Reprinted by permission from Springer Nature, *Journal of Materials Science* (full set), Hydrogen-induced cracking in two linepipe steels, K. K. Chawla, J. M. Rigsbee, and J. D. Woodhouse, Copyright (1969.)

cracks, occurs easily. Large internal pressure would enhance void growth and crack propagation. A good example of this phenomenon is the blister formation in steels on cathodic charging. One would expect such cracking to vary with inclusion distribution.

Figure 16.6 shows such hydrogen induced cracking in a microalloyed steel sample.[7] This extensive stepwise cracking resulted after cathodic charging for 24 hours. Such cracking or voiding is frequently associated with the presence of inclusions.

Figure 16.7 shows an aluminum-based inclusion (possibly alumina) in the interior of a void produced by hydrogen charging.[8] The micrograph on the right in Figure 16.7 shows the mapping of aluminum, indicating an aluminum-based inclusion.

The solubility of hydrogen is greatly influenced by the presence of lattice defects and impurities. For example, the solubility of hydrogen in a commercial steel at room temperature can be as much as 100% greater than that in a clean and well-annealed steel. Thus, although the solubility of hydrogen in iron is small, a large amount of it can be trapped rather easily at various defect sites.

[7] K. K. Chawla, J. M. Rigsbee, and J. D. Woodhouse, *J. Mater. Sci.*, 21 (1986) 3777.

Gas or oil containing $H_2S$ can lead to sulfide stress corrosion cracking or hydrogeninduced blistering in steel.[8,9] This form of HIC, also called *blistering*, is presumed to occur when hydrogen atoms generated in a wet, sour gas environment enter into the steel and precipitate at or around inclusions or other unfavourable microstructural sites. In this regard, manganese sulfide inclusions, elongated in the rolling direction, are perhaps the worst culprits. Hydrogen atoms, generated at the surface, penetrate and diffuse into the steel. These atoms are trapped at matrix–inclusion interfaces and at ferrite–(pearlite+bainite+ martensite-austenite) interfaces.[8] Here it is appropriate to point out an important microstructural feature of in-rolled low-carbon steels. It is tacitly assumed that the solute atoms in a solid solution are uniformly distributed in the matrix. More often than not, this is not the case. Interdendritic segregation of solutes starts during the freezing of alloys. Specifically, in Mn-C steels interdendritic segregation of Mn, followed by rolling, can result in pronounced banding. Pearlite layers in the microstructure coincide with Mn segregation. Such a microstructure consisting of alternate layers of ferrite and pearlite is very anisotropic and susceptible to hydrogen-induced cracking. In quenched and tempered steels, even high-Mn steels do not show such segregation; these steels have superior resistance to HIC.

## Surface Energy

According to this theory, hydrogen is adsorbed on the free surfaces of a crack and reduces the surface energy. This results in a decrease in the work of fracture as per the Griffith criterion. This theory, however, would not explain the reversible degradation attributed to hydrogen.

## Enhanced Plastic Flow

Beachem[10] proposed a hydrogen-assisted cracking model in which hydrogen enhances dislocation motion. The hydrogen diffuses in front of the crack tip, increases the mobility of dislocations there and causes, locally, enhanced plasticity.

Figure 16.8 shows this model schematically. In the absence of hydrogen, a ductile metal fractures by microvoid coalescence within a large plastic zone at the crack tip (see Chapter 8). In the presence of hydrogen, however, locally plastic deformation becomes easier and crack growth occurs by severely localized deformation at the crack tip. This model has been supported experimentally by the work of Tabata and Birnbaum.[11,12] They used an *in situ* deformation stage in an environmental cell of a

[8] D. D. J. Thomas and K. R. Doble, in *Steels for Linepipe and Pipeline Fittings*, London, U.K.: The Metals Society 1983, p. 22

[9] T. Taira and Kobayashi, in *Steels for Linepipe and Pipeline Fittings*, London, U.K.: The Metals Society, 1983, p. 170.

[10] C. D. Beachem, *Met. Trans.*, 3A (1972) 437.

[11] T. Tabata and H. K. Birnbaum, *Scripta. Met.*, 17 (1983) 947.

[12] T. Tabata and H.K. Birnbaum, *Scripta Met.*, 18 (1984) 231.

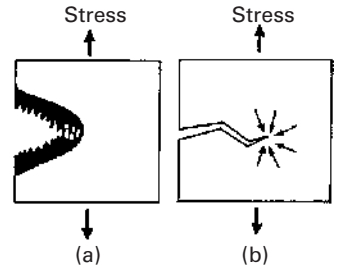


**Figure 16.8** Schematic of crack growth in a high-strength steel: (a) without hydrogen, crack growth occurs by microvoid coalescence within a large plastic zone at the crack tip, (b) with hydrogen, plastic deformation becomes easy and crack growth occurs by severely localized deformation at the crack tip.
(Reprinted by permission from Springer Nature, *Metallurgical and Materials Transactions B*, A new model for hydrogen-assisted cracking (hydrogen "embrittlement"), C. D. Beachem, Copyright (1972).)

high-voltage transmission electron microscope to investigate the effects of hydrogen on the behavior of dislocations in iron. It was observed that the introduction of hydrogen into the environmental cell increased the velocity of screw dislocations. This resulted in softening of the specimen in the early stages of deformation as the density of the mobile dislocations increased. In the later stages of deformation, this higher dislocation density may also contribute to work-hardening. These authors also studied the *in situ* fracture behavior of iron of different purities in the presence of hydrogen gas and observed that the presence of hydrogen enhanced fracture. The main conclusions of this work of are:

- Basic fracture mechanisms in iron in vacuum and in hydrogen atmosphere are the same, but the morphology of fracture is very different.
- Hydrogen-enhanced fracture is caused by the localization of plasticity and by the enhancement of dislocation motion and generation in the presence of hydrogen, as first suggested by Beachem.[11]

## Hydride Formation

Certain metals, such as Ti, Zr, V, Nb, Ta, Mg, Al, etc., could suffer hydrogen degradation by diffusion of hydrogen and reaction with the metal to form a hydride at the crack tip. The hydride phase, being brittle, cracks easily on continued loading. Crack arrest occurs when the crack tip reaches the matrix phase. A new hydride phase forms and the cycle is repeated, as shown schematically in Figure 16.9.[13] In pure iron, carbon and low-alloy steels, a hydride phase is not formed or is unstable. This is attributed to the extremely low solubility of hydrogen in iron and steels. Other no-hydride-forming systems include Mo, W, Cr, and their alloys.

[13] H. K. Birnbaum, in *Atomistics of Fracture*, New York, NY: Plenum, 1983, p. 733.

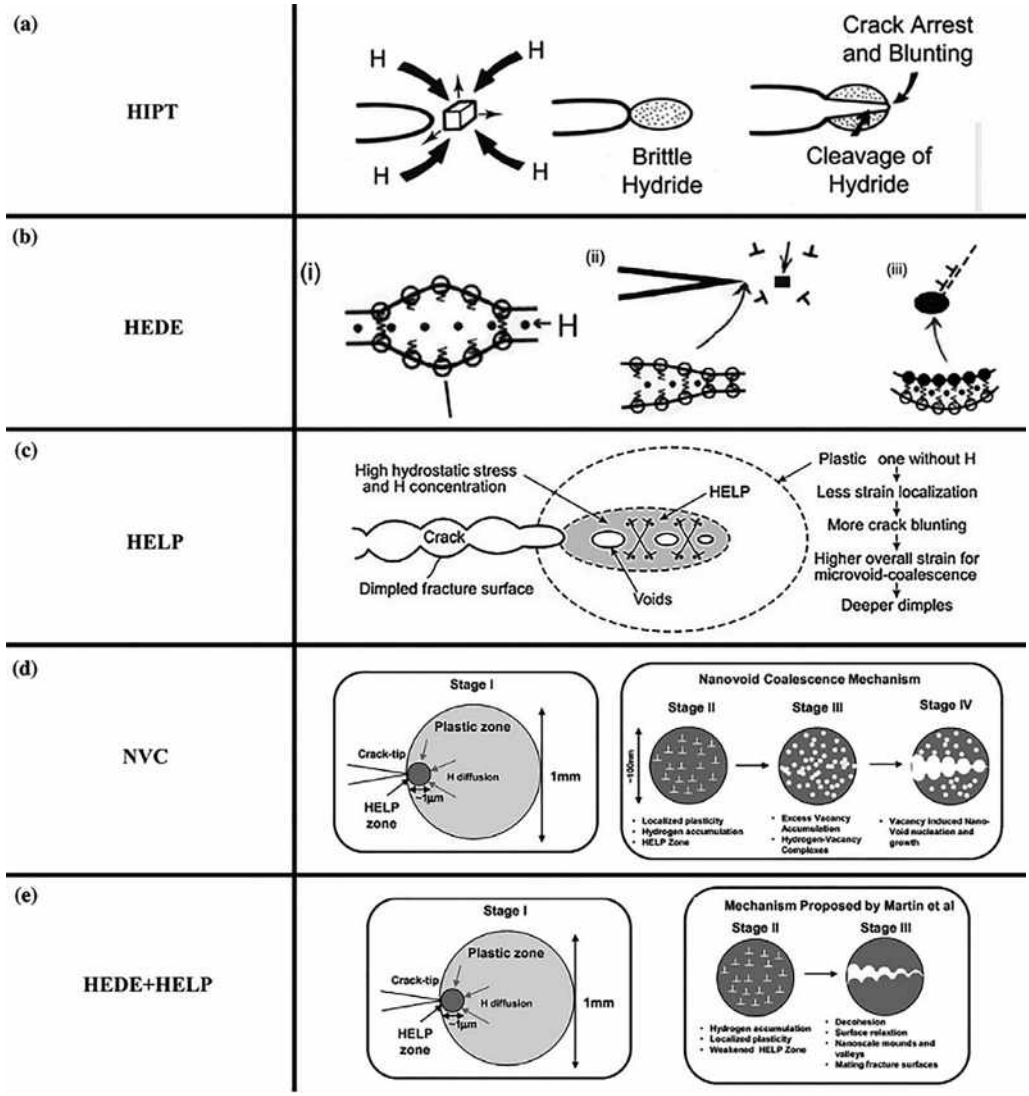


**Figure 16.9** Schematic diagrams of hydrogen embrittlement mechanisms.
(Li, X., Ma, X., Zhang, J., Akiyama, E., Wang, Y., and Song, X. (2020). Review of hydrogen embrittlement in metals: hydrogen diffusion, hydrogen characterization, Hydrogen embrittlement mechanism and prevention. *Acta Metallurgica Sinica* (English Letters), 1-15.)

## Alleviating the Hydrogen Damage

While it is very difficult to provide simple recipes for alleviating the hydrogen damage in all materials, we may list the following general guidelines as possible solutions:

- *Avoid entry of hydrogen.* This involves a control of the external environment, i.e., use of inhibitors or suitable alloying elements to protect the base metal surfaces against a hydrogen ion discharge reaction.

- *Improve the material resistance to hydrogen damage*. An effective way of doing this is to modify the morphology and/or decrease the number of inclusions. Lowering the sulfur content (maximum S about 0.010%) is a very important item in inclusion content control. Because the elongated inclusions such as MnS stringers in steel are highly susceptible to hydrogen damage, inclusion shape control through use of rare earth metals is of great help. Modifying the alloy composition is yet another way. For example, chromium as an alloying element is very beneficial in steels. The reasons for this effect may be varied. The addition of chromium decreases the solubility of hydrogen in steels, perhaps, because chromium alters the electrochemical conditions on the surface of steel, enhances the oxidation of sulfur, or depresses adsorption of atomic hydrogen.

### 16.4.3 Liquid and Solid Metal Embrittlement

Metals that fail in a ductile manner under normal conditions can fail in a very brittle fashion in the presence of certain active liquid or solid environments. This phenomenon has been variously referred to as *metal-induced embrittlement* (MIE), *solid metal embrittlement* (SME), and *liquid metal embrittlement* (LME). LME of brasses and bronzes by mercury is a well-known example. Gallium, which is a liquid at room temperature, causes a catastrophic failure in aluminum without any apparent diffusion. Carbon and low-alloy steels are embrittled by cadmium. Amorphous metals are generally known to show excellent corrosion resistance, primarily because of the absence of grain boundaries and other defect sites. It has been observed, however, that several iron-based amorphous alloys show LME in the presence of Hg, Hg-In, or $Sn_6Pb_4$.[14]

LME is different from SCC in that positively and negatively charged ions in aqueous solution interact with solid metal in SCC, while, apparently, no electrochemical dissolution is involved in LME. There are certain prerequisites for LME to occur. The metals involved do not form any stable intermetallic compounds. The liquid metal must wet the solid metal and the metals must not have mutual solubility.

Among the models proposed to explain the phenomenon of LME are: reduction in surface energy of the solid metal by the adsorbing liquid metal species and localized reduction of the strength of the atomic bonds at the crack tip by the embrittling species.[15,16] It would appear, however, that similar to the hydrogen effects in metals and alloys, different mechanisms seem to be responsible for LME under different conditions. For example, LME of many crystalline metals can be explained satisfactorily by enhanced shear or decohesion while solid

[14] S. Ashok, N. S. Stoloff, M. E. Glicksman, and T. Slayin, *Scripta Met*., 15 (1981) 331; N. S. Stoloff and T. L. Johnston, *Acta Met*., 11 (1963) 251.

[15] M. H. Kamdar, in *Advances in Strength and Fracture*, vol. l, Oxford, U.K.: Pergamon Press, 1977, p. 387.

[16] F. N. Kelly and F. Bueche, *J. Polymer Sci*., 50 (1961) 549.

metal-induced embrittlement is accomplished by grain boundary penetration by the embrittling species. LME of amorphous metals, on the other hand, involves enhanced shear.

Finally, it should be pointed out to the reader that although the phenomenon of LME is generally considered as something undesirable, it is possible to use liquid metals, such as Pb-Sn eutectics, to facilitate drilling steels, titanium alloys, and heat-resistant Ni-Cr alloys. Increased drilling tool life and a better quality of the machined surface are improvements. Such beneficial effects have been known in nonmetallic fields for quite some time. For example, in the drilling of quartz rock, addition of $AlCl_3$ to the water lubricant allows one to double the drilling speed without increasing the wear of the drilling bit.

## 16.5 Environmental Effects in Polymers

Polymers can undergo a variety of changes due to environment, some of which can lead to severe embrittlement. Although polymers generally show good chemical resistance to various acids and alkalis, certain organic liquids and gases can affect their performance markedly. In particular, the fracture process can suffer rather drastic changes in the presence of certain environments. An example of such environmentally assisted fracture in polymers is that of polycarbonate, which fails at a low stress in a solution of sodium hydroxide in ethanol. Essentially, a specific combination of environment and stress results in a premature breakdown of the long-chain polymeric structure. Although our main concern in this section is the environmental effects on the mechanical behavior of polymers, it is worth pointing out that there is great interest in producing biodegradable polymers. This concern, of course, stems from the unsightly discarded plastic trash, which can be injurious to plant and human life. Yet another related topic, but which we shall not discuss in the book, is that of biocompatibility and stability of polymers in the body's environment, tissue-fluid interaction, etc.

Exposure to oxygen, moisture (ambient or otherwise) or other solvents, and ultraviolet radiation can lead to static fatigue or reduction in strain-to-failure. Swelling and/or dissolution are some of the most common phenomena. A liquid or solute molecule can diffuse in a polymer and cause swelling, leading to dimensional changes. Also the liquid molecules push apart the chains so that secondary bonding is reduced and the polymer softens. The structural features responsible for such attack on polymers are the following:

- *Random chain scission:* The polymer breaks down at random points along the chain, with an attendant decrease in molecular weight and mechanical properties. The decrease in the molecular weight and/or changes in the molecular weight distribution, can lead to a deterioration of the mechanical properties.
- *Successive loss of monomer units:* This can occur at one extremity of the polymer chain and result in chain depolymerization. This is generally manifested in a gradual change in the molecular weight. Examples of such a phenomenon are

exposure to different kinds of radiation, oxygen, ozone, etc. Rubber in the presence of ozone is particularly susceptible to this form of environmentally assisted failure. The ozone reacts at the surface of rubber and cracks nucleate and grow at low stress levels.

We provide below a brief description of different environmental effects in polymers.

### 16.5.1 Chemical or Solvent Attack

Thermoplastics can be dissolved by various organic solvents (e.g., xylene). Generally, the higher the molecular weight $M_w$, the lower the solubility. For example, in a polymer having a distribution of various $M_w$ fractions, the low $M_w$ fractions can be dissolved and extracted by a solvent. Cross-linking of molecules, as in a thermoset, reduces solubility. Thus, a cross-linked epoxy is more resistant to chemicals than linear chain polymers such as polyethylene.

### 16.5.2 Swelling

Absorption of solvent molecules can be regarded as a form of solvent attack. Different polymers can absorb ambient moisture to different degrees. This phenomenon results in swelling of polymers and thus leads to dimensional changes. Such dimensional changes can be very important in polymers used as gaskets and seals. They also become important in polymer-matrix composites, for example carbon-fiber-reinforced polymer. Because the polymer matrix will absorb moisture while the carbon fiber will not, there will be internal stresses due to a differential in swelling. One can get an idea of the seriousness of this problem by the following observation of carbon-fiber-reinforced polyimide composite. Polyimide is a high-temperature polymer with a service temperature of 370 °C. However, retained moisture can result in a reduction of service temperature to 250 °C.

Generally, in monolithic polymers (i.e., not composites) swelling-induced changes are reversible, i.e., the polymer will revert to its original dimensions when the absorbed molecule is removed. Moisture acts as a plasticizer, i.e., moisture absorption results in an increase in the impact toughness of a polymer, while its strength decreases.

Swelling of a polymer can occur if a gas or a liquid permeates it. Typically, these swelling agents have small molecules and can easily penetrate the main polymeric network, where they reduce the cohesive force between the primary chains. Nylon, for example, can absorb moisture up to 1% of its weight, which can change its dimensions by about 1%. Moisture typically acts as a plasticizer, i.e., it lowers the glass transition temperature $T_g$ of the polymer, with the result that deformation, crazing, and cracking occur at lower stress and strain values. If a polymer is uniformly swollen because of the permeation of a liquid, it will behave as a homogeneous polymer with a lower $T_g$. It should be pointed out that the $T_g$ of a polymer generally varies in a nonlinear manner with the plasticizer volume fraction.

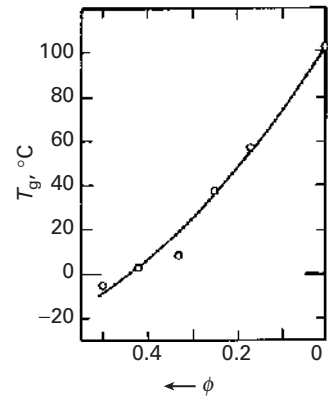


**Figure 16.10** Decrease in glass transition temperature of polymethyl methacrylate as a function of increasing volume fraction of the plasticizer diethyl phthalate.
(Adapted from F. Bueche and Frank N. Kelley, Viscosity and glass temperature relations for polymer-diluent systems, *Journal of Polymer Science*, 50, issue 154 (2003), With permission from John Wiley and Sons.)

Figure 16.10 shows the glass transition temperature of polymethyl methacrylate (PMMA) as a function of the volume fraction of the plasticizer diethyl phthalate.[17] The solid line in the graph is given by:

$$\left[T_g - T_g^*\right]/\left[T_g - T\right] = 1 + r[1 - \phi]/\phi$$

where $r = V_f/V = 0.5$, $T_g^* = -65^\circ C$, $V_f$ is the free volume, $V$ is the total volume of the polymer, and the asterisks indicate the values for the plasticizer. At $\phi = 1, T_g = T$, as expected. The absorption of the plasticizer facilitates the molecular motion. Generally, the plasticizer has a smaller molecule size but similar chemical structure to the polymer into which it penetrates. The plasticizer molecules separate the main chains and thus reduce the intermolecular forces, i.e., their presence makes it easier for the chains to slide past one another. However, more often than not, the swelling of the polymer is not uniform, because diffusion of liquid or gas in a polymer depends on many variables, such as the size of the diffusing molecule, the microstructure of the polymer, etc. Frequently, stresses are set up at the boundary between the part penetrated by the liquid and the unpenetrated part. One can easily imagine this phenomenon to be of great concern in polymer-matrix composites. In general, polymers having high bond energies, high degrees of crystallinity and cross-linking, etc. will show a reduced amount of swelling.

Figure 16.11 shows the decrease in tensile strength of an epoxy with increasing water content.[18]

### 16.5.3 Oxidation

Oxidation of polymers occurs throughout their life because it is impossible to avoid interaction with the oxygen in the atmosphere. More dangerous is ozone, sometimes

[17] P. Nogueira, C. Ramirez, A. Torres, et al., *J. Appl. Polymer Sci.*, 80(1), (2001). 71-80.
[18] G. R. Rugger, in *Environmental Effects on Polymeric Materials*, vol. I, D. V. Rosato and R. T. Schwartz (eds.) New York: Interscience, 1968, p. 339.

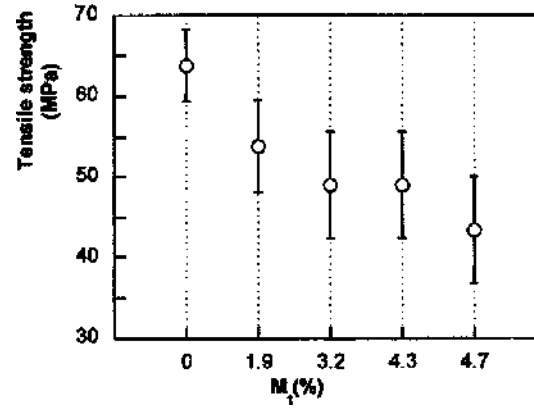


**Figure 16.11** Tensile strength (MPa) of an epoxy resin with water content. (Reprinted by permission from John Wiley and Sons, *Journal of Applied Polymer Science*, Effect of water sorption on the structure and mechanical properties of an epoxy resin system, P. Nogueira, C. Ramírez, A. Torres, et al., Copyright (2001).)

present in the atmosphere but always in outer space because ozone is much more reactive than oxygen. Oxygen can permeate a polymer and increase cross-linking, thereby decreasing its toughness and flexibility. Ozone attacks any elastomer with unsaturated bonds. This is especially important in rubbers and elastomers where cracking on the surface results after prolonged exposure to air. Most of us have experienced this type of damage to the sidewalls of automobile tires.

### 16.5.4 Radiation Damage

Radiation (ultraviolet, X-rays or other energetic particles such as neutrons) can lead to ionization, which can result in breaks in polymeric chains, called chain scission. (See Figure 16.12 for a schematic of this phenomenon.) Carbon-carbon (C-C) bonds form the backbone of polymers. Such bonds, however, can be ruptured by ultraviolet (UV) radiation. Rupture of molecular bonds in polymers (not in metals and ceramics) by UV radiation is commonly manifested as discoloration and loss of mechanical properties. Bond rupture can cause changes in molecular weight, degree of cross-linking, and reaction with oxygen. Physical changes such as discoloration, surface embrittlement, cracking, and loss of strength are other manifestations of radiation damage in polymers.

### 16.5.5 Environmental Crazing

In general, environmentally induced crazes have a faster growth rate and grow to sizes much larger than those grown in inert environments. Certain organic liquids act as crazing and cracking agents. For example, the crazes shown in Figure 8.43 in a sample of polycarbonate, were produced under dead load in a specimen of polycarbonate immersed in alcohol, which is a good crazing agent. The problem, however, is much more complex than might appear at first sight, particularly in glassy polymers. Organic liquids which act as cracking or crazing agents can also raise the toughness of the polymer, i.e., the crack propagation rate is slowed down. For example, cracks propagate in a stable manner in PMMA in air. In the presence

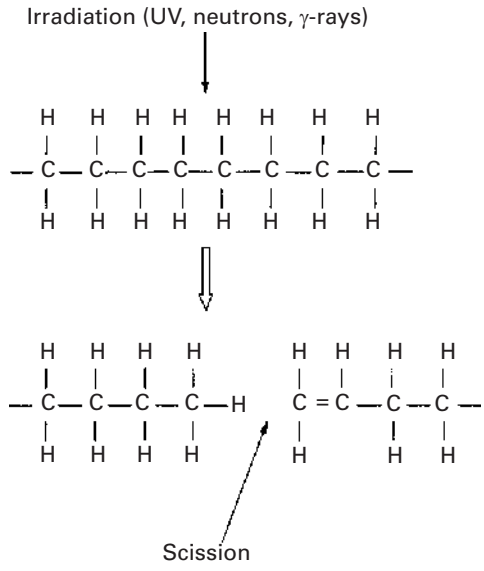


**Figure 16.12** Exposure to UV radiation breaks bonds in the polymeric chains and decreases tensile strength of high density polyethylene. Tensile strength decreases with UV exposure time.

of methanol, a crazing agent, cracks grow in a stick-slip manner reminiscent of the behavior of thermosetting polymers in inert environments. The stick-slip mode of crack growth occurs in thermosets because of crack blunting due to shear yielding. In PMMA, however, the crazing agent causes multiple crazing at the crack tip and blunts the crack.[19] Thus, multiple craze formation can lead to an enhanced toughness.

Although the organic liquids can cause a reduction in the surface energy, it would appear that the plasticizing effects connected with the absorption of the crazing agents into the polymer on a molecular scale are more important. Most organic liquids generally diffuse rather slowly in a bulk polymer. The same organic liquids might penetrate rapidly in a craze and plasticize it. This is because the crazed volume in a polymer is highly porous and has a high surface-area-to-volume ratio. Even a very short diffusion time can plasticize the drawn out polymer chains in the craze, i.e., a drop in the $T_g$ will occur and it will become easier plastically to draw more polymer into fibrils at the craze surface.

### 16.5.6 Alleviating the Environmental Damage in Polymers

Additives or coatings may be introduced into thermoplastic materials to promote resistance to certain adverse environmental affects. Additives are usually introduced during the mixing and processing of thermoplastics, while coatings are applied after the thermoplastic has been consolidated or processed.

Antioxidants and stabilizers are added to polymers. A well-known household example is butylated hydroxytoluene (BHT), which is added to food products to

[19] A. J. Kinloch and R. J. Young, *Fracture Behavior of Polymers*, London, U.K.: Elsevier, 1985, p. 79.

prevent oxidation. Antioxidants help a polymer retain its properties and thus provide a proper service life. Carbon black is a commonly used additive to stabilize polyolefins and other polymers against UV degradation. The UV resistance is very dependent on the amount, type, and particle size of the carbon black used. Carbon black particles of small size provide the greatest UV resistance, but they tend to agglomerate into aggregate clusters.[20]

Antiozonants are additives that protect an elastomer against attack by ozone. Physical and chemical antiozonants (for example, derivatives of *p*-phenylenediamine (*p*-PDA) are used to protect rubber.

## 16.6 Environmental Effects in Ceramics

Ceramics, especially the crystalline and fully dense variety, are quite inert compared to metals and polymers. This conventional wisdom about the refractoriness of ceramics notwithstanding, it turns out that moisture can be quite a damaging species, especially to silica-based glass. For example, identical glass fibers are three times stronger when tested under vacuum than in moist air. In a vacuum, freshly drawn glass fibers can show strength as high as 14 GPa, among the strongest of all materials. Exposure to ambient air for periods of two to three weeks will reduce this strength to about 5 GPa. This effect has been known for a long time. American Indians would soak their flint stones in water before fracturing them for making arrowheads. Artisans would wet scratches made into glass with saliva prior to fracturing.

Figure 16.13 shows the effect of increasing vapor pressure of water on crack propagation in a Hertzian contact fracture test on soda-lime glass.[21] This figure shows a plot of crack velocity as a function of crack extension force for different vapor-pressure values. Liquid water is the most active promoter of crack growth in glass, as indicated by line *A* in Figure 16.13. As the water vapor pressure decreases, the crack velocity versus crack extension force curves shift to the right from *B* to *E*. Not unexpectedly, different chemicals have different effects.

Commonly, a fall in strength as a function of time in an aggressive environment in the ceramic literature is referred to as static fatigue. Figure 16.14 illustrates the phenomenon of static fatigue for glass, i.e, failure occurs under a constant applied stress lower than the tensile stress to cause failure. The drop in strength is greater under moist conditions than dry conditions. Mechalske and Bunker[22] studied the effect of moisture on glass in detail. The phenomenon is referred to in the literature as *stress corrosion cracking of glass*. The water molecule can penetrate to the crack tip, where it attaches itself to the silica molecules. Figure 16.15 shows how two silica molecules hydrolyze in the presence of moisture as per

$$SiO_2 + 2H_2O \rightarrow Si(OH)_4.$$

[20] W. L. Hawkins, M. A. Worthington, and F. H. Winslow, *Rubber Age*, 88 (1960) 279.
[21] M. V. Swain and B. R. Lawn, *Int. J. Fract. Mech.*, 9 (1973) 481.
[22] T. A. Mechalske and B. Bunker, *Sci. American*, 257 (No. 6) (1987) 122.

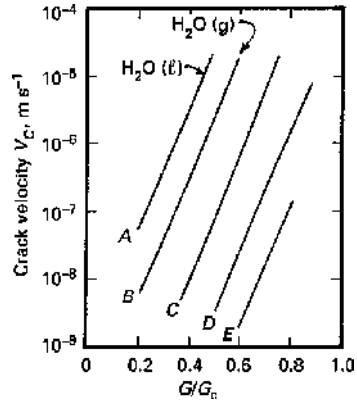


**Figure 16.13** Crack velocity as a function of crack extension force for different vapor pressure values in a soda-lime glass. As the water vapor pressure decreases, the crack velocity versus crack extension force curves shift to the right. Liquid water is the most active promoter of crack growth in glass, line *A*. (Reprinted by permission from Springer Nature, *International Journal of Fracture*, A microprobe technique for measuring slow crack velocities in brittle solids, M. V. Swain and B. R. Lawn, Copyright (1969).)

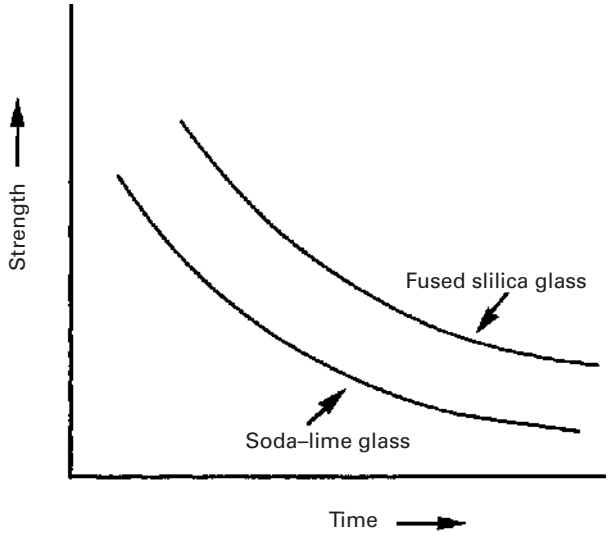


**Figure 16.14** Schematic of static fatigue in fused silica and soda-lime glass. Although fused silica has a higher strength than soda-lime glass, both show a fall in strength as a function of time in an aggressive environment.

As described in Chapter 1, silica tetrahedra are the basic building blocks of the structure of glass. The water molecule, shown floating at the crack tip, attaches itself to two silica tetrahedra. This decreases the bond strength of silica by about 20-fold and allows a much smaller applied stress to break the ring of silica tetrahedra. The process repeats itself; with water molecules penetrating the crack-tip region and weakening the bonds as shown in Figure 16.15. The low magnification optical micrograph of Figure 16.16 shows vivid proof of condensation caused by moisture at a crack tip in glass. The viscous nature of the crack-tip condensate indicates a

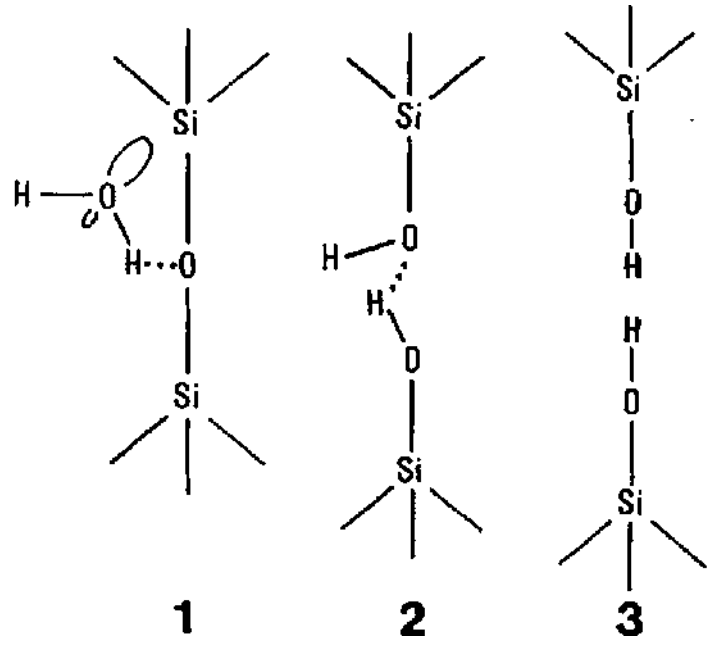


**Figure 16.15** Interaction of the water molecule with silica at the crack tip. Reaction steps involve: (1) adsorption of water to Si-0 bond, (2) concerted reaction involving simultaneous proton and electron transfer, and (3) formation of surface hydroxyl groups.
(Reproduced from John Wiley and Sons: *Journal of the American Ceramic Society,* A molecular mechanism for stress corrosion in vitreous silica, Stephen W. Freiman, Terry A. Michalske, Copyright (2006).)

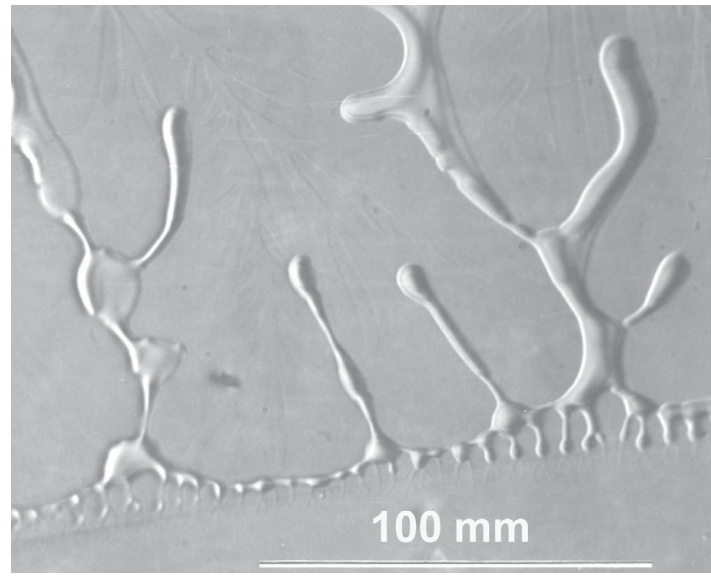


**Figure 16.16** Condensation caused by moisture at a crack tip in glass. Note the viscous nature of the crack-tip condensate, indicating a chemical reaction between water and the glass.
(Courtesy of S. Wiederhorn.)

chemical reaction between water and the glass. The effect of other molecules is not so drastic and depends on their size and reactivity.

Wiederhorn[23] modelled the effect of humidity on crack propagation velocity in a soda-lime glass. He treated the corrosion reaction at the crack tip to be an

[23] S. M. Wiederhorn, *J. Amer. Ceram. Soc.*, 50 (1967) 407.

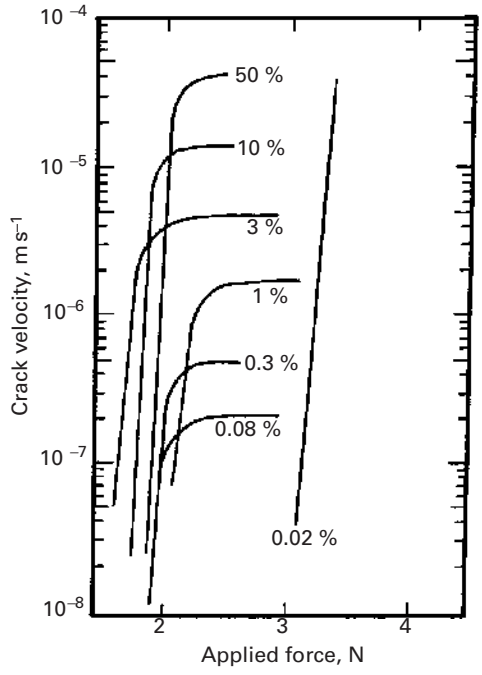


**Figure 16.17** Crack velocity as a function of applied force in sapphire (single-crystal alumina) for different relative humidities. (Adapted by permission from Springer Nature, *International Journal of Fracture Mechanics*, Moisture assisted crack growth in ceramics, S. M. Wiederhorn, Copyright (1968).)

interactively controlled process with stress-dependent activation energy. The final expression for the crack velocity is:

$$v = Cx^n \exp bK,$$

where $C$ is the mole fraction of water vapor at the crack tip, $n$ is the number of water molecules of water reacting with a bond B:

$$n\mathrm{H_2O} + \mathrm{B} \rightarrow \mathrm{B}^*$$

and forming an activated complex B*. $K$ is the stress intensity factor and $b$ is a constant. Thus, crack velocity $v$ increases as $\exp bK$ and linearly with $C$. The factor $C$ is a function of the water vapor pressure.

Alumina is also affected by the presence of moisture. Figure 16.17 shows the crack velocity as a function of applied force.[24] The test was done on a cantilever beam specimen at different relative humidities. The sapphire (single-crystal alumina) specimen was precracked along the (1011) rhombohedral plane. This is the plane that has the lowest surface energy in sapphire. The crack velocity values reach a plateau, the values of these plateaux increase with increasing humidity. The data points for 0.02% humidity are on a line that is nearly vertical.

[24] S. M. Wiederhorn, *Int. J. Fract. Mech.*, 4 (1968) 171.

### 16.6.1 Oxidation of Ceramics

Oxide ceramics such as alumina, mullite, silica, etc. are inherently stable in oxidizing atmospheres. That is the reason oxides such as silicates, aluminates, etc. are abundant in the Earth's crust. Nonoxide ceramics such silicon carbide, silicon nitride, molybdenum disilicide, etc. invariably have a surface layer. They tend to get oxidized at high temperatures in air.

One can represent the oxidation of structural ceramics such as SiC and $Si_3N_4$ at low oxygen partial pressures (<140 Pa) by the following reactions:

$$2SiC_{(s)} + 3O_{2(g)} \rightarrow 2SiO_{(g)} + 2CO_{2(g)},$$
$$2Si_3N_{4(s)} + 3O_{2(g)} \rightarrow 6SiO_{(g)} + 2N_{2(g)}.$$

In a vacuum, or an inert atmosphere, silica can degrade by:

$$2SiO_{2(g)} \rightarrow 2SiO_{(g)} + O_{2(g)}.$$

Catastrophic oxidation can occur for some ceramics in the 300–700 °C range. In the literature this has been referred to as the *pesting* phenomenon. $MoSi_2$ has excellent oxidation resistance outside the pesting range because a protective layer of $SiO_2$ forms. This silica layer can protect $MoSi_2$ to 1000 °C.

## SUGGESTED READING

S. Al-Malaika, Oxidative degradation and stabilisation of polymers, *Intl. Mater. Rev.*, 48 (2003) 165.

H Arup and R. N. Parkins (eds.), *Stress Corrosion*. Alphen aan den Rijn, the Netherlands: Sijthoff & Noordhoff, 1979.

I M. Bernstein and A. W. Thompson (eds.) *Hydrogen Effects in Metals*. Warrendale, PA: TMS-AIME, 1981.

M. R. Louthan, R. P. McNitt, and R. D. Sisson (eds.) *Environmental Degradation of Engineering Materials in Hydrogen*. Blacksburg, VA: Virginia Tech Printing Dept., 1981.

H. G. Nelson, in *Treatise on Materials Science and Technology*, vol. 25. New York, NY: Academic Press, 1983, p. 275.

D. Talbot and J. Talbot, *Corrosion Science and Technology*. Boca Raton, FL: CRC Press, 1998.

## EXERCISES

**16.1** Steel products are commonly protected by chromium or zinc coatings. Based on the galvanic series, what difference would you expect in their ability to protect steel?

**16.2** Explain why a small anode/cathode area ratio will result in a higher corrosion rate.

**16.3** Alclad aluminum consists of a thin layer (5–10% of total thickness) of one Al alloy metallurgically bonded to the core alloy. Generally, the cladding layer is anodic to the core. Why?

**16.4** Tinplate (commonly used in the canning industry) is not a plate or sheet of tin. It is actually a steel strip with a thin coating of tin. Discuss the pros and cons of using tin to protect steel.

**16.5** Describe how galvanizing (coating steel with zinc) works as a cathodic protection for steel.

**16.6** Describe some methods of protecting the inside of a metallic pipe against chemical attack.

**16.7** A form of corrosion called pitting corrosion can occur in aluminum in fresh water. As the name suggests, pits form on the surface of aluminum in this type of corrosion. The pit depth $d$ follows a cube root relationship with time $t$:

$$d = At^{1/3}.$$

Normally, a 5 μm thick $Al_2O_3$ film forms on the surface of aluminum. If we double the thickness of the film, by what factor will the time to perforation increase?

**16.8** Structural ceramic materials such as SiC, $Si_3N_4$, $MoSi_2$, etc. oxidize in the presence of oxygen at high temperatures. Give the oxidation reactions and indicate how the reaction products serve to protect these materials from further oxidation. Does it have a deleterious effect on the high temperature capability of these materials?

**16.9** A Ni-based super alloy has a 0.2 μm thick oxide layer. When placed in a burner rig to test for oxidation, it was observed to grow to 0.3 μm in1 h. If the superalloy follows a parabolic oxidation law ($x^2 = a + bt$, where $x$ is the thickness, $t$ is the time, and $a$ and $b$ are constants), what is the thickness after one week?

**16.10** The velocity of a crack in a material submerged in an aggressive medium such as humid air can be represented by:

$$V = \frac{\mathrm{d}a}{\mathrm{d}t} = 0.5K_{\mathrm{I}}^{20}.$$

Using the relationship $K_{\mathrm{I}} = \sigma\sqrt{\pi a}$, compute the time to failure for this material. $K_{\mathrm{Ic}}$ for the material is 5 MPa $\mathrm{m}^{1/2}$.

**16.11** For a silica-based glass, the following data are available for a $V = AK_{\mathrm{I}}^{n}$ type of relationship:

| Relative humidity | Preexponential constant A | Crack velocity exponent $n$ |
|---|---|---|
| 10% | 2.8 | 25 |
| 100% | 4.0 | 22 |

Take $K_{\mathrm{Ic}} = 1$ MPa $\mathrm{m}^{1/2}$. For a crack length $a = 1$ nm, compute the fracture strength $\sigma_{\mathrm{c}}$ in an inert atmosphere. Then compute the lifetime of the material under $0.3\sigma_{\mathrm{c}}$ in 10% and 100% relative humidity.

**16.12** The stable, slow crack growth in a polymer in an aggressive environment can be represented by:

$$\frac{da}{dt} = 0.03K_I^2,$$

where $a$ is the crack length in meters, $t$ is the time in seconds, and $K_I$ is the stress intensity factor in MPa $m^{1/2}$. $K_{Ic}$ for this polymer is 5 MPa $m^{1/2}$. Calculate the time to failure under a constant applied stress of 50MPa. Use $K_I = \sigma\sqrt{\pi a}$,

**16.13** It has been observed experimentally that, in cold-worked brass under stress-corrosion conditions, crack propagation is adequately described by:

$$\frac{da}{dt} = AK^2,$$

where $A$ is a constant and the other symbols have their normal significance. Derive an expression for the time to failure of the material $t_f$, in terms of $A$, the applied stress $\sigma$, the initial crack length $a_0$, and the critical stress intensity corresponding to $a_f$ (i.e., $K_{Ic}$).

# Appendixes

## UNIT CONVERSION FACTORS

| *Length* | |
|---|---|
| 1 m = $10^{10}$ Å = 0. 1 nm | 1 Å = $10^{-10}$ m |
| 1 mm = 0.0394 in | 1 in = 25.4 mm |
| 1 cm = 0.394 in | 1 in = 2.54 cm |
| 1 m = 3.28 ft | 1 ft = 0.3048 m |

| *Mass* | |
|---|---|
| 1 Mg = $10^3$ kg | 1 kg = $10^{-3}$ Mg |
| 1 kg = $10^3$ g | 1 g = $10^{-3}$ kg |
| 1 kg = 2.205 $lb_m$ | 1 $lb_m$ = 0.4536 kg |
| 1 g = $2.205\times10^{-3}$ $lb_m$ | 1 $lb_m$ = 453.6 g |

| *Density* | |
|---|---|
| 1 kg $m^{-3}$ = $10^{-3}$ g $cm^{-3}$ | 1 g/$cm^3$ = $10^3$ kg/$m^3$ |
| 1 kg $m^{-3}$ = 0.0624 $lb_m$ $ft^{-3}$ | 1 lbm /$ft^3$ = 16.02 kg/$m^3$ |
| 1 g $cm^{-3}$ = 62.4 $lb_m$ $ft^{-3}$ | 1 $lb_m$ /$ft^3$ = $1.602\times10^{-2}$ g/$cm^3$ |
| 1 g $cm^{-3}$ = 0.0361 $lb_m$ $in^{-3}$ | 1 lbm /$in^3$ = 27.7 g/$cm^3$ |

| *Force* | |
|---|---|
| 1 N = $10^5$ dynes | 1 dyne = $10^{-5}$ N |
| 1 N = 0.2248 $lb_f$ | 1 $lb_f$ = 4.448 N |

| *Stress* | |
|---|---|
| 1 MPa = 145 psi | 1 psi = $6.90\times10^{-3}$ MPa |
| 1 MPa = 0.102 kg $mm^{-2}$ | 1 kg/$mm^2$ = 9.806 MPa |
| 1Pa = 10 dynes $cm^{-2}$ | 1 dyne/$cm^2$ = 0.10 Pa |
| 1 kg $mm^{-2}$ = 1422 psi | 1 psi = $7.03\times10^{-4}$ kg/$mm^2$ |

| *Fracture Toughness* | |
|---|---|
| 1 psi $in^{1/2}$ = $1.099\times10^{-3}$ MPa $m^{1/2}$ | 1 MPa $m^{1/2}$ = 910 psi $in^{1/2}$ |

| *Energy* | |
|---|---|
| 1 J = $10^7$ ergs | 1 erg = $10^{-7}$ J |
| 1 J = $6.24\times10^{18}$ eV | 1 eV = $1.602\times10^{-19}$ J |
| 1 J = 0.239 cal | 1 cal = 4.184 J |
| 1 J = $9.48\times10^{-4}$ Btu | 1 Btu = 1054 J |
| 1 J = 0.738 ft-$lb_f$ | 1 ft-$lb_f$ = 1.356 J |
| 1 eV = $3.83\times10^{-20}$ cal | 1 cal = $2.61\times10^{19}$ eV |
| 1 cal = $3.9710^{-3}$ Btu | 1 Btu = 252.0 cal |

| *Power* | |
|---|---|
| 1W = 0.239 cal/s | 1 cal/s = 4.184 W |
| 1W = 3.414 Btu/h | 1 Btu/h = 0.293 W |
| 1 cal/s = 14.29 Btu/h | 1 Btu/h = 0.070 cal/s |

| *Viscosity* | |
|---|---|
| 1 Pa s = 10 P | 1 P = 0.1 Pa s |

| *Temperature, T* | |
|---|---|
| $T$(K) = 273 + $T$(°C) | $T$(°C) = $T$(K) – 273 |
| $T$(K) = [$T$(°F) – 32] + 273 | $T$(°F) = 5[$T$(K) – 273] + 32 |
| $T$(°C) = 5/9[$T$(°F) – 32] | $T$(°F) = 5[$T$(°C) + 32] |

| *Specific Heat* | |
|---|---|
| 1 J $kg^{-1}$ $K^{-1}$ = $2.39\times10^{-4}$ cal $g^{-1}$ $K^{-1}$ | 1 cal $g^{-1}$ $°C^{-1}$ = 4184 J $kg^{-1}$ $K^{-1}$ |
| 1 J $kg^{-1}$ $K^{-1}$ = $2.39\times10^{-4}$ Btu $lb_m^{-1}$ $°F^{-1}$ | 1 Btu $lb_m^{-1}$ $°F^{-1}$ = 4184 J $kg^{-1}$ $K^{-1}$ |
| 1 cal $g^{-1}$ $°C^{-1}$ = 1.0 Btu $lb_m^{-1}$ $°F^{-1}$ | 1 Btu $lb_m^{-1}$ $°F^{-1}$ = 1.0 cal $g^{-1}$ $K^{-1}$ |

# STANDARD PREFIXES, SYMBOLS, AND MULTIPLICATION FACTORS

| Prefix | Symbol | Factor by which unit has to be multiplied |
|---|---|---|
| Tera | T | $10^{12}$ |
| Giga | G | $10^{9}$ |
| Mega | M | $10^{6}$ |
| Kilo | k | $10^{3}$ |
| Hecto | h | $10^{2}$ |
| Deca | da | $10^{1}$ |
| Deci | d | $10^{-1}$ |
| Centi | c | $10^{-2}$ |
| Milli | m | $10^{-3}$ |
| Micro | μ | $10^{-6}$ |
| Nano | n | $10^{-9}$ |
| Pico | p | $10^{-12}$ |
| Femto | f | $10^{-15}$ |
| Atto | a | $10^{-18}$ |

# IMPORTANT CHARACTERISTICS OF SOME ELEMENTS

| Symbol | Atomic number | Atomic weight (amu) | Density of solid, 20 °C (g $cm^{-3}$) | Crystal structure, 20 °C |
|---|---|---|---|---|
| Al | 13 | 26.98 | 2.70 | FCC |
| Ar | 18 | 39.95 | – | – |
| Ba | 56 | 137.33 | 3.5 | BCC |
| Be | 4 | 9.012 | 1.85 | HCP |
| B | 5 | 10.81 | 2.34 | Rhomb. |
| Br | 35 | 79.90 | – | – |
| Cd | 48 | 112.41 | 8.65 | HCP |
| Ca | 20 | 40.08 | 1.55 | FCC |
| C | 6 | 12.011 | 2.25 | Hex. |
| Cs | 55 | 132.91 | 1.87 | BCC |
| Cl | 17 | 35.45 | – | – |
| Cr | 24 | 52.00 | 7.19 | BCC |
| Co | 27 | 58.93 | 8.9 | HCP |
| Cu | 29 | 63.55 | 8.96 | FCC |
| F | 9 | 19.00 | – | – |
| Ga | 31 | 69.72 | 5.90 | Ortho. |
| Ge | 32 | 72.59 | 5.32 | Dia. Cubic |
| Au | 79 | 196.97 | 19.3 | FCC |
| He | 2 | 4.003 | – | – |
| H | 1 | 1.008 | – | – |
| I | 53 | 126.91 | 4.93 | Ortho. |
| Fe | 26 | 55.85 | 7.87 | BCC |
| Pb | 82 | 207.2 | 11.35 | FCC |
| Li | 3 | 6.94 | 0.534 | BCC |
| Mg | 12 | 24.31 | 1.74 | HCP |
| Mn | 25 | 54.94 | 7.44 | Cubic |
| Hg | 80 | 200.59 | – | – |
| Mo | 42 | 95.94 | 10.22 | BCC |
| Ne | 10 | 20.18 | – | – |
| Ni | 28 | 58.69 | 8.90 | FCC |
| Nb | 41 | 92.91 | 8.57 | BCC |
| N | 7 | 14.007 | – | – |
| O | 8 | 16.00 | – | – |
| P | 15 | 30.97 | 1.82 | Ortho. |
| Pt | 78 | 195.08 | 21.45 | FCC |
| K | 19 | 39.10 | 0.862 | BCC |
| Si | 14 | 28.09 | 2.33 | Dia. cubic |
| Ag | 47 | 107.87 | 10.5 | FCC |
| Na | 11 | 22.99 | 0.971 | BCC |
| S | 16 | 32.06 | 2.07 | Ortho. |
| Sn | 50 | 118.69 | 7.3 | Tetra. |
| Ti | 22 | 47.88 | 4.51 | HCP |
| W | 74 | 183.85 | 19.3 | BCC |
| V | 23 | 50.94 | 6.1 | BCC |
| Zn | 30 | 65.39 | 7.13 | HCP |
| Zr | 40 | 91.22 | 6.51 | HCP |

Adapted from W. D. Callister, Materials Science and Engineering. New York, NY John Wiley & Sons, 1997.

| Atomic radius (nm) | Ionic radius(nm) | Most common valence | Melting point (°C) |
|---|---|---|---|
| 0.143 | 0.053 | 3+ | 660.4 |
| – | – | Inert | –189.2 |
| 0.217 | 0.136 | 2+ | 725 |
| 0.114 | 0.035 | 2+ | 1278 |
| – | 0.023 | 3+ | 2300 |
| – | 0.196 | 1– | –7.2 |
| 0.149 | 0.095 | 2+ | 321 |
| 0.197 | 0.100 | 2+ | 839 |
| 0.071 | 0.016 | 4+ | (sublimes at 3367) |
| 0.265 | 0.170 | 1+ | 28.4 |
| – | 0.181 | 1– | –101 |
| 0.125 | 0.063 | 3+ | 1875 |
| 0.125 | 0.072 | 2+ | 1495 |
| 0.128 | 0.096 | 1+ | 1084 |
| – | 0.133 | 1– | –220 |
| 0.122 | 0.062 | 3+ | 29.8 |
| 0.122 | 0.053 | 4+ | 937 |
| 0.144 | 0.137 | 1+ | 1064 |
| – | – | Inert | –272 (at 26 atm) |
| – | 0.154 | 1+ | –259 |
| 0.136 | 0.220 | 1– | 114 |
| 0.124 | 0.077 | 2+ | 1538 |
| 0.175 | 0.120 | 2+ | 327 |
| 0.152 | 0.068 | 1+ | 181 |
| 0.160 | 0.072 | 2+ | 649 |
| 0.112 | 0.067 | 2+ | 1244 |
| – | 0.110 | 2+ | –38.8 |
| 0.136 | 0.070 | 4+ | 2617 |
| – | – | Inert | –248.7 |
| 0.125 | 0.069 | 2+ | 1453 |
| 0.143 | 0.069 | 5+ | 2468 |
| – | 0.01 –0.02 | 5+ | –209.9 |
| – | 0.140 | 2– | –218.4 |
| 0.109 | 0.035 | 5+ | 44.1 |
| 0.139 | 0.080 | 2+ | 1772 |
| 0.231 | 0.138 | 1+ | 63 |
| 0.118 | 0.040 | 4+ | 1410 |
| 0.144 | 0.126 | 1+ | 962 |
| 0.186 | 0.102 | 1+ | 98 |
| 0.106 | 0.184 | 2– | 113 |
| 0.151 | 0.071 | 4+ | 232 |
| 0.145 | 0.068 | 4+ | 1668 |
| 0.137 | 0.070 | 4+ | 3410 |
| 0.132 | 0.059 | 5+ | 1890 |
| 0.133 | 0.074 | 2+ | 420 |
| 0.159 | 0.079 | 4+ | 1852 |

## MECHANICAL PROPERTIES OF SOME IMPORTANT CERAMIC MATERIALS

| | Weibull modulus | Flexural strength (MPa) | Young's modulus (GPa) | Poisson's ratio |
|---|---|---|---|---|
| Silicon nitride | 20 | 930 | 320 | 0.28 |
| Silicon carbide | 18 | 634 | 450 | 0.17 |
| Aluminum nitride | 10 | 200 | 320 | 0.22 |
| Tungsten carbide | – | 1930 | 627 | 0.21 |
| Titanium oxide | – | 137 | 228 | 0.27 |
| MgO– stabilized Zirconia | – | 620 | 200 | 0.3 |
| Aluminum oxide (98%) | 10 | 300 | 340 | 0.22 |
| Aluminum oxide (99%) | 10 | 400 | 370 | 0.22 |
| Zirconia toughened | 3 | 912 | 285 | 0.25 |
| Alumina (ZTA) boron carbide | 12 | 450 | 450 | 0.27 |
| Titanium diboride | | 277 | 556 | 0.1 1 |
| Zirconia | 5 | 800–1200 | – | 0.28 |

*Note*: the values given are indicative only

## MECHANICAL PROPERTIES OF SOME IMPORTANT METALS AND ALLOYS

| Alloy | Density (kg $m^{-3}$) | Melting point (°C) | Young's modulus (GPa) | Poisson's ratio |
|---|---|---|---|---|
| Al 2024–T 851 | 2770 | 502 | 72.4 | 0.33 |
| Al 7075–T 651 | 2810 | 477 | 72 | 0.33 |
| Al 7178–T651 | 2830 | 477–629 | 73 | 0.33 |
| Ti–6Al–4V (grade 5) | 4430 | 1604–1660 | 113.8 | 0.342 |
| Ti–3Al–2.5V (alpha annealed) | 4480 | 1700 | 100 | 0.3 |
| 702 Zirconium | 6500 | 1852 | 99.3 | 0.35 |
| 60–40 Soft Solder | 8600 | 183–190 | 30 | 0.4 |
| Stainless steel 4340 | 7850 | – | 205 | – |
| Stainless steel 304 | 8000 | 1400 | 193 | 0.29 |
| Steel 5160 | 7850 | – | 205 | – |
| Tool steel H 11 hot worked | 7800 | – | 210 | – |
| Maraging steel (18 Ni) (before aging) | 8000 | | 183 | |
| Maraging steel (18 Ni) (annealed & aged at 480 °C) | 8080 | | 200 | |
| Superalloy CoCrWNi | 10000 | – | – | – |
| Superalloy Fe based N08330 Ni | 8000 | | | |
| Superalloy H–X Nickel | 8220 | – | – | – |

*Note*: the values given are indicative only

| Compressive strength (MPa) | Hardness (HV) | Tensile strength (MPa) | Fracture toughness (MPa $rn^{1/2}$) |
|---|---|---|---|
| 2100–3500 | 1800 | 350–415 | 6 |
| 1035–1725 | 2300 | 390–450 | 4.3 |
| 1400–2100 | 1 110 | – | 3 |
| 2683 | 1600 | 344 | – |
| 688 | 800 | 51.6 | 3.2 |
| 1750 | 1200 | 352 | |
| 2500 | 1800 | 150 | 4 |
| 3000 | 1800 | 180 | 4 |
| – | 1500 | – | 6.9 |
| 470 | 2700 | | 3.0 |
| 470 | 2700 | – | 6.9 |
| 2000 | 1200 | – | 6–8 |

| UTS (MPa) | Yield strength (MPa) | Strain-to-failure (%) | Fracture toughness (MPa $m^{1/2}$) |
|---|---|---|---|
| 455 | 400 | 5 | 26.4 |
| 570 | 505 | 11 | 24.2 |
| 605 | 540 | 10 | 23.1 |
| 1860 | 1480 | 14 | 55 |
| 620 | 500 | 15 | 100 |
| 379 | 207 | 16 | – |
| 53 | – | – | – |
| 745 | 470 | 22 | 60.4 |
| 505 | 215 | 70 | – |
| 724 | 275 | 17.2 | – |
| 1990 | 1650 | 9 | – |
| 965 | 660 | 17 | |
| 1864 | 1737 | 17.4 | |
| 860 | 310 | 10 | – |
| 586 | 276 | 40 | |
| 690 | 276 | 40 | – |

# MECHANICAL PROPERTIES OF SOME IMPORTANT POLYMERIC MATERIALS

| | Density (g $cm^{-3}$) | Young's modulus (MPa) | Tensile strength (MPa) | Strain–to–fracture (%) | Yield stress (MPa) | Yield strain | Rockwell hardness | Izod impact energy J $m^{-1}$ |
|---|---|---|---|---|---|---|---|---|
| *Thermoplastics* | | | | | | | | |
| Cellulose acetate(soft) | 1.27–1.34 | 593–1723 | 13–32 | 32–50 | 15–28 | – | R49–RI03 | 100–270 |
| Cellulose acetate (hard) | 1.27–1.34 | 1309–2757 | 31–58 | 6–40 | 28–52 | – | RI0I–RI23 | 3140–5060 |
| Cellulose acetate butyrate (soft) | 1.15–1.22 | 510–868 | 13–26 | 60–74 | 8.2–17 | – | R59–R95 | 130–290 |
| Cellulose acetate butyrate (hard) | 1.19–1.25 | 1034–1378 | 34–46 | 38–54 | 24–42 | – | RI08–RI17 | 38–130 |
| Nylon 6/6 | 1.13–1.25 | – | 62–82 | 60–300 | – | – | RI08–RI20 | 50–100 |
| Polycarbonates (unfilled) | 1.2 | 2000–2240 | 55–65 | 20–100 | 55–68 | – | M70–MI80 | 430–850 |
| Polyethylene (low density) | 0.91–0.925 | 96–260 | 6.9–9.6 | 400–700 | 7.5–1 1.7 | 20^0 | – | – |
| Polyethylene (medium density) | 0.926–0.941 | 240–620 | 8.2–24.1 | 50–600 | 10.3–17.9 | 10–20 | – | 26–850 |
| Polyethylene (high density) | 0.941–0.965 | 590–1110 | 21–37 | 15–100 | 16.5–34.4 | 5–10 | R3O–R5O | 80–1050 |
| Methylmethacrylate (PMMA unmodified) | 1.18–1.20 | 2410–3450 | 48–75 | 2–10 | – | – | M80–MI05 | 16–32 |
| Polypropylene (unmodified) | 0.9 | 9.65–11.8 | 29–37 | >220 | 33.8 | 5 | 93 | 53 |
| Polypropylene (copolymer) | 0.9 | – | 19–31 | 200–700 | – | – | R50–R96 | 58–64 |
| Polystyrene (unmodified) | 1.04–1.08 | 2750–4140 | 34–68 | 1–2.5 | – | – | M65–M85 | 13–32 |
| PTFE (unmodified) | 2.1–2.3 | 1030 | 31–41 | 250 | 29 | 10 | J75–J95 | 130–210 |
| *Thermosetting* | | | | | | | | |
| Epoxy (unfilled) | 1.115 | 2070 | 27–89 | 2–6 | – | – | M75–MI 10 | 10–50 |
| Melamine formaldehyde | 1.47–1.52 | 8960 | 48–90 | 0.6–0.9 | – | – | Ml I0–MI24 | 12–18 |
| Polyester (glass fiber mat reinforced) | 1.5–2.1 | 3450 | 206–344 | .5–1.5 | – | – | M80–MI20 | 370–1600 |
| Silicones (mineral filled) | 1.8–2.8 | – | 20–27 | – | – | – | M85–M95 | 13–18 |
| Urea formaldehyde (a–cellulose filled) | 1.47–1.52 | 8970 | 37–89 | 0.6 | – | – | E94–E97 | 12–20 |
| ABS (high–heat resistant) | 1.06–1.08 | – | 48–62 | 1–20 | 28–62 | – | Rl 10–RI15 | 100–210 |

*Note*: the values given are indicative only

# Index